Countering WMD JOURNAL

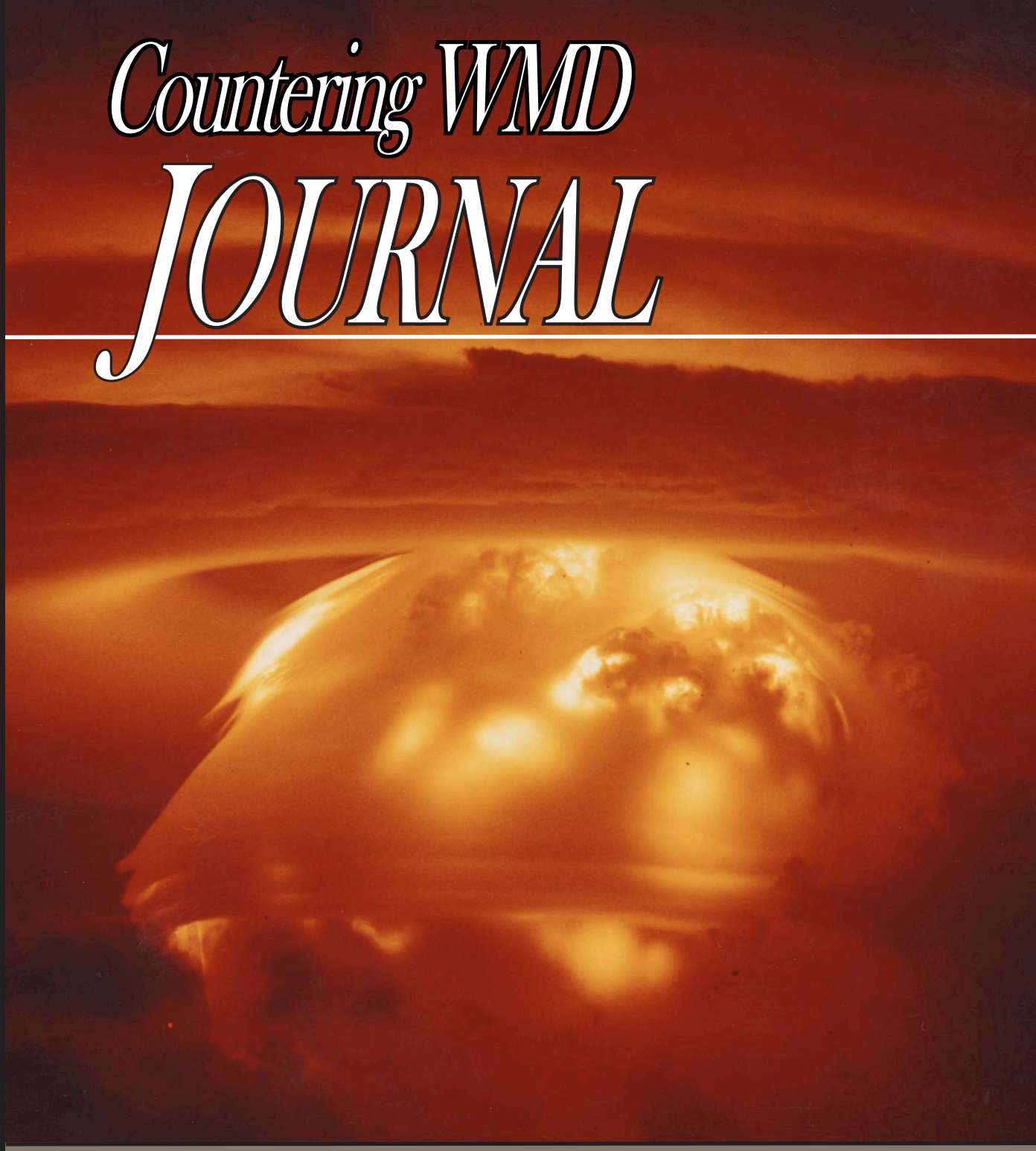

75TH ANNIVERSARY ATOMIC ERA EDITION

Issue 21 • Summer/Fall 2020

U.S. Army Nuclear and Countering WMD Agency

Countering WMD JOURNAL
U.S. Army Nuclear and Countering WMD Agency

Published by the
United States Army Nuclear and Countering WMD Agency
(USANCA)

Disclaimer: The *Countering WMD Journal* is published semi-annually by USANCA. The views expressed are those of the authors, not the Department of Defense (DoD) or its elements. *Countering WMD Journal*'s contents do not reflect official U.S. Army positions and do not supersede information in other official Army publications.

Distribution: U.S. Army organizations and activities with CWMD-related missions, to include combat and materiel developers and units with chemical and nuclear surety programs, and Functional Area 52 (FA52) officers.

Distribution Statement A: Approved for public release; distribution is unlimited.

The Secretary of the Army has determined that the publication of this periodical is necessary in the transaction of the public business as required by law. Funds for printing this publication were approved by the Secretary of the Army in accordance with the provisions of Army Regulation 25-30.

Article Submission: We welcome articles from all U.S. Government agencies and academia involved with Countering WMD matters. Articles are reviewed and must be approved by the *Countering WMD Journal* Editorial Board prior to publication. Submit articles in Microsoft Word without automatic features; include photographs, graphs, tables, etc. as separate files. Please call or email us for complete details. The editor retains the right to edit and select which submissions to print. For more information, see the inside back-cover section (Submit an Article to *Countering WMD Journal*) or visit our website at http://www.belvoir.army.mil/usanca/.

Mailing Address:
Director, USANCA, 5915 16th Street Building 238, Fort Belvoir, VA 22060-1298.

Telephone: 571-515-9948, Fax 703-806-7900, DSN 94-312-515-9948.

Electronic Mail: usarmy.belvoir.hqd-dcs-g-3-5-7.mbx.usanca-proponency-division@mail.mil
Subject line: ATTN: Editor, CWMD Journal (enter subject)

About the cover: 15MT CASTLE BRAVO thermonuclear detonation conducted on 01 March 1954 at the Pacific Proving Ground by Joint Task Force 7. Photo courtesy of the U.S. Department of Energy.

Inside the Journal

Trinity
(C761, Los Alamos National Laboratory, photo by Physicist Jack Aeby)
The Trinity test was the world's first nuclear detonation and a precursor to one of two Los Alamos-developed weapons that helped end World War II just weeks later.

Director Notes

COL Benjamin Miller
Director, USANCA

Welcome to our long-awaited Summer/Fall 2020 issue of the *Countering WMD Journal*. We decided to make the 21st issue a special edition to commemorate the anniversary of the dawn of the nuclear age. Seventy-five years ago, the United States carried out the world's first nuclear detonation (Trinity, July 26, 1945) and the only two nuclear attacks in history (Hiroshima, on August 6; Nagasaki, on August 9, 1945). In light of those historic events, and with an eye toward the Joint Force's role in our national security, we asked the CWMD Community to submit articles for the 75th Anniversary Atomic Era Edition—we were not disappointed.

Ever since the historic events that ushered the world into the Atomic Age, theorists, strategists, and politicians alike have struggled to come to terms with nuclear weapons and the implications of their proliferation and use. The very existence of nuclear weapons poses profoundly difficult questions. How best is deterrence achieved? Is the world now more or less safe? When can nuclear weapons be eliminated—should they be? What role should nuclear weapons play in security strategies? These questions persist today in various forms; therefore, it is important to review the lessons of the past and seek to understand how nuclear strategies changed over time.

Many of the Atomic Era's lessons still resonate today. The Korean War demonstrated that the U.S. nuclear arsenal would neither preclude all belligerence nor deter a regional power from becoming directly involved in a war with a nuclear superpower. Like the Korean War, Vietnam proved that conflicts could be fought below the nuclear threshold. More recently, Desert Storm demonstrated the incredible conventional power of a seemingly unstoppable U.S.-led coalition. America's adversaries took heed. Since then, no enemy has attempted to challenge the U.S. military directly with uniformed forces in symmetrical warfare at the Gulf War scale. That does not mean large conventional future conflicts will not occur, nor does that mean nuclear weapon use against the United States and our allies is not possible.

While the United States has long sought to reduce the role of nuclear weapons in its security strategy, its adversaries have emphasized nuclear weapons development, seeking to put the United States and its allies in a position of relative disadvantage in certain types of conflicts. A regional war that escalates, spilling across borders and domains, presents the most likely path to nuclear weapons use. The risk of escalation grows if our adversaries come to believe they can achieve coercive advantage by threatening nuclear

escalation or by actual first use of nuclear weapons in order to force cessation on terms favorable to them.

The United States may fight its next war with the possibility of nuclear weapon use; we would be unwise to disregard the most dangerous enemy course of action. The best way to prevent a perception of coercive advantage is by preparing our Joint Force to fight on a battlefield shaped by the use or threat of nuclear weapons. This is why USANCA is working with the Army Service Component and Combatant Commands to improve Conventional Nuclear Integration (CNI) in training, doctrine, education, plans, and operations. These important measures will both prepare our Joint Force to fight on a nuclear battlefield and deter our adversaries from pursuing doctrines and policies likely to precipitate such a battle in the first place.

Perhaps one of our toughest jobs as CWMD professionals is staying abreast of the dynamic security situation and the shifting nuances of nuclear capabilities, policies, and treaties. We cannot forget that it is the next war—rather than the last—for which we must prepare to fight. Today, nuclear debates range from the Joint Comprehensive Plan of Action, the Intermediate-Range Nuclear Forces Treaty, the New Strategic Arms Reduction Treaty, declaratory policy, and nuclear modernization. Our nation needs CWMD professionals like you to help senior leaders understand these complexities and prepare them to make decisions concerning some of the toughest security issues we face. I'm excited to share this special edition with you. For everyone who contributed her or his time and energy to make this Atomic Era edition of the *Countering WMD Journal* possible, thank you.

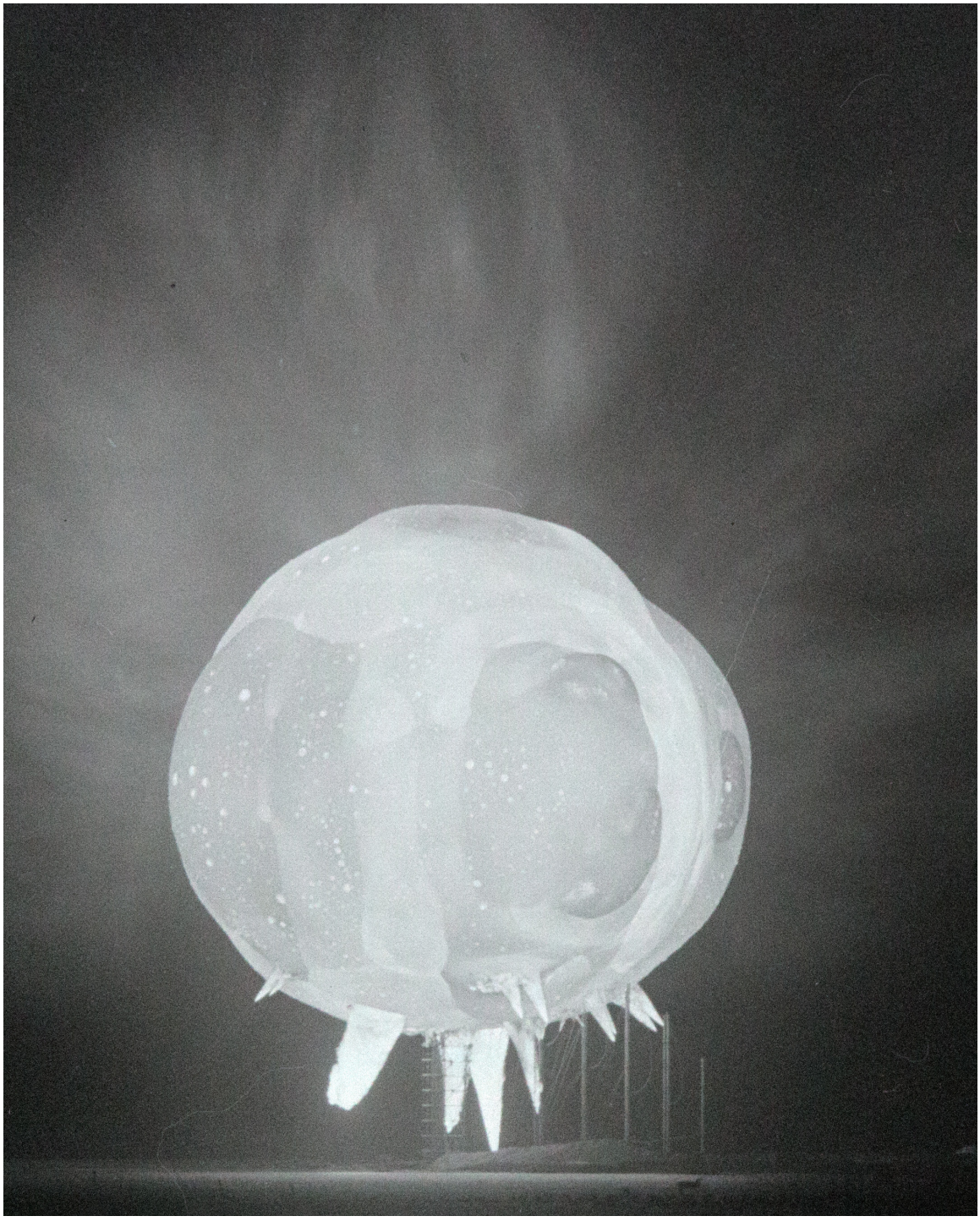

Erie 34249: The Erie nuclear test was conducted by the Los Alamos Lab in 1956 at Enewetak Atoll. Erie's yield was 14.9 kilotons; its fireball consumed the 300-foot tower and guy wires from which it was detonated. Photo courtesy of Los Alamos National Laboratory.

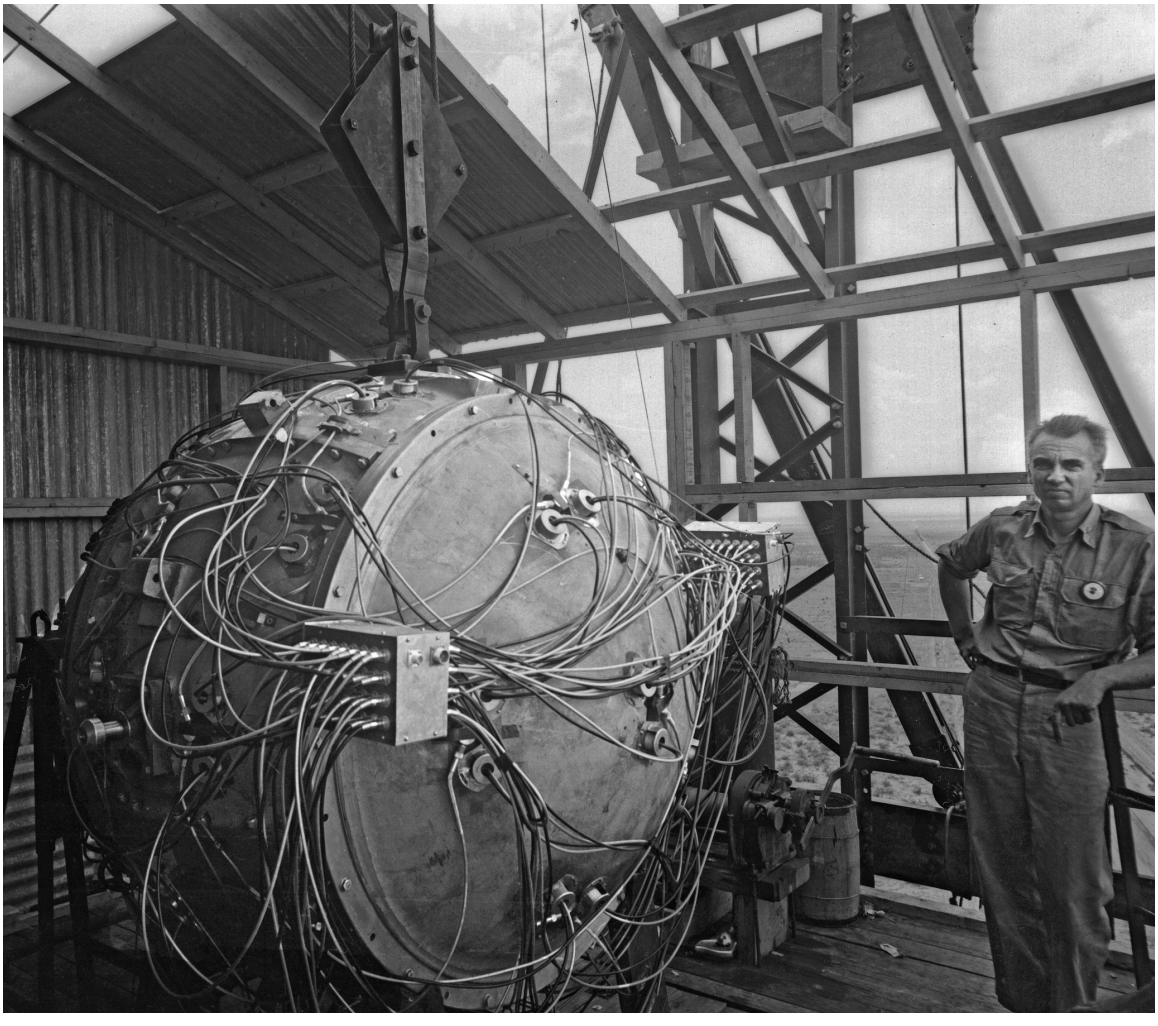

Physicist Norris Bradbury, who would succeed J. Robert Oppenheimer as Los Alamos Director, stands next to the Gadget – the world's first successfully detonated atomic device. The implosion-style plutonium weapon was developed at the Los Alamos Lab and detonated during the Trinity test on July 16, 1945 in the New Mexico desert. This scientific achievement would later help end World War II. The Gadget produced a yield of 21 kilotons. Photo courtesy of Los Alamos National Laboratory (TR-311_4x5).

Of Clouds and Craters: The Incredible Story of U.S. Nuclear Weapons Testing[1]

Alan B. Carr
Los Alamos National Laboratory

"Now!" With that word, the Atomic Age – and the era of nuclear weapons testing – dawned.[2] The advent of World War II's first irresistible weapon, which had been secretly tested in the New Mexico desert in July 1945, would help hasten the inevitable: complete victory for the Allies. Codenamed Trinity, the test was the first of over a thousand conducted by the United States between 1945 and 1992.[3]

Nuclear weapons would change future clashes as well. The looming Cold War, with roots stretching all the way back to 1917, was history's first conflict between two major nations armed with nuclear weapons. The existence of those weapons played an important role in maintaining a tenuous peace between the United States and the Soviet Union; furthermore, nuclear weapons testing played a prominent role in fueling both the arms race and the success of deterrence. Yet, the history of nuclear weapons testing is rarely remembered, even though nuclear tests have been performed in the very recent past.[4] Of the estimated 2,000-plus nuclear tests ever performed, the United States is responsible for approximately half. This is the story of U.S. full-scale nuclear weapons testing.

The United States tested nuclear weapons for many reasons. First, and perhaps most obviously, weapons were tested to verify they would work. The next order of business was to explore what nuclear weapons would do when used in combat. As such, the Department of Defense (DoD) routinely sponsored experiments to assess the effects of nuclear weapons on civilian and military assets. As the Cold War solidified, along with the future of nuclear weapons, tests were performed to advance design (e.g., improve efficiency, adjust yields, etc.); this was the most common type of nuclear test. Though it may come as a surprise, only a very small handful of tests were performed to confirm the reliability of weapons in the stockpile. Known as stockpile confidence tests, these events validated the reliability of stockpiled weapons and assessed their performance. Similarly, there were only a small handful of full-system tests – events in which a test device was deployed in its delivery system. Safety tests were performed to ensure that weapons would not detonate in the event of an accident and to assess potential vulnerabilities. Tests were also performed to study

Alan B. Carr is the Senior Historian at the Los Alamos National Laboratory's National Security Research Center in Los Alamos, New Mexico. He has B.A. and M.A. degrees in History from Texas Tech University. He has served as a historian at Los Alamos for more than 17 years. His email address is abcarr@lanl.gov.

the basic phenomenology associated with nuclear explosions in order to avoid technological surprises. Some nuclear detonations had nothing to do with weapons at all. Rather, these events explored the possibility of using nuclear devices for (very) large-scale excavation and fracking. Finally, as we shall see, nuclear tests were conducted for political reasons

Though the atomic strikes launched against the Japanese cities of Hiroshima and Nagasaki represent the culmination of the Manhattan Project, its scientific crescendo was certainly the Trinity test of July 16, 1945. At its peak, the Manhattan Project simultaneously employed 125,000 workers at installations all over the country.[5] Perhaps the most well-known facility was located at Los Alamos, New Mexico. There, physicist J. Robert Oppenheimer led a technical staff of approximately 1,700 individuals in a quest to design, build, test, and help deliver the world's first nuclear weapons.[6] Codenamed Project Y, the Laboratory produced two entirely different types of weapons during the war. The first was Little Boy, a gun-type device that fired one subcritical mass of enriched uranium at another to achieve supercriticality. The second was Fat Man, a weapon that used thousands of pounds of high explosives to compress a sphere of plutonium at its center.

Little Boy did not require a full-scale test before entering combat. The weapon's relatively simple design and well-understood materials enabled small-scale tests to be performed, which conclusively demonstrated it would work. However, Fat Man required a full-scale test due to its more intricate design and dependence upon relatively crude high explosives. Thus, planning began many months before the test. Trinity, as the test was dubbed by Oppenheimer, would be conducted at the Alamogordo Bombing Range.[7] The range, located relatively close to Los Alamos and controlled by the Army, provided enhanced security. To ensure a minimal number of people in surrounding areas would see the secret test, detonation was planned for 4 a.m.

Los Alamos scientists gave safety a considerable amount of thought, especially in the final weeks leading up to the test. During a nuclear test, particles that come in contact with the fireball are irradiated, and a portion of the material is ejected into the atmosphere. Eventually, these contaminated particles fall back to earth, hence the infamous term fallout. To minimize the dangers of fallout, nuclear tests (including Trinity) were generally performed in very arid or remote regions. Ideally, the irradiated particles would climb high into the atmosphere and be evenly dispersed across the globe at very low levels, which posed no significant threat to people. Precipitation, however, would drive irradiated particles back to earth quickly in a very concentrated area; this concentration of radioactive material could be very hazardous to anyone below. As such, weather was an important consideration in selecting the bombing range as the location for the test.

In the very early morning of July 16, 1945, there was a violent, isolated thunderstorm near ground zero. Oppenheimer's boss, General Leslie R. Groves, was present and ordered that the test be postponed until the storm had passed at approximately 5:30 a.m. This would compromise security, as more people in the surrounding area would see the explosion. However, in this rare case, there was a priority that even trumped security: politics. The next day, July 17, the Potsdam Conference would begin in Germany: President Truman had to know if the United States had successfully developed the atomic bomb before going into negotiations with

Joseph Stalin to decide the fate of postwar Europe.

At 5:29:15 a.m., the world's first nuclear test was performed.[8] Trinity proved remarkably successful: approximately thirteen-and-a-half pounds of plutonium yielded a blast equivalent to 21,000 tons of TNT.[9] Because there were many witnesses in the surrounding area due to the delay, the Manhattan Project reluctantly issued a press release. The news story that followed reported, "'a considerable amount of high explosive and pyrotechnics' in a remote area of the Alamogordo air base reservation was reported by Col. William O. Hareckson, commandant. Although the blast rattled windows 255 miles away … Col. Hareckson said there were no loss of life or injury to anyone."[10] But even today, the assertion that there were no injuries remains hotly debated as those downwind of Trinity's fallout, which was substantial, continue to seek compensation from the federal government.[11]

Trinity was arguably history's greatest, single scientific experiment, and, as might be expected, the scientists who observed it had many things to say about the unique experience. Perhaps the best concise quote encompassing the Trinity experience was uttered by Project Y Physicist Victor Weisskopf: "Our first feeling was one of elation, then we realized we were tired, and then we were worried."[12] The trip back to Los Alamos for the exhausted scientists was apparently a quiet and somber one, as they imagined future wars fought with nuclear weapons. But the business of ending World War II remained.

With Nazi Germany defeated, the Allies gathered strength to deliver the death blow to Imperial Japan. All previous measures employed against the Japanese, including a threat of "prompt and utter destruction" after Trinity, had failed to induce an unconditional surrender, thus nuclear weapons were used against the cities of Hiroshima (Little Boy; 15 kiloton yield) and Nagasaki (Fat Man; 21 kiloton yield) on August 6 and 9, respectively.[13] By the end of the year, approximately 64,500 people had perished as a result of the bombing of Hiroshima; nearly 40,000 died during that time in Nagasaki.[14]

Nuclear weapons played an important role in inducing the unconditional surrender of Japan. On August 14, President Truman stated: "I have received this afternoon a message from the Japanese Government in reply to the message forwarded to that Government by the Secretary of State on August 11. I deem this reply a full acceptance of the Potsdam Declaration which specifies the unconditional surrender of Japan. In the reply there is no qualification."[15] That same day, Emperor Hirohito acknowledged that the use of this "new and most cruel bomb" factored heavily in the government's decision to surrender.[16] Though the Soviet entry into the war against Japan was certainly a crushing blow to Japan's hopes of concluding a conditional peace, it is clear the use of the atomic bombs – perhaps more than any other individual dynamic – helped compel the Japanese to surrender quickly and unconditionally. William J. Donovan, the Director of the Office of Strategic Services, sent a top-secret memorandum to President Truman the day fighting ceased: "The group [of Japanese diplomats in Switzerland] believes that the atomic bomb, not the Soviet entry into the war in the Pacific, caused the Japanese offer to surrender."[17]

Thus, the war came to an end, but not before 60 to 80 million people had been killed worldwide. Oppenheimer almost immediately left Los Alamos, but served as an adviser to the government in

the years following the war. President Truman hoped to eliminate nuclear weapons, thus one of Oppenheimer's first postwar tasks was playing a key role in drafting the world's first, formal nuclear abolition plan. Originally known as the Acheson-Lilienthal Report (and, after modifications, the Baruch Plan), the proposal was rejected by the Soviet Union when it was presented to the United Nations in the summer of 1946. Tensions between West and East gradually escalated as the memory of Hitler, who had served as the adhesive of the wartime alliance, began to very gradually fade.

The future of the Manhattan Project's weapons design laboratory at Los Alamos was very much in doubt in the months following the war. Very few chose to stay at the Laboratory, a facility created to fulfill a single mission, which had been successfully accomplished. Oppenheimer and Groves convinced a wartime Group Leader, Norris Bradbury, to become the Director. Groves believed Bradbury, a Berkeley-trained Stanford physicist and Naval Reserve Commander, would make an excellent successor to Oppenheimer due to Bradbury's knowledge of both technical and military matters. Bradbury reluctantly agreed to take the reins of what appeared to be a dying institution for six months.[18] But rather than evaporating, the future of Bradbury's Laboratory rapidly began to congeal as 1945 came to an end.

On January 10, 1946, President Truman formally approved the plan for Operation Crossroads, the nation's first true nuclear weapons test series.[19] The Joint Chiefs of Staff gave the Navy the assignment and appointed Vice Admiral W.H.P. Blandy its commander. Los Alamos, then tasked with manufacturing the nation's nuclear weapons, would provide test devices for Crossroads, which was purely intended to assess weapons effects. Though the Crossroads devices did not advance weapons design, the operation gave Los Alamos meaningful work to do during very uncertain times.

Crossroads, which would be performed at Bikini Atoll in the Pacific's Marshall Islands, proved an immense operation. The task force included over 40,000 individuals, nearly 250 ships, and over 150 aircraft. Seven hundred fifty cameras would capture the spectacle. The tests would explore how nuclear weapons performed against naval vessels; they would also explore the biological effects of nuclear blasts, therefore the task force included nearly 5,500 test animals.[20]

Not everyone shared the Navy's enthusiasm for Crossroads. According to the official history of the operation, some argued the tests should not be carried out because of the cost. Others feared nuclear testing might produce dangerous tidal waves and "thought cracks might be made in the earth's crust, allowing sea water to rush into the white-hot interior and form catastrophic quantities of steam." Others believed the tests were simply unnecessary, and might even provoke the Soviet Union.[21] As the public head of Task Force One, Admiral Blandy drew the ire of many. After making assurances that the tests would "not blow out the bottom of the sea and let all the water run down the hole" or "destroy gravity," the Admiral defended himself, saying, "I am not an atomic playboy, as one of my critics labeled me, exploding these bombs to satisfy my personal whim."[22] Despite the controversy, Operation Crossroads proceeded in the early summer of 1946.

Crossroads began somewhat inauspiciously. The first test, an airdrop codenamed Able, missed the target ship (the Battleship *Nevada*) by a significant margin. Conducted on June 30, the bomb produced a yield of 21 kilotons, the same

as its similar predecessors the Trinity device and Fat Man. The test failed to sink many of the target ships, but unfortunately sent the *Gilliam*, one of the main instrumentation ships, to the bottom of the lagoon.[23] The mystery of the miss was never fully resolved, though some have suggested Fat Man's poor ballistic design may have contributed; bombardier error has also been suggested.[24] Regardless, this would be the first of many, many, many surprises in the history of nuclear testing.

Crossroads-Baker, the second and final test of the series, produced some of the most iconic photographs of the testing era. The device, another 21-kiloton implosion weapon, was detonated directly beneath the target fleet. Though relatively few ships were sunk, the target fleet was heavily damaged and rendered inoperable by high levels of radiation. In fact, the radiation later prompted Glenn T. Seaborg, a Nobel Laureate and head of the Atomic Energy Commission (AEC), to describe Baker as "the world's first nuclear disaster."[25] A third test, planned for the spring of 1947, was canceled due to withering criticism from many, including General Groves and Bradbury.[26] Thus, Task

Crossroads-Baker, 21kT explosion on July 25, 1946. Photo courtesy of the U.S. Department of Energy.

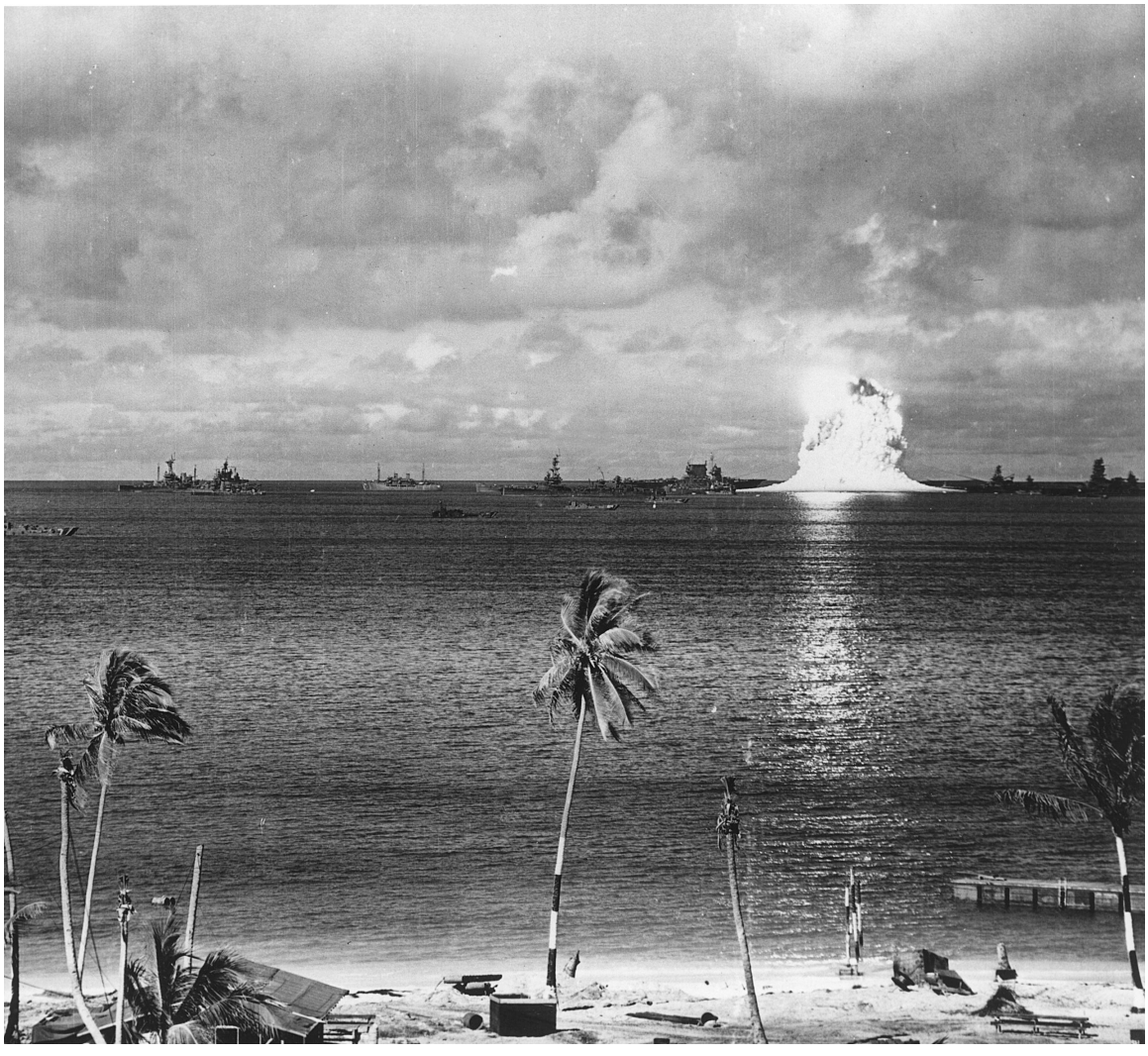

Force One was disbanded in the fall of 1946; the Manhattan Project would soon follow suit.

At midnight on December 31, 1946, the Manhattan Project formally ended; the newly created, civilian-led Atomic Energy Commission (AEC) immediately absorbed the nation's nuclear weapons complex. Though General Groves lost control of the complex, he was appointed leader of the Armed Forces Special Weapons Project (AFSWP). Moving forward, the AEC would assume responsibility for the design and manufacture of nuclear weapons, as well as the handling of special nuclear materials. AFSWP would maintain control of the nuclear weapons stockpile, less the special nuclear material, and participate in field testing.

In the months following Crossroads, relations between the United States and the Soviet Union continued to sour. It was a time of rapid change, tenuous hope, and grave danger. Back at Los Alamos, scientists continued to explore the prospect of a weapon many orders of magnitude more powerful than the fission bombs that had destroyed Hiroshima and Nagasaki. No tests were performed in 1947, but in the spring of 1948, an important series called Operation Sandstone was conducted in the Marshalls, this time at Enewetak Atoll. The Sandstone devices featured changes that significantly increased yield. For instance, the second test of the three-shot series, Yoke, produced a yield of 49 kilotons – more than double that of its predecessors. Thus, Sandstone was the first postwar test series to advance weapons design. The series concluded as the Soviets blockaded Berlin.

The United States maintained a nuclear monopoly for just over four years. During those years, the weapons complex and the stockpile grew at a very slow rate. For instance, at the end of 1945, the United States officially had two nuclear weapons in the stockpile. That grew to nine in 1946, 13 in 1947, and 50 in 1948.[27] But in the summer of 1949, the world changed dramatically. On August 29, 1949, the Soviet Union secretly tested its first nuclear weapon. The device, which was based on Fat Man, was made possible through espionage. Though multiple Soviet agents had penetrated the Manhattan Project, Los Alamos theoretical physicist Klaus Fuchs provided the most substantial contribution. Yuli Khariton, one of the most senior Soviet scientists, once wrote: "The whole Soviet people should be deeply grateful to Klaus Fuchs for the vast amount of information he provided to Soviet physicists."[28] One of history's most prolific mass murderers, Joseph Stalin, now had nuclear weapons; thanks to the atomic spies, he had them more quickly than anyone in the West anticipated. On October 1, Mao Zedong announced the establishment of the People's Republic of China – the world's most populous country had become a socialist dictatorship. Days later, the Sandia Corporation was formed to manage a laboratory at Kirtland Air Force Base in Albuquerque. The Kirtland lab, which had started as a wartime Los Alamos division, would focus on developing non-nuclear components for atomic bombs, freeing Los Alamos to concentrate on weapons design.

By the end of 1949, the United States had 170 nuclear weapons in the stockpile. No full-scale tests were conducted in 1950, as had been the case in 1949, but many important events that would shape the future of testing occurred that year. On January 31, President Truman "directed the Atomic Energy Commission to continue its work on all forms of atomic weapons, including the so-called hydrogen or super-bomb."[29] The development of thermonuclear weapons then became the top priority at Los

Alamos. On May 26, Fuchs confessed to espionage; this led to the discovery of several spies working for the Soviet Union in the United States. On June 25, the North Korean People's Army invaded the Republic of Korea, sparking the Korean War. The fear caused by the setbacks of 1949-50 unfortunately led to one of the darker episodes in America's history: the Red Scare.

With the arms race underway, Los Alamos began exploring more advanced weapons and, as such, additional testing was required. Because the Pacific Proving Grounds lay so far away, testing in the Marshalls was so expensive, and security was questionable, recommendations emerged for a test site within the continental United States. Spurred by the Chinese entry into the war in Korea, President Truman approved the creation of the test site within the boundaries of the Las Vegas Bombing and Gunnery Range on December 18, 1950.[30] Incredibly, testing began only a few weeks later. Operation Ranger, the site's first series, featured five airdrops conducted in just eleven days starting with shot Able on January 27, 1951. Yields ranged from 1 to 22 kilotons; each test was conducted at the same location with, for the most part, very similar heights of burst.[31] These tests, which advanced increasingly efficient design concepts, were the first of over 900 tests that would be conducted at the site (an area only slightly larger than Rhode Island).

1951 proved a very busy year in terms of stockpile growth, research, and testing. That year, the United States had 438 nuclear weapons in the stockpile. In the years that followed, the stockpile would grow exponentially due to the arms race, an expanding role for nuclear weapons in national defense, and the groundbreaking for a new, purpose-built pit production facility. Located 10 miles south of Boulder, Colorado, the

GREENHOUSE-George (B369-11): Conducted by the Los Alamos Lab at Enewetak Atoll in May of 1951, Greenhouse George was the first nuclear test to produce a thermonuclear burn. This validated the principles that would be used for the first full-scale thermonuclear bomb test Ivy Mike one year later. Greenhouse George was detonated on a 200-foot tower and produced a yield of 225 kilotons. Photo courtesy of Los Alamos National Laboratory.

Rocky Flats Plant would enable the United States to produce thousands of nuclear weapons each year. Up until 1951, the United States had introduced four types of weapons into the stockpile. In 1951 alone, four new weapons types were produced. It was a big year for testing as well: the United States had conducted six tests since 1945, but in 1951, there were sixteen.

In addition to Operation Ranger, the AEC also sponsored a test series in the Pacific called Operation Greenhouse and another in Nevada called Buster-Jangle.[32] The spring series, Greenhouse, included four tests; two were significant weapons design firsts. The third test in the series, George, was the first detonation to produce thermonuclear burn. All weapons up to that point derived energy solely from fission: the process of splitting the nucleus of an atom. George was the first test device to produce energy by fusing particles together (thermonuclear fusion). Though not considered a full-scale thermonuclear detonation, George nonetheless produced a yield of 225 kilotons (15 times as powerful as Little Boy) by effectively fusing deuterium and tritium (D-T). The final test of the series, Item, explored the possibility of boosting. In a boosted weapon, D-T gas is injected into the device. During detonation, the gas is compressed and D-T fusion occurs; this results in the creation of additional neutrons, which increases yield.[33]

That fall in Nevada, Buster-Jangle started unfavorably. The first test, Able, did not detonate.

The anxious arming party returned to the 100-foot shot tower to disarm the device. Walt Treibel, a wartime Los Alamos veteran who then worked for Sandia, recalls the team's ascent: "We stopped a lot on the ladder to catch our breaths because of the anxiety and because of our awareness that each step could be our last." As Treibel and his colleagues disarmed the device, soon nicknamed "Unable Able," they discovered the problem: a blown fuze due to the DC power supply being plugged in backward.[34] Two days later on October 22, Able was successfully detonated, but it produced more headlines than yield. At less than one-tenth of a kiloton, the test wasn't visually impressive, prompting newspaper articles such as, "Tiny A-Bomb Blast This Morn Disappoints Watcher Hordes" and "'Baby atom blast' set off; fails to shake Las Vegas."[35] The troubled series ended on November 29 with a cratering test called Uncle. Though some consider Uncle to be the first underground nuclear test since the device was buried 17 feet, it can be argued the shot was an atmospheric test because the blast was never intended to remain below the surface. Uncle produced one of the first of many obtrusive craters at the Nevada Test Site (NTS).[36]

VIP Observers: Observers watch Los Alamos Lab's Greenhouse Dog test from a beach patio on Enewetak Atoll. The April 1951 test was part of the Greenhouse series, which tested principles that led to the development of hydrogen bombs. The blast wave from the 81-kiloton yield arrived at the observers' location an estimated 45 seconds after the initial flash. Photo courtesy of Los Alamos National Laboratory.

The Soviet Union only tested two nuclear weapons in 1951 and did not test at all in 1952.[37] The United States, however, performed two test series in 1952: Tumbler-Snapper, at the NTS, and Ivy in the Pacific. Like Buster-Jangle, Tumbler-Snapper featured a mix of weapons effects and weapons development tests. The third test, Charlie, was the first to be broadcast live on television. William Laurence, the Pulitzer Prize-winning New York Times reporter who also witnessed Trinity, was interviewed as part of the coverage: "You never see a second atomic blast… it's always the first. No matter, I think, how many you see, you always have a new experience as though you had never seen it before."[38] On May 20, a device once again failed to detonate and John Clark, who was in the (dis)arming party for Buster-Jangle-Able, once again had to climb the tower (this time 300 feet) to assess the problem. An experiment had malfunctioned, triggering an interlocking mechanism that prevented the device from detonating. With the problem corrected, Fox was successfully fired five days later.[39]

Late that summer, under pressure from the Air Force, the AEC established a third weapons laboratory. The upstart laboratory was created in Livermore, California, as a branch of the University of California's Radiation Laboratory and tasked with developing diagnostics to support the thermonuclear work at Los Alamos, but soon the young Livermore scientists would begin exploring entirely new and innovative weapons designs. Ernest Lawrence, a Nobel Laureate who led the Manhattan Project's work at Berkeley, played the lead role in establishing the fledgling facility's culture. The laboratory's Director, 30-year-old Herbert York, recalls: "Lawrence firmly believed that if a group of bright young men are simply sent off in the right direction with a reasonable level of support, they will end up in the right place. He did not believe that the goals need to be spelled out in great detail, nor that it was necessary that the leadership consist of persons who were already well known."[40]

Though Greenhouse-George had demonstrated the fusion principle, the feasibility of a full-scale thermonuclear device had proven elusive for the better part of a decade. Edward Teller, a Project Y veteran and one of the driving forces behind the creation of Livermore, and Los Alamos mathematician Stan Ulam jointly proposed a workable idea for a revolutionary new thermonuclear design in 1951. The new architecture would feature a "primary," an imploding descendant of Fat Man that, when detonated, would channel massive amounts of x-rays around a "secondary" stage laden with thermonuclear fuel. On October 31, 1952, this concept was confirmed during Operation Ivy at Enewetak. The Mike test produced a yield of 10.4

Photo on page 17, Tumbler-Snapper-Dog CN70-3473 LA-UR-06-1068: One of the primary objectives of Tumbler-Snapper Dog was to help train troops in the tactical use of nuclear weapons and radiological protection. An estimated 1,950 Marines took part in a troop exercise during the test, which was conducted at the Nevada Test Site. The Los Alamos device was airdropped and detonated at 1,040 feet above the surface, producing a yield of 19 kilotons. Photo courtesy of Los Alamos National Laboratory.

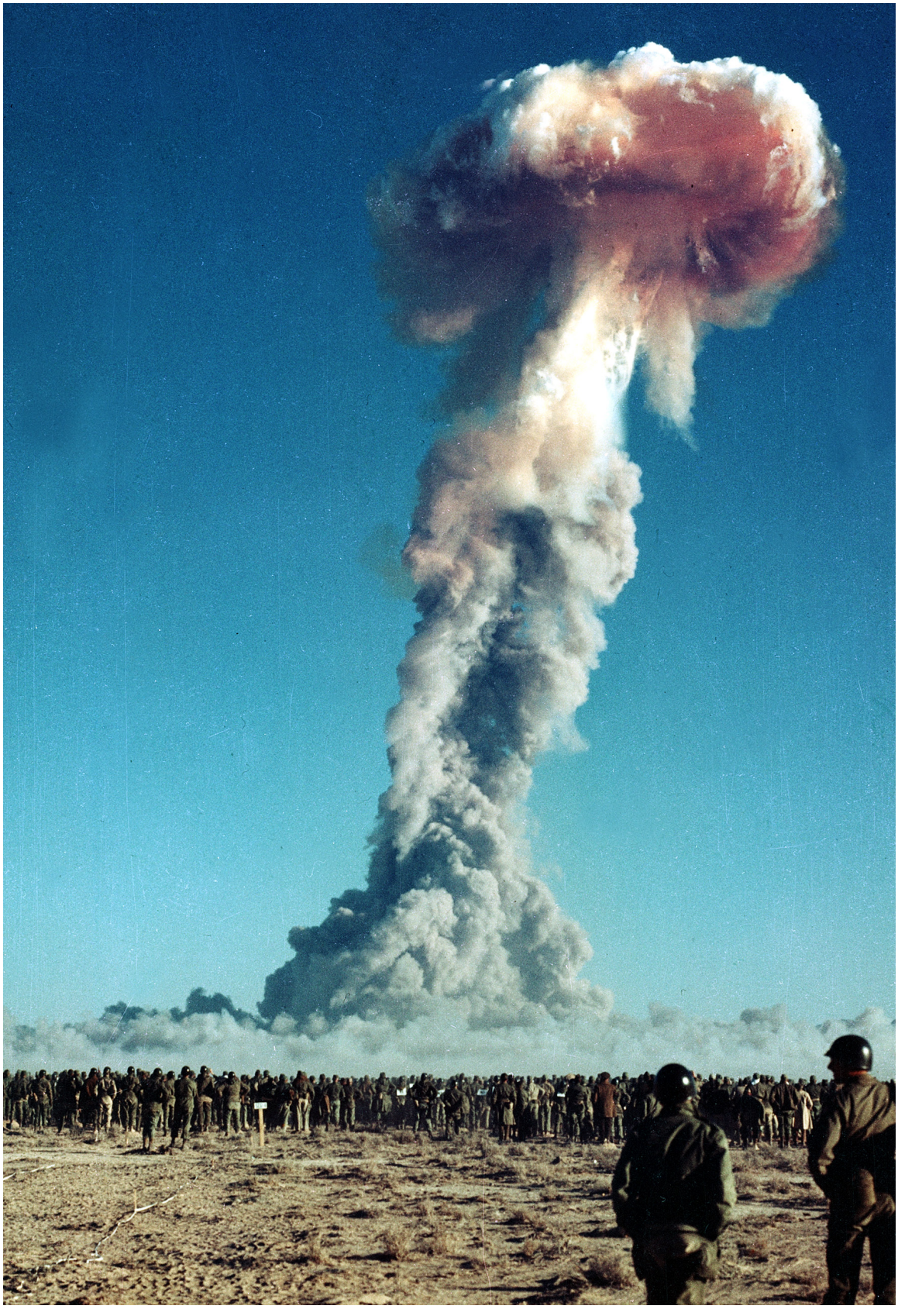

megatons (700 times as powerful as Little Boy) and vaporized the small island it was conducted on, leaving a 164-foot deep, 3,120-foot wide crater in the bottom of the ocean floor in its wake.[41] A patent exists recording Teller and Ulam's breakthrough idea. There is only one word in response to section (E) Results of Tests, and Extent of Use of Invention: "Satisfactory."[42] Fifteen days later, the second and final test of Ivy was fired: King. At 500 kilotons, King was the largest fission-only device the United States ever tested. Despite its immense yield, it was almost an afterthought following Mike.

On March 5, 1953, Joseph Stalin died after suffering a stroke, leading to a time of great uncertainty in the Soviet Union. Only days later, U.S. nuclear testing resumed with an 11-shot series in Nevada. Operation Upshot-Knothole was conducted to test new designs and improve civil defense measures. Additionally, thousands of soldiers participated in military exercises intended to improve tactics for nuclear warfighting. The series also featured Livermore's debut tests, Ruth and Ray. The devices were expected to produce less than a kiloton of yield, but, at only 200 tons each, they were disappointments.[43] The

Photo of IVY MIKE test courtesy of the U.S. Department of Energy. Operation IVY, conducted in 1952, was an atmospheric nuclear weapons test series held in the Pacific Proving Ground at Enewetak Atoll in the Marshall Islands. IVY consisted of two detonations: MIKE on 01 NOV (10.4MT) and KING on 16 NOV (500kT).

Ruth device failed to completely destroy the shot tower; according to a favorite old tale at both Livermore and Los Alamos, a senior leader from the latter institution called the former to inquire about the availability of the tower for future tests![44] Ray's uninspiring performance on April 11 produced unwelcome headlines. The front page of San Francisco's The Call Bulletin proclaimed, "ATOMIC BOMB MYSTERY TEST," with the subhead, "MUSHROOM' CLOUD FAILS TO APPEAR." Unfortunately, things would get worse for the AEC's newest weapons laboratory before they improved.

It has been estimated that the Upshot-Knothole tests produced about 50% of all radiation doses received by populations neighboring the test site during the era of testing.[45] The Harry test alone was responsible for about 50% of the dose produced by the series.[46] The preceding shot, Simon, produced so much contamination that Harry was postponed until cleanup could be completed. Ultimately, Harry was detonated atop a 300 feet tower at 5:00 o'clock in the morning on May 19. The 32-kiloton device produced a considerable amount of fallout, which, due to an unanticipated change in the wind, was carried directly to St. George, Utah. Highways were closed and the local population was sent indoors for a few hours, but large numbers of people and animals were subjected to high levels of radiation.[47] The infamous test eventually became known as "Dirty Harry," and provided an early catalyst for the test ban movement.

In the months leading up to Upshot-Knothole, Los Alamos and Picatinny Arsenal collaborated to produce the world's first artillery-delivered atomic weapons. In the days before missiles, an atomic cannon offered dependable accuracy in all weather conditions. In the event of severed

Upshot-Knothole-Grable (di991877) LA-UR-06-1068: Upshot–Knothole Grable was conducted by the Los Alamos Lab on May 25, 1953 at the Nevada Test Site. It was fired from a 280-millimeter cannon and produced a yield of 15 kilotons. Photo courtesy of Los Alamos National Laboratory.

communication lines, artillery gave commanders in the field the ability to quickly respond to surprise, large-scale attacks. Despite these advantages, and despite the incredible innovation that went into developing a warhead that could survive being launched from a gun, "Atomic Annie," as the system was dubbed, was not an ideal battlefield weapon. The 280-milimeter gun weighed nearly 50 tons and, though it was nimble for its size, was difficult to navigate through the narrow city streets of Europe and too heavy to trundle over the bridges of South Korea. Upshot-Knothole-Grable was one of the rare full-system tests in history. A Mark 9 atomic artillery shell was fired from Annie on May 25; it traveled seven miles and detonated just over 500 feet above the desert floor, unleashing a yield of 15 kilotons.[48] Grable's greatly refined descendants remained in the U.S. stockpile for decades thereafter.

Castle Bravo, March 1, 1954.
Photo courtesy of the U.S. Department of Energy.

A tense peace settled over the Korean peninsula in the weeks following Upshot-Knothole, as the Soviet Union quietly prepared to resume testing. Despite the disarray following Stalin's death, the USSR ended a 22-month testing hiatus on August 12, 1953. The Soviets tested a 400-kiloton air-deliverable thermonuclear device; an enormous shock to the West. The United States had no counter, as Mike was an undeliverable test device weighing tens of thousands of pounds. This prompted the Emergency Capability Program in the United States, which was an effort to weaponize a full-scale thermonuclear device quickly. The United States would fire only six shots in 1954, but the series, Operation Castle, became one of the most important in testing history.

Castle began on February 28 at Bikini. The first test, Bravo, produced a yield 1,000 times more powerful than Little Boy. It was the largest U.S. test ever conducted. Studies from Mike indicated fallout produced by high-yield tests could be mitigated with relative ease, and, in turn, planners for Bravo took a conservative approach to safety based on observations from Mike.[49] Unfortunately, only a few hours after Bravo, dangerous levels of fallout reached Bikini's neighboring atolls. Bravo carried surprisingly large particles into the stratosphere where they only remained briefly before plummeting back to earth. Hundreds of Marshallese Islanders and dozens of Americans were evacuated in Bravo's wake, but the evacuation did not prevent them from receiving significant exposures. A Japanese fishing vessel, ironically named Fortunate Dragon, was in the area of contamination; a member of the crew died upon returning to Japan.[50] At that point in time, most Americans continued to support nuclear testing and maintaining a large nuclear weapons stockpile. But Bravo, which unfolded less than nine months after "Dirty Harry," marked the beginning of a visible shift in public opinion.

The other Los Alamos Castle designs also performed well. In fact, John Richter, who would emerge as one of Los Alamos's premier weapons designers, wrote: "Castle results can be described as sensational."[51] But Livermore's third test, Castle Koon, was a complete failure. The despair induced by Ruth, Ray, and now Koon greatly demoralized Livermore's scientists, but Lawrence's encouragement helped the young staff through these growing pains.[52] The next year, in 1955's Operation Teapot, Livermore would finally find some measure of success. Meanwhile, there was despair at Los Alamos for an entirely different reason. Just weeks after Castle came to a close, the AEC announced J. Robert Oppenheimer's clearance had been terminated. At the height of the Red Scare, one of America's wartime heroes had been martyred in a humiliating fashion.

At 14 shots, Teapot would be the largest operation yet. Tests were performed for a variety of purposes, but the most important was to advance weapon design. Though the Castle weapons worked, they remained incredibly unwieldy. As such, there was a concerted effort to reduce the weight of early thermonuclear weapons; this started with reducing the weight of the primary. Boosting held the key, and therein lay the challenge: Could the yield of a very light primary be increased, by boosting, to the point it would successfully light a secondary? Los Alamos demonstrated it could by introducing the concept of hollow boosting: the process of injecting D-T gas into a void in the center of the device. There were weapons effects tests as well. Teapot ESS (Effects Sub-Surface), for instance, was a cratering experiment. The 1-kiloton device, which was placed 67 feet below the surface, produced

a crater nearly 300 feet wide and nearly 100 feet deep.[53] Apple-2, a 29-kiloton device fired on May 5, supported a large Civil Defense exercise known as Operation Cue. With the U.S. nuclear monopoly a distant memory, the military began exploring the survivability of civilian assets in the event of nuclear war in operations such as Cue.

That fall, a series of very low-yield safety tests was performed as part of Project 56 in Nevada. These important Los Alamos tests were conducted to assess the one-point safety of the new weapons entering stockpile; one-point safety being: "The nuclear safety design principle that states that the probability of achieving a nuclear yield greater than 4 pounds of TNT equivalent in the event of a one-point initiation of the main charge high explosive must not exceed one in a million."[54] It was essential to validate the safety of the lighter new primaries that would be used in the nation's second generation hydrogen bombs. Those bombs would be tested in the Pacific as part of Operation Redwing, which began in May 1956.

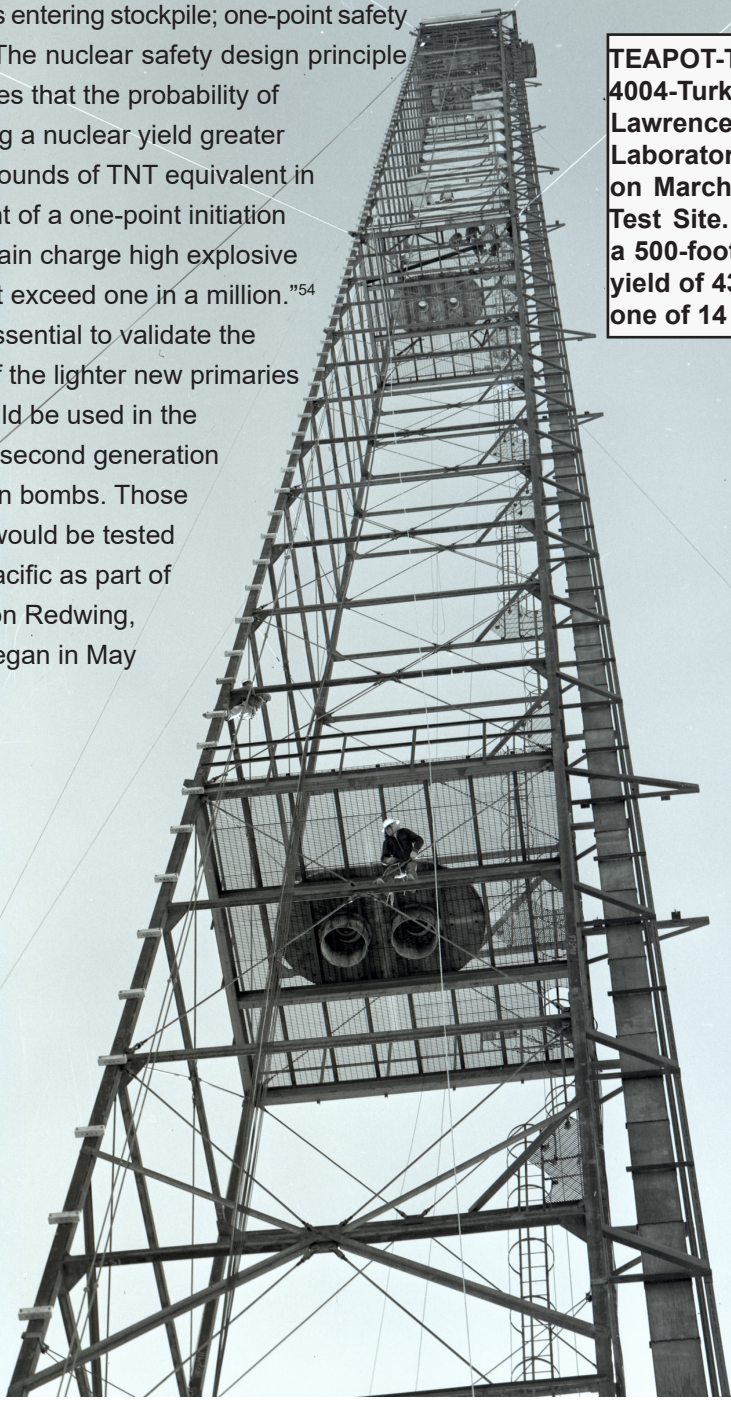

TEAPOT-Turk Tower (LLNL photo 4004-Turk-Tower-1-17-55): This Lawrence Livermore National Laboratory test was conducted on March 7, 1955 at the Nevada Test Site. It was detonated from a 500-foot tower and produced a yield of 43 kilotons. The test was one of 14 in the series.

Redwing began with a very expensive and highly instrumented test called Lacrosse on May 4, but it was the second test in the series that made headlines. Redwing-Cherokee was the first airdrop of a U.S. thermonuclear weapon, prompting headlines such as, "USE OF BOMBER TO UNLEASH BIG BLAST SUCCESS: Explosion Five Times More Destructive Than All Missiles Dropped in World War II; Crew Is Safe."[55] At 3.8 megatons, Cherokee was certainly an impressive sight to behold, but the crew of the plane may not have been as safe as advertised. The crew missed the target by approximately five miles due to "human error."[56] According to an old testing legend, Major General Curtis LeMay, Commander of Strategic Air Command, told the bomber crew to just keep on flying and not come back.[57] Redwing's 17 tests featured innovative ideas from both Los Alamos and Livermore, and demonstrated to the Soviet Union that the United States could effectively put multi-megaton weapons into combat.

By 1957, the United States had 5,543 weapons in the stockpile. That year's test series, Operation Plumbbob, would include 30 tests performed beginning in April and running into October. Public concerns pertaining to fallout coupled with President Eisenhower's interest in limiting (and eventually banning) nuclear testing made it look as if Plumbbob might be the final atmospheric series. Counted among Plumbbob's shots were several safety tests, the first true underground test (Pascal A, performed by Los Alamos), and the largest atmospheric test Nevada would ever host (Livermore's Hood test; 74 kilotons).[58] In addition to the now-traditional tower test, 13 devices were suspended from balloons and detonated.[59] Plumbbob also featured the test of an air-to-air rocket on July 19. The rocket included a W25 warhead that was fired from an F89J fighter in the John test. The warhead produced a yield of about 2 kilotons and detonated nearly 15,000 feet above the dessert floor, where five soldiers looked on in an effort to prove that civilian populations on the ground would be safe from nuclear air defenses.[60] Seconds after the explosion, as the shockwave reached the ground, one of the observers said, "It is over folks...It is tremendous, directly above our heads. It worked! It worked!"[61] On September 9, Livermore performed the first successfully contained underground test (UGT): Rainier. This innovative experiment would provide a basic template for future UGTs. In October, three days before Plumbbob concluded, the Soviet Union successfully launched the first man-made satellite to orbit Earth: Sputnik.

As the '50s progressed, the Bomber Gap gave way to the Missile Gap, an almost entirely unjustified assertion that the Soviets would soon have a vastly superior arsenal of missiles. Eisenhower concealed his skepticism of the gap from the public, as he hoped to negotiate a moratorium on nuclear testing with the Soviet Union. Nonetheless, testing moved forward. Los Alamos closed out 1957 with two safety tests in Nevada; Livermore conducted two more in early 1958. At the same time, both laboratories made plans for an enormous series in the Pacific dubbed Operation Hardtack. But one month before Hardtack commenced, First Secretary Nikita Khrushchev announced the Soviet Union, which had already completed 13 tests in 1958, would enter a unilateral testing moratorium; he advised Western leaders to stop testing as well.[62] They didn't.

Between April 28 and August 18 (113 days), the United States detonated 35 devices. Hardtack commenced with a test called Yucca, part of a subset of DoD-sponsored high-altitude tests called Newsreel. The 1.7-kiloton Yucca device

was attached to an untethered balloon and detonated at 86,000 feet. Highlights from Hardtack included two underwater tests, Wahoo and Umbrella, detonated at 500 feet and 150 feet below the surface, respectively. Hardtack included eight shots that produced at least a megaton of yield, the two most powerful of which being a Los Alamos test, Oak (8.9 megatons), and a Livermore test, Poplar (9.3 megatons). Toward the end of the series, two more Newsreel tests were performed by Los Alamos: Teak and Orange. Carried by rockets to heights of 77 kilometers and 43 kilometers, these tests produced critical data on Electromagnetic Pulse (EMP). The pulse produced by Teak greatly disrupted radio communications throughout much of the Pacific, forcing the delay of civilian air travel for hours.[63]

On August 22, President Eisenhower sent a letter to Norris Bradbury: "I am today announcing that the United States will suspend nuclear weapons tests for a period of twelve months and, under certain conditions of progress toward real disarmament, continue that suspension on a year-to-year basis."[64] This left the design laboratories in somewhat of a bind. The tests of the mid-50s had revolutionized weapons design. In 1958 alone, 12 new weapons-types entered the stockpile; in 1959, nine more would join them. These lighter, boosted weapons were highly advanced, but not thoroughly tested. Fortunately, the United States would not enter the moratorium until the end of October, so testing continued.

August 27 was a bittersweet day in weapons history. Ernest Lawrence, who had played the lead role in creating the laboratory at Livermore, sadly died following surgery for intestinal problems; he had recently turned 57. That day also included the first test of Operation Argus, a three-shot series in the South Atlantic. The Argus devices were fired by rocket and detonated at approximately 300 miles above the surface. The objective of the tests was to determine if electrons introduced into the earth's magnetic field would create an artificial shell, similar to the Van Allen Belts, which would interfere with communications equipment.[65] When the operation was made public the following year, a newsreel proclaimed: "…it was a major breakthrough both for purely theoretical science and for military planners, hinting the possibility of throwing up a shield of radiation as a part of an anti-missile defense."[66]

The final series heading into the moratorium was initially called Millrace, but, according to Los Alamos Test Director Bill Ogle, the name was changed to Hardtack Phase II "for political reasons."[67] Conducted in Nevada, Hardtack II saw 37 tests performed in 49 days beginning on September 12. Looking ahead, Livermore scientists recognized there would be little political support for a return to testing in the atmosphere and, as such, focused on developing techniques for successfully containing UGTs. Livermore performed UGTs in hillside tunnels; Los Alamos chose to detonate devices in vertical shafts, which would ultimately become the preferred underground testing method.

A complete and permanent ban on testing had eluded policymakers in large part because reliable methods of detecting UGTs did not exist; Hardtack II tests would be used to explore possible detection methods. Nearly half the shots were considered safety tests, prompting a member of the operation to write:

Here's to Operation Hardtack
The phase in the early fall
When the safety tests went nuclear
And the nuclear tests went small[68]

The Soviets, seeking to collect as much data as possible before the moratorium, resumed testing on September 30 with a 1.2-megaton atmospheric test at the Semipalatinsk test site in Kazakhstan. A month later, the United States completed Hardtack II by conducting four tests on October 30, just before the moratorium went into effect on November 1. The Soviets, however, did not complete their 21-shot series until November 3, adding tension to an already very anxious situation.[69] As testing operations ceased, the USSR, the United States, and United Kingdom (which had independently become a nuclear power in 1952) would attempt the unprecedented: maintenance of nuclear stockpiles without full-scale nuclear testing.[70]

Though the AEC was expected to maintain the capability to resume testing with 90-days' notice, budget restrictions led to immediate layoffs at NTS.[71] The Hardtack II tests provided data relevant to assessing the one-point safety of the innovative new weapons entering stockpile, but unanticipated problems emerged; problems that could only be resolved by field testing. With no hope of a quick resumption of full-scale testing, the AEC secretly allowed Los Alamos to perform hydronuclear tests on Laboratory property. Hydronuclear experiments, which Livermore had pioneered in the earlier part of the decade, used test devices with greatly reduced amounts of fissile material. Although such tests can produce nuclear yield, the fission yield remains below the yield of the test device's high explosives.[72] Eisenhower personally approved the hydronuclear experiments, which began in January 1960, but a very small number of scientists believed the tests violated the spirit of the testing moratorium. Physicist John Malik, for instance, refused to participate; he temporarily lost his health and permanently lost friends as a result.[73] Nonetheless, dozens of tests were secretly performed at Los Alamos, the largest being a June 1961 experiment that produced four-tenths of a pound of fission energy.[74]

The results of the hydronuclear experiments led to important design changes, but the tests were not definitive. As the moratorium continued, Los Alamos and Livermore debated the ease, usefulness, and costs of underground testing, should the opportunity arise to resume. Bradbury remained highly skeptical of the sanguine promises coming out of California. In fact, to demonstrate his frustration, the Los Alamos director quoted a passage from Alice through the Looking Glass in a classified telegram to General Alfred Starbird, director of Military Applications for the AEC. The passage concluded with the Queen telling Alice, "Why, sometimes I've believed as many as six impossible things before breakfast."[75] Despite the legitimacy of Bradbury's concerns, the Livermore scientists rightly recognized that if full-scale testing had a sustainable future, it lay below the surface.

Halting tests did not translate into a halt in weapons production. In both 1959 and 1960, the United States manufactured over 7,000 weapons pits at Rocky Flats. The moratorium continued through 1960, but not without political challenges. France independently performed its first nuclear test in February. Although France had not agreed to the moratorium, this test by a Western power riled the Soviets. In May, a U.S. spy plane was shot down over the Soviet Union; the pilot, Gary Powers, was captured and tried for espionage in Moscow. This episode killed any prospect of a negotiated test ban. By the end of the year, Eisenhower had concluded the Soviets had no interest in a test ban anyway, but chose not to preemptively return to testing in the final months of his administration; he did not want to "tie the hands" of his successor.[76] In early 1961, John F.

Kennedy became president and almost immediately faced trial by fire. Only weeks after test ban negotiations finally resumed in Geneva, the Bay of Pigs fiasco unraveled in Cuba. France's fourth nuclear test, conducted on April 25, only exacerbated already feverish tensions.

A growing number of insiders believed the Soviet Union would resume testing soon. There was no hard evidence that the USSR was about resume, but according to a CIA intelligence estimate there were "numerous indications which arouse strong suspicion."[77] Back at Los Alamos, in May, Bradbury assured the AEC: "We are doing everything we can to get ready for testing short of getting ready for testing in Nevada!"[78] Large operations in Nevada would have likely been detected, so Bradbury quietly prepared his Laboratory to resume testing if called upon. The debate on how to test had ended. For political reasons, the United States would remain underground if a resumption was ordered. However, a resumption was not ordered, and tensions cooled as the summer progressed. The lull, however, was short-lived.

On August 28, about two weeks after the Berlin Wall started going up, Kennedy received a bulletin claiming the Soviet resumption of testing was imminent. The President's Special Advisor, Arthur M. Schlesinger, recalls Kennedy, "read the bulletin, grimaced and said bitterly: 'Bitched again.'"[79] On August 30, the Soviets formally announced they would begin testing immediately; among other things, they cited the French nuclear tests as one of the reasons for the decision. Then, it happened. The chairman of the Joint Atomic Energy Intelligence Committee reported, "An explosion has been detected as having occurred in the atmosphere at 0700 hours + - 10 minutes Zebra, 1 September 1961." Even Hans Bethe, the imperturbable leader of the wartime Theoretical Division at Los Alamos, said, "I believe that the USSR showed bad faith. It is very likely that they had started specific preparations by March of 1961 when the test ban conference reconvened in Geneva. Therefore, they negotiated for at least six months in bad faith."[80] He went on to add, "We do not need to look far afield for reasons why the Russians resumed testing. They knew as well as we did that they were technically behind in 1958."[81] The numbers alone make it quite clear the Soviet Union had been preparing to test for months, if not years. Between September 1 and November 4 (65 days) the USSR conducted 59 tests, unleashing 86,430 kilotons of energy.[82]

It took two weeks for testing to resume in the United States. According to future Livermore Director Johnny Foster, the resumption was "technically agonizing, operationally painful, and economically very costly."[83] The first shot coming out of the moratorium was a 2.6-kiloton underground test in Nevada performed by Livermore on September 15. Called Antler, it was the first of Operation Nougat's 45 tests and it accidentally vented radioactive steam. Back in February, Bradbury had reaffirmed his concerns regarding underground testing. "I tend to disagree somewhat with the commonly expressed opinion from Livermore that everything can be done as well (or better) in underground testing as it could have in the air," he said, continuing, "This seems to me a very dubious extension of the rather diffident and ambiguous results from two or three underground experiments…"[84] His concerns were not misplaced. The next day, Los Alamos performed a test called Shrew, which also resulted in an accidental release. In fact, all 10 U.S. tests performed in 1961 accidentally released radioactive material into the atmosphere.

Shortly thereafter, in January 1962, a young Public Health Service officer named Chuck Costa arrived in Nevada. "I drove out to Yucca Flat at night and stopped on CP [Control Point] hill. I saw throughout Yucca valley a city of lights as there were probably 30 drill rigs drilling emplacement holes around the clock!"[85] In 1992, Costa became the Los Alamos test director. Meanwhile, testing surged forward in the Soviet Union. After a nearly three-month hiatus, the Soviets resumed testing on February 2. In 1962, the Soviets performed 79 tests cumulatively producing a staggering 133,830 megatons of energy.[86]

Hard lessons were learned during Nougat, which ran through June 1962. The United States focused on containing UGTs, refining smaller primaries, and ensuring their safety. Tests of this nature did not require large yields, but meanwhile the Soviets continued to detonate enormous weapons in the atmosphere for both scientific and political purposes. The largest nuclear blast of all time was unleashed on October 30 west of the Novaya Zemlya test site in the Arctic Ocean. The Tsar Bomba produced a yield of 50 megatons, a blast more than three times as powerful as Bravo. The subheading of The New York Times' front-page article stated, "Test Denounced: White House Asserts Purpose Is to Incite Fear and Panic."[87] As a direct result, President Kennedy publicly announced the United States would begin preparing to resume atmospheric testing. Should the resumption order ever come, Kennedy insisted on a quick series with a minimal number of tests, confiding to his advisors, "We want to do as little as possible to prolong the agony."[88]

The Tsar Bomba test was primarily motivated by politics, but there were scientific aspects to the Soviet atmospheric tests as well. It was greatly feared the Soviets were rapidly advancing their knowledge of EMP and, in doing so, learning to destroy critical American targets (e.g., communication centers, missile defense systems, etc.) as they learned how to harden their own. A February 1962 Department of Defense Position Paper argued, "High altitude nuclear bursts produce widespread and long-lived disruption of certain radio communication systems. Considerations of command and control demand that we understand the magnitudes of the effects…"[89] The United States had maintained the moral high ground by keeping tests underneath it, but technical necessity forced Kennedy to resume atmospheric testing. On March 2, he gave a public speech announcing that the United States would return to testing in the atmosphere at the end of April. The president, with backing from British Prime Minister Harold McMillan, offered a plan for a comprehensive test ban in lieu of a resumption, but it was not to be; Khrushchev promptly rejected the overture. Unfortunately, these desperate actions would help lead to perhaps the single-most dangerous epoch in human history that November. First, however, as Nougat continued, the United States would return to the Pacific for one final series in the atmosphere: Dominic.

Operation Dominic, which was initially conducted near Christmas Island with British concurrence, began on April 25 with a 190-kiloton Los Alamos airdrop called Adobe. The resumption of U.S. atmospheric testing proved no trivial matter. Bill Ogle appeared on the cover of the May 4 issue of TIME magazine. Inside, the feature article ominously described Dominic as, "the U.S. series of nuclear tests in the atmosphere that the free world did not want, but for its survival's sake could not avoid."[90] Two days later, Livermore performed a unique and remarkable test called Frigate Bird. A Polaris missile equipped

with a W47 warhead launched from the USS Ethan Allen and traveled more than a thousand miles before detonating 11,000 feet above the ocean. As Livermore historian Tom Ramos notes, "It was a historic moment. This Frigate Bird event was the first and only fully operational test of a nuclear tipped strategic missile system."[91] After a challenging start, Livermore was clearly entering an era marked by incredible creativity and success.

A few days later, on May 11, Los Alamos demonstrated an additional nuclear capability in the Swordfish event. In the test, an antisubmarine rocket (ASROC) armed with a W44 was fired from the USS AGERHOLM. After travelling over 4,000 yards, the warhead successfully detonated. Though some of the diagnostics failed, important effects information was gathered.[92] These innovative new weapons would give the president new and important capabilities in the arduous days that lay ahead.

Learning to contain UGTs proved far more formidable than early proponents imagined, but significant progress was made quickly as Nougat continued alongside Dominic. There were, of course, setbacks. Twenty-six of Nougat's 45 tests suffered an accidental release of radioactive material, including 17 of the first 21 tests. One of the more dramatic containment failures occurred toward the end of the series on June 13. When the containment broke for a 2.9-kiloton Livermore tunnel shot called Des Moines, "The test vented out of the tunnel mouth with sufficient pressure and flow rate that the radioactive debris was projected entirely across the canyon and deposited on the slope behind a trailer shelter."[93] The cloud traveled to the northeast, where Costa had prepared monitoring equipment 10 miles away. Lacking protective equipment, he asked his supervisor for permission to leave the area. When his request was denied, Costa relates: "I therefore placed a large plastic bag over my head and continued with my monitoring duties. I took a shower that evening at a motel in Tonopah."[94] On June 20, iodine milk contamination was measured at 1,200 picocuries per liter in Spokane, Washington.[95] Nonetheless, the Nougat tests produced a basic formula for safely conducting UGTs that would be refined in the years ahead.

As Dominic continued in the Pacific, Nougat came to a close on June 30 in Nevada. Nonetheless, a new series began almost immediately: Operation Storax. The first Storax test was a Livermore shot called Sedan, but it was not a weapons test. Sedan was conducted as part of the AEC's Plowshare Program, which explored peaceful uses for atomic energy. Sedan, being an excavation experiment, produced the test site's most striking landmark: a 1,280-foot wide, 320-foot deep crater.

Storax and Dominic each included notable DoD-sponsored subsets: Operations Sunbeam and Fishbowl, respectively. Sunbeam's four shots included two tests of the Los Alamos-designed W54 Davy Crocket battlefield weapon. In each test, Little Feller I and Little Feller II, the low-yield weapon was fired from a recoilless rifle. Little Feller I was delayed multiples times, in hopes that President Kennedy would be able to attend; because of these delays, Little Feller II was fired first on July 7. Finally, on July 17, Little Feller I was fired. The president did not attend, but his younger brother Robert, the U.S. attorney general, did. Robert Kennedy, National Security Advisor Maxwell Taylor, and thousands of soldiers witnessed what proved to be the final atmospheric test conducted in Nevada.[96]

Operation Fishbowl commenced on July 9 with a 1.4 megaton Los Alamos burst detonated 250 miles above the Pacific near Johnston Island. The test, codenamed Starfish Prime, produced incredible auroral effects as the ionized fission fragments streamed along magnetic field lines and collided with the atmosphere.[97] John Hopkins, the future leader of the Los Alamos Field Testing Division, witnessed the test's aftermath in Hawaii: "At zero time, the sky instantly turned as bright as a noonday sun, with a thin overcast. After a few seconds, I realized that it was not just a flash but that the brightness was staying…Soon the most fantastic aurora display started over the whole sky…The display was red, white, blue, and every color within that spectrum. It went on and on for well over an hour."[98]

Although Dominic, which had shifted to the Johnston Island area, and Storax continued into the fall, the pace of testing temporarily slowed after a busy summer. But in October, everything changed. Over the course of 1961 and 1962, 15 new weapons types entered the stockpile; in 1962, the United States had 25,540 nuclear weapons. However, the Soviet Union now had thousands of weapons as well, including some earmarked for Cuba. On October 14, aerial reconnaissance confirmed the existence of missile sites under construction in the socialist island nation. After much internal debate, President Kennedy instituted a naval quarantine of Cuba on the 22nd. Over the next two days, nuclear war appeared imminent. Fortunately, Kennedy and Khrushchev made a bargain: In exchange for the removal of Soviet missiles from Cuba, the United States would publicly promise not to invade Cuba and secretly remove missiles from Turkey. The crisis subsided the morning of the 28th when Khrushchev announced the missiles in Cuba would be removed.

Throughout the Cuban Missile Crisis, testing continued in both nations. The United States performed seven tests during the 13-day ordeal; the USSR performed seven as well, including three on the 28th. The first test after tensions subsided was a massive 8.3 megaton Livermore airdrop called Housatonic. The blast produced a seiche, a phenomenon similar to a tsunami, which flooded the coast of Hawaii and caused approximately $100,000 in damages.[99] Los Alamos, which had ushered in the era of U.S. atmospheric testing, would close it out as well. The final Fishbowl test, Tightrope, was fired near Johnston Island on November 4: It was the last above ground yield-producing test the United States would perform. In 1962 alone, the United States conducted 96 tests. After Cuba, the Soviet Union performed 33 tests in 58 days, including four on December 23 and four more on the 24th. On the 25th, the Soviets conducted two airdrops; the second was the final Soviet atmospheric weapons test. The USSR would not perform another nuclear test until March 1964. Storax finally concluded on June 25, 1963, nearly a year to the day after it started. Including its two subsets, Operation Sunbeam and a joint Los Alamos-DoD-U.K. set of zero yield safety tests called Operation Roller Coaster, the series included 56 shots.[100]

For months, the relationship between the United States and Soviet Union remained tepid as diplomats hoped to reignite test ban discussions. President Kennedy chose to try and break the impasse on June 10. During his commencement remarks at American University, he said: "So let us not be blind to our differences, but let us also direct attention to our common interests; and the means by which those differences can be resolved. And if we cannot end now our differences, at least we can help make the world safe for diversity." As a tangible step forward, Kennedy pledged to keep U.S.

testing underground unless another country tested in the atmosphere first.[101] Even the Soviet Union's turgid first secretary reportedly stated it was "the greatest speech by any American president since Roosevelt."[102]

In response to Kennedy's speech, Khrushchev proposed a limited test ban in early July. By the end of the month, the president's team of negotiators had worked with the Soviets to craft an agreement in Moscow prohibiting nuclear tests in the atmosphere, underwater, and in space. On August 5, the Limited (or Partial) Test Ban Treaty (LTBT) was signed in the Soviet capital. After the Senate ratified the treaty by a wide margin in September, President Kennedy signed the LTBT into law on October 7; it went into effect October 10. Tragically, President Kennedy was assassinated six weeks later on November 22. A new technology, largely pioneered by Los Alamos, helped make the agreement possible – satellites designed to hunt for clandestine nuclear tests. This program, codenamed Vela (short for El Velador, which is Spanish for The Watchman), launched its first volley of satellites one week after the LTBT went into effect. Had it not been for the Vela Program, it is reasonable to conclude efforts to ratify the LTBT would have been greatly hindered and perhaps even abandoned.

While test ban negotiations had proceeded in the late summer, a new series began: Niblick. This time, however, there would be no colorful mushroom clouds or ethereal nuclear blasts in space. Niblick did have memorable moments, such as the 249-kiloton Bilby test on September 13 that was felt in Las Vegas. It also included a dubious Los Alamos "leaker," Pike, the following March. A higher yield than expected, a shallow hole, and a layer of alluvium lacking cohesive strength all conspired to produce the mishap.[103]

Going into Niblick, the United States had performed 331 of the 1,054 nuclear tests it would ever undertake. From the fall of 1963 onward, U.S. testing would remain underground. Although the famous, photogenic tests in the atmosphere continue to amaze generations after they first appeared, approximately 80 percent of all U.S. nuclear tests were conducted underground. The yields of a vast majority of these tests remain classified, as these were the tests that produced the modern stockpile. Their technical stories largely remain secret, but many of the innovations that were pioneered during the period of underground nuclear testing are not. For instance, the laboratories greatly miniaturized warheads, and hardened them to increase survivability when under attack. Los Alamos pioneered the development of insensitive high explosives, and was the first laboratory to successfully test and field such compounds in nuclear weapons. Underground testing directly led to advances in design that made weapons lighter, more accurate, more versatile, more robust, and much safer.

Although nearly all U.S. nuclear tests were conducted in either Nevada or the Pacific, there were some exceptions. For instance, New Mexico hosted two more tests in addition to Trinity: Gasbuggy and Gnome. Each was a Livermore Plowshare event. Perhaps the most interesting objective of Gnome, which was fired in December of 1961 as part of Nougat, was to determine if the surrounding salt beds would retain the heat of the blast. It was hoped the trapped heat could gradually be harvested in the form of steam, which could then be converted to electricity. Unfortunately, the blast broke containment and vented; additionally, the heat reservoir failed to materialize. Notably, however, the device produced an underground cavity that scientists entered five months after the test.[104] Gasbuggy followed in 1967, the same year the United States

reached the numerical peak of the stockpile: 31,255 weapons. It was hoped the device would free-up natural gas trapped far below the surface so that it could be more easily collected -- essentially fracking with a nuclear device. Though the experiment failed to impress, similar Plowshare tests were performed in Colorado years later; but again with underwhelming results.[105]

Tests were also performed in Mississippi and Alaska. Both shots in the Magnolia State pertained to underground test monitoring; the 1966 Sterling test was performed in the cavity created by the 1964 Salmon event. Two of the three tests in Alaska also pertained to test detection: Long Shot (1965) and Millrow (1969). The final shot performed in Alaska, Cannikin (1971), was a proof test of Livermore's W71 warhead; it was also the largest U.S. UGT ever conducted.[106] The weather leading up to the shot was dreadful, as Test Director Phil Coyle recalls: "It was at the control point that I watched the storm front move through, the sharpest storm front I've ever seen. On one side of the front, the storm was raging; on the other side of the front the sky was blue and the sun was shining. And chugging along behind that front as it moved down the length of Amchitka, was a Russian trawler, bristling with antennas to capture signals from the test." AEC Chair James R. Schlesinger attended the test along with his family, to help assuage fears that Cannikin might be unsafe. He won a wager with Coyle: The Test Director bet on Cannikin being postponed, and, because it was not, Schlesinger won the opportunity to give Coyle a haircut. Schlesinger's daughter offered to intervene on Coyle's behalf but, like the test, the haircut proceeded as scheduled.[107]

Over time, nuclear testing became increasingly controversial. With the memory of Stalin fading into the past, the United States and USSR signed many treaties to help ease tensions. New priorities, such as arms control and environmental protection, very gradually supplanted fears of violent Soviet expansion. Cannikin had multiple political consequences. Coyle relates, "The success of Cannikin caused Russia to agree to the Anti-Ballistic Missile Treaty;" it also "caused Greenpeace to be created from the coalition of anti-nuclear groups that opposed the test."[108] Of course, Cannikin certainly wasn't the first controversial test. Atmospheric tests had once attracted curious tourists to Las Vegas, but some of the city's denizens had grown weary of nuclear devices being detonated just over an hour's drive from home. The most notable protest of the era came from Howard Hughes, the enigmatic millionaire who had purchased the Desert Inn Hotel on South Las Vegas Boulevard in 1967.

On January 19, 1968, Livermore performed a test in central Nevada near Warm Springs, approximately 200 miles north/northwest of Las Vegas. The shot, called Faultless, dropped the earth in the surrounding area several feet; though the shock was felt over a wide area, the test did not produce any notable damage to private property. Hughes, who had already expressed his qualms pertaining to testing, was likely further startled by post-Faultless headlines in local papers such as "Giant A-Blast Rocks Nevada" and "Earth Crust Split Open."[109] Thus, he became more aggressive in his attempts to lobby the AEC and politicians to postpone the upcoming Boxcar shot at the Test Site. He personally called the governor of Nevada on February 8, who in turn called the AEC's area manager in Nevada, James Reeves, to inquire if all testing could be moved to Alaska.[110] On April 25, the day before Boxcar, one of Hughes's personal assistants, Robert Maheu, called Reeves to discuss the possibility

of a postponement, but to no avail. Deprived of sleep in the hours leading up to Boxcar, the reclusive tycoon told Maheu he would send a short message of protest to President Johnson, but the operation proceeded nonetheless.[111] At 1.3 megatons, Boxcar was the largest test ever performed at the test site. No Las Vegas hotels were harmed in the testing of the device.

The Soviet Union detonated 21 devices in 1970 and continued to steadily increase the number of weapons in its stockpile. Conversely, the much larger U.S. stockpile contracted to 26,008 weapons that year, but 60 devices were tested. Unfortunately, the year ended with one of the more significant disasters in the history of testing. On the afternoon of December 18, Livermore performed a test called Baneberry in Nevada. The 912-foot vertical shaft for the test was drilled, with great difficulty, in saturated clay rather than the alluvium that hosted most UGTs. Making things worse, the saturated clay sat adjacent to a fault. Costa remembers when Baneberry was fired: "The shot went off and all looked normal for the first few minutes. I remember commenting to my team that it looks like we'll enjoy a normal Christmas. At about H+3 minutes, all hell broke loose."[112] John Rambo, a Livermore physicist, explains what happened: "So, you've got this motion along the fault, plus an almost plane wave rarefaction that comes back, and you get a lot of tensile failure around the cavity in this weak material."[113] Baneberry's underground cavity predictably collapsed, but the radioactive effluent escaped through fractures produced by ground shift. Residue quickly vented out of the ground, forming a large plume that resembled the mushroom clouds from the days of atmospheric testing. Even 20 hours after the test, vapor could still be seen escaping from the ground.[114]

The Baneberry debacle unfolded due to a set of unique circumstances that never reoccurred. However, the experience did result in significant changes. Perhaps most notably, a panel was created with members from various stakeholder organizations to review the containment plans for each subsequent test. After Baneberry, nearly 400 more tests were performed. There were only 11 accidental releases and they were all relatively small. Of those, only four resulted in an uncontrolled release due to a containment failure.

In the early 1970s, the United States and the Soviet Union deployed anti-ballistic missile defenses (ABMs). The laboratories designed and tested warheads for use on the Sprint and Spartan missiles, which were intended to defend against the threat of incoming Soviet strategic nuclear weapons. However, the U.S. ABM system was canceled almost immediately after it was deployed in 1975. Mark Chadwick, an Associate Director at Los Alamos, relates: "It was expensive and its efficacy was unclear. And the U.S. and Russia had independently developed a new technology to overcome missile defenses: the MIRV (Multiple Independent Reentry Vehicle)." In a MIRV system, one missile can carry several warheads into space; the warheads can then be deployed independently and with great accuracy against multiple enemy targets. As Chadwick concludes, "Field testing enabled the laboratories to design increasingly compact, powerful and accurate MIRV warheads for this critical mission."[115]

As testing continued at Nevada, the United States and Soviet Union continued to craft arms control treaties in hopes of further improving relations. One such agreement was the Threshold Test Ban Treaty (TTBT), which was completed in the summer of 1974. The TTBT limited underground tests to a design yield of 150

kilotons, but there was a significant problem: The technology did not exist to enforce the treaty. The United States and USSR observed the treaty in the years that followed, but it would not enter into force until the final years of the Cold War. In the interim, the U.S. stockpile continued to shrink and the Soviet stockpile continued to grow. In 1978, the Soviets surpassed the United States in number of weapons; it is estimated that the USSR had approximately 45,000 weapons by 1986. That same year, the United States only conducted 21 tests. It was the last year the United States would perform more than 20.[116]

As the 1980s progressed, relations with the Soviet Union improved dramatically. In fact, several months after the Chernobyl disaster of April 1986, President Ronald Reagan and General Secretary Mikhail Gorbachev met in Reykjavik, Iceland, to discuss a plan for abolishing nuclear weapons. Although the two leaders did not reach an agreement, the October 1986 summit was a clear indication of how much the Cold War had changed.

Two years later, in 1988, a similarly unlikely summit of sorts, known as the Joint Verification Experiment (JVE), unfolded. Unbelievably, Soviet scientists were invited to measure the yield of the Kearsarge test in Nevada on August 17 and American scientists were invited to measure a Soviet test, Chagan, at Semipalatinsk the next month. Neither test exceeded the 150-kiloton limit called for in the TTBT, which had been observed for years, but never ratified. To ensure the historic effort was remembered, Los Alamos filmmakers produced a documentary chronicling the JVE called Trust, But Verify. Legendary Academy Award-winning actor Charlton Heston, who had held a Department of Energy (DOE) clearance since 1983, hosted the program. Heston, a veteran of the Pacific Theater in World War II, never accepted pay for Trust, But Verify or any of his other DOE films; he once mused, "Perhaps my son lives because we bombed Hiroshima, 10 years before he was born."[117]

During the JVE exchanges, American scientists made many memories as they built relationships with their Soviet counterparts. Gy Allen, a DOE team leader, recalls taking his Soviet guests to a Las Vegas supermarket during their visit. They were overwhelmed by the quantity and variety of American goods. "They felt like... this was a Potemkin village for our grocery store; that this was not really the way we lived. We were just trying to impress them." One of Allen's colleagues responded to the Soviets: "Ok, here's a telephone directory: you choose a store and we'll go there."[118] In reflecting on his JVE experiences, the leader of the Soviet team, Victor Mikhailov, recalls: "I have always dreamed of seeing... U.S. experts at the Nevada Test Site and I can tell you they are excellent experts, very friendly, very warm people. We have cut a window into their heart." He continued, "I am certain that the main result of the JVE was not the development of procedures or the extent of nuclear test monitoring or the joint development of technical verification means, but the chance for interpersonal communications with the American nuclear physicists."[119] There was another significant result as well – after awaiting signatures since 1974, the TTBT was finally ratified and entered force on December 11, 1990.

In 1988, the Soviet Union detonated 27 nuclear devices in weapons-related tests. This show of strength was the real "Potemkin village," in that the USSR was rapidly rotting from the inside out. The Soviet economic system was congenitally flawed and increasingly weak; the government was thoroughly corrupt. The Kremlin recognized these problems and responded by

instituting the reform policies of Glasnost and Perestroika, but these relatively liberal policies only seemed to fan the flames of discontent in the nations under Soviet rule. Meanwhile, the United States applied unceasing political, economic, and military pressure to the floundering socialist dictatorship. Throughout 1989, demands for reform swept through the Eastern Bloc: Poland, Hungary, Latvia, Lithuania, Estonia, Czechoslovakia and, that fall, Germany. After the Berlin Wall came down in November, the Soviet Union would only perform one more nuclear test: eight devices were fired in a final, simultaneous salvo experiment on October 24, 1990, at Novaya Zemlya.

In the United States, Operation Julin commenced on October 18, 1991 with a test called Lubbock. Only two months later, at the end of December, the Soviet Union formally dissolved. With the Cold War over, weapons systems currently in development in the United States were quickly canceled, but testing continued in 1992. Julin's final shot, a Los Alamos test to ensure the reliability of the U.S. nuclear deterrent dubbed Divider, was fired the morning of September 23. The United States has not performed a full-scale nuclear test since. On October 2, President George H.W. Bush signed a law including a provision requiring the cessation of testing for nine months. Russia and France had already entered testing moratoriums, so it was no surprise that the United States would stop testing; the surprise was that testing ended immediately and never resumed. The next scheduled test, a U.S.-U.K. shot called Icecap, was canceled, to the particular chagrin of the British. To this day, the Icecap test area in Nevada remains intact and largely undisturbed. Diagnostic trailers wait idly, tethered to hundreds of feet of cable strewn across the desert floor. The rack tower is still standing; the custom-built Icecap test rack hangs inside, suspended over a hole hundreds of feet deep, waiting for a nuclear test device that will never arrive. Today, owls inhabit the upper levels of the Icecap tower and tour groups, often guided by Chuck Costa, gather at ground level to learn about the incredible days of U.S. nuclear testing.

It's been nearly 30 years since Divider, yet the United States continues to maintain seven weapons types in the stockpile: B61, B83, W76, W78, W80, W87, and W88. These sophisticated, highly-optimized designs were not designed to last forever; they contain many types of materials that age in different ways in a hostile, radioactive environment. Full-scale testing enabled scientists to develop weapons with confidence and ensure their reliability, but such testing is no longer an option. As Joe Martz, a Los Alamos scientist, explains: "Nuclear testing was a wonderful tool. It was also the world's biggest shortcut. It meant that we didn't have to understand all the details of a nuclear weapon and how it functions."[120] In 1993, Congress directed the secretary of the U.S. Department of Energy to "establish a stewardship program to ensure the preservation of the core intellectual and technical competencies of the United States in nuclear weapons, including weapons design, system integration, manufacturing, security, use control, reliability assessment, and certification."[121] In order for today's stockpile stewardship program to be effective, scientists need to understand the complex phenomena of nuclear explosions in a far more complete way than was ever required during the full-scale testing era.

At the national laboratories, testing of a different sort continues: dynamic high explosives testing, testing computer codes, and testing the mettle of young new staff members who face the daunting challenge of ensuring the safety and

reliability of America's nuclear deterrent in an age when full-scale nuclear testing is rapidly becoming the stuff of ancient lore. The tools of the trade today include the world's most powerful laser at Livermore, the world's most powerful laboratory radiation source at Sandia, and the world's most powerful x-ray radiography facility at Los Alamos. The laboratories also conduct subcritical plutonium experiments in Nevada, with increasingly sophisticated diagnostics, to assess the stockpile. But perhaps the most valuable asset is the real-world data collected from the nation's full-scale nuclear tests. Though the ground-shaking blasts of the past may be history, their technical and political legacies continue to guide scientists and policymakers alike in an ever-changing and ever-dangerous world.

Notes:

1. The author wishes to thank the many scientists, engineers, librarians, archivists, and historians who contributed to this article. In particular, LANL editor Brye Steeves, LANL scientist Thomas Kunkle, DTRA scientist Byron Ristvet, and Air Force Lieutenant Andrew Port deserve credit for making this publication a reality.
2. Physicist Samuel K. Allison gave the countdown for Trinity. James W. Kunetka, City of Fire: Los Alamos and the Atomic Age, 1943-1945 (Albuquerque: University of New Mexico, 1979), 168. Also see undated War Department press release (Los Alamos National Laboratory, National Security Research Center), 6.
3. The official number, as given in United States Nuclear Tests: July 1945 through September 1992, is 1,054; (DOE/NV—209-REV 16, September 2015), xiii. All U.S. shot dates and yields given in the article come from this source unless otherwise noted.
4. North Korea performed the world's most recent, known nuclear test in 2017, as confirmed in the Central Intelligence Agency's (CIA) World Factbook (cia.gov/library/publications/the-world-factbook/geos/print_kn.html, retrieved 1/23/2020).
5. Historian Alex Wellerstein offers the exact number of 125,310; a figure he obtained from the official history of the Manhattan Project. Even more impressive, Wellerstein estimates approximately half a million people were employed by the project at one point or another during the war (http://blog.nuclearsecrecy.com/2013/11/01/many-people-worked-manhattan-project/, retrieved 2/5/2020).
6. David Hawkins, Edith Truslow, and Ralph Carlisle Smith, Project Y: The Los Alamos Story (Los Angeles: Tomash, 1983), 486-7.
7. Oppenheimer, most certainly inspired by the poetry of John Donne, gave Trinity its name; Alice Kimball Smith and Charles Weiner, eds., Robert Oppenheimer: Letters and Recollections (Cambridge: Harvard University Press, 1980), 290.
8. The official time according to the Test Director is 5:29:15 "plus 20 s minus 5 s error spread." K.T. Bainbridge, "Trinity" (Los Alamos: Los Alamos National Laboratory report LA-6300-H, May 1976), 31.
9. The weight of the plutonium is revealed on page 77 of the report of the U.S. Department of Energy Office of Health, Safety and Security Office of Classification, "Restricted Data Declassification Decisions 1946 to the Present (RDD-8)," January 1, 2002.
10. From the Associated Press story that appeared in the Albuquerque Journal, July 17, 1945.
11. For instance, consider, "Senators, representative working on providing help for downwinders," Albuquerque Journal, October 6, 2019.
12. Richard Rhodes, The Making of the Atomic Bomb (New York: Simon and Schuster, 1986), 675.

13. Point 13 of the Potsdam Proclamation concludes, "The alternative for Japan is prompt and utter destruction," as quoted in Robert J.C. Butow, Japan's Decision to Surrender (Stanford: Stanford University Press, 1959), 244. The official yields of Little Boy and Fat Man are offered in, "The Yields of the Hiroshima and Nagasaki Nuclear Explosions," by John Malik (Los Alamos: Los Alamos National Laboratory report LA-8819, September 1985), 1.

14. United States Army, "Army Pathological Study: Fatalities for Hiroshima and Nagasaki" (from The Report of the Joint Commission for the Investigation of Effects of the Atomic Bomb in Japan), 12.

15. As quoted in, Butow, Japan's Decision, 245.

16. Ibid, 248.

17. Available from the CIA's online library (https://www.cia.gov/library/readingroom/docs/CIA-RDP13X00001R000100270005-0.pdf, retrieved 2/3/2020). This letter also indicates the diplomats were not pleased with the official Japanese public statement. Among other things, they argued the statement should have included a stipulation exempting the Emperor from any criminal culpability for war crimes.

18. Leslie R. Groves, Now It Can Be Told: The Story of the Manhattan Project (London: Andrew Deutsch, 1963), 378. Bradbury remained the Director for 25 years. Today, the Laboratory's museum in Los Alamos is named after him.

19. W.A. Shurcliff, Bombs at Bikini: The Official Report of Operation Crossroads (New York: Wm. H. Wise Co., Inc., 1947), 13.

20. Ibid, 2.

21. Ibid, 5-6.

22. From the film "Adm. Blandy Talks on Atomic Destruction Test," courtesy of the Sherman Grinberg Film Library.

23. As noted in the master script of the film, "The Story of Five Atomic Bombs" (Air Force Special Weapons Project). Both the extract from the script and a copy of the film were made available to the author by Academy Award-winning filmmaker Peter Kuran.

24. Jonathan M. Weisgall, Operation Crossroads: The Atomic Tests at Bikini Atoll (Annapolis: Naval Institute Press, 1994), 204.

25. Ibid., ix. Seaborg wrote the foreword for the book.

26. Ibid., 256-61. The third test, predictably codenamed Charlie, would have seen the detonation of a device thousands of feet below the surface.

27. "Summary of Declassified Nuclear Stockpile Information," (United States Department of Defense and United States Department of Energy), 172. All U.S. stockpile numbers given in the article come from this source unless otherwise noted. A majority of the weapons officially in stockpile in the late 1940s were not war-ready.

28. Yuli Khariton, "The USSR's Nuclear Weaponry: Did It Come From America or Was It Created Independently?" from Myths and Realities of the Soviet Atomic Program, by Yuli Khariton and Yu.N. Smirnov (Arzamas-16: Russian Federal Nuclear Center, 1994), 4.

29. Harry S. Truman, Years of Trial and Hope, 1946-1952 (Garden City, NY: Doubleday, 1956), 309. It's worth noting the President's use of the word "continue," as thermonuclear research at Los Alamos had been going on for years.

30. John C. Hopkins and Barbara Germain Killian, Nuclear Weapons Testing at the Nevada Test Site: The First Decade (www.nucleartestingnevada.com, 2013), 77. John Hopkins served as a Los Alamos Test Director, the Leader of the Field Testing Division, and the Head of the Los Alamos Weapons Program.

31. U.S. Nuclear Tests, 2-3.

32. Although Buster and Jangle are sometimes separated, it is appropriate to consider them an individual operation. The Buster tests focused on

weapons design; the two Jangle shots were DoD-sponsored weapons effects tests.

33. John Vandenkieboom, "Nuclear Weapons Fundamentals," presented at the Nuclear Nonproliferation Seminar, October 30 to November 1, 2001 (Los Alamos National Laboratory: LA-UR-02-1601), 36-37.

34. Hopkins and Germain Killian, 141.

35. Headlines from the Las Vegas Review Journal and the Los Angeles News, respectively.

36. The test area formally became known as NTS on July 8, 1951. The previous test, Sugar, also produced a crater, but a much smaller one since it was detonated 4 feet above the surface.

37. Soviet test data comes from V.N. Mikhailov, ed., USSR Nuclear Weapons Tests and Peaceful Nuclear Explosions 1949 through 1990 (Sarov: Russian Federal Nuclear Center, 1996) unless otherwise noted. Only Soviet weapons tests are accounted for in this article; Soviet peaceful nuclear explosions are not included in annual tallies.

38. "KTLA A-Bomb Coverage April 22 1952," (retrieved from https://www.youtube.com/watch?v=OF3JvVJMtzg, 2/12/20).

39. Robert Cahn, "When an A-Bomb Misfires," Collier's (August 9, 1952), 17-19.

40. Herbert York, The Advisors: Oppenheimer, Teller & The Superbomb (San Francisco: W.H. Freeman and Company, 1976), 131.

41. R.B. Vaile, "Operation Castle Crater Survey: Report to the Scientific Director" (Stanford: Stanford Research Institute, June 1955), 60.

42. Los Alamos National Laboratory, National Security Research Center, VFA-2790.

43. Jean Ponton, et al., Operation Upshot-Knothole 1953 (Washington: Defense Nuclear Agency, 1982) 39 & 123-4. Not only did Ruth produce a smaller yield than predicted, but the instruments failed and little data were collected.

44. There is no, known official record of this, though the story has been passed down through the decades by many reliable sources within the weapons programs of each laboratory.

45. Bernard Shleien, "External Radiation Exposure to the Offsite Population from Nuclear Tests at the Nevada Test Site between 1951 and 1970," Health Physics Volume 41 (August, 1981), 250.

46. Lynn R. Anspaugh and Bruce W. Church, "Historical Estimates of External γ Exposure and Collective External γ Exposure from Testing at the Nevada Test Site. I. Test Series Through Hardtack II, 1958," Health Physics Volume 50, Number 1 (July, 1986), 46.

47. Terrence R. Fehner and F.G. Gosling, Atmospheric Nuclear Weapons Testing, 1951-1963 / Battlefield of the Cold War: The Nevada Test Site (Washington, D.C.: United States Department of Energy, 2006), 104-6.

48. Harry S. Pease, "Atomic 'Annie' Answer to Enemy Manpower," The Milwaukee Journal, July 12, 1953.

49. Thomas Kunkle and Byron Ristvet, CASTLE BRAVO: Fifty Years of Legend and Lore (Los Alamos: Los Alamos National Laboratory, 2004), 46. A jet stream, capable of keeping the fallout aloft, was likely present at Mike.

50. Ibid., 108-9. There is evidence to suggest this fatality may have been due to over-treatment involving dubious medical procedures, rather than exposure to fallout.

51. John L. Richter, Risk Versus Threat: The U.S. Nuclear Weapon Program during and After the Cold War (unpublished memoir, Los Alamos National Laboratory National Security Research Center, 2018), 12.

52. Tom Ramos, From Berkeley to Berlin: The Epic Journey of Heroic Americans to Avert a Nuclear War (unpublished manuscript), 72-3. Ramos is the historian of Lawrence Livermore National Laboratory.

53. Hopkins and Germain Killian, 316.

54. United States Department of Energy Order

DOE O 452.1E (approved: 1-26-2015), 13.

55. The Springfield Union, May 21, 1956.

56. William E. Ogle, An Account of Nuclear Weapons Testing by the United States After the Test Moratorium, 1958-1961 (Las Vegas: United States Department of Energy Nevada Operations Office, 1985), 88.

57. Air Force Colonel Roger Ray, a member of the Redwing Joint Task Force, shared this story with Byron Ristvet; personal communication with the author (2/19/20). Ray helped complete Ogle's history after the latter passed away.

58. Pascal A was stemmed with a concrete plug, but a bluish fire escaped through peripheral channels. Due to this phenomena, Pascal A has been referred to as a Roman Candle test.

59. Nuclear weapons were usually detonated high above the surface (e.g., towers, balloons, etc.) to prevent the fireball from coming in contact with the ground and thereby producing fallout.

60. Frank H. Shelton, Reflections of a Nuclear Weaponeer (Colorado Springs: Shelton Enterprises, 1988), 8-22. Shelton served as the Technical Director of the Armed Forces Special Weapons Project from 1955 to 1959.

61. "Genie Missile Test," (retrieved from https://www.youtube.com/watch?v=1VZ7FQHTaR4, 2/20/20).

62. Glenn T. Seaborg, Kennedy, Khrushchev and the Test Ban (Berkeley: University of California Press, 1981), 11.

63. Shelton, 9-35.

64. Los Alamos National Laboratory, National Security Research Center.

65. Richard G. Hewlett and Jack M. Holl, Atoms for Peace and War, 1953-1961: Eisenhower and the Atomic Energy Commission (Berkeley: University of California Press, 1989), 483.

66. "Project Argus 'Greatest Experiment' 1959/3/19" (retrieved from https://www.youtube.com/watch?v=Ce0-AuLmSkQ, 2/24/20).

67. Ogle, 106. Having already committed to the test moratorium, it's most likely the "political" reason was Eisenhower wanted to give the impression he was concluding an existing series; not initiating a new one.

68. Richter, 16. Though Richter does not offer the author's identity, LANL scientist Thomas Kunkle is confident Malik wrote it on the Los Alamos Control Point 1 office chalk board (personal communication with the author, 2/24/20). John Hopkins believes it may have been written by Air Force Colonel Roger Ray (personal communication with the author, 7/13/2020).

69. Hewlett and Holl, 548.

70. The Mutual Defense Agreement of July 1958 formally made the U.S. and U.K. partners in the nuclear field.

71. M.K. Hertford to AEC Division of Military Application, 11/13/58 (Los Alamos National Laboratory, National Security Research Center, Collection A-1999-019, box 99, folder 20).

72. Robert K. Thorn and Donald R. Westervelt, "Hydronuclear Experiments" (Los Alamos National Laboratory, LA-10902-MS, February 1987), 4.

73. LANL Historian Emeritus Roger Meade, who knew Malik personally, conveys this account (personal communication with the author, 8/23/19).

74. Thorn and Westervelt, 6.

75. Bradbury to Starbird, 6/4/60 (Los Alamos National Laboratory, National Security Research Center, Collection A-1999-019, box 99, folder 22).

76. Dwight D. Eisenhower, Waging Peace: The White House Years, A Personal Account, 1956-1961 (New York: Doubleday, 1965), 481.

77. CIA Special National Intelligence Estimate Number 11-9-61 (John F. Kennedy Presidential Library and Museum).

78. Ogle, 235.

79. Arthur M. Schlesinger, Jr., A Thousand Days: John F. Kennedy in the White House (Boston: Houghton Mifflin, 1965), 459.

80. Hans Bethe, "Disarmament Strategy,"

Bulletin of the Atomic Scientists (September 1962), 18.

81. Ibid, 19.

82. V.N. Mikhailov, Catalog of Worldwide Nuclear Testing (New York: Begell-Atom, 1999), 94. 86,430 kilotons is the equivalent of nearly 5,800 Little Boy-type bombs.

83. As quoted in Ogle, 6.

84. Bradbury to Fisk, 2/3/61 (Los Alamos National Laboratory, National Security Research Center, Collection A-1999-019, box 99, folder 23).

85. Personal communication with the author (2/28/20).

86. Mikhailov, Catalog, 92 & 94.

87. New York Times, 10/31/61.

88. Schlesinger, 488.

89. John F. Kennedy Presidential Library and Museum, National Security Files: Subjects: Nuclear Weapons Testing, 2/16/62, Part I, Box 300.

90. TIME, May 4, 1962, 18.

91. Ramos, 128.

92. Ogle, 415-6. Although Los Alamos designed the warhead, it's important to note this successful full-system test was the work of many organizations including Sandia, Honeywell Industries, and the China Lake Naval Ordnance Test Station.

93. United States Department of Energy, Radiological Effluents Released From U.S. Continental Tests, 1961 Through 1992 (Nevada Operations Office, August 1996), 28-9.

94. Personal communication with the author (2/28/20). Costa, who retired as Test Director in 2008, continues to guide tours at the test site (today the Nevada National Security Site).

95. Radiological Effluents, 29.

96. "Robert Kennedy watches a test of the Davy Crockett. Incredibly RARE!" (retrieved from https://www.youtube.com/watch?v=xHiihPD7bLM, 3/4/20). Zero yield safety tests were performed in the atmosphere subsequently as part of Operation Roller Coaster, but Little Feller I was the final yield-producing atmospheric nuclear test in Nevada.

97. When the word "prime" is appended to a test name, it indicates there was a failure on the first attempt to perform the shot. In the case of Starfish, the Thor missile carrying the warhead exploded prematurely at 30,000 feet on the first attempt (Shelton, 11-36-7).

98. Personal communication with the author (3/5/20).

99. Byron Ristvet, personal communication with the author (4/26/20).

100. The Department of Energy considers Clean Slate III, a zero yield safety test conducted on June 9, 1963 as part of Roller Coaster, to be the final atmospheric test conducted by the United States.

101. "President John F. Kennedy's 'Peace Speech'" (retrieved from https://www.youtube.com/watch?v=0fkKnfk4k40, 3/4/20).

102. Schlesinger, 904.

103. Robert R. Brownlee and Gary H. Higgins, A Review of Containment Failures (Defense Threat Reduction Agency Special Report, October 1, 2004), 5-6.

104. Ference Szasz, "New Mexico's Forgotten Nuclear Tests: Projects Gnome (1961) and Gasbuggy (1967)," New Mexico Historical Review (Volume 73, October 1998, Number 4), 356.

105. Ibid, 365. Detonated at a depth of 8,425 feet, the Rulison test near Parachute, Colorado, was the deepest in U.S. testing history by a considerable margin. In 1973, the Rio Blanco-1, 2, and 3 devices were detonated simultaneously at different depths in the same 6,690-foot hole near Meeker, Colorado.

106. The official yield is "Less than 5 Mt" (DOE/NV—209, 77).

107. Personal communication with the author (3/18/20).

108. Ibid.

109. Las Vegas Review Journal, 1/19/68, and Las Vegas Sun, 1/23/68.

110. James E. Reeves to Nevada Operations Files, 2/9/68. Part of “The Howard Hughes Papers,” at the Nuclear Testing Archives in Las Vegas.

111. “’68 Notes Reflect Hughes’ Varying Moods,” The New York Times, 2/13/72.

112. Personal communication with the author (3/19/20).

113. Jim Carothers and Friends, Caging the Dragon: The Containment of Underground Nuclear Explosives, 561. This report is published by both the Department of Energy (DOE/NV-388) and the Department of Defense (DNA TR 95-74).

114. Radiological Effluents, 157.

115. Personal communication with the author (5/5/20).

116. The Soviets detonated 55 devices in 1978, though several of them were fired simultaneously in various “salvo explosions.”

117. Charlton Heston, "The Peace Movement: Nuclear Freeze," Vital Speeches of the Day (Volume L, Number 1: October 1983), 20. In 1977, the nuclear weapons complex was absorbed by the newly created Department of Energy.

118. "Kearsarge with Paul Robinson video and a Discussion Panel" (https://www.youtube.com/watch?v=KOMrrI2TM6U&feature=youtu.be, retrieved 3/24/20).

119. Ibid., as quoted by Nick Aquilina, retired Area Manager for the DOE Nevada Operations Office.

120. Joe Martz, "Detonation from the Bottom Up," National Security Science Magazine (July 2014), 6.

121. PUBLIC LAW 103-160-NOV. 30, 1993 (https://uscode.house.gov/statviewer.htm?volume=107&page=1946#, retrieved 3/25/20)

History of Nuclear Effects Testing at White Sands Missile Range

Randy M. Brady
White Sands Test Center

The United States realized the need for nuclear effects testing following the first nuclear detonation on July 16, 1945, which took place in New Mexico on White Sands Missile Range (WSMR) at the Trinity Site. The founder of the Nuclear Effects Laboratory (NEL), Glenn Elder, served as its first director from 1955 to 1974. Elder began preparing for nuclear effects testing by developing the laboratory's requirements and establishing its initial infrastructure, which included the Fast Burst Reactor (FBR) (Fission Neutrons); a 14 MeV Neutron Generator (Fusion Neutrons); and the Linear Accelerator (LINAC) [Gamma Dose Rate (GDR)].

Serving the Western Hemisphere's Largest All Land Missile Range

Published in the interest of military and civilian personnel of WSMR and to promote a greater guided missile program for the national defense.

PUBLICATIONS OFFICE: 114 S. CHURCH, LAS CRUCES, N. M.

WIND & SAND

Vol. X—No. 11 White Sands Missile Range, N.M., Friday, Aug. 28, 1964 Eight Pages

PUBLISHED WEEKLY

Distributed To Military and Civilian Personnel on W.S.M.R

Published by Las Cruces Citizen, Las Cruces, New Mexico, a private firm in no way connected with the Department of the Army. Opinions expressed by the publishers and writers herein are their own and are not to be considered an official expression by the Department of the Army. The appearance of advertisements in this publication does not constitute an endorsement by the Department of the Army of the products or services advertised.

Nuclear Effects Laboratory Opens At WSMR

Figure 1: The Nuclear Effects Laboratory grand opening was announced in the WSMR newspaper the Wind and Sand on Aug. 28, 1964.

In 1968, the NEL added the Gamma Radiation Facility (GRF), which used Cobalt-60 and Cesium-137 sources to conduct Gamma Total Dose (GTD) testing. During the following decade, the lab completed the White Sands Solar Furnace, used to test the thermal effects of nuclear weapons, and the White Sands Electromagnetic Pulse Systems Test Array (WESTA), used to test the effects of High Altitude Electromagnetic Pulse (HEMP).

Figure 2: Fast Burst Reactor

Figure 3: White Sands Solar Furnace

Randy M. Brady is the Director of the Survivability, Vulnerability and Assessment Directorate, White Sands Test Center, U.S. Army Test and Evaluation Command, in White Sands Missile Range, New Mexico. He has a B.S. in Electrical Engineering from the University of Missouri – Columbia and a M.A. in Business Administration from Troy State University. He was previously assigned as a Senior Project Officer, Branch Chief, and Division Chief at the Survivability, Vulnerability and Assessment Directorate. His email address is randolph.m.brady.civ@mail.mil.

Figure 4: El Dorado Irradiator

Figure 5: Teradyne A575 (STL)

Figure 6: Reba Facility

In the 1980s, the U.S. Army gave the lab a new moniker, the Nuclear Effects Directory (NED), and added three new facilities: (1) the Semiconductor Test Laboratory, used to test nuclear effects risk mitigation for electronics, (2) the Relativistic Electron Beam Accelerator (REBA), used to test GDR effects on Circuit Card Assemblies (CCAs) and Line Replacement Unis (LRUs), and (3) the El Dorado Irradiator, used to test Enhanced Low Dose Rate Sensitivity (ELDRS) simulating space radiation on electronics and CCAs.

In the 1990s, NED received a new name as well as the EMP facilities at Kirtland Air Force Base (KAFB). Under its new designation as the Directorate for Applied Technology, Test and Simulation (DATTS), it developed the Radiation Tolerance Assured Source and Supply Center (RTASSC), used for obsolescence life-cycle management by the entire Department of Defense (DoD).

In 2000, DATTS became the Survivability, Vulnerability and Assessment Directorate (SVAD), whereupon it began a complete migration and consolidation of all WSMR laboratory missions: Nuclear / Radiation Effects, Electromagnetic Environmental Effects (E3), Directed Energy (High Power Microwave (HPM) and Lasers), and Applied Environments (Natural Environments).

Figure 7: HPD-II EMP Facility

Today, the SVAD and the White Sands Test Center (WSTC) are the DoD's premier nuclear effects support organizations, maintaining testing capabilities ranging from nuclear weapons effects to the unique effects of space environments, as shown in Table 1. Initiated during FY17, Test Resource Management Center (TRMC) funded an Army Major Nuclear Modernization (all capabilities) and a FBR Central Test and Evaluation Investment Program (CTEIP). Currently, SVAD has received all required equipment and capability upgrades from these efforts, except Pulsed Gamma Simulator (PGS) and FBR fuel rings.

Figure 8: VEMPS Facility

From the Directorate's inception to today, SVAD has acquired the test facilities and capabilities to simulate almost all nuclear weapons effects and radiation environments in support of our nation.

Table 1: SVAD's Nuclear Effects Facilities and Capabilities

Environment / Need	Facilities / Capabilities	Comment
Gamma Dose Rate	Linear Accelerator PI-538 Flash X-Ray Pulse Gamma Simulator	Upgraded in 2018 IOC in SEP 2021
Gamma Total Dose	Gamma Radiation Facility	Upgraded in 2019 – 8 Large Sources.
Neutron Fluence	Fast Burst Reactor (FBR)	Completely Re-Fueled in FY23
Nuclear Thermal Radiation	Xenon Lamp Facility Quartz Lamp Facility Thermal Radiation Sources	FOC in 2019 FOC in 2016 IOC in NOV 2020
High Altitude Electromagnetic Pulse (HEMP)	Advanced Fast Electromagnetic Pulse Simulator (AFEMPS) – Horizontal Polarized Vertical Electromagnetic Pulse Simulator (VEMPS) Pulse Current Injection (EMP) and MIL-STD-188-125	FOC – SEP 2012 FOC – DEC 2016 FOC – SEP 2019
Source Region Electromagnetic Pulse (EMP) (SREMP)	PI-538 Flash X-Ray Pulse Gamma Simulator	IOC SEP 2021
Nuclear Airblast	Large Blast / Thermal Simulator Thermal Radiation Sources	FOC in 2019 IOC in NOV 2020
Combined Environments	FBR / PI-538 Flash X-Ray	FOC in 2010
Enhanced Low Dose Rate Sensitivity (ELDRS)	DS-20 Panoramic Irradiator	Upgraded and refueled 2020
Piece-Part Characterization and Evaluation	Semiconductor Test Laboratory (STL)	Upgraded in 2018
Radiation Life-Cycle Management / Obsolescence	Radiation Tolerance Supply and Support Center (RTASSC)	
Circuit Analysis / Design / Hardening	Radiation Engineering	
Radiation Bill-Of-Material Evaluations	Radiation Engineering	
Radiation Shielding and Attenuation	Fast Burst Reactor Gamma Radiation Facility Radiation Correlation Facility	
Radiation Equipment Characterization and Performance	Radiation Performance Laboratory	FOC in OCT 2020
Radiation Metrology	C-Station	Upgraded in 2019.

Figure 9: AFEMPS Facility

Figure 10: Xenon Lamp Facility

Figure 11: DS-20 Irradiator

Figure 12: Quartz Lamp Facility

Figure 13: Upgraded LINAC Section

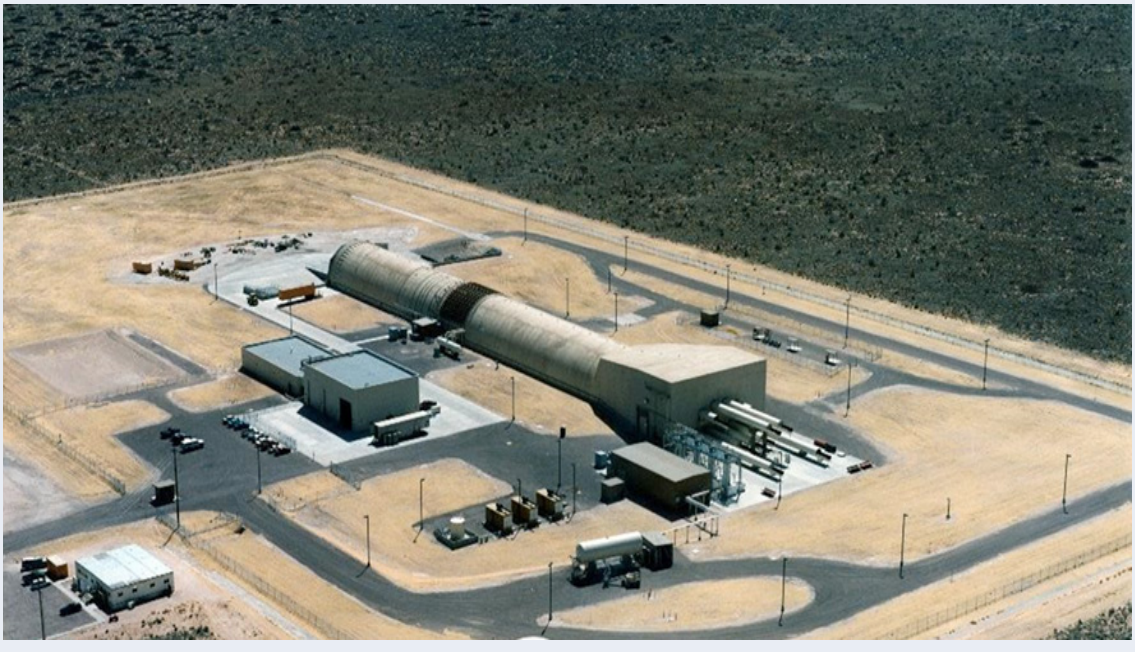

Figure 14: Large Blast / Thermal Simulator

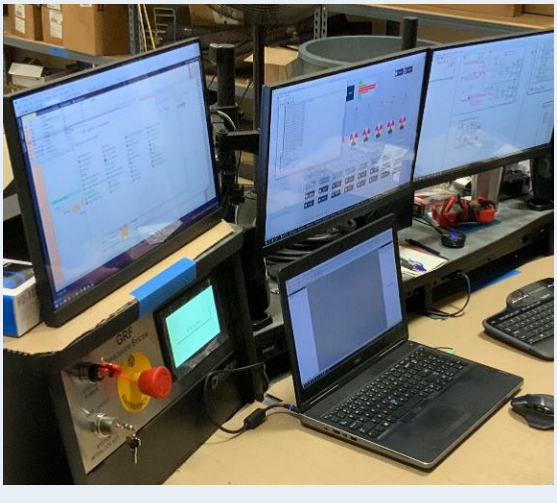

Figure 15: Gamma Radiation Facility Upgrade

The Next Nuclear Arms Control Treaty: Looking Back Beyond New START

Dirk E. Plante
Homeland Defense & Security Information Analysis Center

The Atomic Age began on July 16, 1945, with the detonation in the New Mexico desert of the world's first nuclear device, the "Gadget." Less than one month later, the United States detonated weapons over Japan on August 6, and August 9, 1945, which rapidly led to the end of World War II (WWII). With the atomic bomb no longer a secret, other nations raced to join the nuclear club. In time, more than half a dozen other countries would possess nuclear weapons. Eventually there would be a need to reduce the threat posed by the proliferation of the nuclear weapons. This article will look at the various treaties that the United States has negotiated with Russia over the years to limit the number of weapons each country had to use against the other directly, or against its interests, and the possible road ahead for further treaty negotiations.

Introduction

Although the supply of plutonium was scarce for the United States during the Manhattan Project's development of the first atomic bombs, soon after WWII a steady supply of weapons grade plutonium became available to start building the nation's nuclear weapon stockpile. For a brief four years, the United States was the world's sole nuclear power. That changed on August 29, 1949, when the Union of Soviet Socialist Republics (U.S.S.R., or Soviet Union) detonated its first nuclear device.[1] The nuclear arms race had now truly begun, as both countries sought to develop an arsenal of weapons that provided military capabilities for any number of scenarios. For the United States, its peak year in terms of number of nuclear weapons was 1967, when it had 31,255 weapons in the stockpile.[2]

A few years after that peak, the United States began negotiations with the Soviet Union to reduce the number of nuclear weapons and delivery systems in their arsenals. Russia (and formerly, the Soviet Union) and the United States are the only two nations that have limited the size of their nuclear arsenals through bi-lateral agreements. There has of course been a strong rationale for those two countries doing so, with a significant reason being that they were the two Cold War adversaries whose arsenals had numbered in the tens of thousands of weapons while other nuclear armed nations at the time had weapon numbers at least an order of magnitude less. The various arms control treaties over the years have played a vital role in preventing the growth of each country's arsenals. Over the course of the last 50 years, the United States and Russia

Mr. Dirk Plante is a retired Army FA52 colonel, and he is currently the Deputy Director at the Homeland Defense & Security Information Analysis Center (HDIAC). The HDIAC is one of three IACs sponsored by the Defense Technical Information Center, Fort Belvoir, VA. He has a B.S. in Physics and Astronomy from Texas Christian University, a M.S. in Nuclear Engineering from the Air Force Institute of Technology, and a Master of Strategic Studies from the Army War College. His email address is dplante@hdiac.org.

Table 1: Primary Nuclear Weapon Treaties between the United States and Russia

Treaty	Max Number of Nuclear Weapons	Dated Signed	Date Ratified	Dated Entered into Force
Strategic Arms Limitation Talks (SALT I)	n/a; limit on missiles	May 26, 1972	September 30, 1972	October 3, 1972
Strategic Arms Limitation Talks II (SALT II)	n/a; limit on missiles	June 18, 1979	n/a	n/a
Intermedidate-Range Nuclear Forces (INF) Treaty	n/a; limit on missiles	December 8, 1987	June 1, 1988	June 1, 1988
Strategic Arms Reduction Treaty (START)	6,000	July 31, 1991	October 1, 1992	December 5, 1994
Strategic Arms Reduction Treaty II (START II)	4,250	January 3, 1993	September 26, 1997	n/a
Strategic Offensive Reduction Talks (SORT)	2,200	May 24, 2002	March 6, 2003	June 1, 2003
New Strategic Arms Reduction Treaty (New START	1,550	April 8, 2010	February 2, 2011	February 5, 2011

have conducted bi-lateral negotiations, resulting in a continuous reduction in deployed strategic nuclear weapons from their Cold War highs. Table 1 provides an overview of the primary treaties between the United States and Russia.

A Review of Nuclear Arms Control Treaties with Russia

Today, the New Strategic Arms Reduction Treaty (New START) is the treaty in force between the United States and Russia limiting the number of their deployed strategic nuclear weapons. With New START due to expire in February 2021,[3] it is important to think about what the future of arms control treaties can look like. Even if both countries cannot arrive at a new agreement, and choose instead to agree to a five-year extension, in February 2026, the United States and Russia will arrive at the same point they are now. And by then we could find it to be a different strategic landscape requiring continued efforts at arms control negotiations.

It is worthwhile to look at the various treaties that the United States and Russia have ratified, examining at not only what limits they put on the number of weapons, but also specific language included in the treaties and how that language evolved from one treaty to the next. For example, for New START, both countries chose to count each strategic bomber as being equivalent to one warhead, specifically, "One nuclear warhead shall be counted for each deployed heavy bomber."[4] In the first START, the number of warheads attributable to heavy bombers was ten for the United States and eight for the Soviet Union, but this counting only applied to the first 150 U.S. bombers and the first 180 U.S.S.R. bombers.[5]

Strategic Arms Limitation Talks

Signed during the Nixon Administration in 1972, The Strategic Arms Limitation Talks (SALT) did not directly reduce the number of warheads, but instead placed limits on the number of offensive and defensive missiles. It resulted in the Anti-Ballistic Missile (ABM) Treaty covering defensive strategic weapons. (The United States withdrew from the ABM Treaty in 2002 during the George W. Bush administration). The SALT negotiations also resulted in limits on offensive strategic weapons, known as the SALT interim agreement. The United States was limited to no more than 710 SLBM launchers on no more than 44 submarines, and would not "significantly increase" its ICBM capabilities. Negotiations followed with SALT II to further codify and place limits on offensive capabilities. Due to the Soviet Union's invasion of Afghanistan, the Carter administration withdrew the Treaty from Senate advice and consent in 1980, and it was never ratified nor entered into force.[6]

Strategic Arms Reduction Talks

The Strategic Arms Reduction Talks (START) Treaty sought to reduce the actual number of deployed nuclear weapons that both nations could have. The treaty limited each country to no more than 6,000 warheads

on ICBMs, SLBMs, mobile ICBMs (in the case of Russia), and heavy bombers. START I was signed in July 1991 and was immediately impacted by the breakup on the Soviet Union in December 1991. The George H.W. Bush administration sought to work with the former members of the Soviet Union that now possessed nuclear weapons to become parties to the treaty. It required an additional protocol arrived at through further negotiations, and the treaty entered into force in 1994.[7] Negotiations during the Clinton administration following the original START led to the START II agreement, which sought to further reduce warheads down to 3,800-4,250. Although ratified in 2000, Russia withdrew from the treaty in 2002. START III negotiations were also proposed, but did not materialize as a result of Russia making negotiations contingent on the United States remaining in the ABM Treaty, which it withdrew from in 2002.

New START

The New START Treaty was negotiated during the Obama administration. It set the limit on the number of deployed strategic nuclear weapons at 1,550. It entered into force on February 5, 2011, and required each nation to meet the treaty limit by the beginning of year seven of the treaty (February 5, 2018). Currently each country is below the 1,550 warheads limit as reported by the Department of State.[9] The New START Treaty also put limits on delivery systems, allowing each country to have no more than 700 deployed ICBMs, SLBMs, and heavy bombers.[10] The Russian government stated that it is ready to extend New START for five years without preconditions.[11] The U.S. government has not yet made a similar commitment to the five-year extension, but instead is seeking to negotiate changes to the treaty.[12]

What does it mean to ratify a treaty?

Treaty ratification can be a confusing term. Does it happen when the leaders of a country hold a press conference following negotiations to sign the documents, exchange them, and shake hands? Is the date that the parties agree to begin enforcing the treaty the date of ratification? Answer: It is neither of those dates, and instead falls somewhere between them. To ratify a treaty means to make it the binding law of the signatory. That can only occur when the unique process established by the laws of each country is carried out. For the United States, the Constitution states that the president "shall have Power, by and with the Advice and Consent of the Senate, to make Treaties, provided two-thirds of the Senators present concur" (Article II, section 2). The important point to take away is that a treaty can be negotiated and signed, but unless ratified, it does not legally bind the nation to the terms of the treaty. An example of a treaty that was never ratified is SALT II, although the United States did choose to obligate itself to the limits set in the treaty on the number of strategic nuclear delivery vehicles, which included ICBMs, SLBMs, and heavy bombers.[13]

Strategic Offensive Reduction Talks

The Strategic Offensive Reduction Talks (SORT), also known as the Treaty of Moscow, were held during the George W. Bush Administration and further reduced the number of warheads to 1,700-2,200. The Treaty left it to each country to determine the specific composition of its arsenal.[8] As part of the SORT negotiations there were no new provisions made for verification measures. Instead, both nations agreed to rely on the verification regime from the START Treaty.

Beyond New START

Although the United States and Russia still possess an order of magnitude more operational strategic nuclear weapons that any other nation, a new round of negotiations could lead to both nations getting under 1,000 weapons. This could be a psychological barrier as much as a numerical barrier that would give both nations the leverage to seek other nations' participation in multilateral negotiations. In addition to the number of weapons a nation possesses, there are other significant reasons

for holding negotiations with additional countries. These include limiting the development of nuclear capabilities that can be seen as destabilizing and addressing the proliferation, whether intentional or not, of nuclear weapons technology and material to other nations and even non-state actors.

Whether New START is allowed to expire in early 2021 or extended until 2026 eventually a time will come when the treaty is no longer in force. Today the National Defense Strategy (NDS) outlines a different threat than the one we faced when New START negotiations first began and with which the nation has been focused on for nearly two decades. Furthermore, the Nuclear Posture Review (NPR) has gone through two iterations (in 2010 and 2018) since the negotiations for the treaty first began. Today's NPR points out that the nation does not wish to regard Russia and China as our adversaries and "seeks stable relations with both," but their actions point to the challenges that the United States faces,[14] in particular their development and deployment of new nuclear capabilities.

The NDS outlines a world where "every domain is contested – air, land, sea, space, and cyberspace."[15] Indeed, we are no longer focused on a counter-terrorism fight, but on Great Power competition, recognizing that Russia and China are our strategic competitors. Seeking to engage in nuclear arms control negotiations with both nations simultaneously seems like a daunting challenge, but it is one that the United States has considered.

As recently as July 2020, less than seven months before New START expires, the United States sought to bring China into negotiations as part of discussions with Russia. "Though the Trump administration wants China brought into the deal, the U.S. and Russia currently possess some 90 percent of the world's nuclear warheads… China is believed to have around 320 warheads."[16] Given the size of its arsenal, China is reluctant to join the negotiations. "China's director general of arms control Fu Cong said… that Beijing would be willing to join New START talks if the U.S. and Russia agreed to cut their nuclear arsenals to match China's."[17] However, China is not allowing its nuclear stockpile to remain stagnant. A recent report indicates that China is seeking to double the size of its warhead stockpile in the next decade and may even be trying to develop a nuclear triad.[18]

Conclusion

Although it is never a given that the expiration of New START, whether in 2021 or 2026, will lead to a new treaty with Russia or other nations, what is clear is that there has been a continuous downward trend in the number of weapons each country possesses. Beginning in the late 1960s, when negotiations kicked off for the first SALT agreement, both nations have always sought to reduce the number of their weapons and delivery systems in exchange for equal concessions from the other. Today the sizes of both countries' arsenals are dwarfed by their sizes from the highest levels during the Cold War. With each succeeding treaty, the objective of the United States has always been to reach an agreement that meets national security objectives while reducing the size of its stockpile to the optimal number necessary to accomplish those objectives. That the most current NPR does not call for increasing the number of nuclear weapons or delivery systems bodes well for a new treaty that will further reduce each country's arsenal to below current levels.

Notes:

1 Thomas C. Reed and Danny B. Stillman, The Nuclear Express (Minneapolis, MN: Zenith Press, 2009), 111.

2 U.S. Department of Defense, The Nuclear Matters Handbook 2020, (Washington: Office of the Deputy Assistant Secretary of Defense for Nuclear Matters, 2020), 48.

3 At press time there has been no agreement between both countries to agree to the five-year extension written into the New START Treaty.

4 David Brennan, "America is risking a nuclear 'free-for-all' by delaying New START extension with Russia: Former National Security Official,"

Newsweek, https://www.newsweek.com/america-risking-nuclear-free-all-delaying-new-start-extension-russia-national-security-official-1485242 (accessed January 22, 2020).

5 102d Congress 1st Session, Treaty with the Union of Soviet Socialist Republics on the Reduction and Limitation of Strategic Offensive Arms (The START Treaty), (Washington: U.S. Government Printing Office, 1991), 2-6.

6 A comprehensive discussion of SALT can be found on the Nuclear Threat Initiative's website at https://www.nti.org/learn/treaties-and-regimes/strategic-arms-limitation-talks-salt-ii/ (accessed September 14, 2020).

7 A comprehensive discussion of START can be found on the Nuclear Threat Initiative's website at https://www.nti.org/learn/treaties-and-regimes/treaties-between-united-states-america-and-union-soviet-socialist-republics-strategic-offensive-reductions-start-i-start-ii/ (accessed September 14, 2020).

8 A comprehensive discussion of SORT can be found on the Nuclear Threat Initiative's website at https://www.nti.org/learn/treaties-and-regimes/strategic-offensive-reductions-treaty-sort/ (accessed September 14, 2020).

9 As of July 1, 2020 the United States has 1,372 deployed warheads and Russia has 1,326 deployed warheads. The Department of State regularly posts New START fact sheets on its website at https://www.state.gov/new-start-treaty-fact-sheets/ (accessed September 14, 2020).

10 A comprehensive discussion of New START can be found on the Nuclear Threat Initiative's website at https://www.nti.org/learn/treaties-and-regimes/treaty-between-the-united-states-of-america-and-the-russian-federation-on-measures-for-the-further-reduction-and-limitation-of-strategic-offensive-arms/ (accessed September 14, 2020).

11 The full test of the New START Treaty can be found online at https://media.nti.org/documents/new_start_treaty.pdf (accessed September 14, 2020).

12 David Brennan, "Russia Nuclear Treaty Lapse to Degrade Nuclear Influence: Ex-Military Leaders," Newsweek, https://www.newsweek.com/russia-nuclear-treaty-expiry-degrade-us-influence-ex-military-leaders-new-start-1516601 (accessed September 12, 2020).

13 A thorough discussion of the Senate's role in treaties can be found online at https://www.senate.gov/artandhistory/history/common/briefing/Treaties.htm (accessed September 12, 2020).

14 U.S. Department of Defense, Nuclear Posture Review 2018 (Washington: Office of the Secretary of Defense, 2018), 7.

15 U.S. Department of Defense, Summary of the 2018 National Defense Strategy of the United States of America: Sharpening the American Military's Competitive Edge, (Washington: Office of the Secretary of Defense, 2018), 3.

16 Brennan, "Russia Nuclear Treaty Lapse to Degrade Nuclear Influence: Ex-Military Leaders," Newsweek.

17 Ibid.

18 Carla Babb, "Chinese Nuke Arsenal Next on Beijing's 'To Do' List, US Commander Warns," VOA News https://www.voanews.com/usa/chinese-nuke-arsenal-next-beijings-do-list-us-commander-warns (accessed September 14, 2020).

Countering Hostile Technology with Pathway Defeat

MAJ Chris Bolz
Headquarters, Department of the Army (HQDA) G-3/5

Thomas Kuhn took a philosophical approach to scientific revolutions. He postulated that paradigm shifts can only take place once the older generation of thinkers, wedded to their ideas, die out.[1] This may have been true from Copernicus to the 20th century, but in today's ever changing and interconnected space, those that are unwilling to keep pace are left behind at an even quicker rate. In great power competition, technological advantages will be exploited. Breakthroughs in all manners of research are transforming our world. CRISPR technology re-sequences genetic code. Autonomous, self-driving vehicles will replace truck drivers and vehicle ownership. AI computers routinely outmatch Go (Chinese strategy game) and Chess masters in self-developed, innovative ways.[2] We are at the dawn of a new age and cannot yet see what that future landscape will look like. Competing countries, coupled with technological revolution in a globally interconnected system, will undoubtable create challenges with huge implications. The balance of power could be quickly and drastically reversed from the hostile use of emerging technologies. Dealing with hostile technology is not new; countering weapons of mass destruction (CWMD) operations provides a framework. The United States should expand the Department of Defense's (DoD) CWMD pathway defeat special activity to counter current and future hostile technologies.

Weapons of Mass Destruction

The U.S. military defines weapons of mass destruction as any chemical, biological, radiological, or nuclear weapons capable of high order of destruction but does not include the means of delivery as a part of the weapon.[3] The concept of WMD is difficult to address since essentially every department and agency in the U.S. government maintains a different definition. In "Defining 'Weapons of Mass Destruction,'" Dr. W. Seth Carus identified over 50 different definitions.[4] Some included high explosives, other definitions focused on the destructive or casualty producing phenomenon and not necessarily weapons pertaining to chemical, biological, radiological, or nuclear (CBRN) sources. Some agencies have replaced the term "WMD" with weapons of mass effect, or WME, which can include acts that cause psychological or economic damage.[5] Since the introduction of

MAJ Chris Bolz is an FA52 and the Executive Officer for the Director, Strategy, Plans, and Policy, HQDA G-3/5. He has a B.S. in Civil Engineering from West Point, an M.S. in Civil Engineering from the Missouri University of Science and Technology, an M.M.A.S from the School of Advanced Military Studies, and a Professional Engineer certification. He was previously assigned to USANCA at Fort Belvoir, VA, and as a Battalion XO and Company Commander in 1-1 Special Forces Group (A), Okinawa, Japan.

the term WMD in 1946, the U.S. military has excluded everything other than CBRN weapons in its definition of WMD.

This exclusive framework has allowed the CWMD community to concentrate its efforts against CBRN capabilities, ranging from large state-backed programs to non-state, terrorist labs. Battlefield chemical weapons capabilities are treated with the same level of concern as individual nerve agent attacks, such as the use of Novichok in Salisbury[6] in 2018 or VX in Kuala Lumpur[7] in 2017. Yet labeling discrete incidents as WMD is problematic, further complicating the WMD debate.[8] The DoD makes a point to limit WMD to only CBRN. For one, a military that counters high explosives would be severely limiting its operational capabilities. Administrations have found that limiting WMD to CBRN capabilities is beneficial as it allows a suite of traditional military capabilities while limiting the chemical, biological, and nuclear aspects that are a political and military disaster. CWMD frameworks such as the Chemical Weapons Convention (CWC), Biological Weapons Convention, and Nonproliferation Treaty, along with other arms control agreements, such as the Geneva Conventions and Mine Ban Treaty, constrict the conduct of war to America's favor. In this construct, the United States has developed precision fires and targeting capabilities that greatly threaten our adversaries' armies. Competitors seek asymmetric capabilities outside of the traditional, conventional, and CWMD space to counter the U.S. advantage.

Additionally, from both a policy and execution aspect, if everything was a WMD, the process would be convoluted, and it would be difficult to formulate a strategy to counter everything. Emerging technology can have both beneficial and nefarious uses. For example, chemicals are mostly used to produce a host of essential compounds needed on a daily basis, yet chemicals can also be used to kill or maim large numbers of people. The outright banning of chemicals would be impractical, it would stymie innovation, and it would be a detriment to our way of life. Efforts such as the CWC are practical applications to prevent the disreputable use of technology.[9] Preventing further dissemination of knowledge and technology is plausible for existing WMD, but more is needed for emerging threats.

The U.S. government lacks a coherent CWMD architecture. At the national level, the 2002 National Strategy to Counter WMD, published as NSPD-17, outlines a dated response to the September 11th attacks. Additionally, the more recent 2018 National Strategy for Countering Weapons of Mass Destruction Terrorism does not address state sponsored programs. Because of this, each Department has its own approach to CWMD. The Departments of State, Defense, Justice, and Homeland Security all approach different aspects of WMD, with DoD having the most comprehensive approach to CWMD. The military begins its framework with the DoD Strategy for Countering Weapons of Mass Destruction, published in 2014. While beneficial, the Strategy already needs a revision. The DoD has already published Joint Publication (JP) 3-40, Joint Countering Weapons of Mass Destruction, updated in November 2019, and DoD Directive 2060.02, DoD CWMD Policy, signed in January 2017, making the 2014 DoD strategy obsolete. The DoD Directive assigns roles and responsibilities to the DoD enterprise while JP 3-40 outlines how the joint force will address WMD across the globe. Unfortunately, this construct does not assign specific responsibility to an under secretary or assistant secretary, mirroring the disunity at the department level. Yet

these documents do provide a framework for the DoD to address the WMD problem set.

The DoD defines CWMD as *efforts against actors of concern to curtail the conceptualization, development, possession, proliferation, use, and effects of WMD, related expertise, materials, technologies, and means of delivery*.[10] The DoD recently updated its approach to CWMD by designating U.S. Special Operations Command (USSOCOM) as the CWMD global coordinating authority.[11] USSOCOM does not have the responsibility to coordinate operations across the Geographic Combatant Commands, but it did publish a Functional Campaign Plan and issue planning guidance and intelligence collection requirements.[12] The DoD significantly increased its unity of effort when it transferred responsibility of CWMD from U.S. Strategic Command (USSTRATCOM) to USSOCOM. This is partially because USSTRATCOM has a number of important, competing responsibilities: global strike, air defense, cyber operations, and information operations. Furthermore, CWMD shares many similarities with counter terrorism, a mission at which USSOCOM excels.

Pathway Defeat

There are several points in time to counter the maturation of a WMD program: before acquisition, during development, and after a capability has been operationalized. It is better to prevent a program before it starts. There are several areas that can be addressed either sequentially or in parallel depending on how advanced a WMD program is. These aspects are intent, infrastructure, expertise, production, weaponization, and delivery systems. A program can progress along any one of these lines of effort independently and thus can be addressed and targeted independently. In order to achieve the strategic end states of no new WMD, no WMD use, and minimize WMD effects, JP 3-40

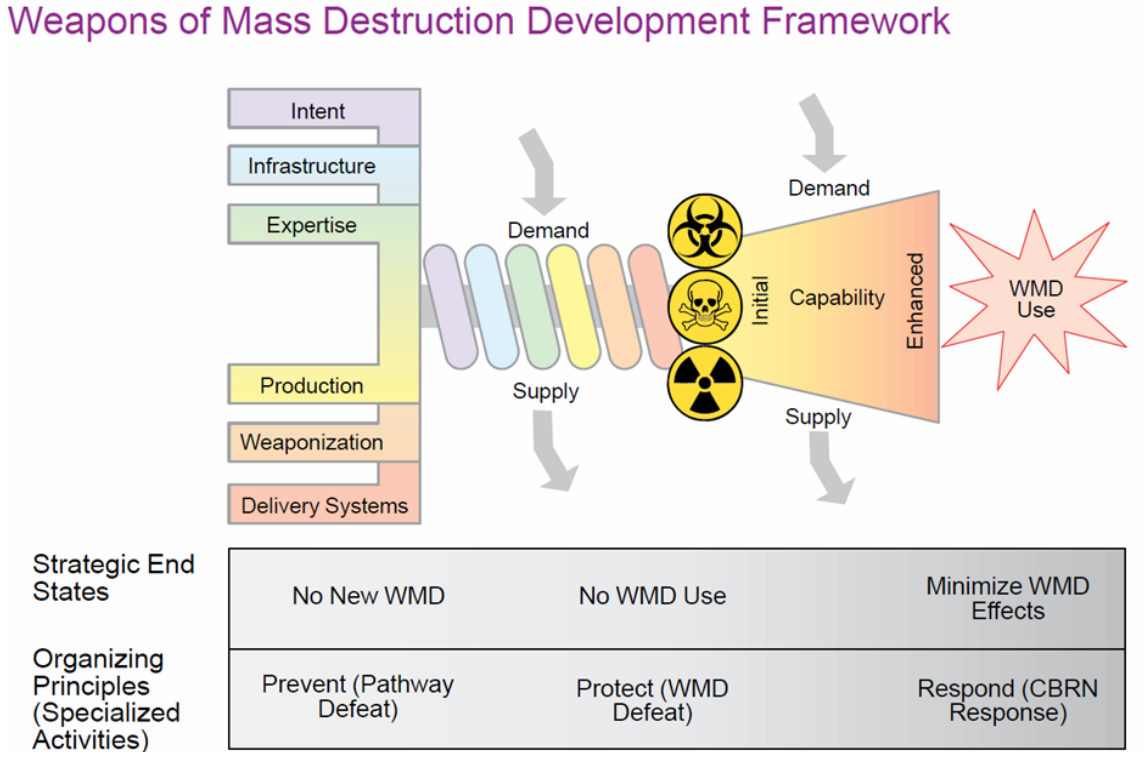

Figure 1: Weapons of Mass Destruction Developmental Framework from JP 3-40[13]

organizes CWMD operations and activities along three principles: prevent, protect, and respond. Most important to preventing the acquisition of WMD is the pathway defeat special activity. Figure 1 provides a visualization of these principles.

Pathway defeat is defined as "activities to dissuade, deter, delay, disrupt, destroy, deny, and assure to complicate conceptualization, development, production, and proliferation of weapons of mass destruction."[14] Figure 2 depicts when these activities are most effective. Pathway defeat includes activities to target the networks and nodes of finance, technology, personality, and knowledge transfer of WMD technology. Pathway defeat activities are upstream of state and non-state actors' WMD procurement and prevent their acquisition through lethal and non-lethal targeting. One way to do this is to place components on control lists such as the Australia Group Common Control Lists for chemical and biological weapons.[15] Nuclear material and component control or trigger lists are managed by the Nuclear Suppliers Group[16] and Zangger Committee.[17] Controlling the import and export of such components prevents a state from building up a weapons program. Other ways to prevent WMD acquisition are to interdict unauthorized shipments of dual-capable components; track financial transactions between known financiers, scientists, and institutions of concern; gather intelligence; and conduct cyber and information operations. Pathway defeat also includes diplomatic efforts to stem the intent of a state to pursue WMD capabilities. Enforcing international norms and agreements greatly contribute to the nonproliferation of WMD. In conjunction with nonproliferation initiatives, a whole of government, pathway defeat approach is the best way to prevent state and non-state acquisition of WMD and hostile use of technology.

The United States and international community aggressively used pathway defeat against Iran's nuclear weapons program. While it is very difficult to dissuade the Iranian regime's desire and intent to pursue nuclear weapons, an international coalition is taking measures to dissuade, deter, delay, disrupt, destroy, deny, and

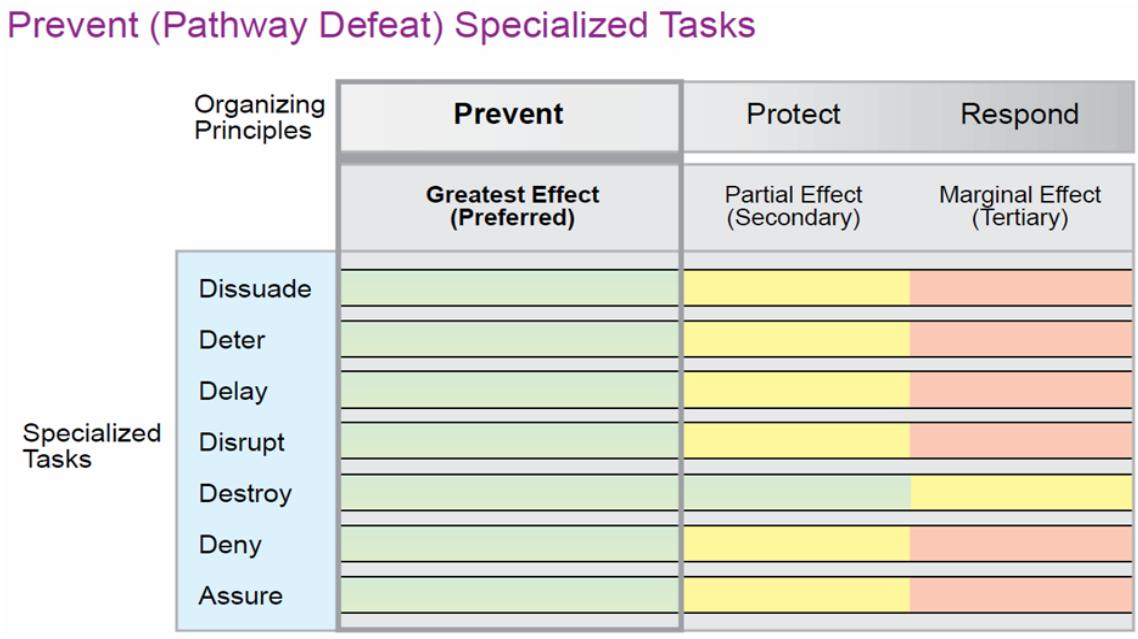

Figure 2: Pathway Defeat Specialized Tasks from JP 3-40[18]

assure Iran in order to prevent its WMD acquisition. The Joint Comprehensive Plan of Action (JCPOA) was endorsed by China, France, Germany, Russia, the United Kingdom, and the U.S. to curtail Iran's nuclear program.[19] In exchange for lifting U.S. EU, and UN sanctions, Iran would stop enriching uranium, dismantle excess centrifuges, cease advance technology development, disable some nuclear infrastructure, and allow the International Atomic Energy Agency (IAEA) to conduct verification inspections. Despite pulling out of the JCPOA, the United States and its partners are committed to aggressively pursuing pathway defeat activities. Prior to JCPOA, Iranian scientists, regime officials, and banks were targeted with sanctions; corporations were prohibited from conducting business with Iranian entities; and Iranian oil exports were limited. Pathway defeat tasks can be even more physically destructive. The Stuxnet cyber-attack probably destroyed a fifth of Iran's advanced centrifuges at Natanz.[20] Some WikiLeaks documents claim that Israel destroyed a nuclear facility in 2011.[21] Meanwhile Iranian nuclear scientists have been detained[22] or killed[23] to thwart their nuclear weapons. Indirectly related, Israel also destroyed a Tehran-funded, Syrian nuclear facility in 2007, a reported hedge for Iran's program.[24] The activities mentioned above highlight the kinetic and non-kinetic actions governments are willing to implement in order to thwart a WMD program.

These actions are not sporadic. They are a part of a network analysis, targeting key linkages and nodes of a complex adaptive system. A determined adversary will continue to adjust its tactics and strategies to achieve its program's goals. A WMD program must be targeted holistically. The financiers, ideologues, researchers, scientists, and machinists are all a part of a human network working on the project. Tracking finances and resources from the government, funneled through intermediaries and corporations, is important to interdict these funds. Seizure of funds cannot be conducted in a vacuum. It must be done in concert with confiscating vital technologies, freezing government assets, restricting travel of key individuals, arresting those violating export controls, and leveraging international legal systems to exert maximum pressure on the government.

Yet pathway defeat can be a mixture of both carrot and stick. Counter proliferation and nonproliferation activities have been successful in convincing states with chemical and biological weapons to abandon their programs and, for some states, like South Africa, to abandon their nuclear programs. With regards to Iran and North Korea, such efforts have delayed their programs. Little can be done if a state or non-state actor is absolutely intent on acquiring WMD, yet their programs can be thwarted and delayed. A cohesive international approach is required to reign in malign actors.

Hostile Technology

The history of chemical and biological warfare predates World War I. Nuclear weapons emerged at the close of World War II. Countering Weapons of Mass Destruction strategies focus on methods that are over 75 years old. Minus treaties and agreements on staging, basing, and delivery systems, little has been done to address emerging technologies. Many weapon system developments since the end of the Cold War have focused on improving existing capabilities: stealth aircraft, precision munitions, and vehicle survivability--nothing that constitutes a revolution in military affairs.

While drone technology has existed since the 1950s, it was not until the widespread use of drones in Iraq and Afghanistan by coalition forces that their effectiveness and lethality became apparent. Unmanned vehicles are readily available for use by armed forces, terrorists, and hobbyists alike. The ease of which unmanned technology has permeated society, law enforcement, and security services highlights the duality of technology. Drones can be used to assist farmers with surveying fields or monitoring livestock. They can be used by police to track criminal activities. Meanwhile, military applications of drone technology are expanding. Conversely, criminals and terrorists have used drones to conduct attacks, challenge national security infrastructure, and even place radioactive material on the Japanese Prime Minister's office building.[25] Moreover, the future of aerial combat could be dominated by swarms of linked drones.[26] Cheap, inexpensive drones could be used to overwhelm or perforate air defense systems or physically disrupt flight paths. Larger drone aircraft could be tethered with piloted planes, creating formations of wingman empowered with Artificial Intelligence (AI) technology. This example alone shows the dual nature of emerging technology. Inexpensive, commercially available Da-Jiang Innovations Technology Company (DJI) drones synched with a smartphone can easily be used as a plaything for children while more robust models are used by the film industry. Other larger systems can be used for medical evacuation or delivery of humanitarian assistance or disaster relief. How do governments control this type of emerging technology? Can elements of CWMD pathway defeat be applied?

Existing export controls are a step in the right direction. There is a great deal of collaboration between the Department of Treasury, Department of State, and Department of Commerce to monitor and enforce multilateral export control regimes. Organizations such as the Australia Group, Nuclear Suppliers Group, and Missile Technology Control Regime work to limit the transfer of WMD and military technology to restricted countries. When reviewing the Wassenaar Arrangement's list of dual-use goods and technologies, much of the flagged items relate to existing military technology.[27] The restricted items are linked to end products or materials for the manufacturing of chemical, biological, nuclear, missile, and aviation technologies. One could argue that this is intended to safeguard existing military capabilities. More needs to be done on emerging, disruptive technology. Export control is key for pathway defeat and disrupting hostile technologies.

Like unmanned vehicles, other technologies are emerging to change not only how we live but how we fight wars. High powered lasers, quantum technologies, autonomous platforms, artificial intelligence (AI), synthetic biology, materials-by-design, and convergent manufacturing all will shape our future. While some technologies already exist, such as lasers, they have not been vastly employed as offensive weapons. Other technologies like hypersonics, while new and have novel propulsion systems, are essentially enhanced cruise missiles. Little can be done to prevent existing weapon programs from advancing.

Truly disruptive technologies are the likes of 3-D printers which can handle special nuclear material or replicate on such a massive scale that supply chains disappear. Networked, autonomous vehicles (land, sea, or air), managed by AI, create a completely new battlefield. The moral and ethical consequences of unmanned machines conducting independent identification and targeting have not been properly addressed.

Recently China used AI facial recognition software to identify and arrest a wanted man at a 60,000 person crowded concert.[28] Synthetic biology, also referred to as living foundries, can create bioengineered structures[29] or self-healing armor.[30] What happens when a state creates an organism that eats or degrades steel or concrete? A government could use CRISPR (Clustered Regularly Interspaced Short Palindromic Repeats) technology[31] to modify plastic eating bacteria,[32] then unleash it on military infrastructure or equipment. This future is not contained to science fiction. The fact that we cannot contemplate all the useful and nefarious aspects of these emerging technologies highlights the need to have a framework in place.

Pathway defeat can be used as a protocol to control the growth of hostile technology. While it is beneficial to support much of the research in these areas, leveraging pathway defeat concepts can thwart malign programs. As sectors explore the full potential of their research, certain areas of risk need to be highlighted. As state research institutions begin to veer down an unwanted path, individuals, institutions, and finances can be flagged and targeted. Diplomatic efforts can highlight emerging nefarious technology and make its pursuit internationally unacceptable.
Instead of debating whether a lethal, autonomous machine (be it robot or aircraft) is a WMD, leaders can employ elements of pathway defeat to stave off such development. Recognizing that there are significant moral hurdles for enabling machines to kill or destroy targets without having humans in the loop, the international community can come together and prohibit this capability. Drafting and enforcing such a treaty is a collective effort. Critical components can be identified and placed on export control lists. Governments, institutions, and individuals associated with research and funding can be targeted with sanctions and legal prosecution. States pursuing said hostile technology can be ostracized and receive sanctions until they abandoned their programs. Pursuing pathway defeat accomplishes the same end state without having to designate a technology as a WMD. The same construct can be applied to all sorts of hostile technology. Disrupting supply chains for rare earth metals, specific to a technology, would also aid in the effect. Even if adversarial development of nefarious technology cannot be stopped, intelligence operations could be employed to map the networks and understand how the systems and nodes are interconnected, which will pay dividends if something more aggressive is warranted.

CWMD and pathway defeat activities are not always successful. Libya and Iraq abandoned their programs while Iran and North Korea continue to develop theirs in the face of staunch sanctions. Despite CWMD operations not providing a perfect framework, pathway defeat activities can address and shape the future conduct of war. As the world enters a new age where technology and interconnectedness will rapidly shape our future, something needs to be in place to address the future threats realized from emerging technology. A pathway defeat construct can address the hostile use of technology. Attempting to wrap every potentially malign use of technology into an already unwieldy WMD definition will not be effective. It is better to use the pathway defeat framework, while leveraging existing export control regimes, diplomatic and legal frameworks, and intelligence activities to prevent the use of hostile, emerging technologies. Our adversaries will continue to search for asymmetric capabilities. The introduction of nuclear weapons three-quarters of a century ago had profound geopolitical repercussions and reshaped international relations and how we fight wars. A broader

pathway defeat concept will allow us to address unseen and unimagined threats in the future.

Notes:

1. Thomas Kuhn, The Structure of Scientific Revolutions, 1962.
2. Matt Reynolds, "Deep Mind's AI Beats World's Best Go Player in Latest Face Off," New Scientist, 23 May 2017, https://www.newscientist.com/article/2132086-deepminds-ai-beats-worlds-best-go-player-in-latest-face-off/#:~:text=AlphaGo%20is%20at%20it%20again,four%20hours%20and%20fifteen%20minutes.
3. Joint Chiefs of Staff, "Joint Countering Weapons of Mass Destruction," Joint Publication 3-40, November 2019, GL-5.
4. Dr. W. Seth Carus, Occasion Paper No. 8 Defining "Weapons of Mass Destruction," National Defense University Press, January 2012, 6.
5. Homeland Security Advisory Council Weapons of Mass Effect Task Force on Preventing the Entry of Weapons of Mass Effect Into the United States, January 10, 2006, 3.
6. "Russia Spy Poisoning: What We Know So Far," BBC, 8 October 2018, https://www.bbc.com/news/uk-43315636
7. "Kim Jong-nam Killed VX Nerve Agent, say Malaysian Police," 24 February 2018, https://www.theguardian.com/world/2017/feb/24/kim-jong-nam-north-korea-killed-chemical-weapon-nerve-agent-mass-destruction-malaysian-police
8. Al Mauroni, "Russia's Chemical Romance: Don't Call it a WMD Attack," 16 March 2018, https://warontherocks.com/2018/03/russias-chemical-romance/
9. Organisation for the Prohibition of Chemical Weapons, "Chemical Weapons Convention," https://www.opcw.org/chemical-weapons-convention.
10. JP 3-40, GL-5.
11. Department of Defense, "DOD Directive 2060.02: DOD Countering Weapons of Mass Destruction (WMD) Policy," 27 January 2017, https://www.esd.whs.mil/Portals/54/Documents/DD/issuances/dodd/206002_dodd_2017.pdf
12. "Statement of LTG Joseph L. Osterman, USMC, Deputy Commander, USSOCOM before the House Armed Services Committee Subcommittee on Emerging Threats and Capabilities, 22 March 2018," https://docs.house.gov/meetings/AS/AS26/20180322/108018/HHRG-115-AS26-Wstate-OstermanJ-20180322.pdf
13. JP 3-40, II-8.
14. JP 3-40, GL-5.
15. The Australia Group, "Australia Group Common Control List Handbooks," https://www.dfat.gov.au/publications/minisite/theaustraliagroupnet/site/en/controllisthandbooks.html.
16. Nuclear Suppliers Group, "NSG Part 1 and Part 2 Control Lists Updated," https://www.nuclearsuppliersgroup.org/en/news/185-nsg-control-lists-updated.
17. Zangger Committee, "Information Circular 209 Rev 5," 5 March, 2020, http://www.zanggercommittee.org/publications.html.
18. JP 3-40, IV-5.
19. UN Security Council, "Security Council Resolution 2231 (2015) Joint Comprehensive Plan of Action on the Islamic Republic of Iran's Nuclear Programme," 20 July 2015, https://www.europarl.europa.eu/cmsdata/122460/full-text-of-the-iran-nuclear-deal.pdf
20. William Broad, John Markoff, and David Sanger, "Israeli Test on Worm Called Crucial in Iran Nuclear Delay," The New York Times, 15 January 2011, https://www.nytimes.com/2011/01/16/world/middleeast/16stuxnet.html.
21. Raphael Ahren, "Wikileaks: Israel Destroyed Iran's Nuclear Program Last Year," The Times of Israel, 27 February 2012, https://www.

timesofisrael.com/israel-destroyed-irans-nuclear-program-already-last-year-leaked-intelligence-claims/.
22. “Iranian Scientist Acquitted in U.S. Trade Secrets Case Deported,” Time, 2 June 2020, https://time.com/5846445/iran-scientist-deported/
23. “How Israel, in Dark of Night, Torched Its Way to Iran’s Nuclear Secrets,” The New York Times, 15 July 2015, https://www.nytimes.com/2018/07/15/us/politics/iran-israel-mossad-nuclear.html.
24. Noah Klieger, “A Strike in the Desert,” Ynet news.com, 11 February 2009, https://www.ynetnews.com/articles/0,7340,L-3799227,00.html.
25. Benjamin Wittes, “Drone with Radioactive Material Lands on Japanese Prime Minister’s Office,” Lawfare, 22 April 2015, https://www.lawfareblog.com/drone-radioactive-material-lands-japanese-prime-ministers-office.
26. James Rogers, “The Dark Side of our Drone Future,” Bulletin of the Atomic Scientists, 4 October 2018, https://thebulletin.org/2019/10/the-dark-side-of-our-drone-future/.
27. Wassenaar Arrangement Secretariat, “Public Documents Volume II, List of Dual-Use Goods and Technologies and Munitions List,” Wassenaar Arrangement, December 2019, https://www.wassenaar.org/app/uploads/2019/12/WA-DOC-19-PUB-002-Public-Docs-Vol-II-2019-List-of-DU-Goods-and-Technologies-and-Munitions-List-Dec-19.pdf.
28. Sara Malm, “Chinese Police Use Facial Recognition Technology to Pick Out a Suspect in 60,000-Strong Concert Crowd and Arrest Him,” Daily Mail.com, 12 April 2018, https://www.dailymail.co.uk/news/article-5607559/Chinese-police-arrest-man-using-facial-recognition-60-000-concert.html.
29. Kevin W. Keating and Eric M. Young, “Synthetic Biology for Bio-derived Structural Materials,” Current Opinion in Chemical Engineering, Volume 24, June 2019, 107-114, https://www.sciencedirect.com/science/article/pii/S2211339818300856.
30. Kris Osborn, “How the U.S. Army Wants to Make Self-Healing Armor,” The National Interest, 4 June 2020, https://nationalinterest.org/blog/buzz/how-us-army-wants-make-self-healing-armor-160606.
31. Jennifer Doudna, “Genome Engineering with CRISPR-Cas9: Birth of a Breakthrough Technology,” iBiology.org, January 2015, https://www.ibiology.org/genetics-and-gene-regulation/crispr-cas9/.
32. Deborah Netburn, “Newly Discovered Bacteria Can Eat Plastic Bottles,” Los Angeles Times, 11 March 2016, https://phys.org/news/2016-03-newly-bacteria-plastic-bottles.html.

Chemical Fractionation Is Not a Constant: Revisiting Bomb Vapor Chemistry

Yves M.X.M. Dardenne, Winifred E. Parker, Kim B. Knight
Lawrence Livermore National Laboratory

Summary

The debris produced by a nuclear explosion forms a hazard to response, can serve as a record used to interpret the event, and may persist in the environment necessitating long term management. Hence, understanding the radiochemical inventory of nuclear debris remains an important area of study, particularly the behavior and resulting distribution of actinides and fission products. Despite formation in a high energy environment, it has been recognized for decades that the chemical and isotopic composition of debris rarely, if ever, captures a homogenized blend of the bomb products. Instead, during cooling and debris formation, a variety of chemical processes cause separation of the different constituents. This process of chemical fractionation creates debris with a variety of different radionuclide inventories. Here we provide an overdue re-examination of our historic basis for understanding chemical fractionation in nuclear explosions through the context of new characterization of a large set of historical nuclear test data. We then discuss the implications of our findings for advancing models of radionuclide distribution and post-detonation chemical fractionation.

Introduction

In the study of radionuclide inventories in nuclear explosion debris, chemical fractionation is defined as "any alteration of radionuclide composition occurring between the time of detonation and the time of radiochemical analysis which causes the debris sample to be non-representative of the detonation products as a whole."[1] Work by E. C. Freiling[2-6] and his contemporaries in the 1960s attempted to describe chemical fractionation systematics for high-yield nuclear explosions based on observation. These empirical studies laid a lasting framework, derivations of which continue to be used today to approximate radionuclide distribution and behavior following a nuclear explosion. Yet even Freiling and his contemporaries recognized that the nuclear test conditions studied at the

Staff Physicist Yves Dardenne is the Debris Diagnostics lead for National Technical Nuclear Forensics at the Lawrence Livermore National Laboratory in Livermore, California. He has a B.S. in Chemistry from Eastern Michigan University and a Ph.D. in Physical Chemistry from Michigan State University. He has worked on interpreting nuclear weapons debris for the past 22 years. His email address is dardenne2@llnl.gov.

Dr. Kim B. Knight is a staff scientist in the Nuclear and Chemical Sciences group of Lawrence Livermore National Laboratory in Livermore, California, specializing in research supporting forensic investigation of nuclear materials as well as the modern study of historic fallout. She has a B.A. in Geology from Carleton College and a Ph.D. in Earth & Planetary Science from the University of California, Berkeley. She was previously a post-doctoral researcher studying cosmochemistry at the University of Chicago.

time represented only a small portion of many possible conditions and contained multiple inconsistencies contradicting their developing theories.

Freiling's foundational work defined a prescriptive set of assumptions governing radionuclide fractionation behaviors, now overdue for critical reevaluation. This document does not attempt a comprehensive review of chemical fractionation theory and simulation up to the modern day. Instead, we focus on exploration of the underlying assumptions and conclusions of the original and impactful Freiling studies. We describe several reasons why the underlying assumptions concluded from these early observations, many of which still surface in modern treatments, may be inadequate to support modeling constructs predicting radionuclide distributions. We then present new evaluations of chemical fractionation behavior based on a comprehensive study of available historical nuclear test data. Finally, we lay out findings motivating the need for development of new understanding of the factors influencing chemical fractionation behavior in nuclear explosions.

The Historic Basis of Post-Detonation Chemical Fractionation

The process of post-detonation chemical fractionation is notionally simple to understand but complicated to predict. As the fireball cools from a temperature many times hotter than the surface of the sun to ambient temperatures over timescales of seconds,[7] radionuclides produced from nuclear fission undergo recombination with electrons, forming compounds with other components in the vapor phase. The specific species formed is likely sensitive to a variety of factors including the composition of the source vapor, the availability of oxygen, and the thermal profile of the fireball.[8,9] As the fireball cools and the condensation temperature of a given radionuclide compound is reached, that compound can condense and be removed from the system in solid form. Species that condense at relatively high temperatures (more refractory species) can thus be removed from the cooling system at earlier times relative to those tending to stay in a vapor form until cooler temperatures are achieved (more volatile species).

Temperature dependent condensation and subsequent removal of radionuclide species causes the radionuclide inventory in the fireball (and correspondingly, the radionuclide inventory captured in fallout) to change as a function of time. The actual picture of the time-dependent fireball radionuclide inventory is, of course, complicated by a multitude of additional factors including concurrent radioactive decay changing the identity of elements (and therefore their chemical properties), the partial pressures between the liquid and vapor phases present in the fireball, and by the probable lack of equilibrium conditions.[10] Furthermore, while it has generally been assumed that abundant oxygen is drawn into the fireball shortly following an explosion, such that radionuclides will tend to combine into oxidized species, multiple recent studies call into question assumptions of a fully oxidized system.[11-12]

Early in the era of nuclear testing, significant work was done to predict the behavior of volatile and refractory species in a nuclear explosion and its subsequent plume with the intent to safeguard a potentially exposed population and to aid in response. This historical work compiled data from a limited number of nuclear tests to provide a simplified framework capturing the order of condensation for different isotopes from a nuclear fireball.[2-6] The foundational framework, referred to as the Freiling ratio, represents for fission products the degree of chemical fractionation for a given mass chain. Variations of the Freiling ratios are used as the basis for defining each radionuclide as refractory or volatile at the time of solidification and govern chemical fractionation behaviors in some post-detonation models to this day.

To arrive at the 'Freiling ratios', Freiling combined observational data from some available sources. In constructing his approach, he started with the premise that chemical fractionation behavior of a given radionuclide is a constant from event to event. A number of consequential assertions fell out from his starting assumption including:

1. Data from one event can be overlapped with data from any other event.
2. The order of condensation, and thus

chemical fractionation behavior, from isotope or mass chain to isotope or mass chain is effectively constant (e.g., the relative degree of refractory or volatile behavior between ^{140}Ba and ^{95}Zr does not vary).

3. Chemical fractionation shares a logarithmic relationship with particulate size (later referred to as the radial power law activity size distribution[3,13]) and can be used to establish activity-size distributions proportional to fallout particle volumes (for refractory species) or surfaces (for volatile species).

Although Freiling's generalization of radionuclide fractionation behavior in nuclear explosions was groundbreaking for its era and has proved adequate for many general radionuclide assessments of nuclear plume inventories, it has long been clear that a variety of exceptions exist to the assumptions upon which these approaches are based. An example of the limitations of historical models is explaining the contrasting volatility behavior of U in air burst compared to surface burst debris. In air burst debris, U behaves with intermediate volatility, being relatively enriched in smaller particles collected on air filters.[5,14] Once detonations incorporate significant amounts of environmental material, depending on the environment and detonation conditions, U is observed to alter its fractionation behavior. In high-yield events conducted over coral, U has been observed to behave as a strong refractory, whereas in explosions over silicate soils, U tends to become more refractory, but still fractionates appreciably from ^{95}Zr and ^{239}Pu. This behavior is not predicted or explained by fallout formation models and is only taken into account by relying on empirical datasets from historic U.S. tests.

Here we will argue why Freiling's initial assumptions are incorrect and show that a more complete data set highlights a variety of deviations from the behaviors he generalized. Through examination of chemical-fractionation metrics from a much larger set of data encompassing a wide range of types of nuclear tests and nuclear test environments, we come to a different set of conclusions. The metric used for this study demonstrates that, for bulk samples, chemical fractionation can be distinctly different from one event to another event. Although this was often recognized historically,[15] data sets were not sufficient at the time to offer better solutions. However, our results now clearly show that data from one event should not be admixed with another event. We also show that there is no robust, predictable relative chemical-fractionation order between fission chains nor between elements. Indeed, based on what we are coming to understand about differences in the local environment and source terms, we argue that there is no reason to expect a constant chemical-fractionation order for nuclear explosions. Past data evaluation likely saw these results due to similarities in the tests and/or local conditions being compared. We find no consistent dependence of chemical fractionation on the energy output from the event, which naively might be thought to dictate the temperature/time and therefore condensation profile. Lastly, we point out that the uncertainty treatment in the historical work was minimal (though appropriate to the mission at the time). New computational capabilities are now hindered by the quality of work that, while cutting edge 60 years ago, now buoys false confidence in modern model outputs. In this work we propagate the uncertainties throughout the analysis to ensure appropriate conclusions.

The Historical Approach to Chemical Fractionation

The 1960s approach to generalize chemical fractionation[2-6] combines data from multiple samples of multiple measured fission products (FP) across multiple events into a single plot. Data plotted[2] comingle samples from four Pacific US tests including a coral surface burst, shallow water surface burst, deep water surface burst, and sub-megaton deep water surface burst. The types of samples include collected particulates from direct fallout onto trays as well as cloud samples collected at the point a plane could 'safely' fly through the cloud and times thereafter. Later work increased the number of events. Measured FPs were converted to a total number of fissions using the fission-chain-yield. Freiling's choice of X-axis (r95,89) represents the ratio of fissions obtained from ^{95}Zr relative to the ratio of fissions obtained from ^{89}Sr. This choice of ^{89}Sr and ^{95}Zr fission products provided a volatility metric, with ^{89}Sr and the 89 mass

chain behaving more volatile relative to ^{95}Zr and the 95 mass chain, considered refractory. The Y-axis in Freiling's plots (rYYY,89) represents the ratio of fissions obtained from any other measured fission product (YYY) relative to the ratio of fissions obtained from ^{89}Sr. Importantly, all plots in these papers were published on a log-log scale.

Chemical fractionation, as applied to post-detonation scenarios, can be thought of as the departure of fission product ratios from what would be expected had the entire radionuclide inventory of debris field been captured. In Freiling's three isotope FP plots, if no chemical fractionation has occurred between any of the three FPs, the data will sit at the (1,1) data point. Deviations in three isotope space should create a linear array going through the (1,1) point with the slope of the line representing the relative volatility for the system. In Freiling's plots, however, only ^{90}Sr meets this criterion (though no error envelopes for the lines are provided). The mismatch of the data to the (1,1) point may result from a number of issues such as 1) incorrect fission-chain-yield data or other nuclear data inconsistencies, 2) issues with sample analysis and/or measurement, and 3) incorrectly assuming (as will be shown) that chemical fractionation is constant from event to event. Thus admixing data from multiple events should provide improved fit. The steepness of the generated slopes for each fission product trend was used as a volatility metric to assign a volatility order, cast as a 'Freiling number'.[2] Accepting that the chemical fraction of different isotopes within events and between events has a constant order, these relationships form the foundational 'rules' used to capture post-detonation fractionation.

The time-dependent condensation of species onto and into fallout was used to develop radionuclide distribution theories for fallout formation suggesting refractory species will be sequestered on the inside of fallout particles, and the volatile species will tend to dominate outer surfaces. If this type of radionuclide distribution is supported by activity distributions in fallout, it would indicate that the surface to volume ratio would be a measure of volatility which would indicate that particle size is a metric for volatile behavior. Such assumptions might be correct for small particles but are definitely not correct for object on the mm size or larger. In Figure 1 we show autoradiography[16] for a representative set of samples of the same size range collected from the same event. Radionuclide distributions measured decades after the event are better imaged due to the absence of short-lived species. Alpha emitters (in this case, representing residual Pu) are sharply outlined whereas long-lived beta emitters such as ^{137}Cs and ^{90}Sr appear more diffuse. (Gamma emissions tend to not be captured by such thin films). While both surface and source distributions exist within the population, neither behavior dominates, and Pu is clearly present in both a surface and volumetric distribution. Many samples appear to be a mixture of multiple effects.

Figure 1. Millimeter scale aerodynamic fallout shown optically (left) and in cross section

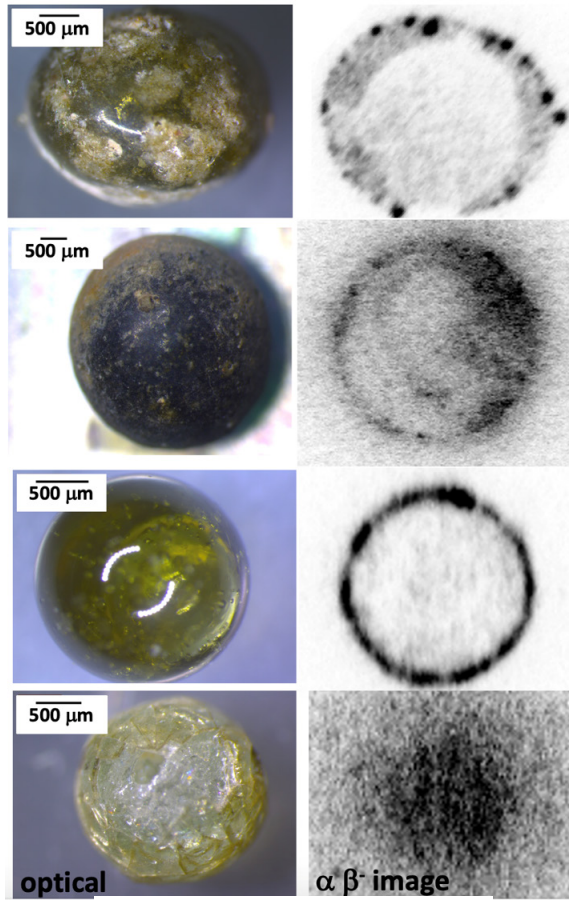

Figure 1. Variations in α/β- Activity Distributions within a Single Size Population and Single Event

as an autoradiograph representing the spatial distribution of long-lived radioactivity (right). Alpha activity is dominated by Pu and provides a sharp outline occurring across volumes and sometimes as a surface deposition. The more diffuse features represent long-lived beta emissions with similarly complex distributions. Simple surface and volume relationships for radionuclide distributions do not necessarily provide the best generalization of such suites of samples.

The approach of combining multiple events together as well as data collected at different times after the explosion (early macroscale fallout collected on plates, for example, relative to air filters collected at different times after the event by flying through the plume) led historical researchers to conclude that chemical fractionation has an inherent logarithmic relationship with particulate size.[3,13] Theory argues that refractory species will tend to precipitate relatively early in the condensation process and the volatile species condense later. In Figure 2, we see measured fractionation data from ground and air samples from a surface detonation overlaid with model activity-size predictions. The construction of theoretical trend lines provides a poor fit to the data. Indeed, drawing such a fit is misleading. While smaller size populations can be expected to capture more contributions of later-formed particles, consideration of gravity alone dictates that larger fallout is much more likely to be the product of early heating and ejection. Thus, these data likely represent distinctly different time steps sampling the radionuclide inventory of the cloud.[17]

Figure 2. Measured fractionation data[14] of from the surface detonation Small Boy overlaid with model predictions after Norman et al, 1970,[18] showing the fractionation of mass chain 89 (considered relatively volatile) from mass chain 95 (considered relatively refractory) plotted as a function of particle size (circles are analytical data, squares are averages). These data are overlaid with predictions assuming refractories become volumetrically-distributed and a diffusion-limited approach. While the diffusion-limited model matches the general trend of the data, it is a poor fit as the plotted data compare populations formed at different times after the explosion.

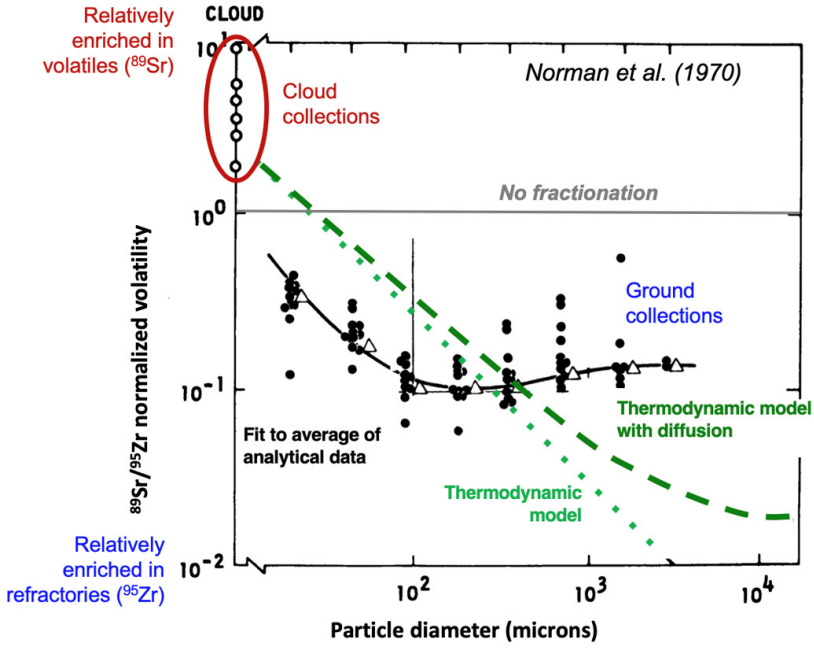

Figure 2. Empirical relationships historically interpreted to relate particle size with radiochemical volatility

The historical approach combined different events and plotted a ratio of FPs. In order to test these hypotheses, we chose data from across wide range of (48) events meeting specific criteria that allowed for robust regression analysis with sufficient event data. These events covered a wide range of yields and depths of burial/heights of burst. We recreate this with a new data set, showing fissions ^{99}Mo/fissions ^{89}Sr vs. fissions ^{95}Zr/fissions ^{89}Sr (Fig. 3a). At first glance, the log-log plots seem to support the Freiling approach, with data able to be fit by a single trend line. Looking at a linear scale plot (Fig. 3b), however, one can see that the dataset contains a subset of linear relationships.

Figure 3. A compilation of historic data from 8 (air only) of 48 events showing ^{99}Mo and ^{95}Zr behavior relative to ^{89}Sr plotted in Freiling's style. a) shows all data in log-log space. b) shows a zoomed in look using linear axes and highlights variations in the data. In c) we see a subset of atmospheric events distinguished by color and suggesting that different events define distinct trends.

In order to better understand these types of data and how best to represent and generalize them, we chose a subset of atmospheric events, only, and replotted these data in Fig. 3b and 3c. As can be better seen within this subset of data, each event suggests a distinct linear trend. Each event however, does not have the same range of data in the X and Y axis. Thus, when looking at plots in Fig. 3a (or indeed, in Freiling's original plots), trends dominated and defined by a few events and combined in log-log space, can appear linear and well behaved. Figure 4 shows (for visual clarity) the extrapolated linear trends for each event that would be observed if all events shared the same range in X and Y data. Clearly each of these atmospheric events has a distinct chemical fractionation trend.

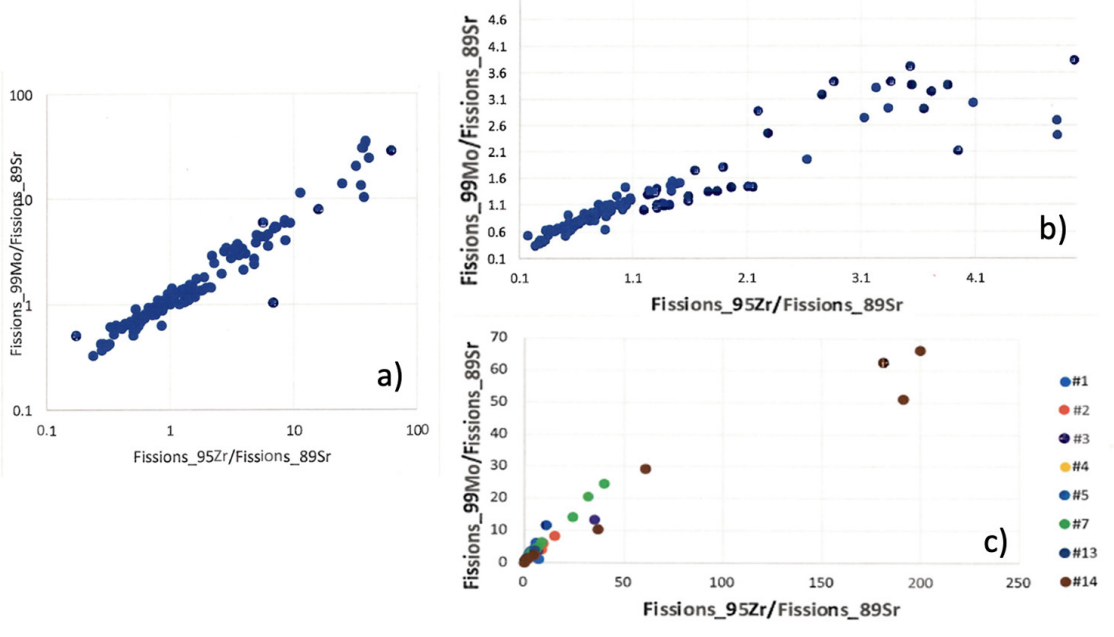

Figure 3. New data sets and observations of chemical fractionation

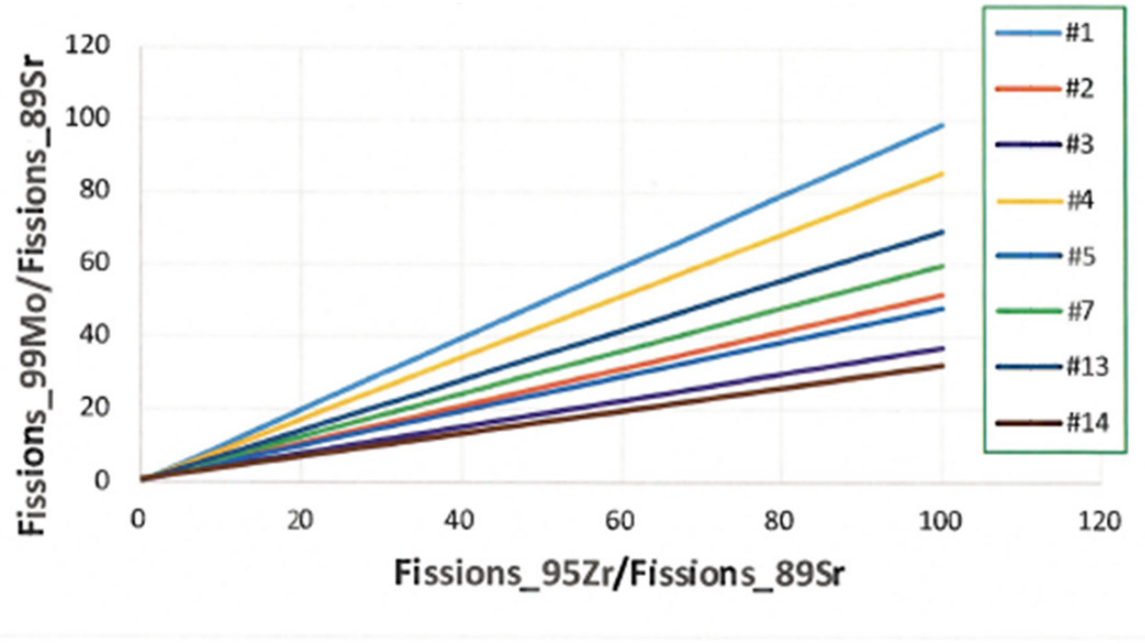

Figure 4. Linear least squares fits for atmospheric events

Figure 4. An extrapolation of event-specific linear least squares fits for the event data shown in Fig. 3c emphasizes the existence of distinct chemical fractionation trends between events.

Patterns in the Linear Fit

A better metric for understanding chemical fractionation is using the slope of the line from the linear fit that the data produce. As demonstrated in Fig. 4, the slope of this line is specific to an event and is due to the extent of chemical fractionation represented in samples all associated with a common source and post-detonation evolution. In the following sections we discuss the meaning of the slopes and present a metric which may be more appropriate to represent event-specific chemical fractionation.

We use the Freiling construct of projecting three isotope plots with the common denominator to represent relative chemical fractionation behaviors between isotopes. Figure 5 is a cartoon representation of the possible patterns that can be observed in data. In Figure 5, the X axis is the ratio of calculated fissions based on ^{89}Sr measurements divided by the calculated fissions based on ^{95}Zr measurements. The Y axis is the ratio of calculated fissions based on ^{137}Cs measurements divided by the calculated fissions based on ^{95}Zr measurements. The purple line is the correlated linear fit,[19-21] the orange curves are the error envelopes, and the cyan lines are the (1,1) point. The green curved line points to the (1,1) point. These patterns are very important as these will be used to define a chemical fractionation metrics that will allow us to cross compare chemical fractionation ranges of the same isotopes from event to event.

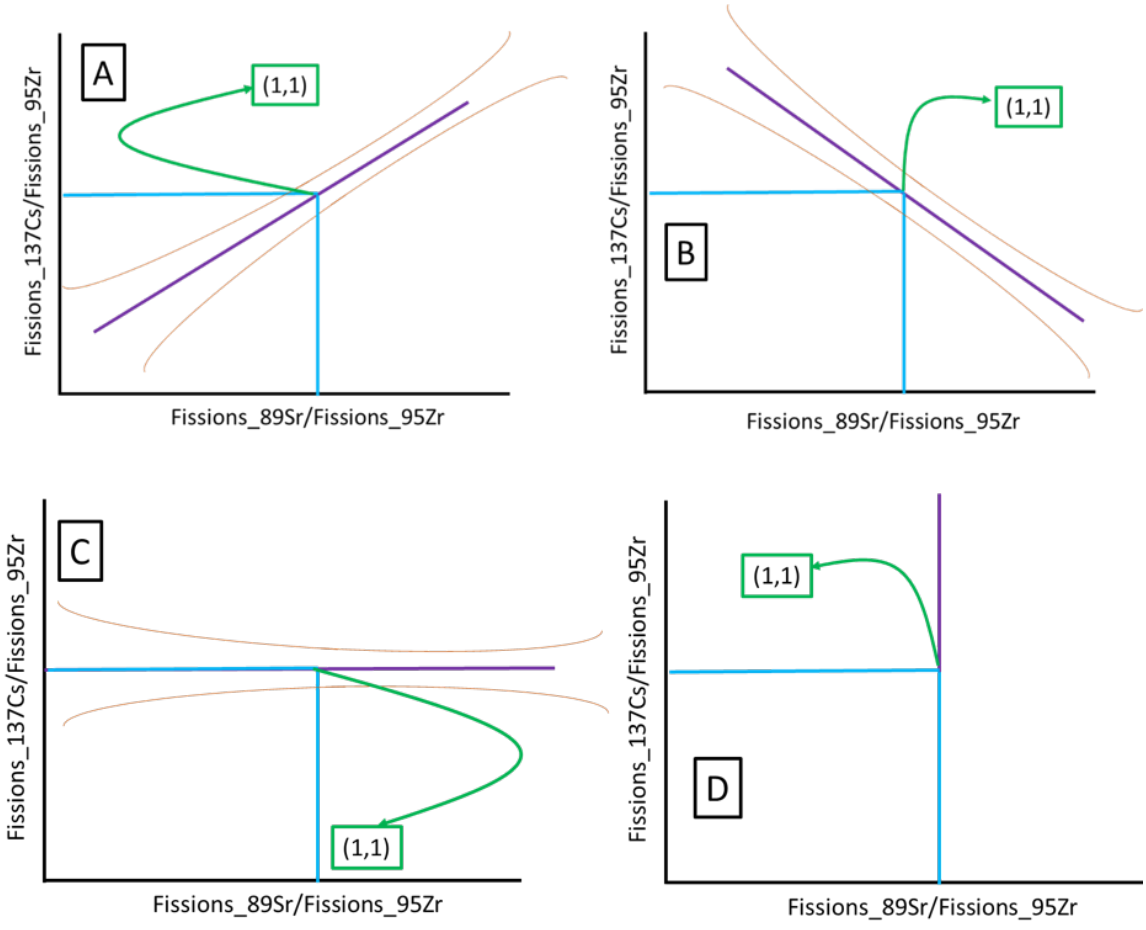

Figure 5. Potential Chemical Fractionation Patterns in Data

Figure 5. Using Freiling's useful construct of projecting three isotope plots with the common denominator to represent relative chemical fractionation behaviors between isotopes, we illustrate potential trends using an example of ^{137}Cs and ^{89}Sr behavior relative to ^{95}Zr: A) shows the positive slope expected if ^{137}Cs is more volatile than ^{95}Zr, B) the negative slope expected if ^{137}Cs is refractory relative to ^{95}Zr, C) the slope=0 expected if ^{137}Cs has the same volatility as ^{95}Zr, and D) the infinite slope expected if ^{89}Sr has the same volatility as ^{95}Zr.

Development of a New Volatility Metric

For this work, we define a theoretical slope representing the chemical fractionation relative to calculated fissions from a given reference (in our work, we used ^{140}Ba measurements). Figure 6 visually shows the concept using ^{89}Sr as a reference as was used in the original Freiling work. Based on knowledge of fission product chain yields it is possible to derive an expected slope for any fission product (FP) (green line in Figure 6). The measured data from one hypothetical event are represented purple crosses with the long-dashed line as the best linear fit to the data. Similarly, the orange crosses with the short-dashed line represent the best linear fit to a second set of hypothetical data. The steepness of the slope allows for an assessment of the chemical fractionation relative to specified references (here, ^{89}Sr and an additional FP, both normalized to a ^{95}Zr basis) within the given event. Choosing a reference and basis with a large potential difference in volatility is optimal, as this results in the best spread of data and a better defined slope. Choosing peak fission products additionally serves to minimize uncertainties.

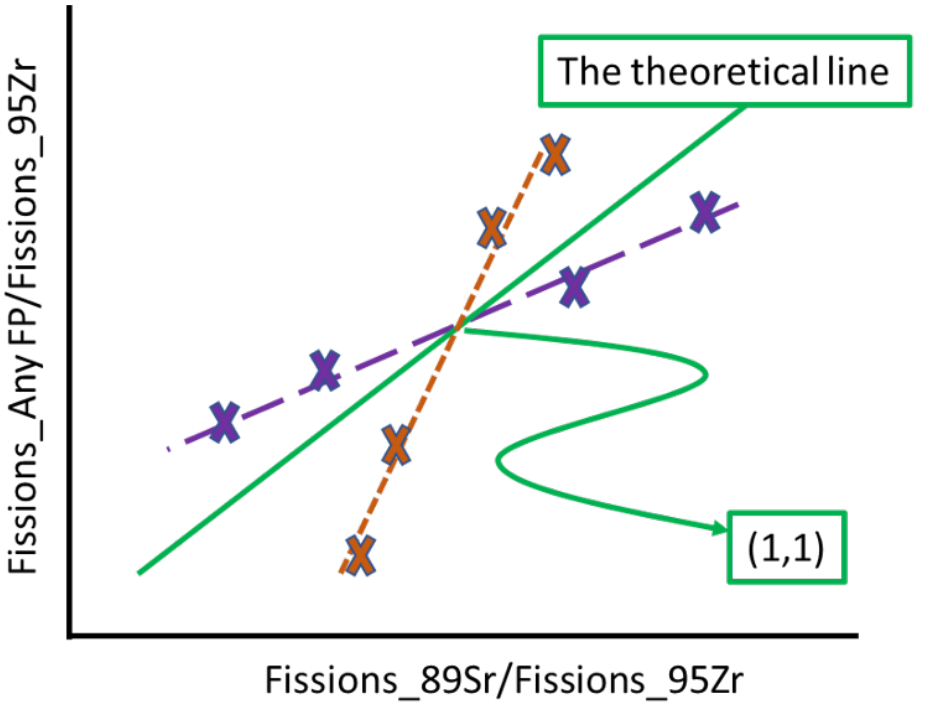

Figure 6. Linear Regression Example

Figure 6. Linear regressions for two fictitious datasets relative to a theoretical slope. Visually, the flatter fit (purple data) represents a relatively less volatile system.

From this understanding, we can develop a metric that will allow us to compare chemical fractionation from event to event. We define this ratio of slopes as the Relative Volatility M

$$RVM = \frac{SLOPE_{measured}}{SLOPE_{theoretical}}$$

The following conclusions can be made about this metric (shown in Figures 5 and 6 relative to a ^{95}Zr basis and a given reference):

1. RVM = 0: means that Fissions_AnyFP and Fissions_basis have the same condensation history
2. 0 < RVM < 1: means that Fissions_AnyFP is more volatile than Fissions_basis but less volatile that Fissions_reference
3. RVM = 1: means that Fissions_AnyFP and Fissions_reference have the same condensation history
4. RVM > 1: means that Fissions_AnyFP is more volatile than Fissions_reference
5. RVM < 0: means that both Fissions_basis and Fissions_reference are more volatile than Fissions_AnyFP

This metric removes multiple dependences and casts behaviors relative to fissions of the chosen reference. For the data summarized here, we used a ^{140}Ba basis. This would not imply that the ^{140}Ba mass chain has the same condensation history from event to event. Instead, this metric allows us to test two of the historical assumptions 1) that condensation from event to event for the same isotope is constant, and 2) that condensation of radionuclides followed the same relative order from event to event as any use of Freiling numbers assumes. Furthermore, a full uncertainty treatment is possible for the linear regressions (i.e., the experimental slopes), any extrapolations, and in the theoretical slope. This concept of the RVM is also applicable to actinides and activations species.

Testing the Relative Volatility Metric

In order to test these hypotheses, we chose data from across a wide range of (48) events meeting specific criteria that allowed for robust regression analysis with sufficient event data. These events covered a wide range of yields and depths of burial/heights of burst. While no data sets contained all of the FPs, actinides, or elements listed, within this compilation we calculated the RVM for the following: ^{89}Sr, ^{90}Sr, ^{91}Y, ^{95}Zr, ^{97}Zr, ^{99}Mo, ^{105}Rh, ^{109}Pd, ^{111}Ag, ^{112}Pd, ^{115}Cd, ^{115m}Cd, ^{125}Sn, ^{126}Sb, 127Sb, ^{129m}Te, ^{132}Te, ^{134}Cs, ^{136}Cs, ^{137}Cs, ^{141}Ce, ^{143}Ce, ^{144}Ce, ^{147}Nd, ^{153}Sm, ^{156}Eu, ^{161}Tb, ^{236}U, ^{238}Pu. Because there is some judgment in which isotope met the criteria for an RVM, particularly choices in extrapolation, this calculation was done independently by two subject matter experts, and then compared.

Figure 7. The Relative Volatility Metric for select FPs plotted as a function of scaled yield. No clear relationship exists correlating with yield.

In Figure 7, we show the RVM with the associated (1-sigma) uncertainties for select FPs. There has long been a question with regard to yield relationships since the original Freiling work was done using data from higher yield pacific events. To address the issue of any first-order relationship between chemical fractionation behavior and yield, we scaled the yields such that the highest yield had a value of 1. As can be seen in Figure 7 there is no strong relationship between degree of chemical fractionation and event yield. Furthermore, it is clear that there is no consistency in the RVM from event to event for these FPs (or, not shown, actinides). Potentially, one could argue that 91Y may approximate constant volatility within 1 sigma uncertainties. In contrast, the Pu shows wide range of volatility. As a whole, however, these data confirm that chemical fractionation trends from one event should not be directly compared to those from another event.

Another way of plotting these data is to create histograms (Fig. 8). To create these histograms, the RVMs were binned for ^{91}Y, ^{236}U, and ^{238}Pu. It is important to keep in mind that this sort of binning does not incorporate uncertainties. It does, however, provide a visualization of the general volatility behaviors across all events and what the generalized trends are (in this representation, relative to ^{140}Ba behavior). As can be seen for ^{91}Y, although there seems to be a tail, the data center about 1,

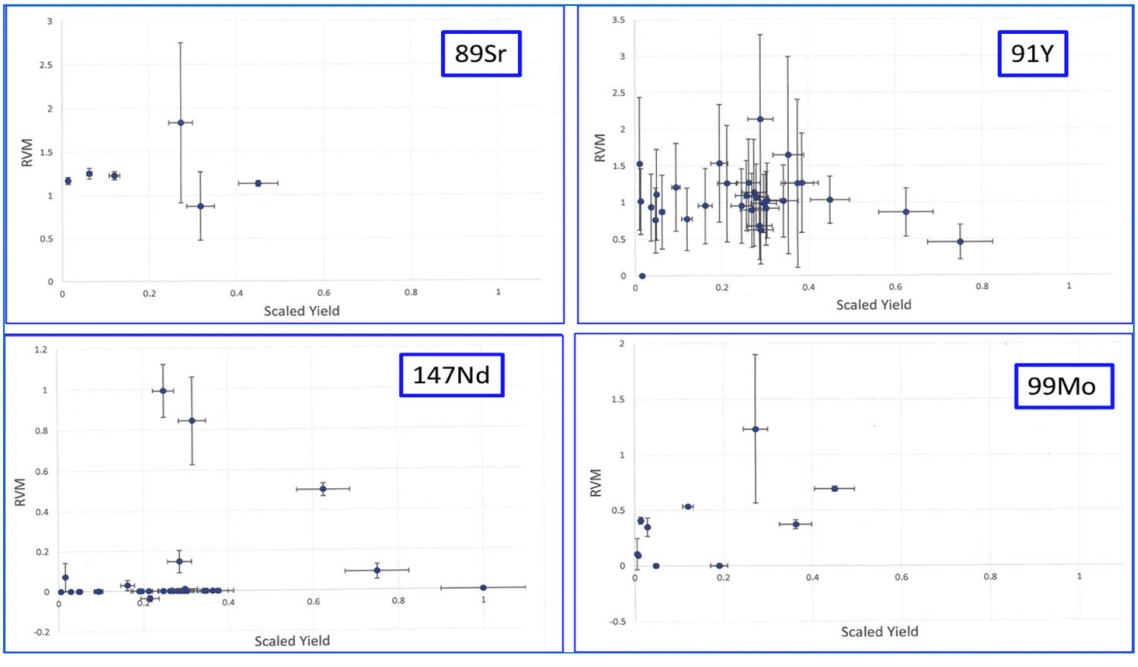

Figure 7. Relative Volatility Metric for select Fission Products and Actinides

implying that ^{91}Y generally behaves similarly to ^{140}Ba. This can also be seen in Figure 8 for the ^{91}Y vs. yield plot (Fig. 7). In contrast, U and Pu display a range of behaviors.

Figure 8. Histograms of the RVM for ^{91}Y, ^{236}U, and ^{238}Pu show a variety of behaviors from event to event. Some relative behaviors such as ^{91}Y show some degree of consistency while others (here, U and Pu) have high level of variation and are likely event-specific.

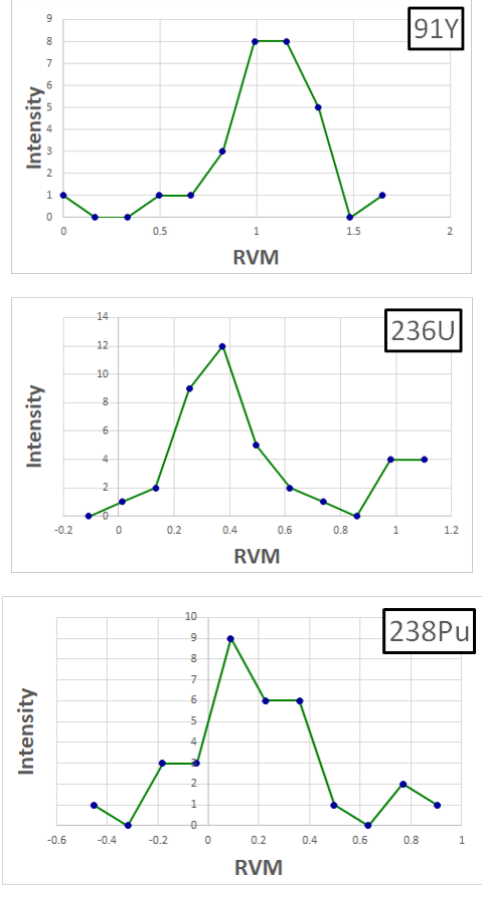

Figure 8. Histograms of the RVM for 91Y, 236U, and 238Pu

To assess if there is a consistent relative order of fractionation from event to event (e.g., if 137Cs fissions are always more volatile than 147Nd fissions), we plot select RVMs relative to one another in Figure 9. No consistency is observed in the relative order of volatility from event to event in these and other (not shown) plots. This again reinforces that data and chemical fractionation behavior from different event are not necessarily comparable. Furthermore, this supports a growing body of data that suggest chemical volatility is not easily predictable and often behaves in ways contrary to the use of Freiling numbers. If Freiling numbers held true, then the different plots in Figure 9 would all be a single point.

Figure 9. RVM comparisons a set of events for ^{147}Nd, ^{144}Ce, ^{238}Pu, and ^{236}U. No consistent behaviors are observed from event to event.

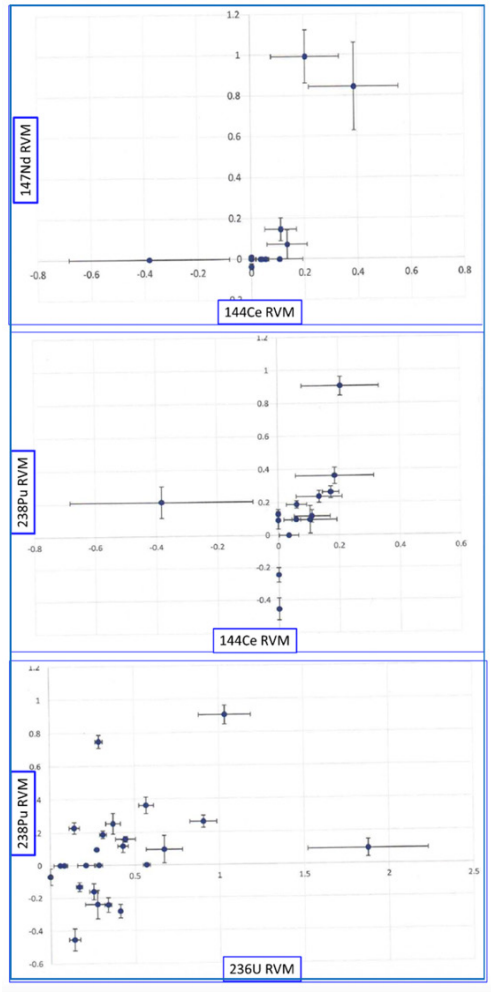

Figure 9. RVM Comparisons for Select Radionuclides

Conclusions

This present work was meant to test the long held and propagated assumptions of foundational work by Freiling to generalize chemical fractionation in nuclear explosions. Specifically, we wished to examine if:

1. chemical fractionation behavior is constant from event to event,
2. the order of chemical fractionation for a given mass chain or element is constant from event to event,
3. data from one event could be overlapped with another event, and
4. chemical fractionation shares a logarithmic relationship with particle size

While such generalization has been sufficient in the past for generalized predictions of chemical fractionation, we have shown that none of these assumptions hold. Instead:

1. Chemical fractionation behavior is not constant from event to event.
2. The order of chemical fractionation (the relative volatilities) observed for given mass chains or elements within a given event are not constant, and there is not yet a basis for understanding if chemical fractionation behaviors observed in one event will apply to another event. This means that Freiling numbers may be used for general modeling purposes, particularly if injects of real data are anticipated, but they do not represent real data trends and are not predictive.
3. Because of #1 and #2, one should not add data together from multiple events when trying to understand the causes of, or develop expectations for, chemical fractionation.
4. Last, the observed logarithmic relationship of the combined data in the original Freiling work is an artifact of fitting a function to data, as the logarithmic behavior was observed by combining data from multiple events. If a logarithmic relationship does exist, it would have to be shown on an event by event basis. Instead, a trend as a function of formation time and expulsion from the fireball is likely to be found and will have some dependency on size (with larger particles sizes becoming depleted from the fireball at earlier times).

We performed linear regressions on the data in order to obtain the slope. Within an event, some FPs (or actinides or activations) had more or less data available than others. In other cases, the range of samples analyzed resulted in a range of different $^{140}Ba/^{95}Zr$ ratios which allowed for a linear fit to be made, but the extrapolation to the (1,1) point was to extreme. For this preliminary study, the choice of which FPs, actinides, and activations included or excluded in a given dataset was based on the level of extrapolation needed to the (1,1) point. To further reduce uncertainties in these conclusions and improve consistency, measurements of additional historic samples, including samples with a greater range of volatilities, would significantly increase select data sets and interpretations.

Within our studied dataset spanning 48 events, we have been unable to discern any universally consistent whole-event chemical fractionation patterns within the data that we accumulated. Additional investigations are warranted, however, as there may exist patterns in multi-dimensional space that will become evident using Principal Component Analysis (PCA) or similar approaches.[22] Most of all, these results emphasize that the assessments and theories of the 1960s may not be sufficient to support the level of prediction and response commensurate with modern computational models. It is clear that the fundamental mechanisms influencing chemical fractionation require additional study such that key physical and chemical processes can be captured into modern models supporting safety and operational response. We conclude that chemical fractionation is much more complex than any comparison (given current data sets) has yet captured, and we predict that variations in chemical fractionation behavior may be strongly influence by secondary factors not traditionally captured in models, such as the material available in and around the fireball, the fireball confinement, non-equilibrium behaviors, and other factors not fully understood.

Acknowledgements

This work was performed under the auspices of the U.S. Department of Energy by Lawrence

Livermore National Laboratory under Contract DE-AC52-07NA27344 and was supported by the LLNL-LDRD Program under Project No. 20-SI-006 and by the Office of Defense Nuclear Nonproliferation Research and Development within the U.S. Department of Energy¹s National Nuclear Security Administration. We additionally thank former students L. Lewis and A. Lundquist for assisting with data and insights associated with this paper. LLNL-JRNL-814770.

Notes:

1. Radioactive Fallout from Nuclear Weapons Tests: Proceedings of a conference held in Germantown, Maryland November 15-17, 1961, ed. A. W. Klement, Jr., US Atomic Energy Commission Division of Technical Information (1962): 541 p.
2. E. Freiling, Radionuclide fractionation in bomb debris, Science 133:1991-1998, 1966.
3. E. Freiling, Theoretical basis for logarithmic correlation of fractionated radionuclide composition, Science 139:1058-1059, 1963.
4. E. Freiling, Estimated degree of fractionation and radionuclide partition for nuclear debris, U.S. Naval Radiological Defense Laboratory, NRDL TR-680, Sep 1963.
5. E. Freiling, G Crocker, and C. Adams, Nuclear debris formation, A. Klement, ed., Radioactive fallout from nuclear weapons tests: Proceedings of the Second Conference, pages 1-43, Washington DC U.S. AEC, 1965.
6. E. Freiling, Mass transfer mechanism in source-term definition, in E. Freiling ed., Radionuclides in the environment, pages 1-12, Wash. DC, American Chemical Society, 1970.
7. S. Glasstone and P. Dolan, The effects of nuclear weapons, US Department of Defense and US Department of Energy, 1977.
8. C. F. Miller, A Theory of Formation of Fallout from Land Surface Nuclear Detonations and Decay of the Fission Products, San Francisco: U. S. Naval Radiological Defense Lab, 1960.
9. Moody K.J, Grant P.M., Hutcheon I.D., Nuclear Forensic Analysis, Second Edition, CRC Press, 502 p., 2015.
10. Weisz, D.G., Crowhurst, J.C., Finko, M.S, Rose, T.P, Koroglu, B., Trappitsch, R, Radousky, H.B., Siekhaus, W.J., Armstrong, M.R, Isselhardt, B.H., Azer, M., Curreli, D., Effects of Plume Hydrodynamics and Oxidation on the Composition of a Condensing Laser-Induced Plasma, J. Physical Chemistry, 122:6, 1584-1591, 2018.
11. W.S. Cassata, S.G., K.B. Knight, I.D. Hutcheon, B.H. Isselhardt, P.R. Renne, When the dust settles: stable xenon isotope constraints on the formation of nuclear fallout, J. Environmental Radioactivity, 137, 88-95, 2014.
12. J.I. Pacold, W.W. Lukens, C.H. Booth, D.K. Shuh, K.B. Knight, G.R. Eppich, K.S. Holliday, Chemical speciation of U, Fe, and Pu in melt glass from nuclear weapons testing, J. Applied Physics, 199, 195102, 2016.
13. Tompkins, R.C., Department of Defense Land Fallout Prediction System – Volume V: Particle Activity. Defense Atomic Support Agency, U.S. Army Nuclear Defense Laboratory, Edgewood Arsenal, MD, NDL- TR-102, DASA 1800-V, AD832239, February 1968.
14. Crocker, G., Kawahara, F. & Freiling, E. Radiochemical Data Correlations on Debris from Silicate Bursts in Radioactive Fallout from Nuclear Weapons Tests: Proceedings of the Second Conference, ed Klement, A. W., U.S. Atomic Energy Commission, 1965, 72–81.
15. R.C. Tompkins, I.J. Russell, M.W. Nathans, A Comparison between Cloud Samples and Close-In Ground Fallout Samples from Nuclear Ground Bursts, Radionuclides in the Environment, E. Freiling Ed., American Chemical Society, 1970.
16. T. Parsons-Davis, K. Knight, M. Fitzgerald, G. Stone, L. Caldeira, C. Ramon, M. Kristo, Application of modern autoradiography to nuclear forensic analysis, Forensic Science International, 286, 223-232, 2018.
17. Lewis, L., The Origin of Agglomerates and their Role in Forming Near-Surface Glassy Fallout, Thesis, Univ. of CA, Berkeley, 2018.
18. Norman, J., Winchell, P., Dixon, J., Roos, B. & Korts, R. in Radionuclides in the Environment (ed Freiling, E.) 13–34 (American Chemical Society, Washington, D.C., 1970).
19. D. York, “Least squares fitting of a straight line” Can. J. Phy. V44 p 1079, 1966.
20. D. York, “Least squares fitting of a straight line with correlated errors” Earth Planet Sci. Lett. 5, 320-324, 1969.
21. D. York, “Unified equations for the slope, intercept, and standard error of the best straight line” Am. J. Phy. V72, No. 3 March 2004.
22. K. Mardia, J. Kent, and J. Bibby “Multivariate analysis”, Academic press. 1979.

Phase Formation in Nuclear Fallout

Capt Tim Genda, Emily E. Moore, Aurélien Perron, Zurong Dai, Enrica Balboni,
Peter Hosemann, Kim B. Knight
Lawrence Livermore National Laboratory

Summary

An understanding of the physical and chemical process occurring in a nuclear explosion enables predictions of the effects of nuclear weapons, including characteristics of radioactive fallout resulting from the explosion.[1] Near-surface nuclear explosions are of particular interest due to the potential for significant amounts of environmental material to interact with and alter the physical and chemical behavior of the fireball. Such interactions have the potential to affect the distribution of radioactive species in the fireball and subsequently become incorporated into fallout through a process known as radiochemical fractionation.[2] Studying variations in fallout formed in different historical testing environments allows us to understand the influence of local environments on fallout formation processes. In particular, constraining variations in thermal evolution and redox conditions during the evolution of the fireball can be useful to understanding how sensitive fallout radiochemical fractionation may be to the local explosion environment. However, untangling these conditions in complex, multicomponent fallout is a challenge. Here we present one method of constraining and interpreting fallout formation conditions by relating computationally derived phase stability predictions to observations in historic fallout. Development of such approaches will help improve physics-based models of fallout formation and radiochemical fractionation in complex, near surface nuclear detonations.

Historic Nuclear Fallout

Many historic nuclear weapons tests were conducted on and over land at heights of burst low enough to cause the resulting fireball to significantly interact with the surface of the earth. Soils entrained into the fireball formed molten silicates that became laced with bomb vapor, before quenching to generate fallout in the form of silicate-rich glasses on the scale of micrometers to centimeters.[1] Such fallout often preserves strongly aerodynamic shapes suggesting the molten silicate quenched after leaving the fireball but while still lofted,[3] and thus has the potential to record a 'snapshot' of fireball conditions immediately prior to quench. Residual fission products in historic fallout glasses have been used to constrain cooling timescales as well as local redox conditions at the time of fallout formation.[4] In addition, partially molten or unmelted soil grains and relict minerals have been reported and used to place constraints on the fallout thermal histories.[5] A variety of compositional phases are observed in historic samples of nuclear fallout. Because cooling occurs rapidly, most aerodynamic samples formed from surface-interacting nuclear tests quench to glass. In fallout glasses derived from tests conducted in metal-rich environments (such as tower-based nuclear tests or tests involving other significant, proximate structure), additional metal-rich cooling textures are reported.[5,6] At least some of these metal-rich textures may be the result of phase formation from the host melt during cooling, such as liquid immiscibility phase separation and crystalline growth prior to quenching. Although the formation mechanisms for these metallic textures remains to be evaluated, metallic phases formed during the cooling of the host silicate melt have the potential to provide new, quantitative constraints on redox conditions and cooling behavior of the fireball.

A typical fallout sample showing inferred immiscibility textures and crystalline growth textures is depicted in Figure 1. Semi-quantitative energy dispersive X-ray spectroscopy measurements establish the average composition of the sample surface shown in Fig. 1 to be 60 mol% SiO2, 15 mol% FeO, and 15 mol% Al_2O_3, 4.7 mol% CaO, 2.3 mol% MgO, 2.1 mol% K2O, 1.5 mol% Na2O, and <1 mol% TiO_2. In this example, partially molten entrained soil grains are evident on the both the surface and the interior of the fallout glass (Figs. 1a, 1b). In contrast, crystalline textures (confirmed using diffraction-based analysis) are present only in the iron-rich regions of the sample, generally located near the rim (Figs. 1c, 1d). We hypothesize that these metal-rich structures are the result of phase separation from the host melt during cooling. If the alloy and metallic structure associated with these features can be identified, and the thermodynamic and kinetic behavior attending the phase formation are well known, the occurrence of these textures and measurement of their composition offers an independent means of constraining local fireball conditions immediately prior to fallout formation.

Of particular interest are textures which may result from liquid immiscibility processes such as those suggested in Fig. 1c. The structural relationships between the polymerizing SiO_2 and the respective ion species in multicomponent melts (Fe^{+2}, Fe^{+3}, Al^{+3}, Ca^{+2}, Mg^{+2}, etc.) is quite complex, and results in sensitivity of the field of liquid immiscibility to compositional variations, temperature, and redox conditions. Understanding these sensitivities is a necessary starting point for using phase formation approaches to constrain the fireball environment. To identify what temperature ranges, oxygen partial pressures, and multicomponent melt compositions are necessary for such liquid immiscible phases to form, predictive computational thermodynamic

Capt Tim Genda is a graduate student at the University of California, Berkeley. He has a B.S. in Physics from the U.S. Air Force Academy, a M.S. in Nuclear Engineering from the Air Force Institute of Technology, and is a candidate for a Ph.D. in Nuclear Engineering from The University of California, Berkeley. He was previously assigned as a Nuclear Debris Collections and Analysis Senior Evaluator at the Air Force Technical Applications Center, Air Combat Command. His email address is timothy_genda@berkeley.edu.

Dr. Zurong Dai is a Physicist at the Lawrence Livermore National Laboratory, in Livermore, California. He has a B.S. in Materials Science and Engineering from the Zhejiang University, China, a M.S. in Materials Engineering from the North University of China, and a Ph.D. in Materials Physics from University of Science and Technology, Beijing. He was previously assigned as a Research Scientist II at the Georgia Institute of Technology, a Visiting Scientist at the University of Washington, and a Lecturer at the North University of China.

Dr. Enrica Balboni is a Research Scientist at the Lawrence Livermore National Laboratory in Livermore, CA. She has a B.S. and M.S. in Earth Sciences from the Universita' degli studi di Ferrara, Italy, and a Ph.D. in Civil and Environmental Engineering and Earth Sciences from the University of Notre Dame.

Dr. Kim B. Knight is a staff scientist in the Nuclear and Chemical Sciences group of Lawrence Livermore National Laboratory in Livermore, California, specializing in research supporting forensic investigation of nuclear materials as well as the modern study of historic fallout. She has a B.A. in Geology from Carleton College and a Ph.D. in Earth & Planetary Science from the University of California, Berkeley. She was previously a post-doctoral researcher studying cosmochemistry at the University of Chicago.

methods can be used. We outline one such approach, here.

In our example sample, the inferred immiscible region (containing the lighter greyscale features in Fig. 1c) is enriched in iron relative to the bulk sample, with a composition of approximately 43 mol% FeO, 38 mol% SiO_2, 12 mol% Al_2O_3, 2.8 mol% CaO, 2.3 mol% MgO, 1.6 mol% Na_2O, 1.5 mol% K2O, and <1% TiO_2. The immiscible region contains a population of distinct blebs made up of two distinct compositions. The first phase is relatively enriched in Fe, and relatively depleted in Si and Al. The second phase is relatively depleted in Fe, and relatively enriched in Si and Al. Measured compositions and relationships observed in these immiscible regions are consistent with compositional ranges associated with silicate immiscibility in geologic immiscible silicate melt observations.[7]

Calculation of Phase Diagrams (CALPHAD) Approach

One approach to identify temperature ranges, oxygen partial pressures, and multicomponent melt compositions such as those observed in metal-rich fallout is to apply a CALPHAD approach.[8-10] This method uses self-consistent mathematical models with adjustable parameters to describe Gibbs energy functions of various phases in a system to best reproduce

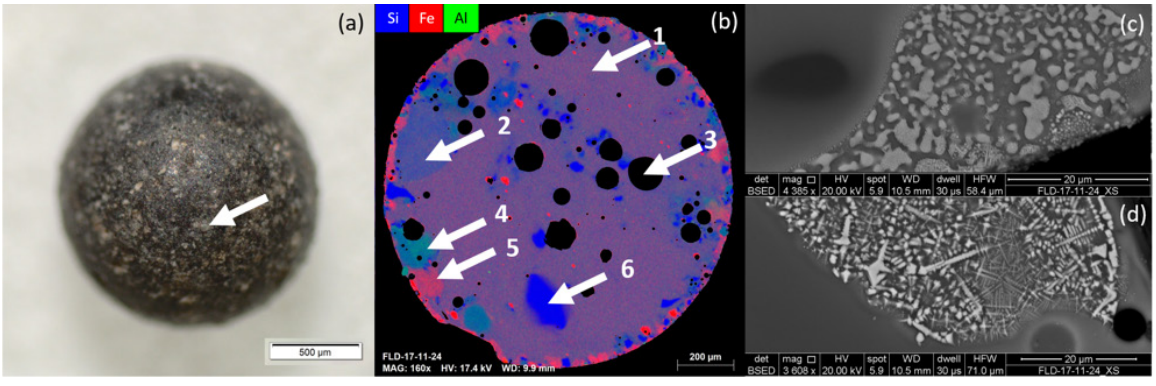

Figure 1. Historic Fallout with Metal-Rich Features

Figure 1: Nuclear fallout glass from an iron-rich nuclear test showing a typical aerodynamic form. (a) Optical image of a representative mm-scale particle. Partially molten or unmolten grains can be observed across the surface and give the sample a dull appearance (arrowhead). (b) An energy dispersive X-ray spectroscopy mosaic map showing the relative abundances of Si, Fe and Al from a cross section of the sample reveals compositional heterogeneities throughout the particle and highlights the Fe-rich sample rim. In this sample the interior preserves a relatively homogeneous melt composition (arrow 1) with Fe-poor melt regions (arrow 2), vesicles (arrow 3), Al-rich melts (arrow 4), Fe-rich melts (arrow 5), and partially molten entrained quartz grains (arrow 6). The Fe-rich regions of the sample often exhibit distinctive textures as illustrated by the lighter grey areas seen in backscatter electron images (c and d). Examples include (c) rounded, often interconnected textures we hypothesize are caused by liquid immiscibility, and (d) dendritic textures.

phase diagram and thermodynamic data (from experiments and ab initio calculations) across multicomponent systems. By minimizing the total Gibbs free energy of the system considered as functions of composition and temperature, the thermodynamically grounded CALPHAD method permits prediction of phase stability across temperature and composition ranges. This permits the association of observed compositional phases with defined physical conditions. In the case that phase formation in fallout occurred in the brief period between ejection from the fireball and deposition on the ground, such fallout will record a snapshot of the historic fireball conditions.

The thermodynamic description of the Si-Fe-Al-O system used for this work is taken from the Thermodynamics of Advanced Fuels-International Database (TAF-ID)[11] and includes the Gibbs energy parameters of Fe-Si-O,[12] Al-Si-O,[13] and Al-Fe-O.[14] The CALPHAD method allows us to explore a novel application for silicate glasses formed in nuclear explosion environments, namely use compositions and phases preserved in fallout to constrain the thermal and oxidation conditions of the fireball during fallout formation. In the present study, we provide initial exploration of contributions from Fe-rich environments to silicate-based fallout along with the interaction of elements commonly reported in near-surface fallout glasses (Al, Ca, etc.)[5,6] and differing oxidative environments.

The primary form of fallout produced in silicate-rich environments is glass, suggesting non-equilibrium formation conditions. While the kinetics of phase formation may be significant for non-equilibrium conditions, understanding the stable phases that can form through the immiscibility of the silicate melt and their sensitivities to a range of parameters is a relevant starting point to apply preliminary constraints to the chemistry of debris formation. Minor components such as CaO, K_2O, MgO, and Na_2O may alter the field of liquid immiscibility,[7] but as a first approach, we investigate phase formation in a generic Fe-Si-Al-O system (i.e., considering the major elements of the melt). We use this approach to predict liquid immiscibility as a function of the composition, oxygen partial pressure, and temperature that might contribute to the formation of nuclear fallout microstructures. We also investigate parameter sensitivity for the region of stable liquid immiscibility that we hypothesize gives rise to the textures such as those observed in Fig. 1c.

Fe-Si-Al-O Phase Formation

Using the CALPHAD approach, we calculate pseudobinary phase diagrams to explore the miscibility gap, defining where a separation of phases will occur, across the FeO-SiO2 system with variable addition of Al_2O_3. In Figure 2, the deviation in SiO_2 (with constant Al_2O_3) is plotted as a function of temperature for two different oxygen partial pressures. In high oxygen environments where $p(O_2)$ = 1 atm (Fig. 2a), the two-phase liquid miscibility gap extends across a temperature range of from 1620 - 1950°C without the addition of Al_2O_3 and exists between silicate compositions of approximately 35-95 mol% SiO_2. The addition of Al_2O_3 alters the stability of the two-phase liquid domain, decreasing the maximum temperature of the two-liquid region by 77 and 167 °C for 5 and 10 mol% Al_2O_3, respectively, but extending the stability range to lower temperatures. The presence of Al_2O_3 also shifts the phase boundaries towards enrichment in FeO (depletion in SiO_2). Similar trends are observed in Fig. 2b for lower oxygen content system ($p(O_2)$ = 10-5 atm), where the maximum temperature of the liquid miscibility gap decreases with higher Al_2O_3 content and the phase boundaries are shifted towards a more Fe-rich, Si-depleted portion of the phase diagram. In the absence of Al_2O_3 (black dotted lines), a noticeable contraction of the miscibility gap at lower oxygen pressures is predicted, such that the two-phase domain is stable across a smaller composition range. The presence of Al_2O_3 (a comparison of the blue lines) causes an overall shift in the phase boundary for both higher and lower oxygen systems but results in relatively similar range of realized compositions. The Al-containing systems at lower partial pressures (Fig. 2b) stabilize the two-phase liquid domain to a lower temperature compared to atmospheric pressures, $p(O_2)$ =1 atm.

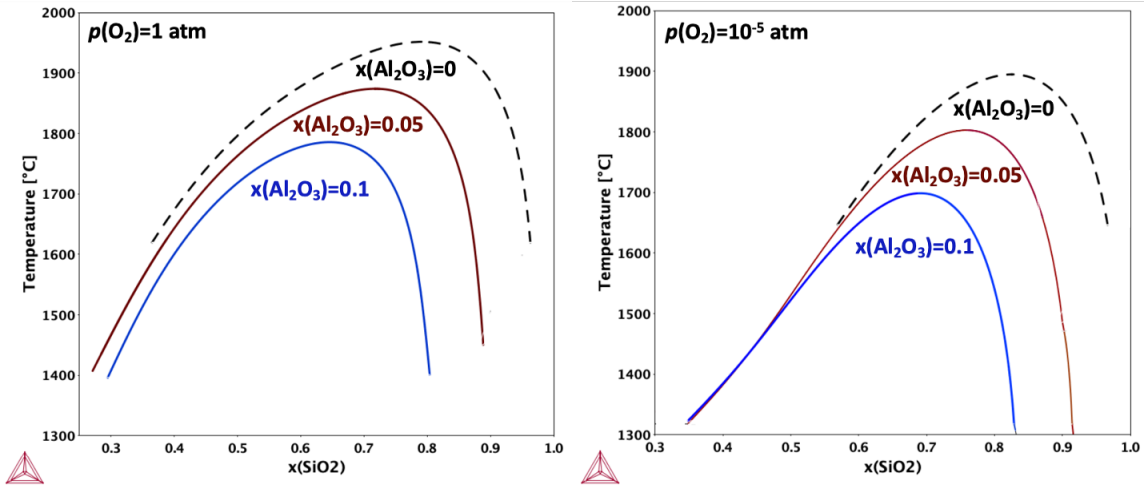

Figure 2. Calculated FeO-SiO2 Pseudobinary Phase Diagrams with Variable Al2O3 Contribution

Figure 2: Calculated FeO-SiO_2 pseudobinary phase diagrams with variable contributions of Al_2O_3 for two oxygen partial pressures (a) $p(O_2)$ = 1 atm and (b) $p(O_2)$ = 10-5 atm. The black dashed line shows the liquid miscibility gap in the absence of Al_2O_3, the red line illustrates the system including 5 mol% Al_2O_3, and blue line illustrates 10 mol% Al_2O_3.

As a first approach, this calculation demonstrates the utility of the CALPHAD approach in understanding fallout sensitivities to a range of parameters (composition, oxygen partial pressure, temperature) and the potential for these types of models to place quantitative constraints on phase formation thereby independently constraining the physical parameters attending fallout formation. While we have only illustrated a three component oxide system here (Fe-Si with Al), inclusion of other minor components such as Ca, Na, K into the calculation may allow CALPHAD predictions to be directly compared with real world compositional measurements in fallout glass. Future considerations of minor components and the kinetics of phase formation will further enhance our understanding of phase formation in nuclear fallout.

Conclusion

A variety of compositional phases are observed in historic samples of nuclear fallout. Because cooling occurs rapidly, most aerodynamic samples formed from surface-interacting nuclear tests quench to glass. For nuclear tests where significant metal-rich interaction occurred during the explosion, metal-rich textures are observed to be preserved within the glassy matrix. These textures are consistent with formation by solidification from the host melt during cooling and can consist of multiple compositional phases. The formation of such phases is governed by the thermodynamics and kinetics of the multicomponent system. Understanding the thermodynamics of the multicomponent system can be explored using a CALPHAD approach to predict the stability of the liquid immiscibility region to understand the composition and temperature ranges of the melt and of the separated phases. We showed that constraints on the miscibility gap as a function of temperature, composition, and oxygen content can be calculated using the CALPHAD method and can be used as a guide to predict the conditions attending phase formation in historic nuclear fallout. The development of CALPHAD predictions of phase stability and the ability to use such predictions alongside characterization of historic fallout provides a new, interpretative tool, with such textures in fallout providing a snapshot in time of fireball conditions immediately prior to fallout quench. Further development of this approach will provide new data constraining fireball evolution and fallout formation in addition to advancing models of fallout formation and radioactivity distributions for compositionally complex, near surface nuclear explosions.

Acknowledgements

This work was performed under the auspices of the U.S. Department of Energy by Lawrence Livermore National Laboratory under Contract DE-AC52- 07NA27344 and was supported by the LLNL LDRD Program under Project No. 20-SI-006. LLNL-JRNL-814018.

Notes:

1. S. Glasstone, and P.J. Dolan, “The Effects of Nuclear Weapons” Third Edition. United States Department of Defense and the United States Department of Energy (1977).

2. E.C. Freiling “Radionuclide Fractionation in Bomb Debris”. Science Vol 133, No. 3469, 1991-1998 (1961).

3. A.W. Klement, “Radioactive Fallout from Nuclear Weapons Tests”. Proceedings of the Second Conference, Germantown, Maryland. U.S. Atomic Energy Commission, Division of Technical Informaiton. (November 1965).

4. W.S. Cassata et al, "When the dust settles: stable xenon isotope constraints on the formation of nuclear fallout," Journal of Environmental Radioactivity 137, 88-95 (2014).

5. G.N. Eby et al. "Trinitite redux: Mineralogy and petrology," American Mineralogist, 100, 427-441 (2015).

6. T.E. Bunch et al. “Very high-temperature impact melt products as evidence for cosmic airbursts and impacts 12,900 years ago,” Proceedings of the National Academy of Sciences, 109 (2012).

7. E. Roedder, "Silicate liquid immiscibility in magmas and in the system K2O-FeO-Al2O3-SiO2: an example of serendipity," Geochimica et Cosmochimica Acta 42, 1597-1617 (1978).

8. L. Kaufman, H. Bernstein, Computer Calculation of Phase Diagrams with Special Reference to Refractory Metals, Refractory Materials, Academic Press, 1970.

9. N. Saunders, A. Miodownik, CALPHAD (Calculation of Phase Diagrams): A Comprehensive Guide, Pergamon Materials Series, Elsevier Science, 1998.

10. H. Lukas, S. Fries, B. Sundman, Computational Thermodynamics: The CALPHAD Method, Cambridge University Press, 2007.

11. OECD NEA/NSC: Thermodynamics of Advanced Fuels – International Database (TAF-ID), (n.d.). https://www.oecd-nea.org/science/taf-id/taf-id-public.

12. M. Selleby, “An assessment of the Ca-Fe-O-Si system” Metall Mater Trans B 28 (4) (1997) 563-576

13. H. Mao and M. Selleby, “Thermodynamic reassessment of the Si3N4-AlN-Al2O3-SiO2 system – Modeling of the SiAlON and liquid phase”. Calphad, 31 (2007) 269-280.

14. Huahai Mao and Malin Selleby, unpublished assessment 2007.

An In-Depth Look at the Minimum Safe Distance

LTC Jeff Kendellen
Defense Threat Reduction Agency

Introduction

We have all heard the joke about giving the Soldier, the Sailor, the Marine, and the Airman an order to "secure the building!" The Soldier (Hooah!) posts guards around the building; the Sailor (Hooyah!) turns out the lights and locks the doors; the Marine (Oorah!) kills everyone inside and sets up a headquarters; and the Air Force (Haaaayyy!) takes out a 5 year lease with an option to buy. The words people use matter and precise language is important, especially in the military. Be it orders given by commanders to subordinates or the extreme case where nuclear weapon preclusion analysis products are provided and briefed to staffs.

The Minimum Safe Distance (MSD) is perhaps the most frequently conveyed and most important element of preclusion analyses and nuclear strike warning (STRIKWARN) reports. Unfortunately, for briefers and those receiving the information, sometimes MSDs are conveyed as: "personnel outside of this area are 'safe'." And 'safe' is then translated to the colloquial meaning which is: "free from harm or risk" or "unhurt".[1] The problem with oversimplifying MSDs in this manner is that the term loses precision in what MSDs strictly represent in the definition and analytical calculations. With that in mind, this paper defines MSD and addresses some of the complexities to understand how 'safe' MSDs really are.

What is a Minimum Safe Distance?

Joint doctrine defines MSD as "the distance from desired ground zero at which a specific degree of personnel risk and vulnerability will not be exceeded with 99% assurance."[2] This MSD definition is made up of dozens of sub-terms and their associated definitions. To further complicate matters, there are two MSDs; MSD1 and MSD2. To truly understand what an MSD is and the protection it affords, one must start dissecting the term itself into its basic elements starting with the definition above.

The first term – 'distance' – is given in meters as part of the 'preclusion oriented analysis' and STRIKWARN message.[3] In the preclusion analysis, the MSD is overlaid on a map as a radius and circle (of the same radius). The distance is also rounded up to the nearest hundreds of meters. 'Ground zero' is another common term referring to the "point on the earth's surface immediately below (or above) the point of detonation."[4] Risk, specifically personnel risk, refers to the possibility of injury from the nuclear weapon effects such as blast, thermal, and/or radiation. Vulnerability,

LTC Jeff Kendellen is a planner at the Defense Threat Reduction Agency, Fort Belvoir, VA, where his current focus is conventional-nuclear integration. He has a B.S. in Physics, an M.S. in Strategic Intelligence, and an M.S. in Aeronautical Science. LTC Kendellen is a former Navy officer, previously certified to operate the S5W, S6G, and S8G submarine nuclear power plants. His email address is jeffrey.c.kendellen.mil@mail.mil.

specifically personnel vulnerability, refers to how exposed one is to injury from nuclear weapon effects.

Next, the reference to "specific degree of" risk and vulnerability requires us to further delve into each element. The risk component of MSD is connected to the risk categories which are 'negligible', 'moderate' and 'emergency'. In almost all cases, MSDs are calculated using negligible risk as the 'specific degree of risk'.[5] Negligible risk is quantified as 1% risk of latent ineffectiveness (LI). Prior to addressing the definition of LI, we need to understand the application of a '1% risk'. This is applied in much the same way as a lethal dose is communicated for hazardous substances. Often written as lethal dose-50 (LD50) which is the dose which will cause death to 50% of the exposed population. When applied to LI, negligible risk means that the commander understands that 1% of exposed personnel at the MSD will experience LI.

Latent ineffectiveness is where: "personnel will become performance degraded within three hours and remain so until death some weeks post-exposure or become combat ineffective at any time within six weeks post-exposure."[6] Understanding LI requires understanding the following two performance capability definitions: (1) performance degraded means personnel can function at between 25% and 75% of their pre-exposure performance level; and (2) combat ineffective means personnel function at 25% or less than their pre-exposure performance level.[7] Given the potentially broad views on what 'performance' would mean (e.g., a Netflix marathon versus an ultramarathon), the performance level in question refers to 'physically demanding tasks'[8] such as marching uphill, loading artillery rounds, and digging foxholes.

The "specific degree" of vulnerability is a reference to specific vulnerability categories associated with the personnel and is also what differentiates MSD1 and MSD2. The first category is associated with MSD1 and includes personnel that are warned and protected; meaning "personnel are assumed to have significant protection against blast, and thermal and nuclear radiation. Protected categories include personnel in tanks, armored personnel carriers, and foxholes."[9] The second category, associated with MSD2, is: 'unwarned and exposed'.[10] Unwarned and exposed means "personnel are assumed to be standing in the open at the time of the detonation, but will have dropped to a prone position by the time the blast wave arrives."[11]

In the paragraphs above, we have only described the distance created by the 'radius of safety' through an understanding of the 'specific degree of risk and vulnerability.' To understand how the final element of the definition, which is the reference to "with 99% assurance", the equation for MSD must be disclosed:

Minimum Safe Distance = Radius of Safety + Buffer Distance (Eq. 1)[12]

The buffer distance is revealed in Equation 2.

Buffer Distance = 2 x Circular Error Probable (Eq. 2)

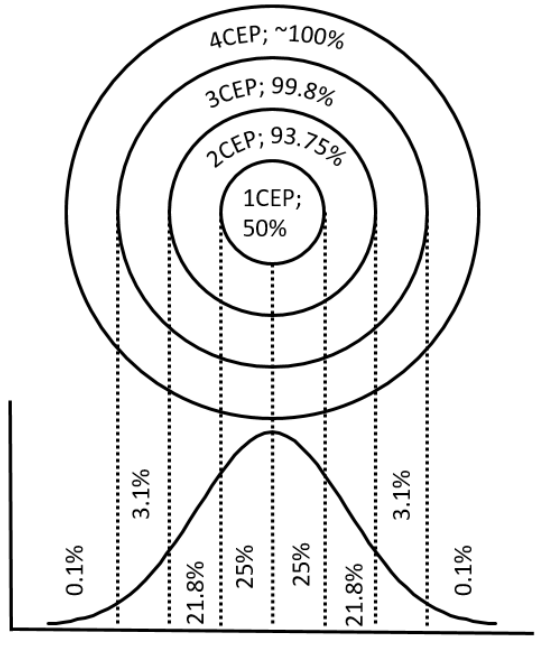

Figure 1. Shows the normal distribution overlaid with a circular error probable.

Circular error probable (CEP) is defined as the radius of a circle within which 50% of the weapons will fall. The MSD includes a buffer distance because the radius of safety is related to weapon effects on personnel and does not take into account the accuracy of the nuclear weapon delivery systems. Adding 2CEP to the radius of safety accounts for the assurance element within the MSD definition.

Those familiar with weapon delivery systems, their accuracy, and CEPs might have noticed that 99% of weapons do not fall within 2CEP and therefore the buffer distance appears to not afford 99% assurance. Instead, 2CEP calculates to 93.75% using Equation 3 and can be seen visually in Figure 1. However, it is the case that for a specific personnel arrangement 2CEP affords 99% assurance, but its application is limited and nuanced.

$$P(0 \le r \le R) = 1 - e^{-\ln(2)\frac{R^2}{CEP^2}}$$

(Eq. 3)[13]

First, as described in the Staff Officers Field Manual Nuclear Weapon Employment (FM 101-31-1, 1963) and as seen in Figure 2, only troops that are positioned to the left of the tangent line are afforded 99% assurance as part of the MSD definition.[14]

To prove that '1% fall to the left of the tangent' requires using the Polya-William Approximation which allows one to adapt circular pattern normal distributions to a square normal distributions.[15] Equations 4 and 5 are used to compute the equivalent radii and widths (or length; denoted as width = 2a).

$$\pi R^2 = 4a^2$$ where *a* is half of the width (or length) of the square (Eq. 4)

$$Equivalent\ radius\ R = \frac{2a}{\sqrt{\pi}}$$ (Eq. 5)

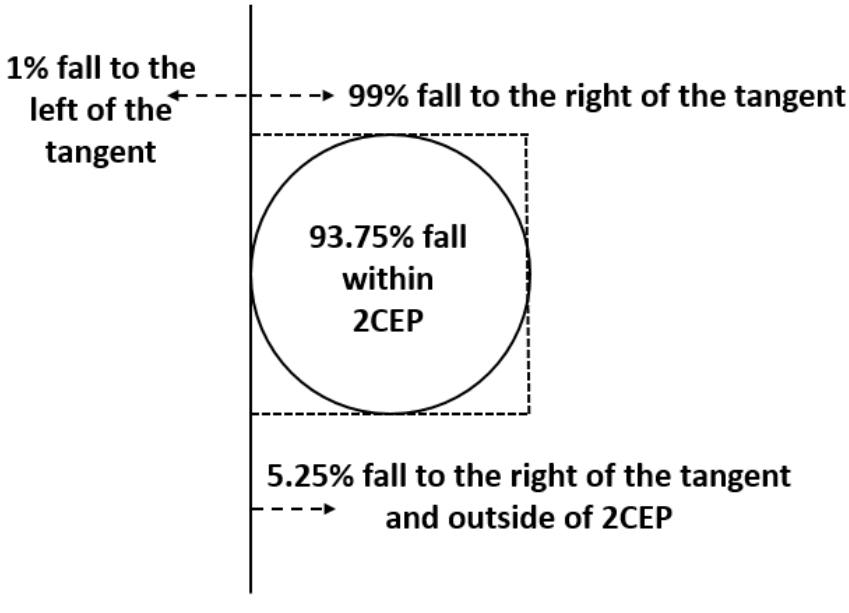

Figure 2. Depicts the percentages of weapons that will fall within the 2CEP circle and in different regions around the CEP circle. Adapted from the Staff Officers Field Manual Nuclear Weapon Employment (FM 101-31-1, 1963).

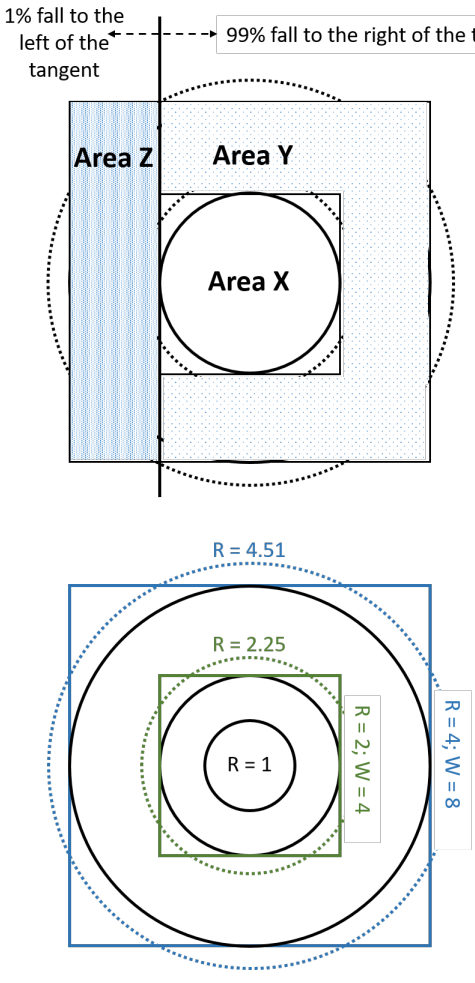

Figure 3. Figure on the left shows a visual application to the Polya-Williams Approximation where the blue circle and square and green circle and square enclose the same number of weapons respectively. The figure on the right shows Areas X, Y, and Z and the relationship to Figure 2.

Figure 3 provides a visual representation of the relationship where, as an example, the same number of weapons will land within the green square of width 4 (or a = 2) as the green circle of radius 2.257. As we are concerned with MSDs, assume CEP = 1 and therefore we can calculate the number of weapons landing within the green a circle of radius 2.257 which is 97.07%. Likewise, the same is true for the blue square of width 8 (or a = 4) and blue circle of radius 4.513 which will capture 99.99% of the weapons. One sees that 2.93% (= 99.99% – 97.07%) of the weapons will land within Areas Y and Z. Likewise, 97.07% of the weapons fall within Area X. An analysis of the actual areas demonstrates that Area Z (which is the same as the area to the left of the tangent line in figure 2) accounts for only 1% of the weapons thereby proving what Army Officers knew all along back in 1963.

For more complex troop arrangements, 2CEP is inadequate and does not provide 99% assurance. Again, referring back to the 1963 Staff Officers Field Manual Nuclear Weapon Employment, the instructions for calculating MSDs took this into account and had further calculations for other personnel arrangements. If we consider the worst case, which is where personnel are arranged continuously around the MSD, then equation 3 informs us that the buffer distance must equal 2.6 x CEP in order to provide 99% assurance for all personnel in all arrangement cases.[16]

When analysts today are performing preclusion analyses and calculating MSDs, they use 2CEP for the buffer distance. The primary reason for this is that it is unlikely an individual, let alone multiple troop formations, will be in close proximity to where a U.S. nuclear weapon is employed and as such, a unit located at the tangent line would be considered 'worst case'.

To reflect back on the question 'how safe are personnel physically located at the minimum safe distance?' – MSDs only tell planners and commanders that no more than 1% of personnel will be LI. Considering some personnel at LI will be combat degraded, combat ineffective, and/or fatalities in the days and weeks after the detonation, more information is certainly needed about the status of the remaining 99%. To explain this 1% / 99% a different way, if a commander received a report after completing a military operation that 1% of his personnel are killed in action, surely the commander could not rate the combat effectiveness of his unit based on that percentage alone. He or she must fully understand the condition of the remaining personnel (and weapons systems).[17] MSDs, while generally very conservative, unfortunately provide significant ambiguity

and uncertainty in the condition of the remaining 99% when personnel are in close proximity to the safe distances.

This article presents a thorough analysis of each component (and subcomponent) of the MSD definition. As previously stated, the MSD is the most frequently conveyed and most important element of preclusion analysis. Therefore, the definitions must be fully understood by nuclear weapon effects analysts and operations analysts that are charged with briefing preclusion analyses to potentially non-technical planning staffs. This paper is, however, incomplete. Additional topics that should be addressed in future articles include how weapon outputs (i.e., blast, thermal, and radiation) are translated to MSDs, compound injuries, and environmental considerations such as surface albedo (e.g., snow versus damp soil) as well as atmospheric conditions (e.g., clear skies versus cloud cover). Lastly, this article provides evidence of how important it is to be knowledgeable, trustworthy, and factual when communicating complex terms to personnel hearing them potentially for the first time.

Notes:

1. Merriam Webster's Collegiate Dictionary, Tenth Edition, Springfield, MA, 1994.
2. Joint Publication 3-12, Doctrine for Joint Nuclear Operations, March 2005, GL-4, GL-5.
3. Preclusion oriented analysis is a responsibility of Director, U.S. Army Nuclear and Countering Weapons of Mass Destruction Agency (USANCA). Typically performed by USANCA analysts and operations officers and by definition is "analysis on nuclear targets to ensure integration of weapons effects, and mitigate the impacts of nuclear weapons effects on the friendly scheme of maneuver." Army Regulation 10-16, August 29, 2019.
4. Glasstone, Samuel; Dolan, Philip, The Effects of Nuclear Weapons, 39.
5. Using moderate or emergency risk would be reserved for extreme situations when the commander deemed it appropriate.
6. Moakler, Martin., VanHorne-Sealy, Jama., Bosley, William., Countering WMD Journal, Issue 17, Summer/Fall 2018, 18-19
7. Ibid., 18.
8. Ibid., 18.
9. Ibid.
10. Ibid., 21. Another category is 'warned and exposed', but it is not used for MSD calculations.
11. Ibid.
12. Ibid., 17.
13. St. Ledger, John., Nuclear Targeting Terms for Engineers and Scientists, Los Alamos National Laboratory, LA-UR-17-20752, February 1, 2017, 4.
14. Staff Officers Field Manual Nuclear Weapons Employment, Field Manual 101-31-1, Headquarters, Department of the Army, February 1, 1963, 94.
15. Strickland, Jeffrey. Fundamentals of Combat Modeling - Military Applications of Mathematical Modeling, 2010, Second Edition, 26.
16. The 1963 Staff Officers Field Manual Nuclear Weapon Employment had three options: 1) 2CEP when troops were tangentially opposed; 2) 2.3CEP when troops were arranged in a quarter circle along the MSD; and 3) 2.6 CEP when troops were in more complex arrangements such as a half circle.
17. Army Doctrine Publication, Terms and Military Symbols, ADP 1-02, August 14, 2018, 4-27.

Positive Indifference: Conventional-Nuclear Integration, an Old Idea Whose Time Has Come Again

Bret Kinman
Joint Staff J8/Joint Requirements Office for CBRN Defense

The 2018 Nuclear Posture Review (NPR) states: "Combatant Commands and Service components will… plan, train, and exercise to integrate U.S. nuclear and non-nuclear forces to operate in the face of adversary nuclear threats and employment."[1]

Conventional-Nuclear Integration (CNI) refers to the seamless planning and operations of nuclear and conventional forces, in sequence and in parallel, across a spectrum of conflict, up to and through a nuclear employment environment.[2]

The U.S. Department of Defense (DoD) is re-learning the intricacies of Great Power competition. The broad learning effort underway includes: Development of new operational concepts to account for improved military and commercial technology, incorporation of 20+ years of counter-terrorism operations and nation building and improving understanding of how all of this changes military strategy, planning and operations. The resurgence of Near Peer competitors, primarily Russia and China, presents new economic and technological challenges as well as traditional military competition. These changes in the global security environment spanning the past 15 years are driving a variety of reassessments of how the United States is postured to respond to different threats and mobilize both its military and industrial capacities and capabilities. The DoD and the military services individually, and collectively as the Joint Force and in multi-Service alignments, are all renewing interest in Large Scale Combat Operations (LSCO), a significantly different scope and scale of military operations than the past 20+ years of operations have provided. In terms of terminology, LSCO is the context and Multi-Domain Operations (MDO) is the operational doctrine and conceptual baseline. Additionally, the development of Cyber, Space, and Missile Defense forces and capabilities varies the operational construct the Joint Force has traditionally used to plan and conduct operations. MDO is still maturing as both a concept and a doctrine and the graphic below is intended as thumbnail view of what is a complex and still developing concept.

Mr. Bret Kinman is a Senior Analyst at the Joint Requirements Office for CBRN Defense in the Pentagon, Washington DC. He has a B.S. in Political Science from North Georgia College and a M.A. in Defense Decisonmaking and Planning from the Naval Postgraduate School. He was previously assigned as the Director of Training at the Defense Nuclear Weapons School, Kirtland AFB, NM; Nuclear Policy Advisor, US Mission to NATO, Brussels, Belgium; Nuclear Disablement Team Chief at the 20th CBRN Command, APG, MD; and Warfare Support Division Chief at EUCOM Joint Analysis Center Molesworth, United Kingdom.

Operational Construct

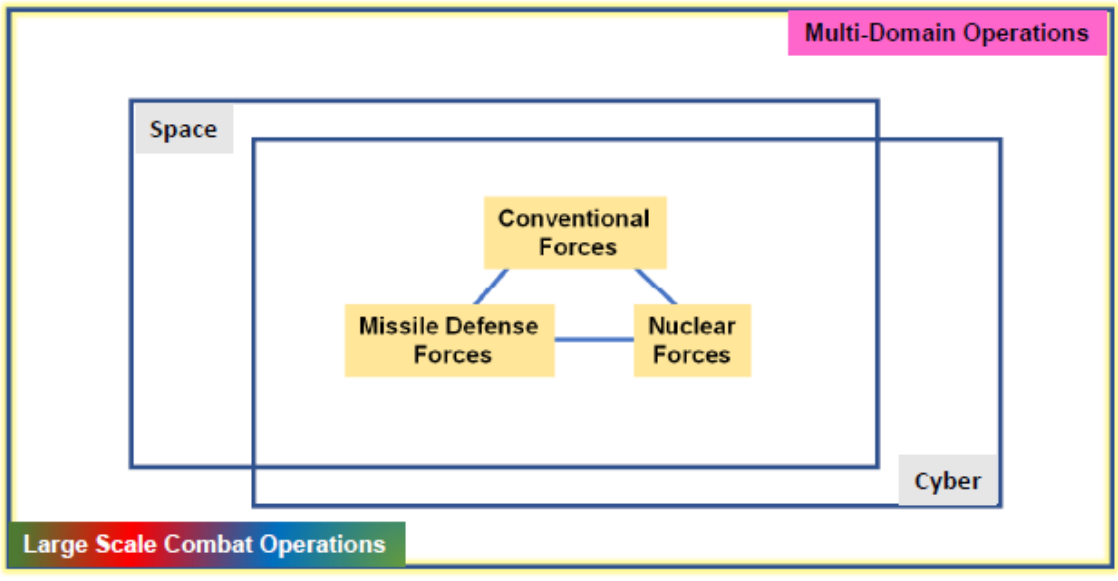

Except for the Air Force and Navy nuclear delivery communities, the U.S. military services have not taken nuclear weapons into planning or operational considerations for over 20 years. Similarly, nuclear deterrence has not been a primary focus of intellectual effort at either the operational or institutional level. Deterrence has been viewed as a byproduct of conventional force capabilities developed and utilized over the past 20 years. This atrophy has led to a state of positive indifference[3] among the preponderance of the military services: A generally affirmative view of U.S. nuclear forces, but in general a lack of clarity or distinct concern about the roles, missions, and operational implications of those forces or those of an adversary.

The revised National Security Strategy outlines five main threats (Russia, China, Iran, North Korea and Violent Extremist Organizations) – four of those threats are nuclear armed or, in one case, poised to develop nuclear weapons. The shift from counter-terrorism to great power competition means that significant parts of the DoD are studying and analyzing these threats and the potential operational environments to understand the needed doctrine, organization, training, material, leadership, policy and facilities (DOTMLPF) updates in order to compete. New operational concepts such as Multi-Domain Operations (MDO), the increased networking of systems, and the emergence of additional threats such as cyber and electronic warfare mean military leaders have a new set of parameters to operate within and through. Given the potential adversaries with or pursuing nuclear weapons, the 2018 Nuclear Posture Review provided direct guidance to the DoD to improve its ability to "operate in the face of adversary nuclear threats and employment." More recently, Office of the Secretary of Defense (OSD) Policy has provided a useful operational construct called Conventional-Nuclear Integration (CNI) and established a working group to engage the discussion across the DoD.

Planning and executing operations under the threat of adversary nuclear weapons use is a significant alteration from the past 30 years of U.S. military operations in the Balkans and - save for the initial aspects of the invasion of Iraq - operations in Iraq and Afghanistan. Operating "in the face of adversary nuclear threats and employment" is an operating condition few leaders below the General Officer level in the Services have had to contemplate. However, simply not thinking about it is no longer a viable intellectual pathway. The need for both training and education across the Joint Force on nuclear leadership is imperative if CNI is going to become

an integral part of the concepts and doctrine of MDO. The scope of nuclear leadership extends from strategic to tactical in terms of the training, education, and exercising of the force. This is first a U.S. military challenge; however, it must also eventually expand to include our Allies.

Throughout the Cold War, the U.S. military, and specifically the U.S. Army, continually struggled with the prospect of reacting and responding to nuclear weapons at the tactical and operational level. The limited threat environment of the last 20 years has allowed a withering of the knowledge base and tactical and operational experience outside the already small CBRN community of the U.S. Army (in this case, the Chemical Corps and the Army FA 52 - Nuclear and Countering WMD Officer and Health Physicist career fields.) Now, as the Army reorients to MDO and begins to relearn the art and science of combined arms fire and maneuver on a grand scale, the changes to the operational environment are considerable. Given the emerging threat environment, the Army faces nuclear escalation challenges that, even as part of a larger Joint Force, require it to be prepared to deal with the operational impacts of nuclear weapons. At a minimum, these threats may alter the desired operational design of U.S. commanders. This alteration could be in the form of more extended and constrained logistics, degraded command and control ability, constrained fires support, and a more dispersed operational and tactical arrangement. Impacts may also result from the use of cyber or electronic warfare means, but nuclear weapons present additional physical and psychological effects on humans and materials. The immediate challenge for the U.S. Army and the Joint Force is to develop training and education for leaders and formations that enhances the understanding of nuclear weapons in the multi-domain environment, more specifically, how nuclear weapons affect operations and are integrated into MDO.

CNI should be viewed as a concept that can become a useful forcing function to enable the Joint Force and services to reintroduce leaders and units to nuclear operations and deterrence. This should include both U.S. offensive nuclear operations and the implications and effects of U.S. and adversary use. As the military services and the Joint Force continue to refine the concepts and doctrine needed to actualize MDO, or whatever MDO becomes over time, their remains the need for leaders and units to apply the tenet of CNI, mainly the seamless planning and operations of nuclear and conventional forces, in sequence and in parallel, across a spectrum of conflict, up to and through a nuclear employment environment. CNI and the needed development of nuclear leadership require a starting point for education and training of leaders and units. Nuclear leadership is centrally focused on renewing the knowledge base of the Army and the Joint Force about nuclear weapons, their effects on military operations, and how our adversaries might use them. The broad outlines of nuclear leadership should require the following:

- Understanding of deterrence encompassing both conventional and nuclear
- Understanding of escalation dynamics
- Understanding of nuclear operations and weapons effects to enable decision making
- Understanding of adversary thinking

The baseline above is important as the Joint Force reorients to a LSCO operational construct. The acknowledgement that nuclear weapons (U.S. and adversary) are an integral aspect of that construct is essential. This does not imply that nuclear use is inevitable, either by an adversary or the United States, in any of the variety of possible conflicts planners envision. Rather, the intent is to redress a longstanding thought disparity in the Joint Force and the Army - especially given that our future primary adversaries have or are close to having nuclear weapons.

What must also follow this effort is a reimagining of the Army's (and Joint Force's) operational doctrine regarding nuclear weapons employment and effects. The development of Army and joint operational doctrine for LSCO should review the Army's efforts through the 1960s, 70s, and early 80s to define a maneuver doctrine that accounts for the adversary threat and incorporates the reality of tactical nuclear weapons and relevant doctrine to address their use or effects. Within the Army there will

undoubtedly be some effort to "hand wave" the nuclear aspects to focus on combined arms fires and maneuver in a multi-domain environment. This dialogue is important; the Army found itself in a doctrinal cul-de-sac in the mid-80s regarding nuclear weapons. The Army acknowledged the reality of nuclear weapons on the battlefield but was unable to articulate doctrinal outlines of their use and potential impact to operations. Some things have changed: the operating environments were different, the number of nuclear weapons and delivery systems was greater than today, the thresholds for use were different, and the capability of the weapons has improved. Yet even with these differences, some of the fundamental challenges for the Army remain now as then. For instance, in Training and Doctrine Pamphlet 525-3-1 "The US Army in Multi-Domain Operations in 2028" this very pitfall is codified:

> Neither the U.S. nor adversaries will employ nuclear weapons. The use of such weapons would so significantly alter the strategic context that different operational approaches would be required. (This assumption does not mean that this concept ignores the threat of nuclear weapons. Army forces must be resilient against all possible forms of attack. Furthermore, commanders will have to account for the possibility of nuclear attack in formulating schemes of maneuver and accounting for the risk of escalation that might lead to operational restrictions on where and how the Joint Force operates.)[4]

The Army cannot simply rely on the faith argument that nuclear weapons will never be used. The quote above makes for inconsistent logic, nuclear weapons will not be employed, but leaders and units must prepare for their use in any case. The ambiguity of nuclear weapons use by adversaries, in circumstances that are difficult to pre-define makes it more logical to account for that ambiguity in planning, training and unit and leader education. The more useful approach is to acknowledge that nuclear weapons may be employed by adversaries with direct or indirect effects on operations, at all three levels of war. MDO will not change that circumstance. For as much progress that has been made in developing a new operational construct there remain several long-standing doctrinal challenges the Army must continue to analyze. In a 1980 article titled "Tactical Nuclear Doctrine", LTC Andrew E. Andrews identified a few key points:

Potential nuclear adversaries: As the nuclear club grows, is the Soviet Union the only possible nuclear adversary? Is Europe the only battlefield where nuclear weapons could be used?

Decentralization of control: For example, what is the appropriate level for the employment decision vis-a'-vis tactical nuclear weapons? Does control at corps and higher level inhibit responsiveness so much as to negate tactical utility?

Accuracy, range and safety considerations: With the improved accuracy of today's munitions, to include precision guided munitions, are nuclear warheads now suitable for employment close to friendly forces? Does the trend toward greater mechanization of forces offer greater protection in the troop safety sense? What range weapons systems are really needed to support the maneuver commander?

Depth of the Army's battlefield: What distance past the forward edge of the battle area concerns the corps commander, the division commander, the brigade commander, and so forth? How does this relate to target acquisition?

Combatant density and other battlefield characteristics: What is the relationship between firepower and combatant density? What density represents a lucrative nuclear target? What is the relationship of probability to the employment decision? How can a logistics system, dispersed for survivability, be responsive to the combatants? Do cities now offer sanctuary because of collateral damage concerns?[5]

The Joint Force is continuing to develop a multitude of capabilities that are increasing in range, precision, lethality, and speed, and which are increasingly networked. This evolution, along with the increasing roles of Space and Cyber capabilities, presents an increasingly challenging operational environment. When nuclear weapons are added to the equation, challenges are amplified across the operational spectrum from the tactical to the strategic theater level. The Army's doctrinal efforts must consider not only the vulnerability assessments of operational plans to adversary nuclear weapons use, but also how U.S. nuclear weapons could impact operational maneuver. While doctrine and planning efforts are essential to developing an operational approach to potential adversaries and to address specific Combatant Command contingencies, this alone is not enough. There is also a need to resume the use of nuclear and other WMD effects in training and exercises, including efforts to update both training and education regarding nuclear weapons effects, operations, and deterrence.

CNI and nuclear leadership both require conceptual and doctrinal development and integration with other tenets of emerging operational concepts, which must be codified into doctrine at both the Joint and Service levels. This will include ongoing commitment to the exchange of ideas, the incorporation of developing capabilities, and the integration of intelligence of adversary plans and actions. Concurrently, the need for the development of training and education for leadership and unit staff will aid in growing the overall knowledge base on nuclear matters. A final feature is the increased integration of nuclear operations and adversary use during training and exercises.

Regarding Doctrine:

Throughout this article, the terms Joint Force and Army have been used somewhat interchangeably. This is indicative of the increasing inter-relation of all Services in the planning and execution of MDO. Services will have to incorporate the challenges laid out in the CNI charter and NPR and continually integrate through doctrine, exercises, and training. How the Joint Force operates will clearly be guided by the operational environment - different in INDOPACOM versus EUCOM and CENTCOM - each with unique adversary dynamics within their areas of responsibility. This also highlights one of the differences from the Mid-80s, when the Army developed AirLand Battle doctrine to maximize its current and near expected capabilities and incorporated those of the United States Air Force to address the expected methods of Soviet offensives in Europe. AirLand Battle was ultimately a service and bi-service doctrine, which took almost 15 years to complete.[6] Such a time frame no longer exists for developing doctrine and operational constructs between 2 Services much less across the Joint Force.

The Joint Force and the Services will now have to commit to developing and changing doctrine in a more integrated process than has been the norm of the past. Capabilities that are developed to better enable MDO, and the related Joint and Service doctrines that flow from it, must account for nuclear weapons (and chemical and biological [natural or manmade] agents). Much like the AirLand Battle doctrinal development, developing and refining MDO will require a healthy exchange between, and within, Services. Yet ignoring the implications of nuclear weapons in near and mid-term operational environments means only greater unpreparedness should it occur. Further, although reliance on a cadre of experts is helpful, the small size of the "nuclear community" relative to the increased scale of challenges requires increased nuclear knowledge across the DoD.

Regarding Education, Training, & Exercises:

Training and education of leadership and unit staffs will also enhance understanding of the challenges in future operational environments, and grow future leaders who are "nuclear natives" and not, like the previous generation, working hard to learn (or in some cases relearn) nuclear and CBRN threat knowledge. Training courses for the Joint Force exist already, albeit limited to a few institutions, with small throughput. Expanding this capacity will help; however, expanding the audience is something that will require advocacy and agency from the leadership of the Services and the Joint Staff. In other Professional Military Education

(PME) venues, the zero sum nature of curricula management will also require senior leadership direction to modify or alter existing coursework to better include study and discussion of deterrence, nuclear operations, effects, and related characteristics for MDO.

For exercises, senior leadership emphasis will be needed to incorporate nuclear operations. The constant fear, and reluctance, from exercise planners is that nuclear weapons use will "derail" the exercise, either by immediately moving to strategic level exchanges, or by creating war-stopping levels of damage. There are very few nuclear specific exercises, but there are a significant number of conventional exercises that could effectively integrate nuclear aspects. Those are done mostly under the auspices of USSTRATCOM and USNORTHCOM and their Service Components. The challenge is to translate useful exercise design aspects from those existing nuclear related exercises into other CCMDs as well as Service exercise programs. The Army Mission Command Training Program (MCTP) Warfighter Exercise (WFX) is a good example of a venue that could integrate scenario and adversary aspects from USSTRATCOM exercises to aid in intensifying the scenarios faced by Army Corps and Division staffs.

This is an opportunity for the nuclear community to develop and clearly articulate approaches to integrate conventional and nuclear operations into exercises in ways that do not overwhelmingly impact an exercise. This should be a goal in any case, as the intent is to use exercises as a way to train and educate units and leaders on the realistic effects of nuclear weapons, and utilize the exercise operational environment and adversary weapons and tactics as a platform to increase the knowledge base. This, as with other aspects of relearning nuclearmatters, will take time and likely be somewhat uneven in initial application. Exercise design teams face challenges similar to those faced by curricula managers in that there is a limit to the number of "events" - not only nuclear but also cyber, space, and other emergent operational threats - that can be covered in an exercise. The integration of these operational threats, along with relearning large-scale fire and maneuver in the expanse of the Asia-Pacific region, as well as Eastern Europe and South-Central Asia, presents a window to reorient the Joint Force to preparing for possible next-generation conflicts and adversaries.

Conclusion

The current and near future security environments require a credible U.S. deterrent encompassing nuclear, conventional, missile defense, space, and cyber capabilities, all which have distinct and complementary roles to play in deterring multiple adversaries. These adversaries have or are actively seeking nuclear capabilities to offset other aspects of their force mixture. As the Army learned the challenges of potentially dealing with nuclear weapons on the battlefield during the Cold War, those challenges informed the larger Army debate about how it would operate and fight. Even then, the Army still never completely resolved the challenges of nuclear weapons in relations to its operational preferences. This institutional frustration of positive indifference ended with the Cold War - and has now returned. The Army may never fully achieve doctrinal harmony regarding nuclear weapons. It is still appropriate to expend the intellectual effort to develop doctrine that is "right enough" and refresh the knowledge base.

The increased number of adversaries arrayed multi-dimensionally against the United States and its allies presents greater security challenges today than in recent history. Army leaders and staffs will still have to understand the dynamics of deterrence, and how the Army and the Joint Force conventional and nuclear capabilities can enhance and communicate deterrence in the operational environment. Understanding the effects of nuclear weapons and how the Joint Force will still need to operate "in the face of adversary threats and employment" will be critical across operational levels and commands - both Joint and Service. CNI is a needed construct for expanding the knowledge and training of the Joint Force. CNI is not a new idea - but it has new aspects and a different operational environment in which to be applied by the Joint Force and the Army to improve capability in the emergent security environment.

Notes:

1. Department of Defense, 2018 Nuclear Posture Review, p 21, Washington DC.

2. Department of Defense Conventional Nuclear Integration Community of Interest Charter-DRAFT, p.1, para A, Pentagon, Washington DC, July 2020.

3. Taken from remarks by the Belgian Defense Minister Peter de Crem during a US delegation visit to Kleine Brogel Air Base, 2013.

4. Department of the Army, Training and Doctrine Command (TRADOC), Pamphlet 525-3-1 The US Army in Multi Domain Operations 2018, December 6, 2018, p.A-1.

5. Tactical Nuclear Doctrine, LTC Andrew E. Andrews, Military Review, October 1980, p17-18.

6. Lessons from the Past: Making the Army's Doctrine "Right Enough" Today, BG Huba Wass de Czege, Landpower Essay No. 06-2, AUSA Institute for Land Warfare, September 2006, p. 1

A Cruel Wind from the East: China's DF-17 and DF-ZF

MAJ Christopher J. Mihal
National Nuclear Security Administration

While dwarfed in size by both U.S. and Russian nuclear arsenals, the Chinese nuclear arsenal is rapidly being expanded and upgraded. The DIA projects it will double in size from its current quantity of approximately 300 warheads over the next decade.[1] While there has been considerable discussion over incorporating China into a variant of the now-terminated Intermediate Nuclear Forces (INF) treaty or into the New START treaty,[2] China has displayed little public inclination towards joining either treaty. China routinely cites the huge disparity in nuclear arsenals, with both Russia and the United States having approximately 20 times as many warheads as China,[3,4] as the primary reason for ignoring calls to join arms control treaties. Furthermore, China is unlikely to agree to a deal resembling the INF treaty as 95% of their nuclear warhead delivery systems would be in violation of such a treaty, and China now possesses the largest stockpile of ground-launched missiles in the world, with approximately 2,200 ground-based missiles from a variety of launch systems in total.[5]

The composition of the Chinese arsenal indicates a strong preference for ground-launched ballistic and cruise missiles. The Chinese ballistic missile development program is active, diverse, and growing.[6] One of the most advanced developments in the Chinese ballistic missile program is the new DF-ZF hypersonic glide vehicle (HGV), along with its delivery system the Dong Feng-17 (DF-17) medium range ballistic missile, also known as "East Wind-17" or WU-14 in the West. Dong Feng is the designation given to all of China's ballistic missiles. The DF-ZF was declared officially operational in the People's Liberation Army Rocket Forces at a military parade in Beijing on 1 October 2019.[7] Previously secretive about the appearance of the DF-17, China fully unveiled the new HGV at the same parade, pictured below.

Figure 1 DF-17 Unveiling at Chinese Military Parade in 2019 (Greg Baker/AFP via Getty Images)[8]

China has been at the forefront of testing hypersonic weapons, with Under Secretary of Defense for Research and Engineering noting in 2018 that China has conducted twenty times the number of hypersonic tests that the U.S. had at that point.[9] Hypersonic weapons rely on rockets to ascend to the upper atmosphere, whereupon they are released to subsequently glide towards their targets at extreme speeds. In the case of the DF-ZF, its aerodynamic properties and heat-resistant skin allow it to reach purported speeds of up to Mach 10.[10] Additionally, in at least one test, the DF-ZF conducted "extreme maneuvers" while travelling at hypersonic speeds.[11] Unlike conventional re-entry vehicles mounted on missiles, HGVs can have irregular ballistic trajectories that make them exceedingly difficult to intercept with contemporary missile defense systems, and their great speed can cause immense damage even without nuclear warheads. China is touting hypersonics as a means of defeating both ballistic missile defense systems and aircraft carriers.[12] It logically follows that hypersonics are the means by which China hopes to undermine or negate a portion of the U.S. nuclear deterrent.[13] It is currently unclear if China will choose to make the DF-ZF nuclear-capable, although Russia has claimed their similar HGV, the recently-deployed Avangard, will carry a two megaton warhead.[14] Though China has stressed the conventional role of the DF-ZF weapon system, a nuclear capability is clearly feasible to be mounted as well.[15]

The delivery system for the DF-ZF is the Dong Feng 17, a solid-fueled medium-range missile with a range of 1,800-2,500 km which was first confirmed to exist in 2014,[16] currently carried by a 10x10 wheeled vehicle. The DF-17 is possibly based off of the DF-16B, which would have sped development considerably.[17] The DF-17 is currently ground-launched, although a ship-launched version has been announced, lending credence to Chinese claims that the DF-17 may be used in an anti-ship role.[18] The accuracy of the DF-17/DF-ZF system was confirmed in a November 2017 test, where the HGV impacted "within meters" of the intended target,[19] although reportedly the circular error probable (CEP) – the circular radius around a target where a projectile is designed to most likely impact - is 30 meters.[20]

The DF-11, DF-15, DF-16, DF-21, and DF-26 have all been identified as possible additional launch platforms for the DF-ZF.[21] The DF-21 and DF-26 are designed as "carrier killer" missiles as well, supporting the theory that the system is designed to counter U.S. naval superiority,[22] while the DF-11, 15 and 16 are shorter-ranged tactical weapon systems.

The DF-17's range of approximately 2,500 km is an indicator that the weapon system is designed primarily against regional adversaries, including India and Taiwan, but also potentially U.S. naval forces in the region. Given the region's numerous U.S.-supplied missile defenses (Taiwan, South Korea and Japan), and the presence of Russian missile defense systems (Russia, India and Vietnam), it is logical that China would develop weapon systems to counter the prevalent missile defense platforms in the region.

The development of greater numbers of new and more advanced weapons systems capable of delivering nuclear warheads may serve as a harbinger of a shift in Chinese nuclear policy. As discussed in a previous review of Susan Haynes' "Chinese Nuclear Proliferation," there is evidence that Chinese strategic policy is shifting away from a policy of minimal deterrence to one of limited deterrence, which would signify a more active nuclear posture.[23] The rapid expansion and modernization of China's nuclear armaments would indicate a shift in this direction, and are potential indicators of China

Major Christopher J. Mihal is the Executive Director at the National Nuclear Security Administration Office of Systems Engineering and Integration, NA-18, in Albuquerque, NM. He has a B.S. in History from the U.S. Military Academy, a M.S. in Engineering Management from the Missouri University of Science and Technology, and a M.S. in Nuclear Engineering from the Air Force Institute of Technology. He is a certified Project Management Professional. He was previously assigned as an Exchange Officer with 2 Canadian Mechanized Brigade Group. His email address is christopher.mihal@nnsa.doe.gov.

flexing its muscles regionally. China's politicians have made it plain that incorporating China into existing nuclear treaties is a non-starter, but there may be indications China is willing to enter into other sorts of agreements than what currently exist. Whether China is willing to agree to these agreements out of a genuine desire to decrease international tensions, or they believe an arms control agreement is in their best interest to weaken their potential adversaries, remains to be seen.

Notes:

1. Ashley, Robert P., "Russian and Chinese Nuclear Modernization Trends," Remarks at the Hudson Institute, May 29, 2019. Accessed at https://www.dia.mil/News/Speeches-and-Testimonies/Article-View/Article/1859890/russian-and-chinese-nuclear-modernization-trends/

2. Zakheim, Dov S., "China Needs to Play Straight on New START Nuclear Treaty," in The Hill, July 22, 2020, accessed at https://thehill.com/opinion/national-security/507211-china-needs-to-play-straight-on-new-start-nuclear-treaty

3. "China Views US Attempts to Involve it in Talks on New START Treaty as a Political Hoax," in TASS, July 10, 2020, citing Chinese Foreign Minister Spokesman Zhao Lijian, accessed at https://tass.com/world/1176897

4. The Associated Press, "China Rejects Prospect of Joining Arms Control Talks with U.S.," in ABC News, July 10, 2020, accessed at https://tass.com/world/1176897

5. DePetris, Daniel R., "Fact: 95% of China's Cruise and Ballistic Missile Inventory Would Violate INF Treaty," in The National Interest, June 6, 2020, accessed at https://nationalinterest.org/blog/skeptics/fact-95-chinas-cruise-and-ballistic-missile-inventory-would-violate-inf-treaty-161426

6. Defense Intelligence Ballistic Missile Analysis Committee, Ballistic and Cruise Missile Threat, National Air and Space Intelligence Center (NASIC) report, June 2017, accessed at https://www.nasic.af.mil/LinkClick.aspx?fileticket=F2VLcKSmCTE%3d&portalid=19

7. Yeo, Mike, "China Unveils Drones, Missiles and Hypersonic Glide Vehicle at Military Parade," in Defense News, October 1, 2019, accessed at https://www.defensenews.com/global/asia-pacific/2019/10/01/china-unveils-drones-missiles-and-hypersonic-glide-vehicle-at-military-parade/

8. Ibid.

9. Tirpak, John A., "Griffin Says Hypersonics, Acquisition Reform are Top Priorities," in Air Force Magazine, March 6, 2018, accessed at https://www.airforcemag.com/Griffin-Says-Hypersonics-Acquisition-Reform-are-Top-Priorities/

10. Weitz, Richard, "China and Hypersonic Weapons," in Defense.info, January 18, 2019, accessed at https://defense.info/air-power-dynamics/2019/01/china-and-hypersonic-weapons/

11. Gertz, Bill, "China Successfully Tests Hypersonic Missile," in The Washington Free Beacon, April 27, 2016, accessed at https://freebeacon.com/national-security/china-successfully-tests-hypersonic-missile/

12. Keller, John, "The Emerging China Hypersonic Weapons Threat to Surface Vessels at Sea," in Military & Aerospace Electronics, April 24, 2019, accessed at https://www.militaryaerospace.com/unmanned/article/16711522/the-emerging-china-hypersonic-weapons-threat-to-surface-vessels-at-sea

13. Saalman, Lora, "Factoring Russia into U.S.-Chinese Equation on Hypersonic Glide Vehicles," in SIPRI Insights on Peace and Security, January 2017, accessed at https://www.sipri.org/sites/default/files/Factoring-Russia-into-US-Chinese-equation-hypersonic-glide-vehicles.pdf

14. "Russia Deploys First Hypersonic Avangard ICBM Missile [sic]," in The Moscow Times, 27 December, 2019, accessed at https://www.themoscowtimes.com/2019/12/27/russia-deploys-first-hypersonic-avangard-icbm-missile-a68768

15. Solem and Montague, "Updated-Chinese

Hypersonic Weapons Development."

16. Missile Defense Project, "DF-17," Missile Threat, Center for Strategic and International Studies, February 19, 2020, last modified June 23, 2020, https://missilethreat.csis.org/missile/df-17/

17. Panda, Ankit, "Introducing the DF-17: China's Newly Tested Ballistic Missile Armed With a Hypersonic Glide Vehicle," in The Diplomat, December 28, 2017, accessed at https://thediplomat.com/2017/12/introducing-the-df-17-chinas-newly-tested-ballistic-missile-armed-with-a-hypersonic-glide-vehicle/

18. Keller, "Emerging China."

19. Panda, "Introducing the DF-17."

20. "DF-17" in Military Today, accessed at http://www.military-today.com/missiles/df_17.htm

21. Solem, Erika and Montague, Karen, "Updated-Chinese Hypersonic Weapons Development," in China Brief, Vol 16, Issue 7, April 21, 2016, accessed at https://jamestown.org/program/updated-chinese-hypersonic-weapons-development/

22. Roblin, Sebastien, "See These Missiles? China Might Use Them To Someday Sink an Aircraft Carrier," in The National Interest, July 8, 2020, accessed at https://nationalinterest.org/blog/reboot/see-these-missiles-china-might-use-them-someday-sink-aircraft-carrier-164269

23. Mihal, Christopher, "Book Review: Chinese Nuclear Proliferation – How Global Politics is Transforming China's Weapons Buildup and Modernization," in U.S. Army Countering WMD Journal, Issue 19, Summer/Fall 2019, accessed at https://www.nec.belvoir.army.mil/usanca/CWMDJournal/CWMD%20Journal%20Issue%2019.pdf

Contingency Elimination Preparedness

Maj Emily J. Pollard and Kimberly Z. Heyne
Defense Threat Reduction Agency

The Security and Elimination (S&E) Department of the Defense Threat Reduction Agency's (DTRA) Cooperative Threat Reduction (CTR) Directorate is comprised of three programs: Strategic Offensive Arms Elimination, Chemical Security and Elimination, and Global Nuclear Security. DTRA CTR works with partner countries to prevent the proliferation of WMD and eliminate chemical, biological, radiological, and nuclear threats, and it has over 25 years of experience conducting WMD elimination. Nonetheless, in the current strategic environment, challenges are more diverse and can arise quickly, resulting in unforeseen contingencies. Chemical weapons elimination missions in Libya and Syria (Figure 1 and 2) demonstrated that WMD elimination capability requirements can emerge rapidly in challenging, unstable environments.[1,2,3]

Figure 1. Bulk CW precursor is loaded in a shipping container for transport on board the ship; inset: U.S. M/V Cape Ray at sea.

Similar WMD elimination opportunities will likely arise in unexpected, formidable situations, possibly with limited windows of opportunity for execution, a reality highlighted during notional planning for Final Fully Verified Denuclearization (FFVD) of North Korea. To remain flexible and adaptive when unexpected threats arise, S&E is proactively investing in Contingency Elimination Preparedness (CEP) with dedicated funding and personnel. To ensure CTR can continue to accomplish the mission of eliminating WMD capabilities, S&E developed a comprehensive, proactive approach to preparedness that accounts for the challenges posed by the current strategic environment, modern WMD threats, and the priorities of the National Defense Strategy (NDS).[4,5]

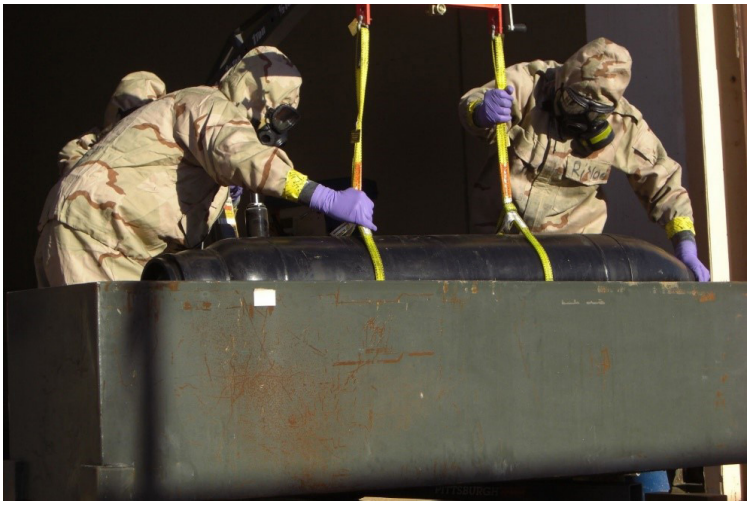

Figure 2. Workers wearing CW protective suits remove a chemical weapon from a transportation container during the process of destroying the munition.

In 2019, S&E initiated a paradigm shift to posture DTRA for agile and rapid response to future contingency WMD elimination missions. When implemented, S&E will be able to capitalize on limited duration, high return-on-investment threat reduction opportunities. Under Title 50 USC Ch. 48, the CTR Directorate has the authority and responsibility to establish and institutionalize the S&E approach to improve CEP. This will allow the USG to maintain preparedness that is based on intelligence analysis, provides a clear cost-benefit, and establishes agility and flexibility for rapid worldwide application. By codifying its approach to CEP, S&E is signaling to the interagency its leadership role in preparing for WMD elimination missions.

While this shift toward CEP is essential, it does not change an important lesson learned in recent CTR elimination missions: interagency and multilateral cooperation is critical to success. Coordination across the interagency and with international partners will be essential in S&E's preparedness initiative and future missions. The breadth of potential elimination scenarios linking interagency responsibilities necessitates a cooperative approach to CEP. There are many related capabilities among interagency partners and other organizations; however, S&E can play a proactive and pivotal role in leveraging and synchronizing those unique capabilities and areas of expertise.

Components of Preparedness

Successful preparation for WMD elimination scenarios needs to consider and address several components; S&E considered a wide range of components and identified seven as being vital to preparedness.[6] While S&E does not have the ability to directly impact all of these components, each impacts holistic preparedness. S&E collaborates across the Department of Defense (DoD) and the interagency to enhance CEP posture.

Maj Emily J. Pollard has a B.S. in Chemistry from Colorado State University, a Professional Science Master's Degree in Material and Chemical Synthesis from the Illinois Institute of Technology, and a Ph.D. in Analytic Chemistry from the University of Florida. In her previous assignment, she was a project officer in the Cooperative Threat Reduction Directorate at the Defense Threat Reduction Agency.

Kimberly Z. Heyne is the Strategic Offensive Arms Elimination Program Manager at the Defense Threat Reduction Agency in Fort Belvoir, VA. She has a B.A. in Political Science from the James Madison University, and a M.A. in International Affairs from the George Washington University Elliott School of International Affairs. She was previously assigned as a project officer in the Cooperative Threat Reduction Directorate at the Defense Threat Reduction Agency.

The seven identified components of preparedness are:

1. Technical Solutions: Elimination of WMD and WMD delivery systems requires specialized technical solutions and proven operations protocols to ensure safe and effective threat reduction. Capability gaps exist between required and available technologies for some types of contingency elimination missions. S&E is partnering with other organizations to address elimination capability gaps and to understand and influence materiel solutions in advance of any elimination operation. This not only reduces the need for CTR to lead and directly invest in technology development but also ensures that materiel solutions will be available when needed.
2. Logistics: Fundamental to any successful elimination mission is detailed logistical planning and flexible execution for deployment and sustainment of personnel and equipment. The logistics preparation undertaken during pre-deployment is key to mission success. These activities focus on identifying host-nation or commercially provided resources and ensuring access to those resources. This includes in-country transportation, lodging, medical care and evacuation, food, office space, communications, personal protective equipment, fuels, infrastructure assessment (military and commercial), site security, interpreter services, etc. Given that S&E is an interagency leader in logistics coordination for elimination missions, applying CEP to logistics ensures the USG will be able to rapidly respond to future missions.[7]
3. Acquisition Vehicles: In the event of an elimination mission, S&E would leverage government contracts to acquire goods and services necessary for the mission. Rapid and flexible contracts will allow S&E to use American or international companies, as well as host-nation companies. For example, a contract vehicle with the option for multiple task orders and pre-drafted statements of work will expedite the response process. S&E has experience with unique acquisition vehicles, which can put a contractor to work within days or weeks of the initial identification of a requirement.
4. Personnel Readiness: To ensure personnel readiness to quickly respond to contingency elimination missions, several factors must be addressed in advance, including the identification of team members, administrative requirements , mission specific training, and travel requirements (e.g., passport, visa, medical clearance, military orders). When possible and reasonable, S&E's proactive CEP aims to reduce personnel readiness timelines to allow teams to deploy safely and quickly.
5. Legal: Determining the applicable treaties, regimes, laws, and policies for a contingency elimination is complex, and depends largely on the specific elements of the scenario and the host nation. For example, the type of material will determine which United Nations convention or international treaty is applicable. Other considerations include sanctions, export controls, notwithstanding authority, indemnification, and liability protection. By analyzing the legal requirements and restrictions in advance, S&E can identify strategies to alleviate potential barriers to success and accelerate implementation when a contingency arises.
6. Policy: In a contingency elimination scenario, the Office of the Undersecretary of Defense for CTR Policy is responsible for policy decisions that impact CTR execution of an elimination mission, such as country determinations and/or permissions, activating interagency and international coordination mechanisms, providing guidance for navigating political sensitivities, etc. Opportunities exist to preempt challenges that may arise during a contingency elimination operation, for example pre-drafting memorandums of understanding and interagency agreements, or establishing other structures, processes, or guidance that enable an expedited response. As policy decisions will significantly impact S&E's ability to effectively respond it is important for the department to consider, discuss, and coordinate on these matters as part of CEP.
7. Operational Concepts and Plans: Planning for success requires coordination across DoD, the interagency, and integration into plans. Planning is a deliberate process used to develop responses to potential scenarios across the interagency and Geographic Combatant Commands (GCC). It is an iterative process led by the GCCs that allows S&E to be adaptive to situational changes to the GCC

Figure 3. DOS hosted a medical exercise as the culminating event to a Radiation Specialist training program. S&E coordinates with the Non-Proliferation Disarmament Fund of DOS to ensure medical response in nuclear contaminated areas and mobile secure communications.

Operational Plans (OPLANS) and Concept Plans (CONPLANS). This component combines the other six components of preparedness to synchronize a coordinated, integrated, and whole-of-government response. OPLANS and CONPLANS should be exercised on a recurring basis in order to maintain a credible elimination response capability.[8]

CEP Coordination and Collaboration

Confronting today's complex strategic environment requires coordinated effort across the USG to effectively and efficiently employ all dimensions of national power for long-term strategic success, as articulated in the 2018 NDS.[9] In line with the NDS and DTRA's Strategic plan, S&E is leveraging existing relationships across the interagency and international partners while continuing to seek new and expanded partnerships.[10]

An example is S&E's partnership with the Department of State (DOS) Non-Proliferation Disarmament Fund Office (NDF)—a critical partner in past contingencies and current planning efforts. In 2019, NDF invited S&E to observe a medical exercise that demonstrated the ability of medical personnel to provide care in a nuclear contaminated environment, and also afforded an opportunity to test their mobile classified communications capability (Figure 3).

This collaboration illustrates S&E's focus on developing and strengthening partnerships to improve CEP through informal action officer engagement, formal agreements, cooperative plans development, and table-top and field exercises.

Another example lies in our ongoing efforts with the Department of Energy (DOE) National Nuclear Security Administration (NNSA). S&E maintains a robust relationship with the DOE/NNSA Office of Material Management and Minimization (M3) Office of Nuclear Material Removal. This office negotiates and coordinates the removal and/or disposition of excess highly enriched uranium and separated plutonium from countries around the world. The partnership has required strategic coordination to understand and define the scope of roles, responsibilities, and capabilities of each agency in responding to emerging elimination opportunities.[11] S&E is well-positioned to support logistical requirements of M3 with rapid transport of response equipment and personnel globally by air, sea, and land; provide sustainment via commercial operating base and resupply of fuel and consumables; and support secure transportation of nuclear materials. These capabilities are integral to WMD elimination operations and allow S&E to bring significant value to DOE and complement their technical expertise. Over the past few years, S&E and M3 have successfully partnered to exercise nuclear

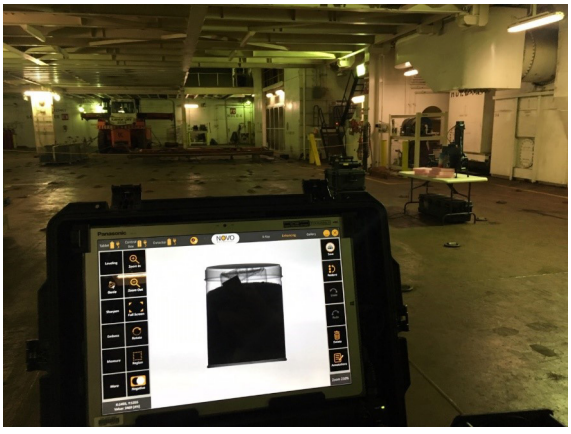

Figure 4. DOE/NNSA M3 and S&E partner to exercise nuclear material removal equipment and processes onboard a ship.

material packaging in a maritime environment (Figure 4) and to conduct joint planning.

S&E worked with DOE/NNSA's Office of Global Material Security to support the removal of Cesium-137 irradiators from Mexico. Additionally, S&E supported a collaborative, multi-year effort with M3 and the United Kingdom to transport approximately 700 kg of highly enriched uranium to the United States for downblending to low enriched uranium (Figure 5).

Figure 5. S&E supported DOE/NNSA M3 with the transport of highly enriched uranium from the United Kingdom to the United States to be downblended to low enriched uranium.

S&E is playing a major role in planning for an upcoming DOE/NNSA exercise that will bring together DOE and DoD organizations sharing similar, but distinct, roles within the nuclear material removal mission space. The primary objective is to exercise the USG's mission of nuclear material removal and the foundational logistics required to execute the mission. This exercise will present a realistic scenario to test and build the interoperability of these teams, allowing them to achieve their common nonproliferation objectives. DOE and S&E collaborate to share technologies, training, and information to allow the USG to construct a comprehensive strategy to enable the expedited removal and verification of nuclear materials under austere conditions.

Looking Forward

S&E has historically identified and implemented long term, highly effective solutions for contingency elimination missions. As a result of its rich history, S&E has established a wealth of program management knowledge, accumulated resident subject matter experts, and cultivated experienced implementing contractors, all of which can be drawn on to improve CEP in concert with the interagency. As S&E transitions from reactive contingency response to proactive posture, S&E invites interested partners to strengthen interagency coordination to address CEP across the seven components of preparedness. In today's dynamic world, it is impossible to predict when a regime will collapse, a WMD will be interdicted, or when a country may voluntarily give up its WMD program; therefore, it is imperative to prepare agile solutions across the whole-of-government to rapidly respond to and quickly execute WMD elimination missions.

Notes:

1. Joseph P Harahan, "With Courage and Persistence: Eliminating and Securing Weapons of Mass Destruction with the Nunn-Lugar Cooperative Threat Reduction Programs," Defense Threat Reduction Agency. 2014.

2. Karen DeYoung, "Removal of Syrian chemical arsenal was result of unprecedented collaboration," The Washington Post, June 29, 2014. https://www.washingtonpost.com/world/national-security/2014/06/29/3f6b6a88-fe1f-11e3-8176-f2c941cf35f1_story.html.

3. Ralf Trapp, "Elimination of the Chemical

Weapons Stockpile of Syria," Journal of Conflict & Security Law 19, no. 1 (2014): 7-23. doi:10.2307/26296277.

4. Jennifer A. Vincent, Edmund B. Zaballa, and Kimberly Z. Heyne, "Strategic Context and Traceability," Unpublished paper in the authors' files.

5. United States. Department of Defense. Summary of the 2018 National Defense Strategy of the United States of America: Sharpening the American Military's Competitive Edge. Department of Defense, 2018.

6. Michelle B. Nalabandian, Sophia Y. Hunt, and Emily J. Pollard, "Approach to Contingency Elimination Preparedness," Unpublished paper in the authors' files.

7. Norman M. Wade, "SMFLS4: The Sustainment & Multifunctional Logistician's SMARTbook: Warfighter's Guide to Logistics, Personnel Services, & Health Services Support," 4th ed., The Lightning Press, 2019.

8. Michael A. Santacrose, "Joint/Interagency SMARTbook: Joint Strategic & Operational Planning," 2nd ed., The Lightning Press, 2019.

9. United States. Department of Defense. Summary of the 2018 National Defense Strategy of the United States of America: Sharpening the American Military's Competitive Edge. Department of Defense, 2018.

10. United States. Defense Threat Reduction Agency. DTRA Strategic Plan FY2018-2022. Department of Defense, 2018.

11. Schuyler D. Bates, Tiffany C. Watts, and Randall D. Holmes, "S&E and NNSA Information Paper," Unpublished paper in the authors' files.

References:

Bates, Schuyler D., Tiffany C. Watts, and Randall D. Holmes. "S&E and NNSA Information Paper." Unpublished paper in the authors' files.

Defense Threat Reduction Agency. "DTRA Strategic Plan FY2018-2022." United States Department of Defense, 2018.

DeYoung, Karen. "Removal of Syrian chemical arsenal was result of unprecedented collaboration." The Washington Post. June 29, 2014. https://www.washingtonpost.com/world/national-security/2014/06/29/3f6b6a88-fe1f-11e3-8176-f2c941cf35f1_story.html.

Harahan, Joseph P. "With Courage and Persistence: Eliminating and Securing Weapons of Mass Destruction with the Nunn-Lugar Cooperative Threat Reduction Programs." Defense Threat Reduction Agency. 2014.

Nalabandian, Michelle B. Sophia Y. Hunt, and Emily J. Pollard. "Approach to Contingency Elimination Preparedness." Unpublished paper in the authors' files.

Santacrose, Michael A. "Joint/Interagency SMARTbook: Joint Strategic & Operational Planning." 2nd ed. The Lightning Press. 2019.

Trapp, Ralf. "Elimination of the Chemical Weapons Stockpile of Syria." Journal of Conflict & Security Law 19, no. 1 (2014): 7-23. doi:10.2307/26296277.

"Summary of the 2018 National Defense Strategy of the United States of America: Sharpening the American Military's Competitive Edge." United States Department of Defense. 2018.

Vincent, Jennifer A., Edmund B. Zaballa, and Kimberly Z. Heyne. "Strategic Context and Traceability." Unpublished paper in the authors' files.

Wade, Norman M. "SMFLS4: The Sustainment & Multifunctional Logistician's SMARTbook: Warfighter's Guide to Logistics, Personnel Services, & Health Services Support." 4th ed. The Lightning Press. 2019.

Developing the Next-Generation of AI Systems to Push the Detection of Foreign Nuclear Proliferation further "Left of Boom"

Angela Sheffield
National Nuclear Security Administration

Following the Trinity test and the end of World War II, the United States called for the development of technologies to monitor foreign nuclear testing programs and detect atomic explosions. Drawing from the same expertise and capabilities that developed the nuclear bomb, the United States began to build technologies capable of detecting nuclear explosions around the globe. While nuclear test detection is as old as the bomb, the development of technologies to detect early nuclear proliferation activities has been an intractable challenge; emerging technologies and approaches from AI and data science present new opportunities. Leveraging the expertise of the DOE's National Laboratory Complex – which was established to advance nuclear science and technology for civilian and military applications – NNSA's Office of Defense Nuclear Nonproliferation Research and Development (DNN R&D) is building AI systems to detect very early indicators of foreign activities to develop nuclear weapons-usable capabilities.

Current proliferation detection technologies exploit unique signatures of the chemical effluents and electromagnetic emanations produced by the specialized industrial processes and equipment used in uranium enrichment, plutonium reprocessing, weapons fabrication and assembly, and weapons testing. However, technologies to enable detection of indicators of nuclear proliferation before a proliferator can produce weapons-grade nuclear material would afford the United States more options for intervention. Early proliferation activities may involve the research and development or acquisition of specialized equipment, technologies, expertise necessary to produce nuclear weapons. Indicators of these activities may be detectable long before weapons testing or the production of weapons-grade nuclear materials. DNN R&D has long pursued the development of technologies to detect indicators of nuclear weapons development activities earlier than enrichment and reprocessing of special nuclear material; however, the development of technologies to detect indicators this early in the nuclear weapons development process, or "left of boom," is incredibly challenging.

Recent advances in data science, artificial intelligence, and computing present new opportunities for early proliferation detection. For example, scientific and academic experts expect that indicators revealing relevant, specialized expertise may be detectable in text-based data sources like technical publications. Data science methods and AI technologies developed to read

Ms. Angela Sheffield is the Senior Program Manager for Data Science and Artificial Intelligence at the Department of Energy (DOE) National Nuclear Security Administration's (NNSA) Office of Defense Nuclear Nonproliferation Research and Development. She has a B.S. in Economics from the United States Air Force Academy and a M.S. in Operations Research from Kansas State University. Prior to joining NNSA, she led project teams at DOE's Pacific Northwest National Laboratory (PNNL) to develop modeling and simulation and data science methodologies to inform CWMD policy and operations. She joined PNNL after a distinguished career as an Operations Research Analyst in the U.S. Air Force. Her email address is angela.sheffield@nnsa.doe.gov.

and process text present powerful new tools to analyze millions of documents without human intervention. However, AI tools developed for commercial applications are inadequate for the high-consequence missions of proliferation detection.

Conventional machine learning-based AI technologies learn complex patterns from datasets of millions of commonplace examples. However, these technologies are not suitable in specialized applications or where events of interest are rare. National security analysts may be overwhelmed by data in the proliferation detection domain, but there are few examples of what they should be looking for. Standard machine learning models notoriously ignore the laws of physics; when there is enough data, learning the laws of physics is believed to be unnecessary. However, the nuclear proliferation domain is far too data sparse for this approach. Instead of ignoring physics and domain information, AI for proliferation detection must leverage domain knowledge and learn from information provided by experts and other sources. National security analysts need to be able to understand and predict when an AI system will (and will not) work and explain model results to decision makers, who reject "black-box models" and require AI systems that "show their work." DNN R&D is developing the next-generation of AI methods and approaches that advance the state-of-the-art in AI to overcome these limitations and build AI systems that are suitable for proliferation detection.

While AI presents new capabilities to address current limits in proliferation detection, AI alone is not enough. The development of AI systems that meaningfully enhance the U.S. government's early proliferation detection capabilities requires tight alignment with unsolved mission challenges and a solid understanding of operational constraints. Working closely with national security mission partners from across the U.S. government, research efforts at the National Laboratories focus on specific proliferation detection areas. Project teams take their research as close as possible to the mission to drive research into the right new scientific techniques to detect early nuclear proliferation indicators.

DNN R&D's project teams are making significant progress. DNN R&D's Advanced Data Analytics for Proliferation Detection (ADAPD) multi-laboratory project team has developed AI models that enable the discovery of scientists with nuclear fuel cycle expertise and the facilities in which they work. This increases the possibility of early identification of illicit activities before nuclear material production begins. In FY21, ADAPD will apply this method against targets of interest and work with mission partners to validate the results. In another effort, Los Alamos National Laboratory (LANL) has developed AI models to identify automatically influential researchers in relevant domains through the analysis of open-source publications from around the globe. After demonstrating this method on relevant use cases, LANL is working closely with mission partners to transition the capability into operation.

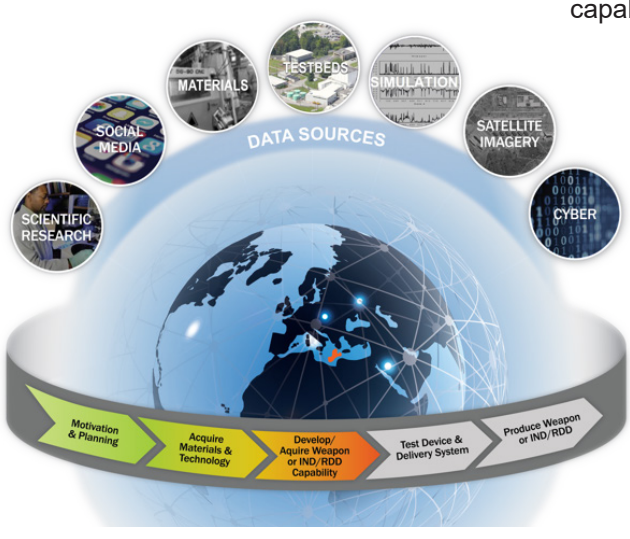

Figure 1. DNN R&D's ADAPD project is developing next-generation AI methods to detect early indicators of foreign nuclear proliferation, pushing detection "left of boom"

Wherever appropriate, DNN R&D's National Laboratory project teams transition enabling technologies throughout the lifecycle of each project, from data management architectures and processing algorithms to AI models and technical reports. In one recent example, Pacific Northwest National Laboratory (PNNL) identified a Department of Defense (DoD) data source from which subtle indicators of proliferation activity could be extracted. The architecture of the database severely limited its interoperability with AI, but PNNL developed a software solution and worked with the DoD development team to test it against known constraints. DoD plans to share the solution broadly, particularly among data scientists and AI developers.

The U.S. government's nuclear proliferation detection capabilities trace their origins to the Manhattan Project. While the test programs are the heritage of the U.S. government proliferation detection programs, AI brings future opportunities, particularly in the challenging domain of early proliferation detection. To continue to drive the development of the next generation of AI methods and technologies, DNN R&D seeks strong partnerships with mission partners, including the U.S. Army.

By better understanding the Army's missions and limitations for countering weapons of mass destruction, DNN R&D can drive the right science to close gaps and, where appropriate, transition technologies that are interoperable with existing capabilities. While the goal is proliferation detection, the potential for impact extends far beyond nuclear nonproliferation. The challenges posed by the nuclear security domain are so demanding that, in building AI to detect early nuclear proliferation, DNN R&D and the National Laboratories will advance the entire field of AI.

Authors of "Fallout Cloud Regimes" (page 103):

Dr. Gregory D. Spriggs is the Principle Investigator of the Film Scanning and Reanalysis Project at the Lawrence Livermore National Laboratory in Livermore, CA. He has a B.S., M.S., and PhD. from the University of Arizona. He was previously assigned as a Nuclear Weapon Designer at the both the Lawrence Livermore National Laboratory (2002-present) and at the Los Alamos National Laboratory (1982-2002). His email address is spriggs1@llnl.gov.

Stephanie Neuscamman is a Staff Scientist at Lawrence Livermore National Laboratory, in Livermore, CA. She has a B.S. in Aerospace Engineering from the University of California, Los Angeles, an M.S. in Aerospace Engineering from Cornell University, and is currently pursuing a Ph.D. in Nuclear Engineering from the Air Force Institute of Technology.

Dr. Kim B. Knight is a staff scientist in the Nuclear and Chemical Sciences group of Lawrence Livermore National Laboratory in Livermore, California, specializing in research supporting forensic investigation of nuclear materials as well as the modern study of historic fallout. She has a B.A. in Geology from Carleton College and a Ph.D. in Earth & Planetary Science from the University of California, Berkeley. She was previously a post-doctoral researcher studying cosmochemistry at the University of Chicago.

Fallout Cloud Regimes

Gregory D. Spriggs, Stephanie Neuscamman,
John S. Nasstrom, and Kim B. Knight
Lawrence Livermore National Laboratory

Summary

The U.S. Department of Defense (DOD), Department of Energy (DOE), and other organizations maintain operational nuclear explosion and atmospheric dispersion models to provide critical guidance on the expected effects of an accidental or deliberate explosion of a nuclear weapon (in this paper simply referred to as "device"). To be effective, these models must represent, as accurately as possible, the complex interactions of the blast, fire, and residual radiological hazards with the environment and population. One hundred atmospheric nuclear tests that form the basis for many models were conducted at the Nevada Test Site (NTS) (now referred to as the Nevada Nuclear Security Site, NNSS) in a dry desert environment.[1] Other environments should be studied, but have less data available and are beyond the scope of the work presented in this paper.

The debris clouds produced by the NTS tests, frequently called "mushroom clouds," are familiar, with common structural elements such as a buoyant cap connected to a skirt of raised dust at the desert surface by a thin, dirt-filled stem. The film scanning project at LLNL[2] has investigated historical film records of nuclear weapons tests. In this paper, we summarize findings showing that the mushroom cloud behavior, for historic U.S. tests conducted in Nevada, has similar characteristics based on the distance of the device from the ground surface or Height of Burst (HOB), scaled by the energy release, or yield, of the device. This scaled height is referred to as the scaled-height-of-burst (SHOB).

The findings discussed below show that mushroom clouds look and behave similarly when detonated at the same SHOB. The amount of residual radiation that is produced by a nuclear detonation is proportional to the yield, but the amount of that residual radiation that actually becomes local fallout is strongly dependent on the SHOB and the type of surface over which the detonation occurs. In order to develop a more comprehensive model that predicts the fraction of the residual radiation that becomes local fallout, it is convenient to define a series of regimes based on SHOB values in which all detonations that occur within a given regime can be modeled using the same algorithms. The purpose of this paper is to provide a framework for defining different regimes, and, in a qualitative way, a basic understanding of the fundamental characteristics of each of these regimes.

Modeling Nuclear Cloud Rise and Fallout

The motion of the visible debris cloud from U.S. atmospheric nuclear tests was recorded on motion picture film during the period from 1945 to 1962. Making use of recent high-quality digital scans of the debris cloud films, data on the rise rate of the buoyant gases, debris cloud interaction with the ambient atmosphere, environmental material entrainment, and final stabilized cloud size, shape, and position are being measured by a team of scientists at the Lawrence Livermore National Laboratory as part of the Film Scanning and Reanalysis Project lead by the first author. The purpose

of the project is to measure the aforementioned quantities to a higher degree of accuracy than previously reported (see DASA-1251 for collected historical test data[3]). The geometry of the mushroom debris clouds resulting from testing at various heights above the surface is of particular focus, and a framework that makes use of the observed self-similarity of debris cloud behavior with similar SHOB is proposed for use in operational fallout models. Figure 1 shows an example of three detonations of different yields having different Height of Burst (HOB), but the same SHOB (given by equation shown in section below). In each of these three examples, the HOB is two times the fireball radius, *R*. The resulting mushroom clouds produced by these three detonations would be almost identical in appearance and characteristics, such as activity-height distribution, after scaling by the energy release, or yield, of the device.

of fallout particles. Characterization of general debris cloud regimes aids in understanding the second of these three phases. For surface and near-surface events, current fallout models use radioactive debris source terms that have been empirically or semi-empirically derived from low-yield, near-surface tests, where the fission products can be assumed to be distributed throughout the initial cloud.[4-7] Evidence exists that events occurring at higher SHOB result in mushroom clouds where the fission product material cannot be reasonably assumed to be uniformly distributed across all parts of the debris cloud structure.[8] Fallout models are needed to help respond to risks from a variety of nuclear detonation threats at different heights of burst.[9] Therefore, model improvements must be developed and validated for a wider range of SHOB.

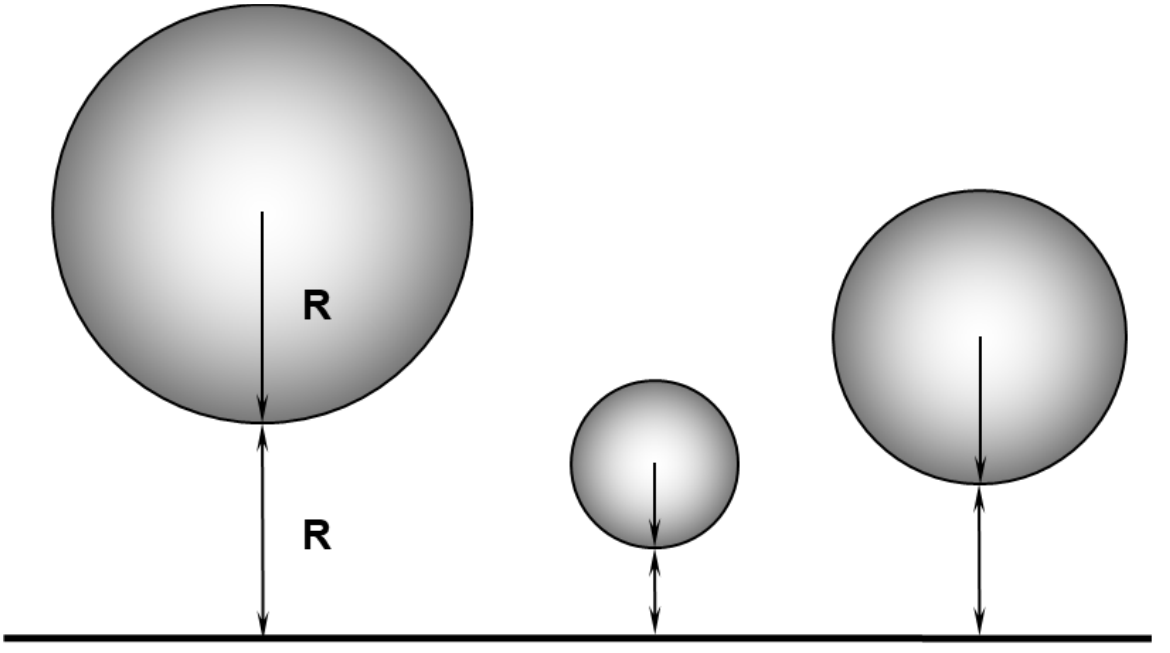

Figure 1. An example of three detonations having the same Scaled Height of Burst (SHOB), because the height of burst is two times the fireball radius, *R*, in each example.

The behavior of the fallout material generated within or swept into the rising buoyant cloud (the familiar mushroom cloud) can be broken down in a modeling framework to three distinct phases: particle growth from condensation and agglomeration, particle mixing and transport during the buoyant cloud rise, and downwind dispersion and deposition

Film Scanning and Reanalysis

Since 2011, the Film Scanning and Reanalysis Project[10] has been an effort between Lawrence Livermore National Laboratory, Los Alamos National Laboratory, the Air Force Institute of Technology and other organizations to preserve and study the historical films recorded

during the United States above ground nuclear tests (AGT) from 1945-1962. The primary goal of the project is to support the nuclear weapons complex by preserving AGT data and creating better data sets for future work. The films must be scanned and digitally archived. The high-resolution scans can be analyzed using sophisticated digital tools that were not available for the original analysis conducted by Edgerton, Germeshausen and Grier, Inc. (EG&G), the Defense Nuclear Agency (DNA), the DOD and other researchers back in the 1940s, 1950s and 1960s. As the digital films are analyzed, improvements to yield determination and other aspects of the tests are made. In addition to determining the yield more accurately, the digital films allow a deeper investigation of post-detonation physics including shock phenomena, light output, thermal blast, mushroom cloud formation, the dynamics of the buoyant cloud rise, and nuclear fallout. The data are being collected by the research team at LLNL to form benchmarks for verification and validation of computer modeling codes for weapons effects and fallout predictions.

Post-detonation debris cloud behavior is studied using two general types of films recorded by EG&G: early- and late-cloud films. Both types of films were recorded with intermediate-speed, intermittent cameras. These cameras were typical motion picture cameras where the film is stopped in the gate to be exposed and then advanced to the next frame. The early debris cloud films were typically recorded at 100 frames per second, whereas the late-cloud films usually ran at 1 frame per second.

The early-cloud films were used to study late-time shockwave phenomena, when the shock has separated from the fireball and interacts with the surroundings, as well as the early motion of the buoyant cloud cap and initial lofting of surface material, as applicable. The evolution of debris cloud behavior captured by this type of film varies widely across different testing campaigns and individual tests. For later series, when the procedure for filming was more mature, the amount of cloud behavior captured on the film depends on the yield of the device. For a typical recording period of an early debris cloud film, the debris cloud from a smaller yield event would go through more of its evolution towards stabilization than one from a larger yield, even at the same SHOB.

Some of the early debris cloud films record long enough times that the cloud motion can be visibly affected by the ambient wind conditions. Investigations of the cloud behavior beyond the point where the cloud motion is being affected by ambient winds can only be accurately analyzed with the use of the cloud triangulation. If the motion of the cloud towards or away from the camera is not accurately assessed, the assumed magnification of the cloud image will not be correct, and the observed cloud dimension will not be correct when obtained from the film record. The triangulation analysis requires pairs of films of sufficient quality over a matching time frame in order to calculate cloud trajectories.

The tests conducted at the Nevada National Security Site usually included several late-cloud films captured from different angles. These films were often a series of snapshots with a framerate of 2 to 4 frames per minute. These records track the cloud motion through stabilization time and often until the debris cloud begins to dissipate in the ambient atmosphere. When pairs of these late cloud films survive, they can be analyzed to determine the cloud motion relative to the fixed camera locations and correct the magnification of the image, giving accurate data on cloud growth and rise rates.

Efforts to analyze the debris cloud motion for the Above-Ground-Tests (AGT) is ongoing, and early efforts to conduct correct debris cloud trajectory calculations have been promising. Fortunately, the current work describes phenomenological, self-similar behavior in which the exact cloud dimensions are not required. The cloud behavior, and how it relates to SHOB described below, is evident in individual films (no triangulation required) and even in some cases from still photographs of the debris cloud at or near its stabilization time. Below we present a summary of cloud regimes generalized from observed SHOB relationships.

Defining the Debris Cloud Regimes

Scaled Height of Burst

The self-similarity of the debris cloud in the minutes after explosion is evident when the initial height at which the detonation occurs is expressed in terms of its SHOB. Based on scaling laws derived from the shock wave equations, the SHOB can be defined as

$$SHOB = \left(\frac{\rho_0}{Y}\right)^{1/3} \times HOB$$

where ρ0 is the ambient atmospheric density at the Height of Burst (HOB) in feet above ground level, and *Y* is the device yield in kt. In the nuclear weapon effects literature, e.g., book by Glasstone and Dolan,[13] the density term ρ_0 is usually ignored. For most atmospheric tests, the variation from a unity density is small, and when raised to the 1/3 power, the effect of including a reference density is negligible. Therefore, SHOB values used in this paper are determined from the yield and HOB defined simply as

$$SHOB = HOB \times Y^{-1/3}$$

Two nuclear events of different yield can have very similar debris-cloud behavior if their HOB is such that the distance of the asymptotic fireball to the ground is the same, relative to the asymptotic fireball radius of each event. The effect is illustrated in Figure 2. Encore was a 27 kt test at 2423 ft above the surface. Wasp was a much smaller test at 1 kt, occurring at a much lower HOB, 762 ft. However, the SHOB for these tests (808 ft/kt$^{1/3}$ and 762 ft/kt$^{1/3}$, respectively) differ by only 6% and the fireballs in relation to the surface are very similar. The fireball images shown in Figure 2 are obtained after the separation of the shockwave, when the fireball has reached an asymptotic size and is no longer growing with time. At some time after these images, the hot, buoyant bubble will begin rising through the ambient atmosphere and transition to the familiar toroidal shape and then to the mushroom cloud cap.

For events occurring below the ground surface, the scaled-depth-of-burial (SDOB) is defined in an analogous way:

$$SDOB = DOB \times Y^{-1/3}$$

When defining regimes for the buried tests, we shall stick to this definition even though the crater dimensions appear to correlate better with $Y^{-1/3}$.[4] as reported by Teller, et al.[12]

Regime Characteristics

The nuclear debris cloud behavior can be divided into eight regimes.[11] The expected fallout deposition from a given nuclear

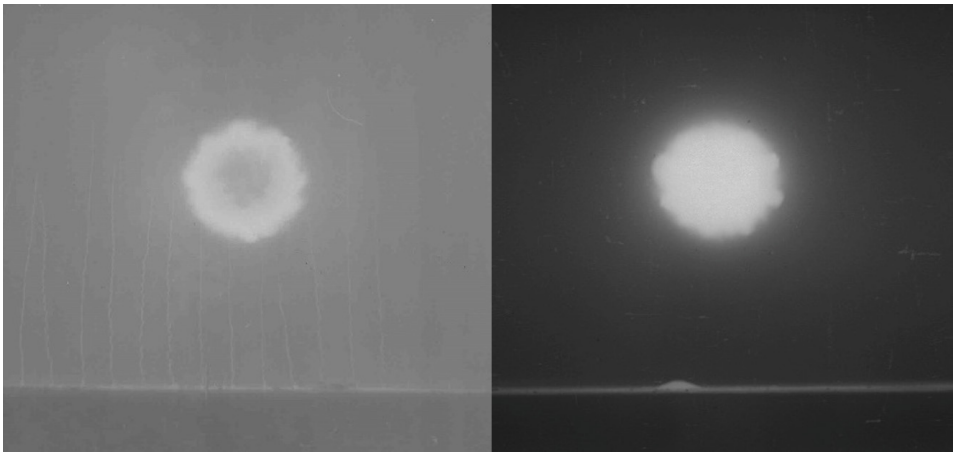

Figure 2. The asymptotic fireball radii of Encore (left) and Wasp (right) with ground surface illuminated. The Encore fireball radius is 659 ft. The Wasp fireball radius is much smaller at 214 ft. However, since the HOB of Encore is much greater, the ratio of the fireball radius to the distance from fireball center to the ground in each test is very similar: 0.27 for Encore and 0.28 for Wasp.

detonation event depends on the characteristics of the regime into which it falls, as influenced by the yield, HOB, and the emplacement of the device. While Ambient, environmental conditions, such as air density and ground density, can also affect the behavior of the cloud. We have neglected the air and ground density in the definition of the SHOB in order to use a single definition of SHOB that is applicable to both above-ground and below-ground detonations (i.e., SDOB is synonymous with a negative SHOB). If we included the ambient medium density in our definition of SHOB, there would be a sudden change in scale going from a detonation just above the surface where the air density is ~1 kg/m^3 to one just below the surface where the ground density is ~2000 kg/m^3. When developing specific algorithms to model each of these regimes, air density will be incorporated into the equations.

geology, can produce significantly different local fallout due to differences in particle size distribution and the associated settling times of the lofted particles. This work does not address the influence of entrained materials and native particle size distributions. These kinds of details will be incorporated in the future in the specific algorithms for each fallout regime.

Nuclear Debris Cloud Regimes

The behavior of the debris cloud in which no surface interaction is observed is defined as Regime 1. Events in Regime 1 occur with the largest SHOB values. Deeply buried events are defined as being in Regime 8. Events occurring between these extremes are divided into Regimes 2-7 based on key characteristics of the observed debris cloud behavior.

Regime	1	2	3	4	5	6	7	8
SHOB (ft/kt$^{1/3}$)	> 1500	800 to 1500	500 to 800	200 to 500	20 to 200	-10 to 20	-150 to -10	-300 to -150

Table 1. Approximate SHOB value ranges for fallout regimes based on film observation from historic events at the Nevada National Security Site.[1]

The following regime framework is presented as a useful tool to help guide improvements to current fallout source term methodology previously used in consequence management applications. Values for SHOB to delineate the regimes are given which apply to many historic U.S. nuclear tests. While the specific SHOB values would change in different environments, such as that of an urban event, the framework presented should be broadly applicable to any nuclear debris cloud.

The character of nuclear fallout depends strongly on the SHOB as well as the type of surface over which the nuclear event occurs. The presence of surface material which can easily be lofted, such as the dry loose dirt typical of the Nevada National Security Site testing conducted in the dry alluvial beds of Frenchman Flats and Yucca Flats, has a strong effect on the amount and distribution of nuclear fallout. The same event, occurring at the same HOB over different

Events in which there is no interaction with the ground surface are in Regime 1, defined as SHOB > 1500 ft/kt$^{1/3}$. The fireball does not reach the ground surface. The cloud cap contains only bomb debris that has condensed onto itself; no significant environmental carrier material is present within the cloud cap. No significant dust stem or dust skirt are formed during the negative wind phase, when the low-pressure region below the rising cloud cap draws air and material from the surroundings back towards the burst point and into the cap. A bomb debris stem may form during the formation of the rising buoyant vortex. This bomb debris stem is far removed from, and does not interact with, the ground surface. Residual radiation in the vicinity of ground zero is in the form of low-level, fixed ground activation. Examples of atmospheric tests categorized as Regime 1 events include Teapot HA (27,734 ft/kt$^{1/3}$), Plumbbob John (11,771 ft/kt$^{1/3}$), and Upshot-Knothole Dixie (2708 ft/kt$^{1/3}$).

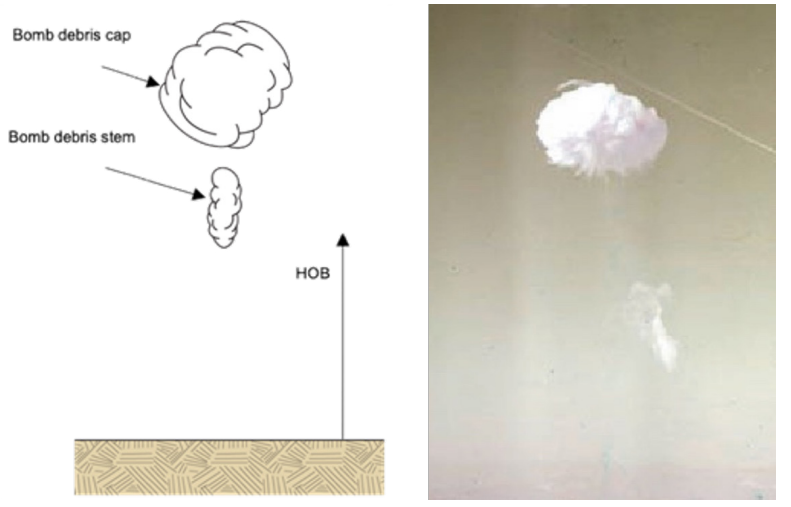

Figure 3: Characteristic debris cloud in a Regime 1 event (left) and the cloud from the Upshot-Knothole Dixie test (2708 ft/kt$^{1/3}$).

Regime 2 events are closer to the surface than Regime 1, between 800 ft/kt$^{1/3}$ < SHOB < 1500 ft/kt$^{1/3}$. As in Regime 1, the fireball does not reach the surface and the cloud cap contains only bomb debris that has condensed on itself. However, Regime 2 is distinct in that at these SHOB, a dust stem and skirt form. The dust stem remains separate from the bomb debris in the cap. Though the dust stem may reach the bomb debris stem (which forms under the cap), it does so only at late time after significant cooling of the bomb debris has occurred. The lofted dust is radioactive due to neutron activation of the soil. No cratering occurs. The residual radiation in the vicinity of ground zero is due to activation of the ground, and groundshine dose rates are higher than observed in Regime 1. Examples of atmospheric tests categorized as Regime 2 include Tumbler-Snapper tests Baker (1109 ft/kt$^{1/3}$) and Charlie (1097 ft/kt$^{1/3}$), Hardtack II tests DeBaca (1153 ft/kt$^{1/3}$) and Rushmore (872 ft/kt$^{1/3}$), and Upshot-Knothole Encore (808 ft/kt$^{1/3}$).

Regime 3 occurs between 500 ft/kt$^{1/3}$ < SHOB < 800 ft/kt$^{1/3}$. The debris cloud behavior is similar to Regime 2, described above, with the distinction that mixing of the bomb debris stem and the dust stem occurs at earlier time and more extensively. The Buster-Jangle tests Baker (736 ft/kt$^{1/3}$) and Dog (514 ft/kt$^{1/3}$), the Wasp (762 ft/kt$^{1/3}$) and Wasp Prime (512 ft/kt$^{1/3}$) tests and the Doppler (674 ft/kt$^{1/3}$) event all show Regime 3 debris cloud behavior.

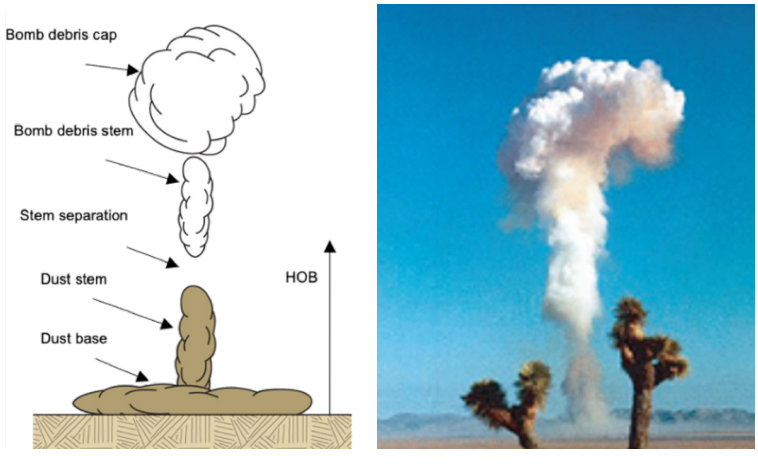

Figure 4: Characteristic debris cloud in a Regime 2 event (left) and the cloud from the Hardtack II DeBaca test (1153 ft/kt$^{1/3}$).

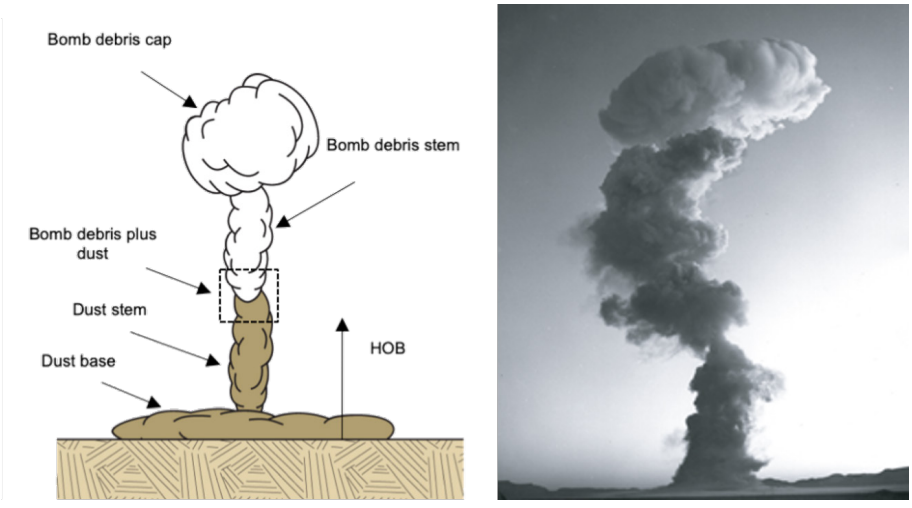

Figure 5: Characteristic debris cloud in a Regime 3 event (left) and the cloud from the Doppler test (674 ft/kt$^{1/3}$).

Regime 4 events have SHOB between 200 ft/kt$^{1/3}$ and 500 ft/kt$^{1/3}$. The nuclear fireball still does not touch the ground. Dust is drawn into the fireball during the initial fireball phase, quenching part of the plasma in the fireball. At the lower end of Regime 4, interaction of the ground reflected shock and the debris fireball results in a bifurcation of the partially quenched fireball, resulting in a main cloud cap and a bulge in the stem. Both the main cap and the stem bulge contain bomb debris and activated dust from the surface. The stem and skirt contain activated dust particles. Local fallout will be formed and deposit in the form of the activated dirt that was lofted and carried downwind. Slight cratering occurs. Examples of Regime 4 tests include Buster-Jangle Easy (418 ft/kt$^{1/3}$), Tumbler-Snapper Dog (390 ft/kt$^{1/3}$), Grable (212 ft/kt$^{1/3}$) and Priscilla (210 ft/kt$^{1/3}$).

As the SHOB is further decreased, the amount of material mixing between the bomb debris and the environmental material entrained from the surface increases. In Regime 5 (20 ft/kt$^{1/3}$ < SHOB < 200 ft/kt$^{1/3}$), the surface material noticeably mixes throughout the cap. The fireball contacts the surface and some soil melt or vaporization occurs. The dust stem and base are both formed and immediately drawn into the buoyant cap. The molten or vaporized soil and bomb debris solidifies or condenses onto lofted dust during the mixing phase in the cap, leading to local fallout which contains both fission and activation products. Examples of Regime 5 tests include Hornet (189 ft/kt$^{1/3}$), Tesla (157 ft/kt$^{1/3}$) and MET (143 ft/kt$^{1/3}$), as well as Tumbler-Snapper George (122 ft/kt$^{1/3}$) and Nancy (104 ft/kt$^{1/3}$).

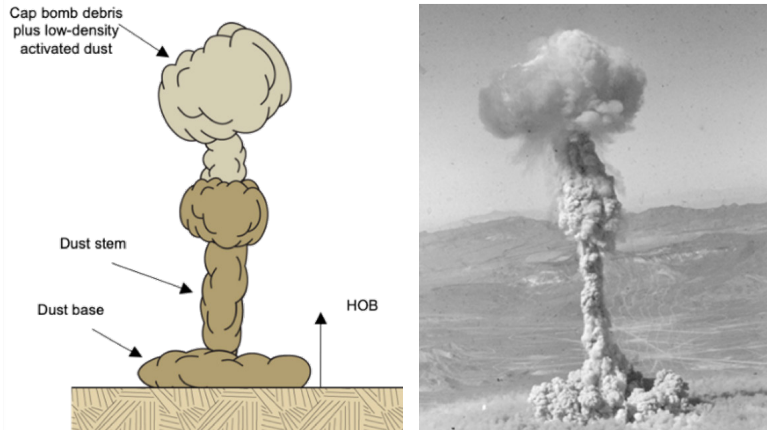

Figure 6: Characteristic debris cloud in a Regime 4 event (left) and the cloud from the Tumbler-Snapper Dog test at SHOB of 390 ft/kt$^{1/3}$.

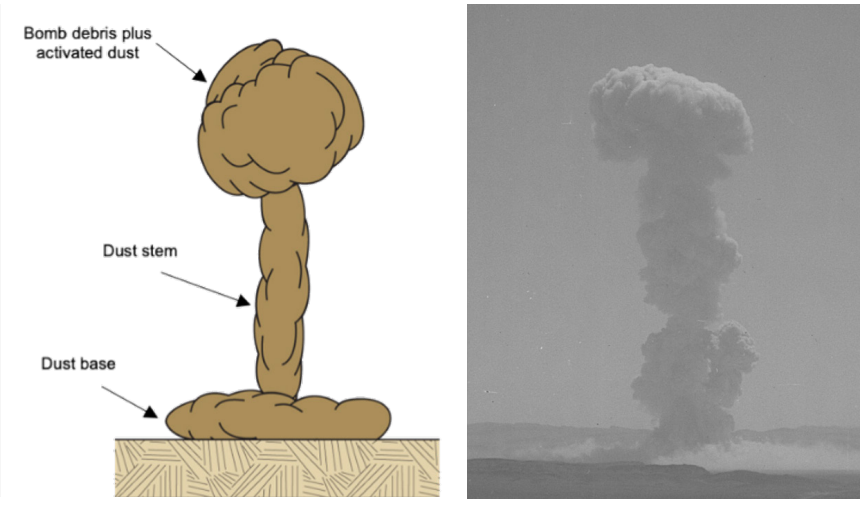

Figure 7: Characteristic debris cloud in a Regime 5 event (left) and the cloud from the MET test (143 ft/kt$^{1/3}$).

The familiar fallout-free height of burst (FFHOB), as frequently included in the discussions of nuclear effects literature, would be found in the upper portion of Regime 5. The value of FFHOB is also scaled by yield (in this case, $Y^{0.4}$) and is intended to represent the height at which local fallout, as stated by Glasstone and Dolan13 "ceases to become a serious problem". As presented in that Glasstone and Dolan book, the FFHOB should be treated as an approximation only, with a quoted error value of ±30%. However, the lofted activation products from the soil can be carried by the wind to form a distributed local radiation hazard well above this scaled height, which makes the FFHOB something of a misnomer.

Surface bursts, as well as events with SHOB < 20 ft/kt$^{1/3}$ and SDOB > -10 ft/kt$^{1/3}$, compromise Regime 6. The fireball contacts the surface and melts or vaporizes a significant amount of soil material. Large amounts of dust are immediately drawn into the cloud cap where it is mixed with bomb debris. Bomb debris and molten soil condense onto dust lofted into the cloud, producing significant local fallout. The near-surface nuclear explosions conducted in Nevada tended to be smaller yield events to limit this effect. Sugar (4 ft/kt$^{1/3}$) and Johnny Boy (-2.4 ft/kt$^{1/3}$) are examples of Regime 6 tests.

Events with scaled depth of burial of 10 to 150 scaled feet below the surface (-150

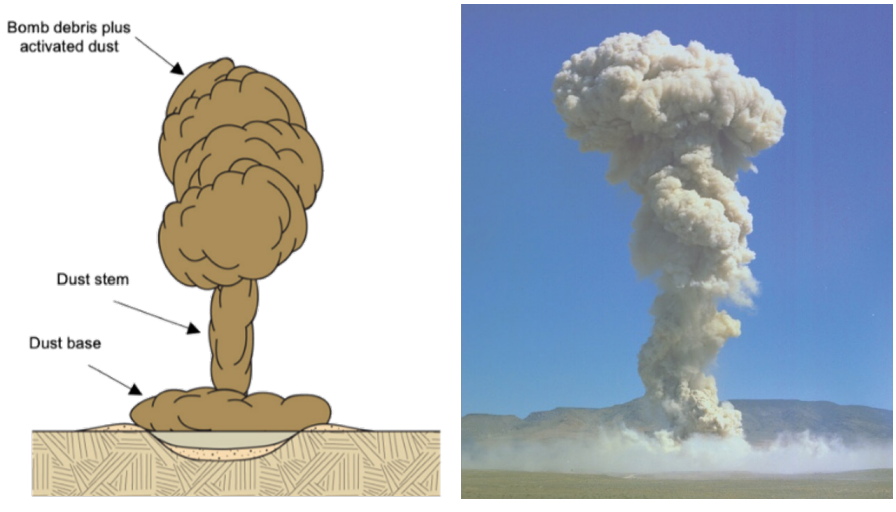

Figure 8: Characteristic debris cloud in a Regime 6 event (left) and the cloud from the Johnny Boy test, a shallow-buried device with SDOB of -2.4 ft/kt$^{1/3}$.

ft/kt1/3 < SDOB < -10 ft/kt$^{1/3}$) are categorized in Regime 7. In this Regime, the rock and soil material around the device is vaporized or melted and this material is mixed with bomb debris. The device is shallow enough such that the fireball breaches the surface and a large crater is formed. A base surge cloud is formed, lofting gaseous and particulate material. Crater ejecta quickly settles back to the surface. The bomb debris and activated soil products mix and condense in the dust cloud. Buster-Jangle Uncle (-16 ft/kt$^{1/3}$), ESS (-67 ft/kt$^{1/3}$) and Sedan (-135 ft/kt$^{1/3}$) and Danny Boy (-146 ft/kt$^{1/3}$) were buried tests which produced a Regime 7 debris cloud.

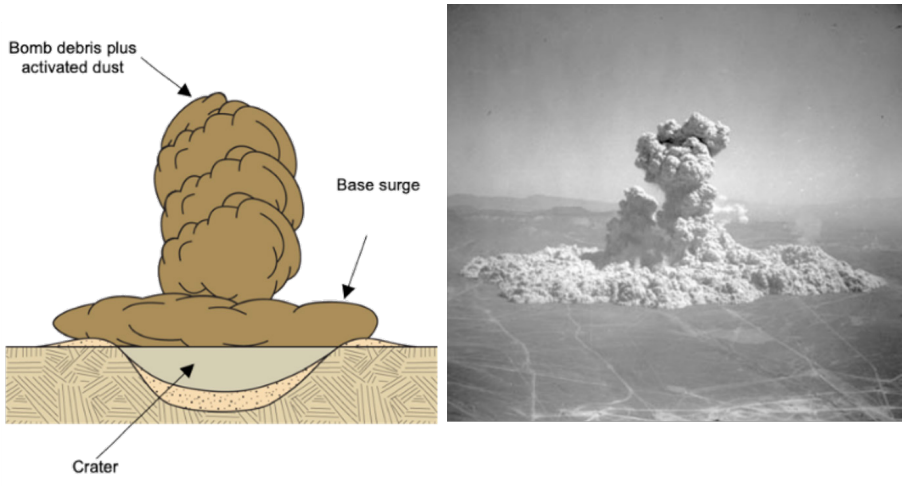

Figure 9: Characteristic debris cloud in a Regime 7 event (left) and the cloud from the Sedan test (-135 ft/kt$^{1/3}$).

More deeply buried bursts are grouped into Regime 8, defined as -300 ft/kt$^{1/3}$ < SDOB < -150 ft/kt$^{1/3}$. The fireball vaporizes and melts the soil surrounding the device but does not break the surface. The earth above the explosion point is fractured and temporarily lofted. A small, non-radioactive base surge forms from the disturbed ground as the earth falls back into the crater. The vast majority of the condensed fission products are contained within the ground and not released to the environment. Some radioactive gases and dust particles can escape through the rubble bed formed above the explosion point. The Sulky test (-197 ft/kt$^{1/3}$) is an example of a Regime 8 tests.

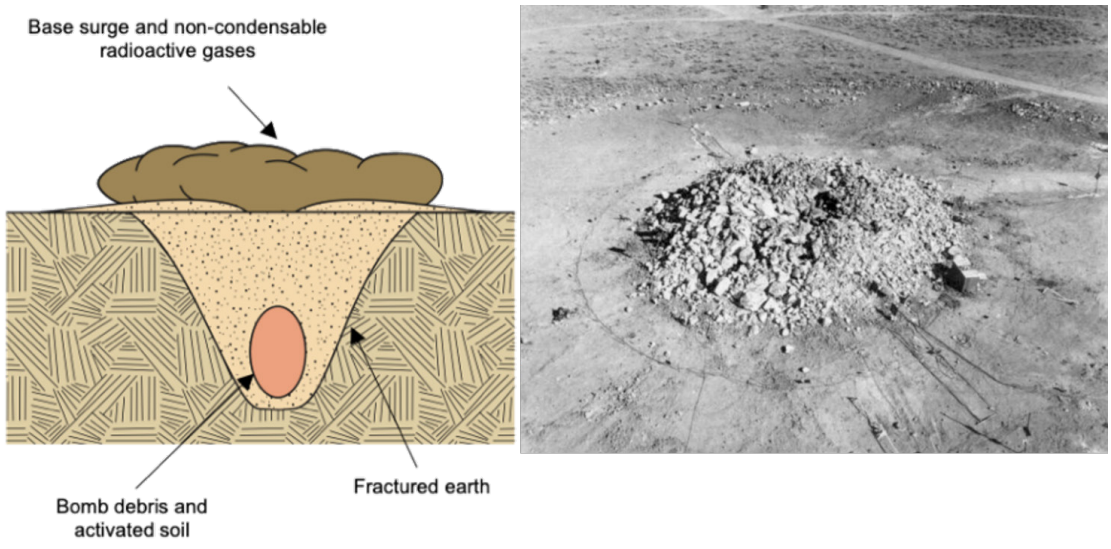

Figure 10: Characteristic debris cloud in a Regime 8 event (left) and the rubble from the Sulky test (-197 ft/kt$^{1/3}$).

Expanding Debris Cloud Behavior Models

We have presented a generalized framework for capturing the similarity of nuclear debris cloud formation for detonations with similar SHOB values. The nuclear debris cloud regimes were defined here based on debris cloud behavior observed in a dry, dusty environment with loose, easily lofted surface material. The same conceptual framework could be adopted when considering post-detonation effects in other environments. The fallout regimes framework can be used to formulate fallout dispersion models that better account for the fallout particle formation processes for fission vs. activation products, and for lofting of activation products for above ground nuclear explosions. The adoption of a regime framework allows for greater flexibility in defining the radioactive source term for a given model. As new information on how expected material entrainment and mixing is affected by the surrounding environment becomes available, adjustments to the regime SHOB ranges are easy to adopt. Both fast-running fallout codes and higher-fidelity cloud rise and fallout codes need to be validated against the existing experimental test data.[7, 14-15] These types of comparisons would allow us to determine if our understanding of the basic physics involved Is correct.

Grouping tests into the regimes describe above, with similar cloud rise and surface interaction, can be useful in future model development for cases for which there is no historical dataset. Cloud features, especially the mixing of material within the familiar cloud structures of the cap, stem, and skirt, could guide the delineation of the regimes. This framework could be applied to the distribution of the nuclear debris source term in fallout simulations to improve model predictions. For example, parameterized particle activity-size distributions and activity-height distributions that vary with SHOB, in a manner consistent with the fallout regimes, could be developed for simpler models. Appropriately placing the fission and activation products within the model fallout source term is necessary to accurately assess the radiation dose and health consequences for nuclear events for a range of yield, HOB, and surrounding environments, and remains to be done by taking advantage of data beyond the limited data at which fallout models are currently validated against. SHOBs that define each regime are preliminary. It is our intention to analyze as many nuclear debris cloud films as possible and refine the SHOBs that further define each regime. When completed, we want to have a set of regimes in which a single set of algorithms can be used to describe all of the detonations that occur within each regime.

Acknowledgements

Prepared by LLNL under Contract DE-AC52-07NA27344. This work was supported by LDRD project 20-SI-006, "The Influence of Environment on Post-Detonation Chemistry and Debris Formation." We thank Susan Mangles for her graphics work on the original Fallout Regimes poster,[11] which formed the basis of this work. We thank Jim Moye, Pete Kuran, and Stephen Murray on the LLNL Film Scanning and Reanalysis project team as well as our many students. A printable poster with several examples of cloud images for each of the Regimes can be made available by request to authors.

Notes:

1. United States Nuclear Tests July 1945 through September 1992 prepared by the U.S. Dept. of Energy NNSA Nevada Field Office, Las Vegas, NV. DOE/NV-209-REV 16. September 2015.
2. Lawrence Livermore National Laboratory, LLNL Atmospheric Nuclear Tests, YouTube playlist, July 3, 2018, https://www.youtube.com/playlist?list=PLvGO_dWo8VfcmG166wKRy5z-GIJ_OQND5
3. Hawthorne, H. Compilation of Local Fallout Data from Test Detonations 1945-1962 Extracted from DASA 1251. Volume 1. Continental U.S. Tests. Technical Report. 1979.
4. Harvey, T., Serduke, F., Edwards, L., and Peters, L. KDFOC3: A Nuclear Fallout Assessment Capability. Lawrence Livermore National Laboratory, Livermore, CA. UCRL-TM-222788. 1992.
5. Nasstrom, J.S., Sugiyama, G., Baskett, R.L., Larsen, S.C., and Bradley, M.M. The National Atmospheric Release Advisory Center (NARAC) modeling and decision support system for radiological and nuclear emergency preparedness and response. Int. J. Emergency Management, 4. 2007.
6. Norment, H.G. DELFIC: Department of Defense Fallout Prediction System, Fundamentals, Vol. I. Technical Report. Atmospheric Science Associates. Bedford, MA 1979.
7. Rolph, G.D., Ngan, F., and Draxler, R.R., Modeling the fallout from stabilized nuclear clouds using the hysplit atmospheric dispersion model. J. Environ. Radioactiv., 136, 41-55. 2014.
8. Larson, K., Neel, J., and Associates, Summary Statement of Findings Related to the Distribution, Characteristics, and Biological Availability of Fallout Debris Originating from Testing Programs at the Nevada Test Site. University of California, Los Angeles School of Medicine, UCLA-438, 1960.
9. National Council of Radiation Protection and Measurements, Responding to a Radiological or Nuclear Terrorism Incident: A Guide for Decision Makers. NCRP Report No. 165, January 11, 2010, National Council on Radiation Protection and Measurements, 7910 Woodmont Avenue, Suite 400, Bethesda, MD 20814-3095, https://ncrponline.org/shop/reports/report-no-165-responding-to-a-radiological-or-nuclear-terrorism-incident-a-guide-for-decision-makers/
10. Spriggs, G.D. and Gaunt, R. Scientific Objectives of Scanning Project, Lawrence Livermore National Laboratory, LLNL-PRES-491856, August 24, 2011.
11. Spriggs, G.D., Fallout Regimes, Lawrence Livermore National Laboratory, UCRL-POST-219627. March 6, 2006.
12. Teller, E., Talley, W.K., Higgins, G.H., and Johnson, G.W. The Constructive Uses of Nuclear Weapons. McGraw-Hill, Inc. New York, NY. 1968.
13. Glasstone, S. and Dolan, P. The Effects of Nuclear Weapons. Technical Report, U.S. Department of Defense. 1977.
14. Miller, A.D., A Comparison in the Accuracy of Mapping Nuclear Fallout Patterns using HPAC, HYSPLIT, DELFIC FPT and an AFIT FORTRAN95 Fallout Deposition Code. Air Force Institute of Technology, WPAFB, OH. 2011.
15. Arthur, R.S., Lundquist, K.A., Mirocha, J.D., Neuscamman, S., Kanarska, Y., and Nasstrom, J.S. Simulating nuclear cloud rise within a realistic atmosphere using the Weather Research and Forecasting model. Submitted to Atmos. Environ. 2020.

Proliferation Considerations of Laser Enrichment Technology

MAJ Lorin D. Veigas
Defense Threat Reduction Agency

Introduction

Although the international community has made great strides to limit the proliferation of nuclear weapons with the Treaty on the Non-Proliferation of Nuclear Weapons (1970) and the Comprehensive Test Ban Treaty (1996), counterproliferation remains a dire technical challenge in the 21st Century.[1] The Democratic People's Republic of Korea (DPRK) continues to develop nuclear weapons in violation of United Nations Security Council resolutions; in the wake of the U.S. withdrawal from the Joint Comprehensive Plan of Action, Iran has surpassed agreed upon enrichment levels for its stockpile of uranium.[2] With the speed of technological innovation, it is critical that regulators remain astutely aware of emerging technologies that could facilitate the acquisition of fissile materials.

The challenges a proliferator encounters using first- or second-generation enrichment technologies such as gaseous diffusion and centrifugation can present advantages to regulators. For example, neither technique is capable of producing weapons grade material in one step, so a cascade of individual machines must be constructed.[3] This means that enrichment plants require large facilities that can be difficult to conceal from the international community. Hundreds of machines arrayed in stages and cascades also draw thousands of kilowatt hours of electricity and can emit a unique signals intelligence (SIGINT) signature. Laser isotope separation, however, is an emerging technology that could enrich weapons grade uranium within a small, discrete footprint while emitting a signature no more noticeable than a large grocery store.

First and Second-Generation Enrichment Methods

The first commercial uranium enrichment process carried out utilized the gaseous diffusion method. Proven to be a durable and reliable method of enrichment, gaseous diffusion accounts for about 40 percent of global enrichment capacity today.[4] The method involves pushing pressurized uranium hexafluoride (UF6) gas through a series of vessels containing a porous membrane. Because $U^{235}F_6$ molecules are slightly lighter than $U^{238}F_6$, they move faster and have a slightly better chance of passing through the membrane pores. The gas that diffuses through the membrane is slightly enriched while the gas that passes directly through the containment vessel is slightly depleted. The major components of each stage include a compressor to pressurize the UF_6 for optimal interaction with the membrane, and a heat exchanger to remove the heat of compression. Both components draw electricity, significantly increasing the overall power consumption of a gaseous diffusion plant. Due to the inefficiency of the process, roughly 1,200 stages would be required to enrich up to 3

MAJ Lorin Veigas is the DTRA Liaison to JSOC, in Fort Bragg, NC. He has a B.S. in English Literature from the United States Military Academy and a M.S. in Nuclear Engineering from the Air Force Institute of Technology. He was previously assigned as a future plans officer at the 75th Ranger Regiment. His email address is lorin.d.veigas.mil@mail.mil.

weight percent U^{235}. In short, gaseous diffusion is commercially reliable, but is inefficient and requires a large footprint and a massive amount of electricity.

Centrifugation is a second-generation enrichment technology that matured in the 1960s and has largely replaced gaseous diffusion as the dominant commercial uranium enrichment method used today.[5] As with gaseous diffusion, the feed is UF_6 gas that is pumped into a vertical cylinder, or rotor, connected to a motor drive and enclosed in a vacuum casing. As the rotor spins, the centrifugal force drives the heavier $U^{238}F_6$ preferentially toward the outside while the lighter $U^{235}F_6$ molecules stay toward the central axis. This separation is enhanced by a countercurrent flow caused by the difference in heat from the end cap with the motor and the one without. This causes a relatively large assay at the top of the cylinder where the product is collected.[6] A centrifuge plant uses roughly five percent of the electricity of a comparably-sized gaseous diffusion plant, making them significantly more economical.[7]

Laser Isotope Separation: AVLIS and MLIS

The two approaches to laser isotope separation that have been researched are atomic vapor laser isotope separation (AVLIS) and molecular laser isotope separation (MLIS). AVLIS works by first vaporizing uranium metal. The vapor stream passes through a laser precisely tuned to a wavelength which excites and ionizes the U^{235} atoms, but not the U^{238} atoms. The U^{235+} ions are electromagnetically attracted to a negatively charged collection plate and collected. The neutrally charged U^{238} passes through the collector unit and is collected separately as depleted tails.[8]

The MLIS process differs slightly in that the feed stock is gaseous UF_6, the same feed used in both gaseous diffusion and centrifugation, which would allow the process to be more readily adopted into a conventional fuel cycle. An infrared long wavelength laser selectively excites $U^{235}F_6$ molecules. Once excited, a second short wavelength or ultraviolet laser deposits sufficient energy to dissociate the molecules into $U^{235}F_5$ and a loose fluorine atom. Although $U^{235}F_6$ and $U^{239}F_6$ have identical chemical properties, they have different natural vibrational frequencies. The infrared laser used is finely tuned to the frequency of $U^{235}F_6$ leaving the $U^{238}F_6$ to pass through unaltered. The loss of a fluorine atom drives a chemical reaction in which the $U^{235}F_5$ is formed as a powder and will naturally settle out of the feed gas.[9] Unlike both gaseous diffusion and centrifugation which have some inherent probability that molecules of the desired isotope will travel in a certain path or diffuse in a certain way, the MLIS reaction will happen to 100 percent of the preferred molecules if contacted with the laser. This allows for a process that can be as much as 70 times more efficient than gaseous diffusion.

Comparison of Enrichment Methods

Efficiency

Separation factor is simply the multiplicand giving the change in the ratio of two constituents. For gaseous diffusion the separation factor is 1.004. For centrifugation using 2nd generation centrifuges, a separation factor of 1.10 can be achieved. Laser isotope separation technologies can achieve separation factors of up to 70.

While separation factor describes the efficiency of a physical process, the overall capacity of a uranium enrichment plants is described in terms of Separative Work Units (SWU). The SWU measures the quantity of separative work performed to enrich a given amount of uranium to a given enrichment level. Since feed and tails are measured in kilograms, SWU is specifically expressed as Kilogram Separative Work Unit (KgSWU).

Energy consumption

When comparing energy consumption, a useful unit of measure common to multiple enrichment methods is the kilowatt hours of electricity required to produce one Kilogram Separative Work Unit (kgSWU). Of the three enrichment methods considered, gaseous diffusion uses roughly 2500 kWh/kgSWU, ultra centrifuges can perform with as little as 50 kWh/kgSWU, and MLIS has published estimates

of 30 kWh/kgSWU. However, separation of isotopes by laser excitation (SILEX) advertises a capability to perform its procedure with energy consumption as low as 9.80 kWh/kgSWU.[10] The energy required for a laser enrichment process is two orders of magnitude smaller than the energy required for gaseous diffusion. Such significantly reduced energy requirements means not only that a laser enrichment facility could be funded more easily by a non-state actor, but also means that the facility would have a much smaller signature on the electrical grid, thus making it easier to conceal. Total energy consumption in large part drives the overall capital costs to produce weapons-grade material. The low energy cost of a laser enrichment facility could make it an attractive pathway for non-state actors.

Size/Concealability

The inefficiency of the gaseous diffusion method requires hundreds of stages and massive diffusion vessels. The K-25 building of the Oak Ridge Gaseous Diffusion Plant was one mile long and the Lanzhou Uranium enrichment Plant in China covers 7.67 square kilometers. Such a large footprint makes plants easily identifiable with reconnaissance satellites and therefore difficult for a proliferator to operate without attracting the attention of the international community. By comparison, A study prepared by physicist Ryan Snyder for the Program on Science and Global Security at Princeton University outlined a viable SILEX type process within a footprint that is 15m x 20m for a total footprint of 300m^2 or 3229 square feet.[11]

Technical Complexity

Gaseous diffusion was accepted as the most durable and reliable enrichment method for decades in part because the technology is relatively straightforward. The most challenging technical hurdle is either manufacturing or procuring diffusion membrane material. Gas centrifuges involve large forces, high rotational velocities, and the potential for resonant vibrations which can cause destructive failure.[12] Some of the technical hurdles to overcome include regulating the power to motor drives so that speeds can be carefully controlled, perfecting software to monitor large cascades, perfecting advanced manufacturing with materials like maraging steel and carbon fiber, and balancing rotors to avoid excessive vibration. While these are intricate, technical procedures, centrifugation as an enrichment method has been widely used in many countries including the UK, the Netherlands, Japan, Russia, France, and Germany which means expertise in these areas is fairly prolific. Laser isotope separation is the most novel of the technologies discussed and has yet to be demonstrated on a commercial scale. Although the setup is small, establishing a viable laser enrichment facility could require technical expertise in laser technology including tuning a laser's wavelength, narrowing linewidth, Raman shifting, and managing gas stability.[13]

	Separation Factor	Energy Consumption (kWh/kgSWU)	Minimum No. Stages Required (weapons-grade material)	Space Required	Technical Complexity
Gaseous Diffusion	1.004	2500	3000	Very Large	Low
Centrifugation	1.1	50	30	Large	High
MLIS	70	12.7	4	Small	High

Table 1. Characteristics of Enrichment Methods[14,15]

Proliferation Concern and Conclusion

In conclusion, laser enrichment could be an attractive pathway for either a state or non-state actor to produce weapons-grade fissile material. Current assessments estimate that the space required for a laser enrichment facility capable of producing 30 kilograms per year of 90 percent enriched uranium could be assembled in a space roughly 300 m^2.[16] The lower energy requirements and smaller footprint would compromise the detection of a clandestine laser enrichment by either image or signals intelligence means. In addition, lower energy consumption would mean lower capital costs, an attractive consideration for a resource-limited actor. Finally, with efficiency that is an order of magnitude greater than centrifugation, this method could provide a proliferator with a significantly shorter breakout timeline along the pathway to a nuclear weapon.

Notes:

1. C. Herzig, "IAEA Safeguards," International Security, 7:4, 2006.

2. M. Specia, "Iran Says It Has Surpassed Critical Nuclear Enrichment Level in 2015 Deal," New York Times, 8 July 2019.

3. P.T. Greenland, "Laser Isotope Separation," Contemporary Physics 31:6, 1990.

4. M. Ragheb, "Chapter 10 Isotopic Separation and Enrichment," (2015) 28 August 2020 https://www.semanticscholar.org/paper/Chapter-10-ISOTOPIC-SEPARATION-AND-ENRICHMENT-Ragheb/4370e00afd6ba62e6c04987550fb3b2ad0d847f7.

5. Ragheb, 46

6. Ronald Allen Knief, Nuclear Engineering: Theory and Technology of Commercial Nuclear Power Second Edition, (Illinois: American Nuclear Society, 2014) 525.

7. Ragheb, 47.

8. Greenland, 409.

9. Ragheb, 62.

10. Ryan Snyder, "A Proliferation Assessment of Third Generation Laser Uranium Enrichment Technology, Science & Global Security, 2016, 20 August 2020 https://doi.org/10.1080/08929882.2016.1184528, 85.

11. Snyder, 83.

12. Knief, 525.

13. Snyder, 85-86.

14. Knief, 525.

15. Snyder, 85

16. Snyder, 86.

References:

Greenland, P.T. "Laser Isotope Separation." Contemporary Physics 31:6, 1990. 405-424.

Herzig, C. "IAEA Safeguards," International Security, 7:4, 2006.

Knief, Ronald Allen. Nuclear Engineering: Theory and Technology of Commercial Nuclear Power Second Edition. Illinois: American Nuclear Society, 2014.

Ragheb, M. "Chapter 10 Isotopic Separation and Enrichment," 2015 https://www.semanticscholar.org/paper/Chapter-10-ISOTOPIC-SEPARATION-AND-ENRICHMENT-Ragheb/4370e00afd6ba62e6c04987550fb3b2ad0d847f7.

Snyder, Ryan "A Proliferation Assessment of Third Generation Laser Uranium Enrichment Technology, Science & Global Security, 2016, 20 August 2020 https://doi.org/10.1080/08929882.2016.1184528.

Specia, M. "Iran Says It Has Surpassed Critical Nuclear Enrichment Level in 2015 Deal," New York Times, 8 July 2019.

Spatially-Resolved Characterization Techniques and Implications for Nuclear Debris Formation

David Weisz, Kim B. Knight, Peter K. Weber, Peter Boone, Peter Bedrossian
Lawrence Livermore National Laboratory

Summary

Debris from nuclear tests has a complex formation process and can inform multiple fields of study such as geology, atmospheric science, shock physics, and chemistry under extreme conditions. Macroscopic nuclear debris forms as the result of fireball interaction with surrounding materials (e.g., structural and environmental component), which rapidly undergo melting and vaporization followed by condensation, convective/diffusive mixing, and solidification over the course of seconds.[1,2] In atmospheric events, some of this material may disperse over long distances, but much of the material is deposited close-in to ground-zero, often in multicomponent, partially (or entirely) amorphous debris formations. During the U.S. nuclear testing program, this material was collected and analyzed, particularly for radionuclide composition. Fallout formation models were developed from nuclear test data based on such radionuclide compositional analyses.[3,4,5] These models were not just used to understand fallout dispersion (i.e. the spread of radioactivity over geographical regions) but also guide radiochemical interpretations of historical nuclear tests.[6] Developments in analytical techniques over the past several decades have made it possible to make new analyses on historical debris, some of which may be more than a half-century old. For example, inductively-coupled plasma mass spectrometry (ICP-MS) has been used to look at the trace elements in glassy fallout material from aboveground nuclear tests (including the Trinity test).[7,8] Advanced analyses using X-ray absorption allowed for the measurement of oxidation state of fallout constituents, including actinides.[9] The ability to measure trace actinides and their subsequent oxidation

David Weisz is a staff research scientist in the Chemical and Isotopic Signatures Group at Lawrence Livermore National Laboratory, in Livermore, CA. He has a B.S. in Chemistry from Virginia Commonwealth University, a M.S. in Health Physics from Georgetown University, and a Ph.D. in Nuclear Engineering from the University of California, Berkeley. His email address is weisz3@llnl.gov.

Dr. Kim B. Knight is a staff scientist in the Nuclear and Chemical Sciences group of Lawrence Livermore National Laboratory in Livermore, California, specializing in research supporting forensic investigation of nuclear materials as well as the modern study of historic fallout. She has a B.A. in Geology from Carleton College and a Ph.D. in Earth & Planetary Science from the University of California, Berkeley. She was previously a post-doctoral researcher studying cosmochemistry at the University of Chicago.

Dr. Peter K. Weber is a staff scientist and the lead scientist for the NanoSIMS facility at the Lawrence Livermore National Laboratory in Livermore, CA. He has a B.S. in Physics from Antioch College and a M.S. and Ph.D. in Geography (Geochemistry) from the University of California, Berkeley.

Dr. Peter Bedrossian is a staff physicist at the Lawrence Livermore National Laboratory in Livermore, CA. He has an A.B. and a Ph.D. in physics from Harvard University. He was previously a postdoc in the Surface Science Department of Sandia National Laboratories in Albuquerque, NM, and an Alexander von Humboldt Fellow at KFA/Julich.

state is important to understanding how the surrounding environment may have influenced the resultant fallout composition and may have implications for why certain fractionation trends have been observed. Here we present data from historic nuclear test debris illustrating the power of spatially resolved methods to connect interaction of the near-field environment with the explosion and provide new insights into nuclear debris formation.

Introduction

Analytical studies of nuclear debris have been conducted since the inception of the U.S. nuclear test program.[10,11] Historically, these analyses were limited largely to decay counting of fresh debris. These analyses revealed that chemical fractionation – the compositional perturbations due to differences in condensation temperature – was commonplace and significantly complicated the development of models from "first-principles". Instead, semi-empirical models were developed based on the observations and measured compositions from early analyses.[5] While the theoretical process of chemical fractionation and its potential causes has been detailed mathematically in the historical literature to some extent, radiochemical interpretations largely compensate for fractionation by implementing semi-empirical trends derived during the test program.[4,12,13] In such models, the influence of entrained soils and other near-field materials is largely ignored.

Early studies measured the spatial distribution of radionuclides in debris via autoradiographs, revealing interesting but difficult to interpret characteristics for fallout formed under different nuclear test conditions.[10] These studies also conducted limited electron microprobe measurements for gross composition, but were not extensive.[14] Advances in spatially resolved analyses on glassy fallout materials, however, may hold special relevance to interpreting the influence of structural and environmental factors on fallout formation. Recently, such measurements have been made on glassy nuclear debris, including modern electron microscopy and X-ray spectroscopy, laser ablation ICPMS (LA-ICP-MS), and secondary ion mass spectrometry.[15-21] Using these techniques, the spatial distribution of chemical and isotopic species of interest has begun to be measured and interpreted with respect to fallout formation conditions. Particularly, these measurements have been used to interpret the mixing behavior of bomb vapor and environmental material.[15,16,21] Such interpretations range from determining time and temperature of debris formation and system closure to multivariate statistical analysis to derive individual source-term contributions.[22,23]

In this work, we continue to investigate unique mixing behaviors observed in debris. Here we include data and interpretations from the analyses of two debris samples from an underground historical U.S. nuclear test, using a combination of scanning electron microscopy, modern autoradiography, and nano-scale secondary ion mass spectrometry (nanoSIMS) to look at the influence of the local environment (including structural materials) on the overall distribution of bomb vapor into the debris. In particular, we look at how structural materials may affect the fallout chemistry through spatially resolved trace element analysis, as well as constraining the spatial scale of mixing within individual debris samples.

Spatial Imaging Methods

Two glassy debris samples associated with the same event were selected from the archives at LLNL and imaged using an Olympus SZ61 stereomicroscope for overall physical and morphological characterization. The samples were then polished flat to using a series of increasingly fine-grit sand paper and, ultimately, a diamond paste down to a 1 micrometer surface roughness suitable for analysis by autoradiography, electron microscopy, and secondary ion mass spectrometry. The samples were then re-imaged using the stereomicroscope to examine the surface polish quality and observable features.

Polished samples were then placed on photo-phosphor imaging plates for approximately 2 hours in a low-light containment tent. The imaging plates are primarily sensitive to alpha and beta activity. The plates were subsequently developed using a GE Typhoon

7000 scanner at 50-micrometer pixel resolution to reveal the gross activity distribution across the sample surface. The images were digitized in TIFF format and false-colorized using ImageJ software (blue/black = lower activity; orange/white = higher activity).

Scanning electron microscopy (SEM) was conducted to produce secondary electron and backscattered electron images to understand surface morphology and gross compositional variation, respectively. An FEI Inspect F50 SEM was used at 5 kV (secondary electron images) and 15 kV (backscattered electron images and energy dispersive X-ray spectroscopy). Energy dispersive X-ray spectroscopy (EDS) was acquired using a Bruker QUANTAX energy dispersive X-ray spectrometer at a working distance of 11.5 mm. The X-ray spectra were converted to semi-quantitative compositional measurements using the ZAF correction native to the ESPRIT software (Bruker Corporation) and then converted to their approximate stoichiometric oxides.

NanoSIMS was conducted with a Cameca NanoSIMS 50 to understand trace element variation in the samples that could not be detected by the EDS (i.e., species present at less than 0.1 percent by weight). Specific to this study, we used a primary current of 1nA O^- and detected overall Pu, $^{208}Pb^+$, $^{137}Ba^+$, $^{57}Fe^+$, and $^{28}Si^+$ on electron multipliers in pulse counting mode. On the two samples, a total of 28 analyses were acquired using nanoSIMS. These analyses were acquired as 25x25 micrometer rasters (each raster comprised of a total of 15 cycles). All cycles for each raster were summed and the average isotope ratios were calculated from each of the rastered areas using *L'image* software.

Analytical Observations

The debris samples selected for this study are irregularly shaped, mm-scale materials (Figure 1, left-hand side). Optical microscopy reveals these samples are largely amorphous, dark colored glasses. Most samples contain numerous macroscopic voids. For the two samples here, Sample 1, when polished to the mid-plane (Figure 1, right-hand side), showed voids up to ~1 mm in diameter. Sample 2, on the other hand, did not reveal large voids on the

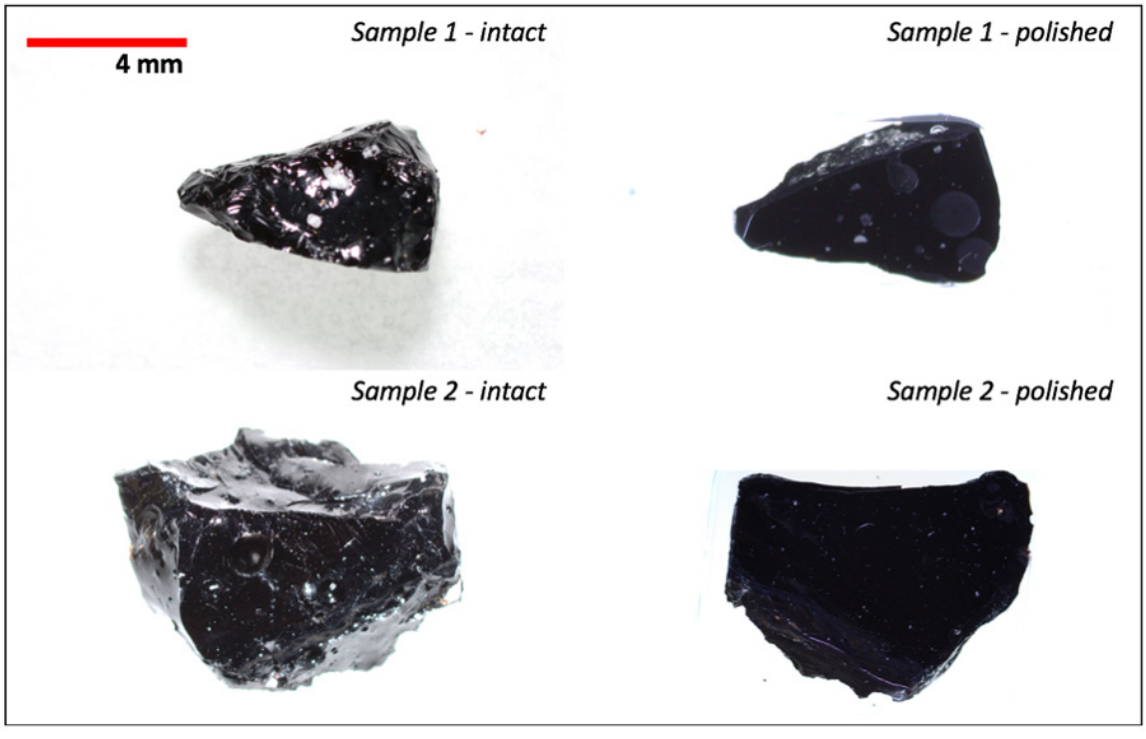

Figure 1. Optical microscopy images of debris Sample 1 and Sample 2 of this study, as sampled at left, and as polished at right.

polished surface, instead presenting as a monolithic glass.

The autoradiographs for both samples indicate variation of radioactivity across the sample surface (i.e., radioactivity is not homogeneously distributed). The voids in Sample 1 are clearly observed in Figure 2a as circular regions devoid of radioactivity. Otherwise, activity in Sample 1 is relatively more homogeneous than in Sample 2, with minor variations of activity distributed across the sample surface. In

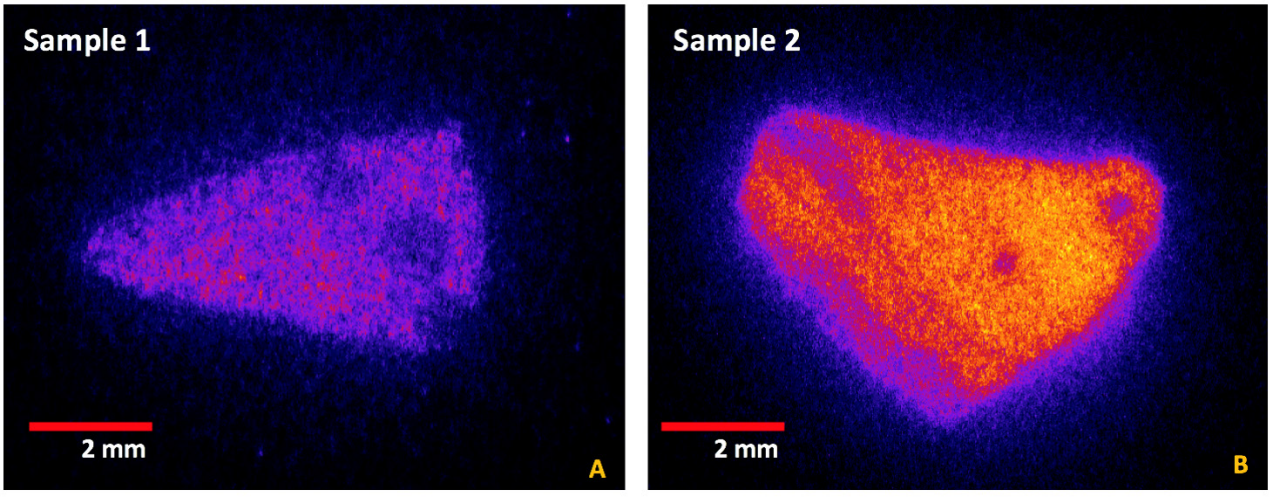

Figure 2. Autoradiographs collected from the polished surfaces of (a) Sample 1 and (b) Sample 2. These autoradiographs have been false-colorized to indicate activity variation (lower activity is black/blue, higher activity is orange/white).

Sample 2, the heterogeneity of radioactivity is much more evident (Figure 2b). There is a significant decrease in relative activity at the edges of the sample to the top left and bottom left as oriented in Figure 2b. There are also locations with a relative decrease in activity apparent within the bulk of the sample. These locations are not associated with voids, but instead with relict minerals in the sample (explained in the following section and shown in Figure 3a). Because the samples were imaged at the same time under the same conditions, their relative radioactivity can also be compared and the residual activity in Sample 2 is more intense than in Sample 1.

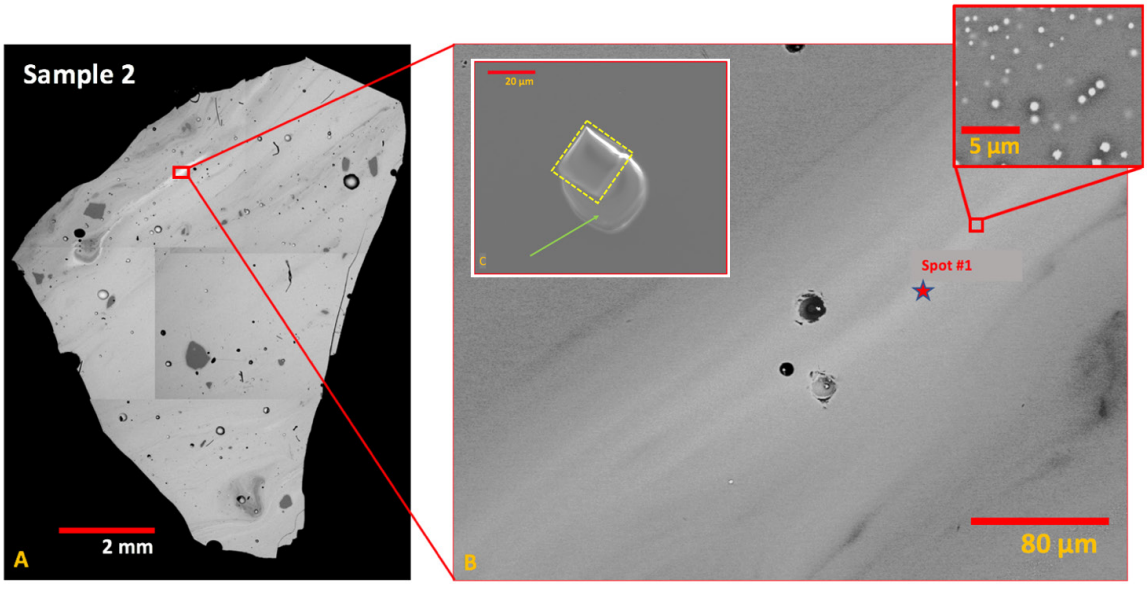

Figure 3. Compositional variation and analytical scales. (A) Backscattered electron micrograph of Sample 2 showing gross compositional variation across the polished sample surface. (B) High-magnification image of the red square indicated in (A), showing the high-Z band and the associated EDS spot analysis as a red star labeled 'Spot #1'. The inset to the top left shows a higher-magnification image of the band, revealing bright high-Z crystallites. (C) The rastered crater formed by nanoSIMS analysis is highlighted by the yellow-dashed box. A green arrow indicates the imaging artifact due to the carbon coating being sputtered away during nanoSIMS analysis.

In Figure 3A, the backscattered electron image of Sample 2 shows the extent of average compositional variation across the polished surface. In backscattered electron images, the average atomic number (Z) of the material is indicated by the gray-scale intensity, with brighter pixels indicating higher average Z. Dark, angular features are likely relict minerals from entrained soils (e.g., quartz). The banded patterns observed throughout the sample indicate advective flow, a commonly observed feature in debris glass. Numerous small voids are also evident. There is also a bright band towards the top of the sample (as oriented in Figure 3A). We conducted EDS to understand the major element composition of this band. In Figure 3B, a backscattered electron image of a high-magnification region of this band is shown, and the EDS spot is indicated by a red star (Spot 1). The results of the EDS analysis of Spot 1 are provided in Table 1, presented as stoichiometric oxides. As determined via EDS, this region of Sample 2 is consistent with a felsic composition (predominantly aluminosilicate), but with high concentrations of Fe, Ba, and Pb generally outside of compositions observed in natural soils.

Na_2O	MgO	Al_2O_3	SiO_2	K_2O	CaO	TiO_2	FeO	BaO	PbO
1.42±0.09	*1.10±0.06*	*16.39±0.43*	*66.17±1.31*	*2.13±0.08*	*4.77±0.13*	*0.21±0.03*	*4.06±0.12*	*2.40±0.09*	*2.18±0.11*

Table 1. Semi-quantitative major-element compositional EDS analysis acquired from Spot #1 (Figure 3b).

The inset in Figure 3B shows an even higher magnification backscattered electron image of the bright band shown in Figures 3A and 3B. As shown in the inset, the structure of this band appears to be dominated by sub-micron scale crystallites of high-Z material interspersed in the silicate matrix. The EDS analysis of individual crystallites, which approximates the spatial resolution of the EDS (~1-3 micrometers at this voltage), indicates that these crystallites are highly enriched

in Fe, in some instances >44% FeO by weight, which is roughly an order of magnitude higher than the average composition of Sample 2.

In Figure 3, secondary electron images acquired via scanning electron microscopy show an example of nanoSIMS craters caused by the analysis (middle inset, Fig. 3c). The nanoSIMS crater is observed as a bright, approximately square feature approximately 25 micrometers on a side (indicated by the yellow stippled box). The feature below the crater, indicated by the green arrow, is an artifact induced by the removal of the conductive carbon coating resultant from the nanoSIMS sputtering process.

Using nanoSIMS, the trace element composition of different spots was measured across the sample surfaces. The trace element comparison of Pb, Fe, and Ba are given as isotope ratios normalized to silicon (i.e., $^{208}Pb^{+}/^{28}Si^{+}$, $^{57}Fe^{+}/^{28}Si^{+}$, $^{137}Ba^{+}/^{28}Si^{+}$, respectively). The silicon concentration is relatively invariant in comparison to the other measured elements, and thus makes for a useful means of normalizing relative variation of trace elements in the samples. Pu was

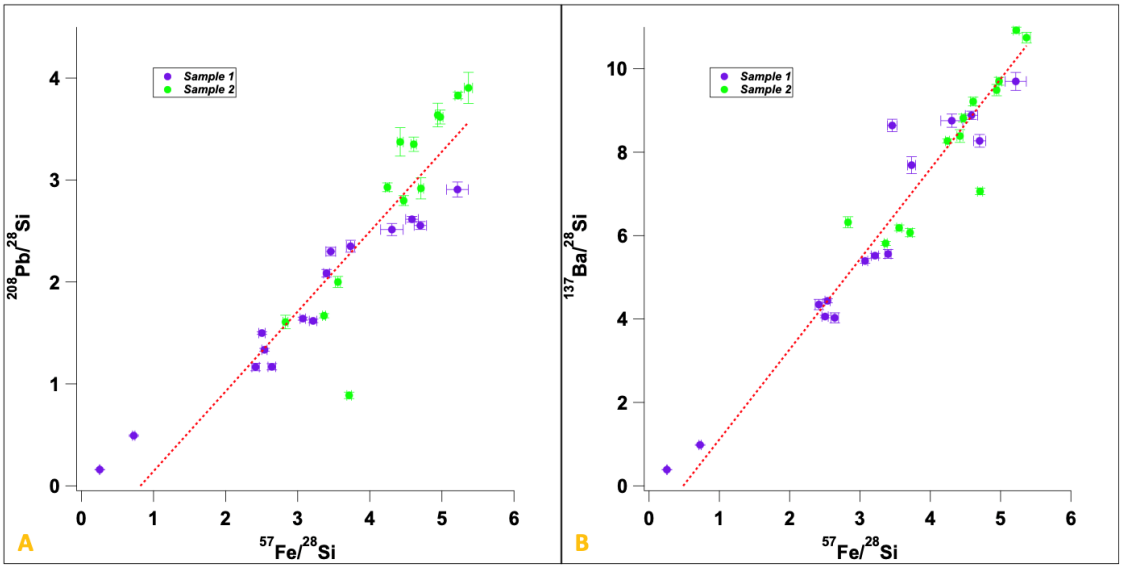

Figure 4. Bivariate plots of (a) $^{208}Pb^{+}/^{28}Si^{+}$ vs. $^{57}Fe^{+}/^{28}Si^{+}$ and (b) $^{137}Ba^{+}/^{28}Si^{+}$ vs $^{57}Fe^{+}/^{28}Si^{+}$, with error bars indicating 1σ uncertainties. The red dashed lines are orthogonal least squares regression fit lines. The purple points indicate analyses from Sample 1 and the green points indicate analyses from Sample 2.

also monitored (as $^{239}Pu^{+}$) as an indicator of bomb vapor contribution. In Figure 4a, a bivariate plot of $^{208}Pb^{+}/^{28}Si^{+}$ vs. $^{57}Fe^{+}/^{28}Si^{+}$ shows the relative change in concentration of Pb as it is related to relative change in Fe. These data were fit with an orthogonal least squares linear fit, indicated by the red line, and have strong significant linear correlation ($\chi 2=2.9$, N=28). A similar linear relationship is shown between $^{137}Ba^{+}/^{28}Si^{+}$ and $^{57}Fe^{+}/^{28}Si^{+}$ in Figure 5b ($\chi 2=2.9$, N=28).

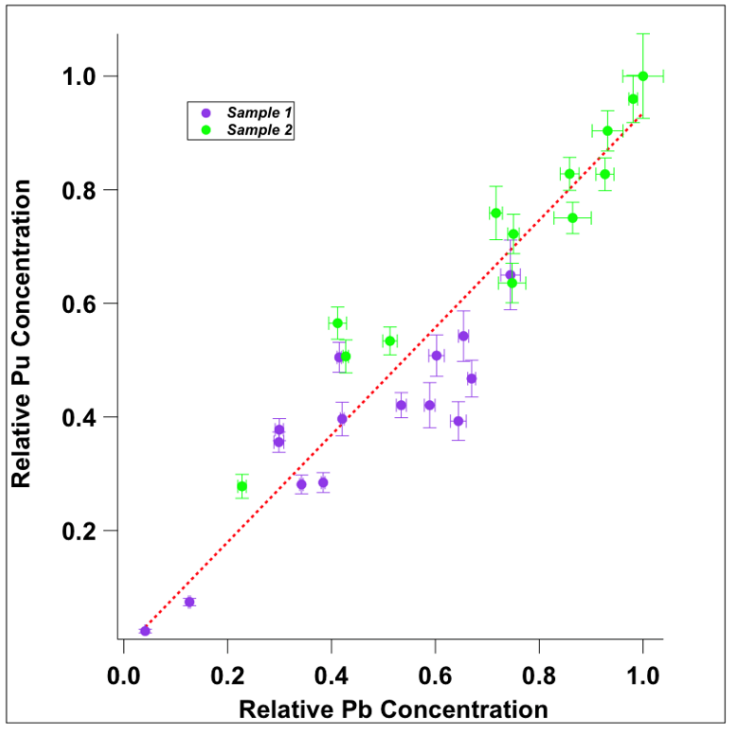

Figure 5. Pu and Pb relationships revealed by spatially resolved characterization. Bivariate plot of relative Pu concentration vs relative Pb concentration. The purple points indicate analyses from Sample 1 and the green points indicate analyses from Sample 2. The red regression line is an orthogonal least squares fit line.

In Figure 5, the relative change in Pu concentration and Pb concentration is shown, as derived from the ratio of the monitored isotope for the respective elements to $^{28}Si^{+}$, normalized to their respective maximum values in order to highlight the relative change in concentration. Further, each data point is color-coordinated to the sample from which it came (purple = Sample 1 data; green = Sample 2 data). Overall, Sample 2 exhibited higher concentrations of both Pu and Pb in comparison to Sample 1 (with a few exceptions). The entire range of data spans nearly two orders of magnitude in relative Pu and Pb concentration (from ~0.02 to 1 and from ~0.04 to 1, respectively). Further, there is a strong linear correlation between relative Pu and Pb concentration in the entire dataset from both samples ($\chi 2$=0.12, N=28).

Mixtures of Near-field Materials into Debris

Mixing of environmental materials, structural materials, and device materials in nuclear debris has been previously observed and discussed in numerous studies; this is particularly true of the Trinity test. Trinitite, or the glassy debris that was formed in large quantities during the first nuclear test, has been studied by a considerable array of analytical techniques. For example, minerals from the local environment have been observed in characterized trinitite since the dawn of the test program (e.g., via optical microscopy and autoradiography).[11] In more recent studies, spatially resolved analyses of debris from surface events has been used to speculate regarding device components and structural features that may have been present at the time of the event. Such spatially resolved measurements encompass major and minor element analyses using SEM/EDS and electron probe microanalysis, as well as isotopic analyses via LA-ICP-MS and SIMS. Multivariate statistical analyses of fallout from Trinity have also been conducted to determine the relationships between various environmental, structural, and device reservoirs.[15,21,23] However, there have not previously been quantitative correlations between device vapor and close-in structural materials, with the exception of the 100-ton steel blast tower for Trinity, and no studies have focused on correlations in underground debris.

Debris from various other tests have also been analyzed using these spatially resolved techniques. Early studies analyzed debris from several tests using autoradiography, though the published images of these early studies are difficult to interpret due to the much higher levels of short-lived radioactivity. Qualitative studies of radioactivity distributions in combination with X-ray diffraction measurements from tower events were used, however, to infer some degree of debris formation incorporating near field materials. In one study, for example, radiographs that showed homogeneously distributed activity were associated with a predominantly iron oxide composition. This led to the conclusion that partially molten tower material intimately mixed with vaporized device material to form one subset of the observed debris from that test.[10] In the same study, they also observed a 'shell' of activity surrounding an inactive core. Thus, another subset of the observed debris consisted of molten calcium oxide onto which vaporized tower and device material co-condensed.

The nuclear debris samples for this study are unusual in that multiple major element contributions could have derived from near-field materials such as instrumentation and structure. For example, the presence of PbO and BaO at >1 weight percent and the presence of FeO at up to 4 weight percent from semi-quantitative EDS measurements (Table 1). These materials, particularly Pb and Ba, naturally occur at the 10-100 ppm range, though Fe may be present at significant concentrations depending on the surrounding lithology. Thus, at these concentrations, an additional reservoir of Pb and Ba must have been present. The use of large amounts of lead shielding in a nuclear test environment would be a logical reservoir of the additional Pb found in these debris samples. Further, baryte aggregate (comprising $BaSO_4$) has been historically used in concrete for radiation shielding applications as well.[24] Thus, if large concrete structures utilizing such an aggregate were also close-in to ground zero, significant amounts of Ba could potentially be incorporated (as well as CaO, a major constituent of concrete, which is present at up to 5 weight percent in these samples, see Table 1).

The distinct linear correlation between Pb and Fe (Figure 5a) as well as Ba and Fe (Figure 5b) indicates that these materials are likely associated with one another during the debris formation process. While FeO may be present in significant quantities (~weight percent) in natural materials, the correlation of Fe with Pb and Ba indicates a predominantly structural origin given the significantly perturbed, non-natural Pb and Ba concentrations. Additionally, the presence of Fe-rich micro-crystallites (Figure 3b) indicates that enough iron was incorporated into these materials during formation that Fe exsolved during quenching. Thus, while previous studies from other historical tests observed large amounts of iron incorporation due to a tower[9,10], we are clearly seeing evidence of other structural components in these samples, perhaps by virtue of the specific event configuration.

In the past few years there have been multiple studies of actinide incorporation into fallout materials from Trinity and other nuclear tests.[7,9,15,16,18] These studies explore actinide isotopic mixing with environmental materials, diffusive mixing during formation, and isotopic studies to identify various components and activations. In one previous study, the correlation between potential structural materials and uranium was observed in deposition layers[16], while other studies have made correlations between uranium as a device constituent and iron as a structural constituent.[15] In this study, we see a clear correlation between Pb and Pu concentration (Figure 6). On one hand, it would make sense from a proximity standpoint – Pu in the device would be physically close to structural shielding materials and would thus be likely to mix readily with them. However, the association with Pu and Pb is, on the other hand, counterintuitive in that Pu is typically a refractory species[25] and Pb is known to be more volatile (i.e., Pu-bearing compounds typically vaporize at significantly higher temperatures than Pb-bearing compounds).[26,27] Due to this difference in volatility, we would not necessarily expect a correlation between Pu and Pb despite the fact that their reservoirs may have been situated physically proximate to one another.

Finally, the physical scale of mixing in these materials has implications not only for formation processes but also for future radiochemical interpretations. Traditionally, radiochemical analysis of these materials has been focused on the dissolution and decay counting of multi-gram samples. Such analyses could 'wash-out' intra-sample inclusions of interest (e.g., structural or device-related materials) that could otherwise prove to useful to understand formation and contributions to radionuclide behavior and speciation. More recently, mg-scale samples have been dissolved and analyzed using ICP-MS[7], which have revealed insights into the isotopics and trace elements relationships captured in debris. Further, spatially resolved analyses on individual samples have demonstrated that variations exist on the ~25-30-micrometer scale through SIMS[15] and LA-ICP-MS[8]. Using SIMS, for example, uranium isotopics varied by several orders of magnitude due to the mixing of device U and environmental U.[15] In this study, we demonstrate that in Pu-bearing materials using 25 micrometer rasters (<<1 micrometer in depth), we can see a 30-fold change in Pu concentration across a single sample. As these spatially resolved techniques become more refined, it may be possible to derive substantive radiochemical interpretations from even a single debris sample, as well as observe physicochemical mixing phenomena at the sub-micron scale.

Conclusions

Using spatially resolved analytical techniques, we are able to discern significant non-natural contributions of Fe, Ba, and Pb in nuclear test debris from a historic underground event. Spatially correlated chemistry in these materials indicate that these elements likely derived structural materials proximate to the device prior to detonation that intimately mixed with each other, as well as environmental materials. A distinct linear correlation was also observed between Pb and Pu – this indicates that the device material in these samples was not separated from these structural materials during the formation process. Given their difference in expected volatility, the inter-mixing between Pu and Pb was not expected, even if they were physically proximate to one another. These relationships were observable in micron-scale analyses across two samples, not only illustrating the spatial scale of mixing in these samples, but also demonstrating the potential of using spatially resolved measurements to better understand debris formation conditions.

Acknowledgments

Lawrence Livermore National Laboratory is operated by Lawrence Livermore National Security, LLC, for the U.S. Department of Energy, National Nuclear Security Administration under Contract DE-AC52-07NA27344. This work was supported by the LLNL-LDRD Program under Project No. 18-ERD-003 and Project No. 20-SI-006. LLNL-JRNL-814284.

Notes:

1. Miller, C.F. "A Theory of Formation of Fallout from Land-Surface Nuclear Detonations and Decay of the Fission Products." 1960. Research and Development Technical Report USNRDL-TR-425. U.S. Naval Radiological Defense Laboratory. 1-131.
2. Freiling, E.C. "Mass-Transfer Mechanisms in Source-Term Definition." 1970. Advances in Chemistry. Radionuclides in the Environment, Chapter 1. 1-12.
3. Freiling, E.C., Kay, M.A. "Radionuclide Fractionation in Air-Burst Debris." 1965. USNRDL-TR-933. 1-16.
4. Freiling, E.C., Kay, M.A. "Radionuclide Fractionation in Air-Burst Debris." 1966. Nature. 209 . 236-238.
5. Norment, Hillyer G. "DELFIC: Department of Defense Fallout Prediction System. Volume I: Fundamentals." DNA 5159F-1. Defense Nuclear Agency. 1-101.
6. Kawahara, Francis K., Freiling, Edward C., Bunney, Leland R., and Crocker, Glenn R. "Fallout from Nuclear Cratering Shot Danny Boy." 1967. B951703. U.S. Naval Radiological Defense Laboratory. 1-39.
7. Eppich, Gary R. et al. "Constraints on Fallout Melt Glass Formation from a Near-Surface Nuclear Test." Journal of Radioanalytical Nuclear Chemistry. 302 . 593-609.
8. Bellucci, Jeremy J. et al. "A detailed geochemical investigation of post-nuclear detonation trinitite glass at high spatial

resolution: Delineating anthropogenic vs. natural components." 2014. Chemical Geology. 365 . 69-86.
9. Pacold, J.I. et al. "Chemical Speciation of U, Fe, and Pu in Melt Glass from Nuclear Weapons Testing." 2016. Journal of Applied Physics. 119(195102). 1-12.
10. Adams, C.E. and O'Connor, J.D. "The Nature of Individual Radioactive Particles IV. Fallout Particles from a Tower Shot, Operation Redwing." 1957. Research and Development Technical Report USNRDL-TR-208. U.S. Naval Radiological Defense Laboratory. 1-24.
11. Ross, Clarence S. "Optical Properties of Glass from Alamogordo, New Mexico." 1948. American Mineralogist. 33 . 1-3.
12. Freiling, E.C. "Radionuclide Fractionation in Bomb Debris." 1961. Science. 133(3469). 1991-1998.
13. Crocker, G.R., O'Connor, J.D., and Freiling, E.C. "Physical and Radiochemical Properties of Fallout Particles." 1965. 12ND NRDL P1 (9/63). 1-32.
14. Norman, J. and Winchell, P. "Cloud Chemistry of Fallout Formation." 1966. USNRDL-R&L-177. U.S. Naval Radiological Defense Laboratory. 12-54.
15. Lewis, L.A. et al. "Spatially-resolved Analyses of Aerodynamic Fallout from a Uranium-fueled Nuclear Test." 2015. Journal of Environmental Radioactivity. 148 . 183-195.
16. Weisz, D.G. et al. "Deposition of Vaporized Species onto Glassy Fallout from a Near-surface Nuclear Test." 2017. Geochimica et Cosmochimica Acta. 201 . 410-426.
17. Bellucci, Jeremy J. et al. "Direct Pb Isotopic Analysis of a Nuclear Fallout Debris Particle from the Trinity Nuclear Test." 2017. Analytical Chemistry. 89 . 1887-1891.
18. Fahey, A.J. et al. "Postdetonation Nuclear Debris for Attribution." 2010. Proceedings of the National Academy of Sciences. 2010. 107(47). 20207-20212.
19. Dustin, Megan K. et al. "Comparative Investigation between In Situ Laser Ablation Versus Bulk Sample (Solution Mode) Inductively Coupled Plasma Mass Spectrometry (ICP-MS) Analysis of Trinitite Post-Detonation Materials." 2016. Applied Spectroscopy. 70(9). 1446-1455.
20. Holliday, K.S. et al. "Plutonium Segregation in Glassy Aerodynamic Fallout from a Nuclear Weapon Test." 2017. Dalton Transactions. 46 . 1770-1778.
21. Bonamici, Chloë E. et al. "A Geochemical Approach to Constraining the Formation of Glassy Fallout Debris from Nuclear Tests." 2017. Contributions to Mineralogy and Petrology. 172(2). 1-23.
22. Weisz, D.G. et al. "Diffusive Mass Transport in Agglomerated Glassy Fallout from a Near-surface Nuclear Test." 2018. Geochimica et Cosmochimica Acta. 223 . 377-388.
23. Fitzgerald, M.A., Knight, K.B., Matzel, J.E., Czerwinski, K.R. "Interpreting Mixing Relationships in Energetic Melts to Estimate Vapor Contribution and Composition." 2019. Chemical Geology. 507. 96-119.
24. Grantham, Jr., William J. "Barytes Concrete for Radiation Shielding: Mix Criteria and Attenuation Characteristics." 1961. ORNL-3130. United States Atomic Energy Commission. 1-61.
25. Moody, Kenton J., Patrick M. Grant, and Ian D. Hutcheon. Nuclear forensic analysis. CRC Press, 2014.
26. Connelly, J. N., and Martin Bizzarro. "Lead isotope evidence for a young formation age of the Earth–Moon system." Earth and Planetary Science Letters 452 (2016): 36-43.
27. Ko, R. "A Single Carrier Method for the Emission Spectrometric Analysis of Uranium-Plutonium Oxides." 1978. Spectroscopic Techniques. 32(3). 325-326.

Challenges in Simulating Ground Interacting Nuclear Explosions

J. Morris, A. Shestakov, A. Nichols, B. Isaac, and K. Knight
Lawrence Livermore National Laboratory

Summary

This paper summarizes recent above-ground nuclear explosion simulations as part of a broader effort to better characterize conditions within a fireball that may influence the chemical evolution of bomb materials and other materials entrained from the local explosion environment. A critical component of this work is validation against historic footage of atmospheric testing, requiring that we understand how the frequency-dependent sensitivity of the utilized film footage influences data captured in such images. We focus first on the early physics of a nuclear explosion in the atmosphere before discussing some of the technical challenges we seek to capture in late-time models that include more complex emplacement conditions and subsurface features. We discuss required physics packages (compressible hydrodynamics, radiation transport, as well as necessary ancillary tables such as equations of state (EOS) and opacities). Additionally, we note reasonable "shortcuts" one may make and their limitations, e.g., using ideal gas EOS, replacing spectrally resolved radiation with spectrally averaged radiation, and exchanging deterministic transport with diffusion. We then discuss an approach to achieving an equilibrated initial stress state for problems where buoyancy and subsurface lithostatic stress are important. Our methodology is presented in the context of LLNL's ALE3D multiphysics code but may readily be implemented in other codes.

In this paper, we start with a description of the challenges of NUDET simulations, followed by a presentation of the simulated intensity (flux) as it would appear on an analysis of the Dixie test. We then progressively introduce additional complexity in subsequent sections (near-surface burst and gravity initialization) before concluding.

Joseph P. Morris, Ph.D. is the Associate Program Leader for Nuclear Effects R&D at the Lawrence Livermore National Laboratory in Livermore, California. He has a B.S. with Honors and a Ph.D., both in Science (majoring in Mathematics) from Monash University, Australia. He previously served as the Computational Geosciences Group Leader at Lawrence Livermore National Laboratory from 2015 to 2020 and worked for the 5 years prior at Schlumberger, the world's largest oil and gas services company at their corporate research laboratory in Boston, Massachusetts. His email address is morris50@llnl.gov.

Dr. Kim B. Knight is a staff scientist in the Nuclear and Chemical Sciences group of Lawrence Livermore National Laboratory in Livermore, California, specializing in research supporting forensic investigation of nuclear materials as well as the modern study of historic fallout. She has a B.A. in Geology from Carleton College and a Ph.D. in Earth & Planetary Science from the University of California, Berkeley. She was previously a post-doctoral researcher studying cosmochemistry at the University of Chicago.

Simulating Nuclear Detonations

This paper discusses recent efforts as part of an internal research project at Lawrence Livermore National Laboratory to improve our understanding of the post nuclear detonation environment, including the chemical evolution of species within the fireball, addressing both bomb debris and entrained material. As part of this effort, we are extending the capabilities of the LLNL ALE3D code to allow us to consider the post detonation environment directly. ALE3D is a multi-physics numerical simulation software tool using arbitrary Lagrangian-Eulerian (ALE) techniques. The code is written to address both two-dimensional (2D) and three-dimensional (3D) problems using a hybrid finite element and finite volume formulation to model fluid and elastic-plastic response on an unstructured grid. Additional ALE3D features include heat conduction, chemical kinetics and species diffusion, incompressible flow, wide range of material models, chemistry models, multi-phase flow, and magneto-hydrodynamics for long (implicit) to short (explicit) time-scale applications. Part of our project extends the chemical and multiphase modules in ALE3D to those relevant to the fireball environment and improves the treatment of radiation transport in order to more accurately track the temperature of the post-detonation material. Variable definitions used here are defined in the 'Nomenclature' section at the end of the paper.

Nuclear detonations (NUDET) differ substantially from conventional explosions in that a tremendous amount of energy is released by a small volume. If yield Y defines the energy released and M the mass of the device, the ratio Y/M is enormous. At stand-off distances, the immediate effects of the energy release consist of a blast (shock wave) and intense radiation in the infrared (IR) and ultraviolet (UV) part of the spectrum (thermal emission). The energy ratio (blast/thermal) varies with height-of-burst H and proximity to ground. For $H < 10$ km, the ratio is approximately 2:1 (Glasstone and Dolan[1]). Such NUDET have a distinctive thermal temporal signature where a brief, bright flash is followed by a reduction of emitted power, which is then followed by an increase to a second, intense, relatively long-lasting emission. The first flash stems from an expanding, incandescent shock. As it propagates, the shock weakens to a level it no longer glows, but is nevertheless still strong. This is the time of emitted power minimum t_{min}, separating the two power maxima. As the shock becomes transparent, it acts as an optical shutter. During the first flash and on its way to minimum power, the shock emits light from its leading edge and blocks light emitted by the fireball left behind. Most of the thermal energy is emitted during the second maximum. Power peaks at time $t = t_{2max}$ to a value P_{2max} then decreases slowly. Most of thermal energy is emitted by $t = 10t_{2max}$.

The rapid expansion of the fireball and shock means that shortly after detonation the size of the fireball and shock position are many times greater than the initial dimensions of the weapon. Consequently, effects are effectively due to a point source. For a free-air burst, or one next to a perfectly reflecting plane, the event has no characteristic length nor time scale. The intrinsic quantities are Y (energy) and ambient density ρ_0 (mass/volume). This implies *self-similarity.* The ratio $(Y/\rho_0)^{1/5}$ multiplied by time$^{2/5}$ has units of length; hence, may define the shock radius. Thus, depending on where one measures and when, all NUDET largely look the same, independent of yield. Quantities-of-Interest such as t_{2max} and P_{2max} scale with yield, e.g., $t_{2max} \approx 42Y^{0.44}$ ms and $P_{2max} = 3.2Y^{0.56}$ kt/s.[1]

Thermal emission is biologically more damaging than blast, if one ignores secondary effects such as impact from projectiles. The *thermal partition*, f, is the fraction of yield emitted as thermal energy. For $Y \in (1, 10^4)$ kT, $f = 0.35$ for free-air burst for $H < 4.5$ km, (Glasstone[1] Table 7.101 and f increases with Y and H). At $Y = 1$ kt, a NUDET emits approximately 0.3 kt ($1.16 \cdot 10^{12}$) joule in $10t_{2max}$ (0.42 sec). Ignoring atmospheric attenuation, an observer 1 km away receives ≈ 1

MW/m^2 thermal power at $t = t_{2max}$. For comparison, on a clear day with sun directly overhead, the solar flux at ground is approximately 1 kW/m^2. One (two) km away, the observer receives a fluence of 10 (2.5) cal/cm^2. A dose of 10 is nearly 66% greater than what causes third degree burns; 2.5 gives first degree burns with 80% probability (Glasstone[1], Tables 12.64-65). For comparison, a 12 psi overpressure is the threshold for lung damage and 5 psi for eardrum rupture (Glasstone[1], Table 12.38). For the same 1 kt yield, the shock delivers 12 (5) psi at 0.21 (0.37) km. At one km distance, the overpressure is a relatively benign 1 psi, (Glasstone[1] Fig. 3.72).

NUDET simulations present unique challenges. Codes able to capture the phenomena require at least two physics "modules," compressible hydrodynamics and radiation transport. The former models the shock and the latter, emitted thermal power. Additionally, the codes must be able to process equations of state (EOS) for the materials being modeled. The radiation module requires spectral (frequency-dependent) tables for the opacity κ, which govern the emission and absorption of radiation. The EOS and opacity tables must cover a wide range of densities ρ and temperatures T; additionally, κ must extend from near IR range (0.1 eV) to hard X-rays (10–100 keV) with a well resolved optical range up to near UV (4.8 eV) since it is those frequencies that readily propagate in cold air.

Even capturing behaviors in a medium as simple as air can be complicated. EOS tables for air use two independent variables of density (ρ) and temperature (T) (or specific internal energy e instead of T) to define necessary thermodynamic quantities: pressure p, specific heat c_v, and T if e is the independent variable. A compact definition uses the ideal gas expressions,

$$e = c_v T \quad \text{and} \quad p = (\gamma - 1)\rho e$$

Figures 1a and 1b display the effective inverse specific heat $1/c_v$ and specific heat ratio $\gamma - 1$ as functions of e for several densities ρ. Given ρ and e, Fig.1a (which defines T) shows that c_v is nearly constant for $e > 10^{12}$ (erg/g), i.e., $T > 2$ eV (23,000 K). However, per Fig.1a, c_v varies by approximately 6× for lower energies (temperatures), which is the range that spans the shock trajectory as it approaches t_{min} (where the fireball becomes transparent.) Figure 1b defines pressure p and γ. The latter term (γ) governs compressibility. Shocks compress: Across a shock, density abruptly increases from an ambient value ρ_0 to a post shock ρ_1. Similarly, pressure jumps from p_0 to p_1. Across an infinite strength shock (defined as $p_1/p_0 \gg 1$), the density ratio $\rho_1/\rho_0 = (\gamma + 1)/(\gamma - 1)$. Figure 1b shows that at sea-level, for $e = 10^9$ (room temperature) and $e = 10^{12}$, $\gamma = 1.4$, 1.2, respectively.

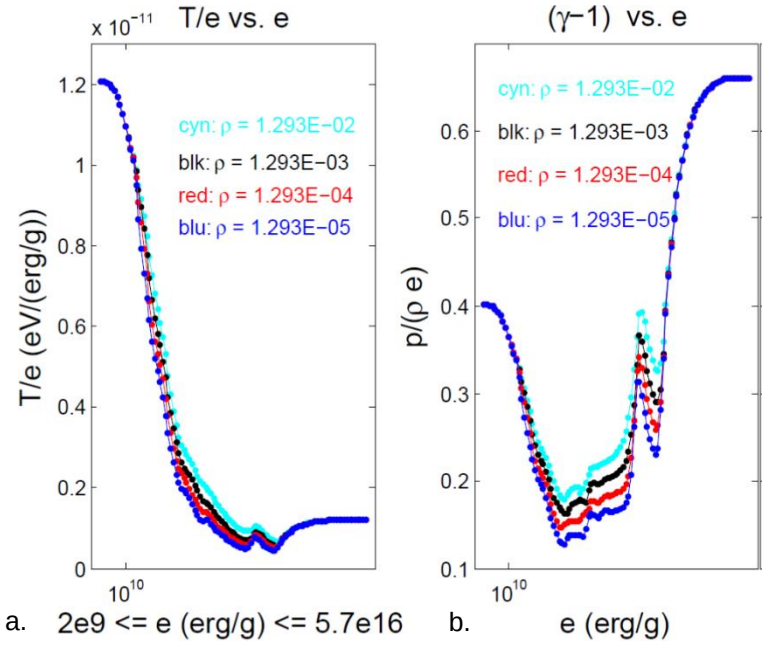

Figure 1. Relating the air EOS to an ideal gas description

Figure 1: (a) displays inverse specific heat *1/cv*; (b) displays compressibility as γ*-1*, relative to specific internal energy (*e*) for a range of densities 10x, 1x, 0.1x, and 0.01x (cyan, black, red, blue) times sea-level value (1.29 x 10^{-3} g/cc). A strong shock at these temperatures amplifies density by factors of 6 and 11, respectively. Since the atmosphere scale height is approximately 7.6 km, a density jump of 11 is equivalent to abruptly dropping from 18.2 km (60 kft) to sea level.

NUDET Simulation Requirements

As noted above, the immediate effects of a NUDET are shock and thermal emission. The latter is largely monodirectional and varies with photon frequency (energy), due to the temperature dependence of the opacity κ of air. Figure 2a displays κ (cm^2/g) vs. photon energy *hv* (eV) for two densities at temperature *T* = 1045 K. To appreciate how opacity affects propagation of radiation, note that the radiation mean free path (mfp), $1/\rho\kappa$, is the distance radiation of that frequency travels before its intensity is reduced by 1/*e*. In the visible spectrum (380, 740) nm equals (3.26, 1.68) eV. Longer (shorter) wavelengths correspond to IR (UV) frequencies.

According to Fig. 2a, air heated to 1000 K (0.09 eV) is largely transparent to visible light. Since its opacity $\kappa \approx 10^{-3}$–10^{-2} cm^2/g, multiplying by sea-level density $\rho_0 = 1.3 \times 10^{-3}$ means the inverse mfp = 1.3 x 10^{-5} cm^{-1}, or 10× less. Hence, light at those frequencies will travel 0.77–7.7 km before its intensity is reduced by 1/*e*. Photons of longer wavelengths (IR) have even longer mean free paths. On the other hand, κ increases sharply for photons with *hv* > 5 eV. For *hv* = 7 eV, $\kappa \approx 100$; hence, mfp ≈ 7.7 cm. The intensity of radiation at that frequency is reduced by a factor of nearly 1000 by traveling only 50 cm. Opacity depends strongly on temperature. Figure 2b displays κ vs. *hv* at *T* = 0.9 eV (10,450 K). Now $\kappa \approx 10^3$ at sea-level density; hence, mfp ≈ 1 cm. Air at 10,000 K is opaque to visible light.

For times t approaching t_{min}, thermal emission is governed by the expanding shock, whose temperature varies from 10,000 to 2000 K, at which point the shock becomes transparent. Thermal emission is largely as from a black body, i.e., from a Planck function $B_\lambda(T)$. According to Glasstone[1] Fig. 7.74, B_λ peaks at 2.5 (5) eV for T = 5000 (10^4) K, i.e., inside and a few eV higher than the visible range. However, Fig. 2a implies photons with energies $h\nu \geq 5$ eV are absorbed within a meter, or less, from the shock. This implies that a given code's radiation module must model unidirectional transport, spectral dependence, and a wide range of absorptivities.

The fundamental radiation variable is the intensity $I(x,t,\nu,\mathbf{\Omega})$, the radiant flux, at position x, time t, per unit frequency ν, per solid angle $\mathbf{\Omega}$. The dependence on x and T is obvious, and spectral dependence (on ν) should be clear given the previous paragraph. Dependence on directionality $\mathbf{\Omega}$, however, also matters. A surface with its normal pointing at the source will receive a large flux on its front and none on its back sides. Radiation modules that evolve the intensity, I, are described as radiation "transport" modules. We use discrete ordinates (S_N) equations for transport[2] in the simulation described in the following subsection. Directionality is modeled by discretizing $\mathbf{\Omega}$ into "rays." For the spherically symmetric cases applicable to free-air NUDET, azimuthal symmetry holds at each radial point x; hence, only the polar direction is discretized.

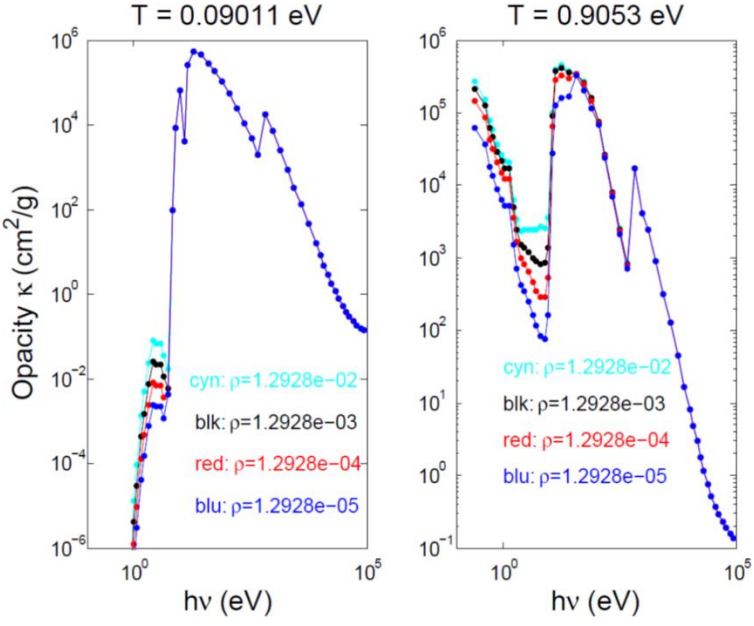

Figure 2. Opacity compared with photon energy for a collection of densities

Figure 2: Opacity κ (cm^2/g) dependence on photon energy $h\nu$ for a collection of densities: 10, 1, 0.1, 0.01 (cyan, black, red, blue) times sea-level value 1.29 x 10^{-3} g/cc. (a) displays κ at temperature T = 0.0911 eV (1045 K); (b) displays κ at temperature T = 0.9053 eV (10,500 K). NB: While abscissae are at same scale, ordinates scales differ; (a) varies over 12 orders of magnitude, while (b) varies over 7.

Transport is essential, since although emission is largely from the surface of a black body, the effect is logged at a remote distance and thus is best characterized as originating from a point source. Transport is required whenever the medium is characterized by long mean free paths (e.g., photons in the IR-UV range, propagating through cold air). For short mean free paths, diffusion is often used instead. In this case, the fundamental variable is the spectral energy density,

$$U(x,t,\nu) = \frac{1}{c}\int_{4\pi} I\, d\omega\,,$$

where c is the speed of light. Diffusion greatly simplifies the representation of physics in a simulation since it reduces the dimensionality of the fundamental variable that describes radiation.

Using Dixie as an Example

Validation of simulations by comparing results with historic footage of atmospheric tests[3,4,5] requires knowing the specific films' sensitivity to the spectrum of received light. In this section, we describe modeling (low-altitude, free-air) immediate NUDET effects and how to determine simulated film response in a camera monitoring the event at a remote location. As noted above, at stand-off distances the two signatures are an expanding shock wave and thermal emission. The latter has a distinctive power vs. time shape. Figure 3 displays a canonical profile. Two power maxima are separated by a deep minimum. The logarithmic time scale belies the fact that most thermal energy is emitted over the second maximum. Typical quantities of interest are the time of power minimum, $t_{min} \approx 0.1$, time of second power maximum, $t_{2max} = 2$, and the power of the second maximum $P_{2max} = 0.54$. These three scale with yield because of self-similarity. Simulations show that t_{min}, $t_{2max} \propto Y^{0.4}$ and $P_{2max} \propto Y^{0.6}$, approximately. In other words, if Fig. 3 is the thermal emission due to yield Y_0, a signature of event with yield $Y_0/1000$ reduces t_{min} and t_{2max} by a 0.063 and P_{2max} by 0.016. If time in Fig. 3 is measured in sec, the time of first max $t_{1max} = 0.02$ sec. Hence, the signature of an event with $Y = Y_0/1000$ has $t_{1max} = 1.3$ and $t_{min} = 6.3$ ms. The power across the first maximum is emitted in a blink of an eye.

The profile displayed in Fig. 3 can represent power vs. time for a single photon frequency band, a sum of several bands of interest, or all power emitted by the event and logged *relatively near* the event itself. The distinction of what measure of power is being captured is important. While emission in distinct bands is qualitatively the same (i.e., double humped), the quantity of interest can differ significantly. For example, blue light has a later t_{min} and a deeper minimum power. Consequently, sums of powers differ depending on the needs of the modeler. In what follows, we consider power in six bands ($257 \le \lambda \le 824$) nm that span the wavelength sensitivity of the medium format (MF) film ($250 \le \lambda \le 710$ nm) in the camera monitoring the Dixie event.[6]

Our simulations of tests such as Dixie use 51 frequency (wavelength) bands. However, power is emitted largely over the lowest 15-16 bands (longest wavelengths) due to the dependence of air opacity on $h\nu$. Dependence on photon frequency illustrates why frequency averaged (gray) transport is insufficient. The nature of the streaming (monodirectional, straight from source to observer) shows why deterministic transport, instead of diffusion, is required. The opacity tables used by the code do not include atmospheric attenuation effects (due to Rayleigh scattering, aerosols, ozone, etc.), a topic we discuss next.

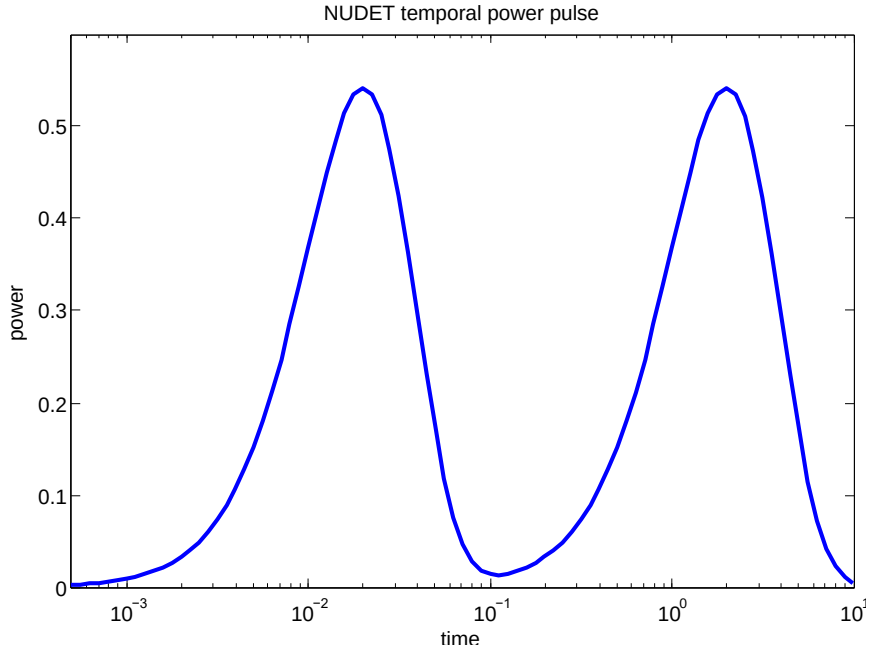

Figure 3. Characteristic profile of NUDET emitted power vs. time

As previously noted, power is logged by the simulation relatively near the event in order to shorten the problem domain and consequently reduce computational expense. Even though the simulations are one-dimensional (spherically symmetric), they may still require many hours to complete due to accuracy demands. For example, the domain may extend from hundreds of meters to kilometers, with certain sections requiring cm to mm zonal resolution. While the near-to-event monitoring of power means that atmospheric attenuation effects may be ignored, they are required in order to convert event power to flux striking a sensor (camera) at a remote distance.

The Dixie event was slightly above 3 km altitude, the camera at height $h \approx 1$ km, approximately $d = 8$ km away[7]. If P_ν represents power emitted at frequency $h\nu$, the resulting spectral flux at the camera,

$$F_\nu = P_\nu \exp(-d a_\nu)/(4\pi d^2), \tag{1}$$

where $a_\nu = a_\nu(h)$, represents the frequency and altitude dependent attenuation due to the processes modeled, e.g., Rayleigh scattering. The attenuations are additive inside the exponential,

$$a_\nu = a_{\nu,R} + a_{\nu,A} + a_{\nu,O},$$

where $a_{\nu,R}$, $a_{\nu,A}$, $a_{\nu,O}$, are the Rayleigh scattering, aerosol, and ozone coefficients (1/km).

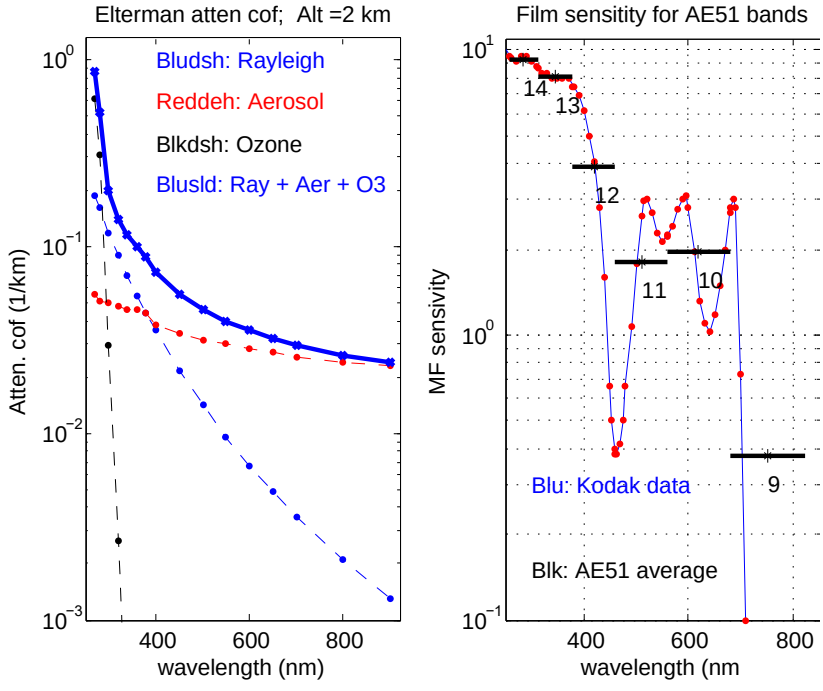

Figure 4. The dependence of attenuation coefficients and film sensitivity on emitted wavelength of light.

Figure 4: (a) Attenuation coefficients (1/km) vs. wavelength for a NUDET.[8,9] Dashed blue, red, black curves display Rayleigh, aerosol, ozone contributions; the solid represents the total. (b) displays MF film sensitivity vs. wavelength (blue curve with red dots); black lines represent AESOP51 average sensitivity over the spectral bands 9 through 14.

In 1964, Elterman[8] listed coefficients covering the IR–UV wavelength and a series of altitudes. In 1968 Elterman[9] revised the work to include 22 wavelengths (270, 4000) nm, in integral 1 km altitudes from 0 to 50. Figure 4a displays the Elterman data vs. λ at h = 2 km altitude and their sum for wavelengths pertinent to the MF film. The figure shows that at λ = 270, ozone dominates attenuation, but its attenuation decreases sharply as λ increases, as do the influence of attenuation due to Rayleigh scattering and aerosols. At λ = 270 (600) nm, total attenuation is 0.86 (0.024) (1/km). Hence, radiation intensity of those wavelengths, is reduced by factors 58% (2.4%) after traveling 1 km. Thus, the atmosphere has a large effect on the emitted spectrum of light. For other altitudes $h \leq 4$, attenuations vary similarly, decreasing with increasing altitude and wavelength (but not uniformly). For λ = 550 nm and h = 2 km, while Rayleigh scattering attenuation is 30% of aerosol attenuation, the ratio reveres at 4 km where Rayleigh scattering attenuation is 16% greater than aerosol attenuation.

The spectral fluxes striking the camera are further modified by including the MF film sensitivity. Figure 4b displays the sensitivity and corresponding averages onto the bands of the radiation hydrodynamic code. The sharp falloff at λ = 710 implies the film is insensitive to larger wavelengths. Luckily, while the film is most sensitive to the shortest and possibly even to $\lambda < 250$ nm, flux in that part of the spectrum is heavily attenuated by the atmosphere *and* the event emits very little power there, as determined from Power vs. time logs of the simulation.

The spectral dependence of the film is the reverse of that for the atmosphere. That is, while atmospheric attenuation is greatest at the shortest λ (more blue than red is scattered/absorbed), the film is more sensitive to blue light. The product of flux and sensitivity is the optical density (OD, non-dimensional), causing effectively brighter pixels to be observed on the film. Recalling Eq.(1), if $F_{v,j}$ represents the flux in band #j striking the camera and S_j the average sensitivity of the band, the resulting OD is,

$$\mathrm{OD}j = Sj\ Fv,j\ .$$

Figure 4b states that MF sensitivity for spectral bands 13 and 10 are 8, 2, respectively. Consequently the band 13 flux is weighed 4x more than the band 10 flux (according to the 8:2 ratio). After the OD of each Band is computed, they are summed and produce the simulated OD on the film.[7]

Radiation-hydrodynamics Simulation for a Near Surface NUDET

The previous sections considered the case of a 1D, spherically symmetric NUDET using Dixie as an example. In this section, we consider a near-surface burst where spherical symmetry is necessarily broken. Recently, as part of our effort to better characterize the conditions within a fireball, ALE3D's multigroup radiation diffusion method was extended for this class of problems. The multigroup system is solved using the method presented in Shestakov.[10]

For the 51 group system solved here ($G = 51$), group energy densities u_i, are solved using the finite element method in a random order, and a partial temperature update is performed in between group energy density solves. The transport equations for group energy density and temperature are as follows:

$$\frac{\partial u_i}{\partial t} = \nabla \cdot D\nabla u_i + \mathrm{c}\rho\kappa(B_i(T) - u_i)$$

$$\rho c_v \frac{\partial T}{\partial t} = -\mathrm{c}\rho\kappa \sum_{i=1}^{G} (B_i(T) - u_i)$$

The diffusion coefficient D is defined as:

$$D = \frac{c}{3\rho\kappa}$$

A linearization is performed on the Planck function (B_i) around a known T, which allows the temperature equation to be solved in terms of known quantities.

It is convenient to define a radiation temperature which identifies how close the radiation energy is to equilibrium with matter energy:

$$T_r = \left(\frac{c}{4\sigma} \sum_{i=1}^{G} u_i \right)^{1/4}$$

where σ is the is the Stefan-Boltzmann constant. Due to the disparity in opacities exhibited in these systems, an Sn transport method such as the one used in the previous sections would be

preferred. In its absence, the extended treatment for multi-group diffusion has been used with an appropriate flux limiter to address large mean free path of the air at lower temperatures and densities.

Preliminary results using the extended diffusion method in ALE3D are shown in Figure 5. The calculation shown is for an idealized energy pill with 100 kT yield, and a height of burst of 120 m. A simple gamma law gas was used for the equation of state for air ($\gamma = 1.4$) and AESOP 51 opacities. The rows of the figure from top to bottom represent different states in time (t = 0.25s, 0.5s, and 1.0s). The variables shown from left to right include radiation and matter temperature (Kelvin), pressure and artificial viscosity (Mbar). One can identify a high temperature core with radiation energy unable to pass through the dense opaque shock wave at t = 0.25 s. As time progresses and the shock wave becomes more transparent and a gradual release of the fireball energy is observed.

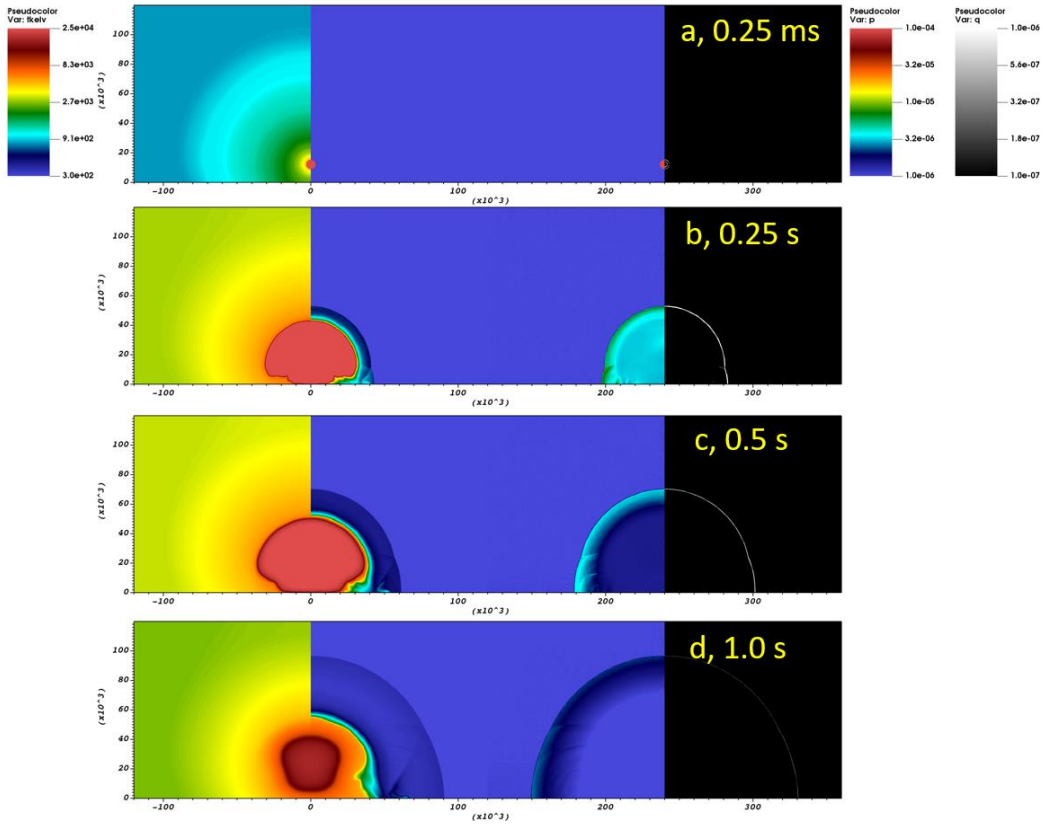

Figure 5. Preliminary example of ALE3D radiation-hydrodynamics model of near surface burst

Figure 5: Preliminary example of ALE3D radiation-hydrodynamics model of near surface burst where rows from top to bottom represent different states in time (t = 0.25ms, 0.25s, 0.5s, and 1.0s). The variables shown from left to right include radiation and matter temperature (Kelvin), pressure and artificial viscosity (Mbar). The artificial viscosity is only active within a shock and so

is useful for highlighting the shock location. Results show the effect of the shockwave on thermal energy as it transitions from opaque to transparent allowing the release of energy.

Modeling Effects with Gravity

Beyond capturing the fundamental physical signatures of a NUDET, if attempting to simulate and understand how the post-detonation environment including chemistry may be influenced by the presence of bomb material and material entrained from the surroundings, we must include gravity. Simulations of near surface nuclear events, for example, require that we include the failure of earthen materials. While the early-time behavior of a NUDET is largely independent of gravitational effects, the late-time fireball behavior including shockwave interaction with the ground and near surface and entrainment of material to form fallout, are all strongly influenced by gravity.

The simplest approach to including gravity in a model adds a body force into the model, without any additional initialization, and requires that the problem equilibrate before introducing the detonation. The majority of effects codes use explicit time integration and there timesteps must be small to satisfy the Courant condition for stability.[11] Consequently, many timesteps must be taken to allow waves to travel through the computational domain, allowing conditions to reach equilibrium. For large problems, however, such an approach adds significant additional computational expense. In addition, the dynamic waves created by the out-of-equilibrium initialization of the model can lead to nonphysical damage to geological and artificial structures within the model. Even small perturbations in initial conditions can result in waves that overwhelm the features of interest.

For both efficiency and accuracy, the cells of the computational domain are instead initialized so that materials are in, or close to being in equilibrium. Such initial states, often referred to as a “quiet start,” are trivial to calculate for simple gas equations of state or even for linear elastic materials. However, for complex equations of state, or sophisticated geologic models that include nonlinear (potentially hysteretic) effects, obtaining the initial state for each cell is more challenging. One approach performs a complete, implicit mechanical analysis (using finite elements, for example) to obtain an initial state in equilibrium. Many geological material models, however, are constructed specifically with the intent of being invoked from an explicit timestepping code and do not lend themselves to being called from within an implicit solver.

We have instead developed an intermediate approach that seeks to quickly estimate a near-equilibrium state without needing to perform an entire implicit analysis. We should note that stress states in a solid can be path dependent. In particular, while the gravitational load must be balanced by a vertical stress gradient, the lateral and shear stresses are not uniquely determined and require making additional assumptions regarding the strain path taken. Simple examples assume isotropic deformation (hydrostatic stress) or uniaxial, vertical deformation. In the work presented here, we assume uniaxial deformation. Our approach adjusts density and stress state in response to any static body forces, of which a gravitational load is the most common, using an iterative process, with an error tolerance.

The force $\mathbf{F}_i$ on node *i* of an element is given by:

$$\mathbf{F}_i = \mathbf{F}^0 - \boldsymbol{\Sigma} \cdot \mathbf{N}_i ,$$

where $\mathbf{F}^0$ is the body force, $\boldsymbol{\Sigma}$ is the stress tensor, and $\mathbf{N}_i$ is the nodal area vector. We need to compute the stress that balances the force on the nodes. We achieve this via the following steps:

1. Compute the total stress and rotations
2. Compute a new target pressure *P* from the trace **T** of the computed stress. (Store new *P* and old **T** so they are not affected by next step)
3. Using the current shear modulus, compute an effective deviatoric strain to apply to the material. (This may require evolving materials with history variables that keep track of effective total strain to compute stress)
4. Restore the stored (*P*, **T**) and then update relative volume and total mass in the cell

Let us consider what each element brings to the overall force calculation. The force can be broken into two basic components - a bulk and local load. Every element and its neighbors are going to provide a consistent bulk load that will be balanced by their neighbors. To speed the calculation, we will compute the bulk load separate from the deviatoric load. The bulk load will have a predominant direction, $\mathbf{G}$, that we will need to solve for:

$$\tilde{\mathbf{F}}_i = \frac{\mathbf{GG}}{\mathbf{G} \cdot \mathbf{G}} \cdot (\mathbf{F}^0 - \boldsymbol{\Sigma} \cdot \mathbf{N}_i)$$

This requires that we choose a direction and two obvious choices are that $\boldsymbol{\Sigma}$ be isotropic ($\alpha = 1$) or uniaxial ($\alpha = 0$):

$$\boldsymbol{\Sigma} = -p\left(\alpha \mathbf{I} + (1-\alpha)\,\frac{\mathbf{GG}}{\mathbf{G} \cdot \mathbf{G}}\right)$$

The initial stages of the calculation are dominated by elements that are not on the bottom of the domain trying to move down and taking an excessive number of steps to equilibrate. To reduce the number of steps needed to converge, we remove the downward tendency for each element. For each node *k*, we compute the acceleration in the direction of the body force:

$$\hat{\boldsymbol{a}}_k = \boldsymbol{g}_k \frac{\boldsymbol{g}_k \cdot \boldsymbol{a}_k}{\boldsymbol{g}_k \cdot \boldsymbol{g}_k}$$

we compare the average normalized acceleration in the load direction ($\bar{\boldsymbol{a}} = \langle \hat{\boldsymbol{a}}_k \rangle$ with the nodal outward normal by taking the dot product:

$$\alpha_k = \bar{\boldsymbol{a}} \cdot \mathbf{n}_k$$

If this dot product is positive, it indicates that the element is seeking to accelerate in the direction of the body force. To avoid this, we prevent the element from accelerating in that direction:

$$\hat{\boldsymbol{a}}_k = \boldsymbol{a}_k - Sign(\alpha_k)\bar{\boldsymbol{a}} \tag{2}$$

where $Sign()$ is the sign of the value times 1. This additional acceleration effectively increases the pressure in the element. Physically, if the element above has a net downward force, we need to increase the pressure of the current element to counteract that force.

We continue iterations until the incremental error, defined as:

$$\epsilon = \left(\frac{\delta P^2 + \delta {J_2}^2}{P^2 + {J_2}^2 + S^2} \right)^{1/2} \tag{3}$$

meets a user selected tolerance. Here J_2 is the second stress invariant, and S is the iteration scale defined by the user.

As mentioned previously, the requirement of gravitational equilibrium does not dictate a unique stress state. Our approach allows for the user to choose the degree to which the solution is closer to isotropic compression or uniaxial loading.

In addition to the initial stress state, the problem requires appropriate boundary conditions to maintain static equilibrium against gravity. In particular, the domain must be constrained to prevent it from falling, and any lateral stresses that develop must also be balanced. In the ALE3D models presented here, we use symmetry boundary conditions on the lateral and bottom boundaries with a pressure boundary condition on the top. Other options could be to utilize a traction boundary with appropriate damping to limit reflections.

Figure 6 shows an example of the final equilibrated stress state obtained using ALE3D with the described initialization algorithm for a 3D problem.

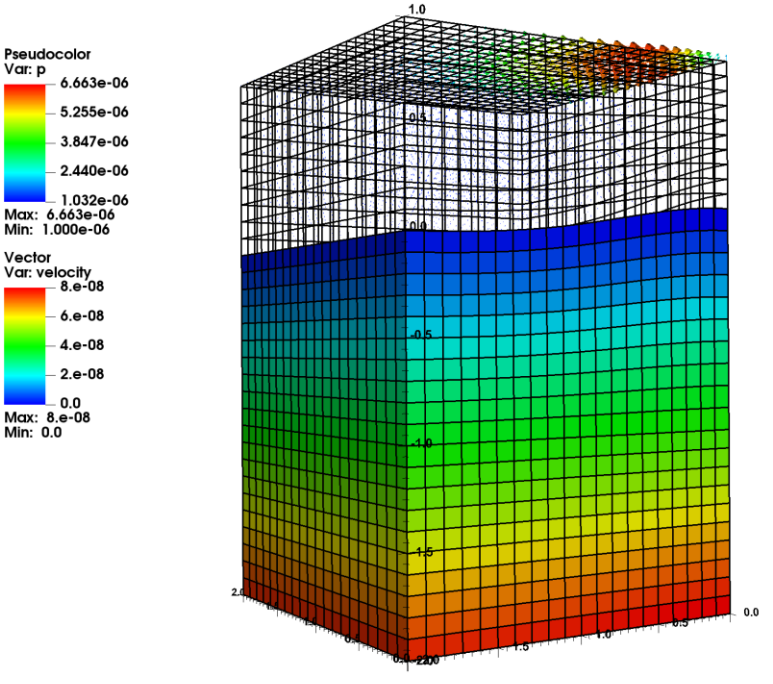

Figure 6. Example of final equilibrated stress state obtained using ALE3D with the described initialization algorithm for a 3D problem with a non-flat ground surface. This snapshot is 100 cycles after start and the largest velocity in the calculation is 1.3 × 10^{-1} cm/μs and we observe a suitable gradation of compression.

6 Modeling Effects with Gravity

An initial NUDET demonstration utilizing the initialization method described in the previous section was performed using ALE3D. The idealized model has an energy pill of 100 kT yield at a height of burst of 150 m. An LEOS material model was used to represent air, and a porous sandstone material[12,13] was used to represent the ground. Figure 7 shows several images of the near surface detonation at different points in time (0.05, 0.6, 2.4, and 10 seconds) with the pressure field (Mbar) on the left, and the temperature field (K) on the right. The radiation diffusion model described in section 4 was not used in these calculations. The initial lithostatic stress gradient is evident and the model is run long enough such that buoyancy has time to drive the fireball upward.

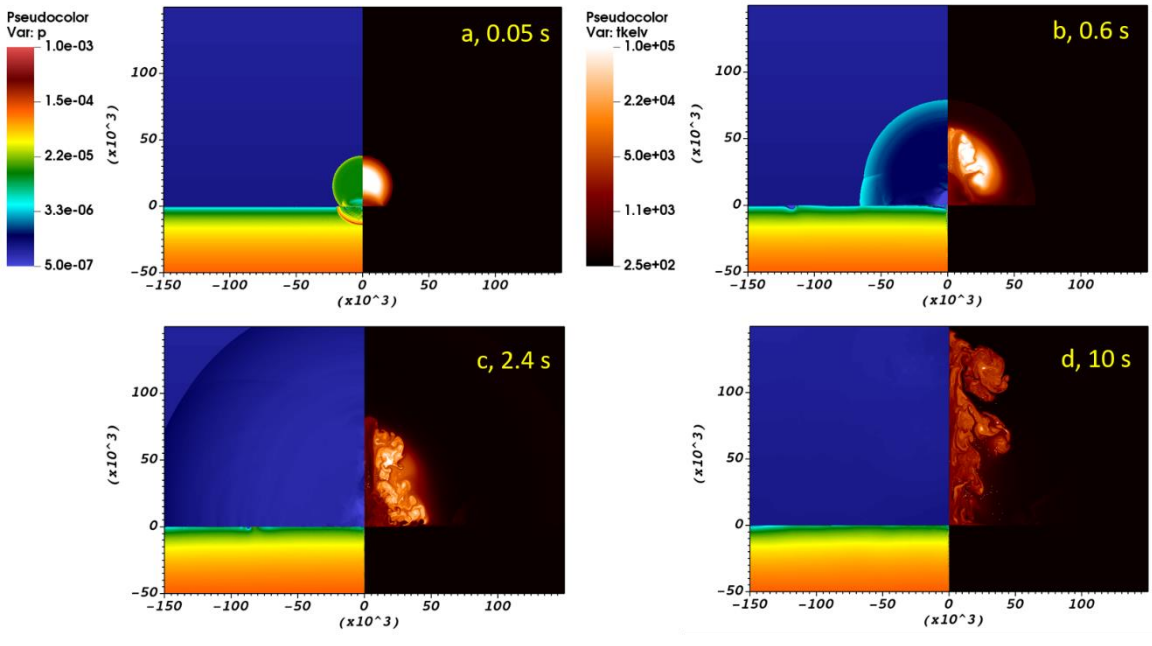

Figure 7. Example of ALE3D model of near surface burst, including geological material. The initial lithostatic stress gradient is evident and the model is run long enough such that buoyancy has time to drive the fireball upward.

Conclusion

We have provided an overview of recent work to improve our understanding of the post-detonation fireball environment (including entrainment of environmental materials) as part of a project investigating the post-detonation fireball chemistry. We discussed the early time coupled radiation-hydrodynamics effects of a NUDET in the atmosphere, including frequency-dependent transport. We demonstrate how this can be convolved with an understanding of the frequency-dependent sensitivity of a specific class of film to predict the observations recorded by a camera. This capability is crucial to the accurate interpretation of historic fireball footage for the purposes of validating our models.

We also discussed our efforts to include radiation effects into our models and the challenges associated with modeling longer-term processes associated with atmospheric NUDET where gravity plays a role, either in the buoyancy of the fireball or in the inclusion of lithostatically stressed subsurface materials and neighboring structures. Such models require that all cells in the calculation be initialized to an equilibrium state, lest energy stored in the domain result in the disruption of the calculation. We presented an efficient, readily implemented approach whereby existing explicit codes can achieve an initial, quiet state without resorting to developing a fully implicit solution. Concurrent with these efforts, improved chemical and multiphase models are being incorporated into ALE3D. Future work will involve predicting the post-detonation chemistry using predicted fireball conditions to drive this updated chemistry model.

Acknowledgements

This work was performed under the auspices of the U.S. Department of Energy by Lawrence Livermore National Laboratory under Contract DE-AC52-07NA27344 and was supported by the LLNL LDRD Program under Project No. 20-SI-006. Release number LLNL-JRNL-814197.

Nomenclature

Unless noted otherwise, symbols have the following meaning and units:

B_i – Planck function for group i; (erg/cc)
c – speed of light; (cm/s)
c_v – specific heat; in AESOP51 ((erg/g)/eV)
D – radiation diffusion coefficient; (cm^2/sec)
e – specific energy; in AESOP51 (erg/g)
G – number of photon energy groups; (-)
H – height of burst (km)
M – source mass (kg)
P – emitted power (erg/sec)
p – pressure (dyne/cm^2)
R – shock position (cm)
T – temperature (K)
t – time (s)
t_{min} – time of min(P) after first max(P) (sec)
t_{2max} – time of second max(P) (sec)
u_i – group i photon energy density; (erg/cc)
Y – yield (kt)
κ – opacity; (cm^2/g)
ξ_o – dimensionless scalar in Sedov-Taylor solution
ρ – density (g/cc)
ρ_o – ambient density (g/cc)
σ – Stefan–Boltzmann constant (erg/cm^2 sec K^4)

Notes:

1. Glasstone, S. and Dolan, P. J., *The effects of nuclear weapons*, Third Edition, 1977

2. Lewis, E. e. and Miller, W. F., Computational Methods of Neutron Transport, John Wiley and Sons, New York (1984)

3. Spriggs, G., "Weapon Physicist Declassifies Rescued Nuclear Test Films," https://www.osti.gov/biblio/1354720, 2017

4. Spriggs, G., "You can now watch declassified Cold War nuclear test films on YouTube," https://www.wired.co.uk/article/nuclear-testing-greg-spriggs-videos, 2017.

5. Myers, A. H., Spriggs, G. D. and Cook, A. W., "New Yield Estimates for Nuclear Detonations Over Water," Lawrence Livermore National Laboratory technical report, LLNL-JRNL-804822.

6. "United States Nuclear Tests, July 1945 through September 1992," Department of Energy technical report, DOE/NV 209, September 2015.

7. Spriggs, G., Personal Communication, 2020.

8. Elterman, L. "Atmospheric Attenuation Model, 1964, in the Ultraviolet, Visible, and Infrared Regions for Altitudes to 50 km," Air Force Cambridge research Laboratories, AFCRL-64-740, Sep. 1964, also at: https://apps.dtic.mil/sti/pdfs/AD0607859.pdf.

9. Elterman, L. "UV, Visible, and IR Attenuation for Altitudes to 50 km, 1968" Air Force Cambridge research Laboratories, AFCRL-68-0153, April 1968.

10. Shestakov, A. I., Vignes, R. M. and Stölken, J. S. "Derivation and solution of multifrequency radiation diffusion equations for homogeneous refractive lossy media", Journal of Computational Physics, 230 (2011) 984-999.

11. Courant, R.; Friedrichs, K.; Lewy, H. (1928), "Über die partiellen Differenzengleichungen der mathematischen Physik", Mathematische Annalen (in German), 100 (1): 32–74.

12. Rubin, M. B., Vorobiev, O. Y., Glenn, L. A. Mechanical and numerical modeling of a porous elastic-viscoplastic material with tensile failure, International Journal of Solids and Structures 37 (13) (2000) 1841 – 1871.

13. Vorobiev, O., Generic strength model for dry jointed rock masses, International Journal of Plasticity 24 (12) (2008) 2221 – 2247.

How to Submit an Article to the

Countering WMD Journal

The Countering WMD Journal is published semi-annually by the United States Army Nuclear and Countering WMD Agency. We welcome articles from all U.S. Government agencies and academia involved with CWMD matters. Articles are reviewed and must be approved by the *Countering WMD Journal* Editorial Board prior to publication. The journal provides a forum for exchanging information and ideas within the CWMD community. Writers may discuss training, current operations and exercises, doctrine, equipment, history, personal viewpoints, or other areas of general interest to CWMD personnel. Articles may share good ideas and lessons learned or explore better ways of doing things. Shorter, after action type articles and reviews of books on CWMD topics are also welcome.

Articles submitted to *Countering WMD Journal* must be accompanied by a written release from the author's activity security manager before editing can begin. All information contained in an article must be unclassified, nonsensitive, and releasable to the public. It is the author's responsibility to ensure that security is not compromised; information appearing in open sources does not constitute declassification. The *Countering WMD Journal* is distributed to military units and other agencies worldwide. As such, it is readily accessible to nongovernment or foreign individuals and organizations. A fillable security release memorandum is provided at http://www.belvoir.army.mil/usanca/.

The *Countering WMD Journal* is published twice a year: Summer/Fall (article deadline is 15 September) and Winter/Spring (article deadline is 15 March). Send submissions via email to usarmy.belvoir.hqda-dcs-g-3-5-7.mbx.usanca-proponency-division@mail.mil, or as a Microsoft Word document on a CD via mail, to: Editor, CWMD Journal, 5915 16th Street, Building 238, Fort Belvoir, VA 22060-5514.

You can get more information about submitting an article to the *Countering WMD Journal*, download an article format, or view and download digital versions of the *Countering WMD Journal* at our website http://www.belvoir.army.mil/usanca/.


U.S. ARMY NUCLEAR AND CWMD AGENCY
Fort Belvoir, Virginia